SUPERCONVERGENT ESTIMATION OF THE GRADIENT FROM LINEAR FINITE ELEMENT APPROXIMATIONS ON TRIANGULAR ELEMENTS

NICK LEVINE

NUMERICAL ANALYSIS REPORT NO. 3/85

ABSTRACT

We consider methods for boosting to second order accuracy ("superconvergence") the gradients of piecewise linear Finite Element approximations on triangular elements.

We show that the component of gradient tangential to any element edge is superconvergent at the midpoint of that edge but that no points exist at which the full gradient can be sampled to this accuracy. To "recover" the full gradient we average its approximation over small patches of elements, choosing weights such that - on a uniform mesh - the scheme would be exact if applied to the interpolant of any quadratic. We present simple schemes for recovery at any point in the domain, for example: nodes, centroids and the neighbourhood of the boundary. We generalise our results to non-uniform meshes. Also, we compare them with Wheeler's flux method.

Superconvergence will not occur unless precisely six elements meet at every node internal to the triangulation. Another condition is that the grid of nodes must be a smooth distortion from uniformity. We show how these requirements can be met on a large variety of domains. Sometimes, near a smooth segment of the domain boundary, the mesh topology will have to reflect the behaviour of a vertex ; we show how this might be achieved in practice.

We prove that our results apply to the approximation of any strongly elliptic self-adjoint problem whose solution has three derivatives. We accept numerical quadrature by the centroid rule and interpolation of both the boundary and the data on it.

We discuss the sense in which our error estimates hold

uniformly across the domain (rather than "on average"), examining in detail the approximation properties of a derivative Green's function. We apply this to the question of "local" superconvergence: there may now exist subdomains in which the smoothness or triangulation requirements fail.

CONTENTS

(continued)

PART 2 - ANALYSIS

1.1 AIMS

It is well known that a Finite Element Method will yield, in an energy seminorm ($|\cdot|_a$), the optimal approximation (Ru) over some finite-dimensional space (S) to the solution (u) of an elliptic partial differenetial equation, thus:

$$|Ru - u|_a \leq |\phi - u|_a$$

for all $\phi \in S$. It is also recognised that in spite of its optimality, the energy error is not particularly small. For example, let S be a space of continuous, piecewise linear functions on some partition into triangles of the domain $\Omega \subset \mathbb{R}^2$ on which the differential equation is posed, with maximum triangle diameter h. Then

$$|Ru - u|_a = O(h)$$

(at best - i.e. provided u is sufficently smooth). On the other hand,

$$||Ru - u||_{L_2(\Omega)} = O(h^2) \ ,$$

even though Ru is not an optimal approximation in the L_2 norm. If we use Ru and ∇Ru as point-by-point approximations to u and ∇u (i.e. to the unknown function and its first derivatives) we know, a priori, that the average errors involved will be $O(h^2)$ and $O(h)$ respectively.

It is ironic that Finite Element Methods should be seen to fail to deliver a good estimate of the one quantity that they are apparently designed to approximate. Our aim is to remedy this position: we seek a procedure for obtaining gradients to the same degree of accuracy as the function values. We will study the commonly used linear elements mentioned above for which this improvement in order - "superconvergence" - is readily accessible

and particularly dramatic. We will show how to construct Finite Element solutions with superconvergence in mind. We will then discuss algorithms which exploit this property to give $O(h^2)$-accurate approximations to unknown gradients for a wide range of problems. A mathematical analysis of our methods follows in Part II. We start in this chapter with some examples which introduce the principal concepts.

1.2 TECHNICAL PRELIMINARIES

Many of our results are presented in the context of Sobolev spaces; for convenience we introduce here the relevant notation and then two key lemmas of these tools of the trade. (Compared with much of the following, this section is abstruse. It can be skipped and used for later reference.)

We work only with bounded open regions in $\mathbb{R}^2$ which have the strong cone property (see Figure 1.2.1 and Bramble & Hilbert, 1970). Let A be such a region: typically this will be the problem domain Ω or a small patch of elements. We denote by $W_p^m(A)$ ($m = 0,1,\ldots$) the Sobolev space of functions which together with their generalised derivatives up to order m inclusive are in $L_p(A)$. The norm and seminorm are given by

$$||\omega||_{m,p,A} = \left[\Sigma_{|\alpha|\leq m} ||D^\alpha \omega||^p_{L_p(A)} \right]^{1/p}$$

$$= \left[\iint_A \Sigma_{|\alpha|\leq m} |D^\alpha \omega|^p \right]^{1/p}$$

$$|\omega|_{m,p,A} = \left[\Sigma_{|\alpha|=m} ||D^\alpha \omega||^p_{L_p(A)} \right]^{1/p}$$

$$= \left[\iint_A \Sigma_{|\alpha|=m} |D^\alpha \omega|^p \right]^{1/p}$$

respectively for $p < \infty$. (α is a multi-index; see e.g. Dupont &

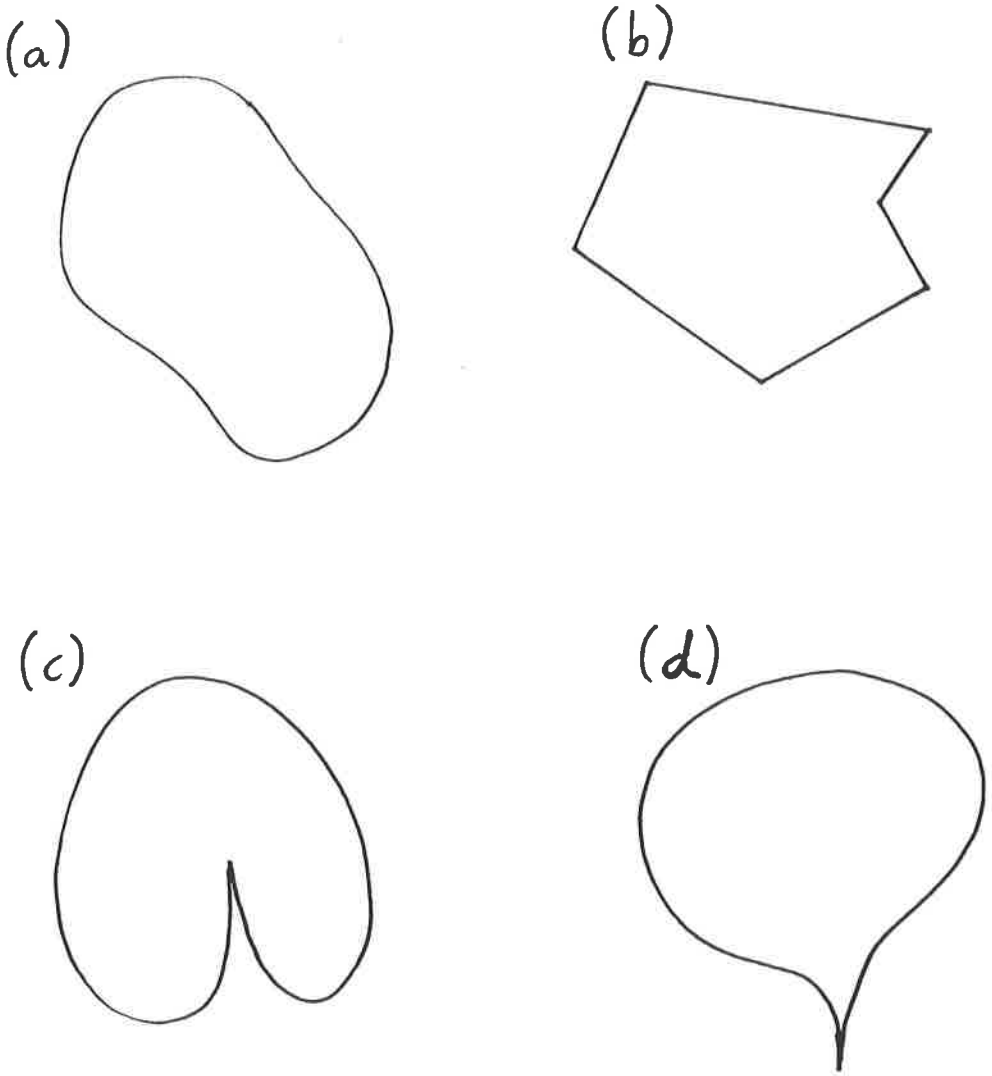

Figure 1.2.1

The strong cone property

This excludes regions with outward-facing cusps; therefore (a), (b) and (c) are acceptable and (d) is not.

Scott, 1980.) We make the usual modification when $p = \infty$:

$$||w||_{m,\infty,A} = sup_{|\alpha| \leq m} ||D^{\alpha} w||_{L_{\infty}(A)}$$

and $$|w|_{m,\infty,A} = sup_{|\alpha| = m} ||D^{\alpha} w||_{L_{\infty}(A)} .$$

We will occasionally need to use norms of fractional order derivatives, defined as follows: let $s = m + \sigma$, $m = 0,1,\ldots$ and $0 < \sigma < 1$. Then (Adams, 1975, page 214)

$$||w||_{s,p,A} = ||w||_{m,p,A} + \Sigma_{|\alpha| = m} \left|\left|\left| \frac{D^{\alpha}(w(x) - w(X))}{|x - X|^{\sigma + 2/p}} \right|\right|\right|_{p,A}$$

where $|||\cdot(x,X)|||_{p,A}$ denotes the $L_p(A)$ norm with respect to (the vector) x of the $L_p(A)$ norm with respect to X.

For the most part we will take $p = 2$ and write H^m , $||\cdot||_{m,A}$ and $|\cdot|_{m,A}$ for W_2^m , $||\cdot||_{m,2,A}$ and $|\cdot|_{m,2,A}$ respectively. We denote the L_2 inner product thus:

$$(w , v)_A = \iint_A w\, v \quad .$$

Throughout, the letter c stands for a generic, positive number, different at each appearance but "constant" in that - unless otherwise stated - it is independent of the coefficients, data and solution of the differential equation under approximation, any function denoted by u, v, w, ϕ or ψ, the element(s) or sampling/recovery point(s) under consideration and the discretisation parameter h. It is not, however, an absolute constant: there is an implicit dependence on the region Ω, smoothness parameters (usually denoted by ϵ) and the algorithms employed for triangulation, recovery and quadrature.

The following result links norms from different Sobolev spaces. It is a combination of the Sobolev Embedding Theorem (Sobolev, 1950) with a simple modification, in $\mathbb{R}^2$ (i.e. $n = 2$), of the Hölder inequality:

$$||u||_{s-k,q,A} \leqslant c\ (diam\ A)^{n(1/q\ -\ 1/p)}\ ||u||_{s,p,A}$$

for all k, q such that $0 \leqslant k \leqslant s$ and $1 \leqslant q \leqslant p$.

"S.E." Lemma 1.2(i) (See Figure 1.2.2.) Let $diam\ A = \rho$. For some $s \geqslant 0$ and $p \geqslant 1$, let $k \in [0,s]$ and $q \geqslant 1$ satisfy

either $k\ p > 2$

or $q < p\ /\ (1 - kp/2)$.

Then

$$W_p^s(A) \subset W_q^{s-k}(A)$$

and

$$||u||_{s-k,q,A} \leqslant c\ \rho^{2(1/q\ -\ 1/p)}\ ||u||_{s,p,A} \qquad (1.2.1)$$

for all $u \in W_p^s(A)$. In particular,

$$sup_{x\ \in\ A}\ |u(x)| \leqslant c\ \rho^{-2/p}\ ||u||_{s,p,A} \qquad (1.2.2)$$

for all $u \in W_p^s(A)$ and $s\ p > 2$. ###

We now give the Bramble-Hilbert Lemma (Bramble & Hilbert, 1970), an important tool in Sobolev space approximation theory. It is often regarded as a non-constructive generalisation of the Peano Kernel Theorem to functions of more than one variable. (By "non-constructive", we mean that no information can be given about the value of the following constant c.)

"B.H." Lemma 1.2(ii) Let $diam\ A = \rho$. Let F be a linear functional on $W_p^m(A)$ and let $k = k(m,p;\rho)$ be given such that

(i) $|F(w)| \leqslant k\ ||w||_{m,p,A}$ for all $w \in W_p^m(A)$

and (ii) $F(w) = 0$ if w is a polynomial on A of degree less than m.

Then

$$|F(w)| \leqslant c\ k\ \rho^m\ |w|_{m,p,A} \quad \text{for all } w \in W_p^m(A),$$

the constant c depending on F, p and m only. ###

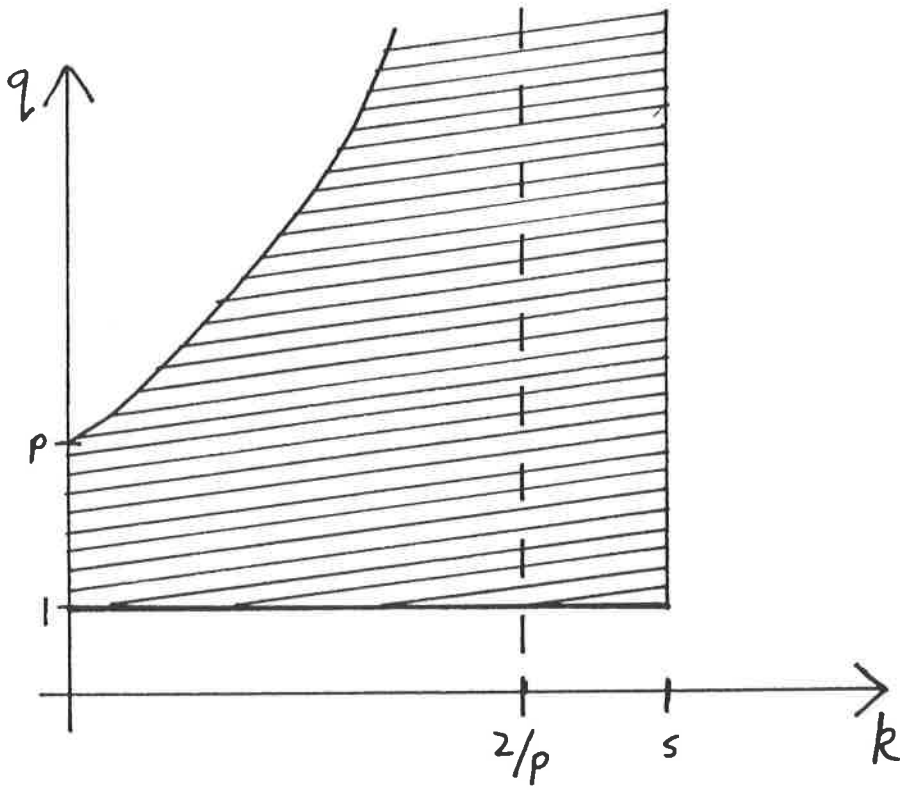

Figure 1.2.2

Sobolev Embedding Theorem

The shaded region indicates the values of (k,q) such that (1.2.1) holds. With the exception of the locus $\{ q = p/(1 - kp/2) \}$ the boundary is included. (In this example $ps > 2$.)

1.3 BACKGROUND FOR QUADRILATERAL ELEMENTS

Gradient superconvergence on quadrilateral elements illustrates many of the concepts that we will meet later, in isolation from the geometrical complications which characterise the corresponding results on triangles. As has often been the case with the Finite Element Method, this phenomenon was first observed in practical work and described (intuitively) by engineers. A fuller theoretical treatment from the mathematicians did not appear until later.

(We note incidentally the "superconvergence" results of Bramble and Schatz, 1977 and Thomée, 1977 which concerned local convolution operators for boosting an $O(h^r)$ error in displacements or their derivatives to $O(h^{2r-2})$. This approach, from which the simple elements that we are interested in cannot benefit, is not related to our variety of gradient superconvergence and we will not mention it again.)

We start then with Veryard (1971). He was able, empirically, to improve the accuracy of the first derivatives of biquadratic Finite Element approximations by sampling them only at the second order Gauss points in each element. (Observations of a similar nature were also made by Barlow (1968) and Too (1971)). These points of exceptional accuracy came to be known as "stress points" and their existance as an example of "superconvergence"; though this term does have a wider meaning we associate it here only with the estimation of gradients to one order of accuracy higher than is generally expected.

The grand prophets of the Finite Element Method, Strang and Fix (1973, pages 168-9) had this to say. "We believe that the

stress points can be located in the following way. The leading term in the errors is gover~ned by the problem of approximating polynomials P_k of degree k [sic], in energy, by the trial functions... Then stress points are identified by the property that the true stresses (derivatives of P_k) coincide with their approximations (derivatives of a lower degree polynomial)." This idea is at the heart of any superconvergence result, for it leads us directly to the stress points of the "unknown" function's interp$\overset{o}{\underset{\wedge}{}}$lant (Barlow, 1976). Now, suppose that - perhaps only under certain conditions - the gradient of the interpolant is at all points a superconvergent approximation to the gradient of the Finite Element solution. Then the stress points for these two functions are identical. A general algorithm for obtaining superconvergent gradients would therefore be as given by Table 1.3.

The first precise statement and full proof of superconvergence at Gauss points was given by Zlámal (1977) for the case of linear and quadratic serendipity elements in up to three dimensions. His work was later extended to cover curved isoparametric elements of any degree with various numerical quadrature schemes (Zlámal, 1978 and Lesaint & Zlámal, 1979). We give in Section 1.4 an example of his method, applied to the simplest possible case: bilinear rectangular elements for a model problem. We will later adapt this to triangles and go on to generalise the problem under approximation, which we now introduce in its model form.

Let u be the ("unknown") solution to Poisson's equation:

$$\left.\begin{aligned} -\left[\frac{\partial^2 u}{\partial x^2} + \frac{\partial^2 u}{\partial y^2}\right] &= f(x,y) \quad \text{in } \Omega \\ u &= u_E \quad \text{on } \partial\Omega \end{aligned}\right\} \quad (1.3.1)$$

(1) Construct a Finite Element approximation whose gradient is close to the gradient of the interpolant.

(2) Locate the stress points of the interpolant.

(3) Take values of ("sample") the gradient of the Finite Element solution at these points. Use them as estimates to the unknown gradient there.

Table 1.3

Superconvergence simplified

where Ω is a rectangle with sides parallel to the x- and y-axes, $\partial\Omega$ is its boundary and u_E is the restriction of some given function

$$\bar{u}_E \in H^1(\mathbb{R}^2) \quad .$$

Let $H^1_0(\Omega)$ be the completion in the H^1-norm of the space of infinitely differentiable functions on Ω with compact support in Ω; let

$$H^1_E(\Omega) \quad = \quad \{ \, w = \bar{u}_E + v \, , \quad v \in H^1_0(\Omega) \, \} \quad \ldots$$

These definitions, though rigorous, are not very helpful. Put more simply,

$$\left.\begin{aligned} v \;&=\; 0 \quad \text{on } \partial\Omega \text{ for all } v \in H^1_0(\Omega) \\ \text{and} \qquad w \;&=\; u_E \quad \text{on } \partial\Omega \text{ for all } w \in H^1_E(\Omega) \quad . \end{aligned}\right\}$$

The "weak solution" of (1.3.1) - obtained from it by Green's Theorem - is a function $u \in H^1_E(\Omega)$ satisfying

$$(\nabla u \, , \, \nabla v \,)_\Omega \quad = \quad (\, f \, , \, v \,)_\Omega \qquad (1.3.2)$$

for all $v \in H^1_0(\Omega)$. The approximations which follow are based on this form rather than on (1.3.1) directly.

If we wish to use the Finite Element Method to approximate the solution of (1.3.2), we must first partition Ω into smaller, polygonal regions, which meet only on common edges or common vertices (as in Rannacher & Scott, 1982). (We assume for now that this can be done exactly.) In this example let us take the elements to be the rectangles A_k, $k = 1, \ldots, k_{max}$:

$$\left.\begin{aligned} &\max_k \, diam \, A_k \;=\; h \\ &\min_k \, edge \, length \, A_k \;=\; ch \quad \text{for some } c > 0 \end{aligned}\right\} (1.3.3)$$

and $S \in H^1(\Omega)$ to be the space of continuous functions which are bilinear on each element, i.e. piecewise of the form

$$\alpha_1 + \alpha_2 x + \alpha_3 y + \alpha_4 xy \quad . \qquad (1.3.4)$$

We let S_E be the subset of S whose members interpolate nodal

values of u_E on the boundary $\partial\Omega$; similarly let $\phi = 0$ on $\partial\Omega$ for all $v \in S_0$. (Note that $S_E \notin H_E^1(\Omega)$ but $S_0 \in H_0^1(\Omega)$.) We define the Finite Element approximation $Ru \in S_E$ to u by analogy to (1.3.2):

$$(\nabla Ru , \nabla\phi)_\Omega = (f , \phi)_\Omega \qquad (1.3.5)$$

for all $\phi \in S_0$. The equations (1.3.5) are known as the "Finite Element" or "Galerkin" equations.

We illustrate the use of S.E. and B.H. (i.e. the lemmas of the last section) for investigating the error inherent in ∇Ru by proving the familiar result, given in Section 1.1, that the difference between the approximate and true gradients is $O(h)$:

$$|Ru - u|_{1,\Omega} \leq ch\, |u|_{2,\Omega} \qquad (1.3.6)$$

for all $u \in H^2(\Omega)$. Note that this result is "global" (the sampling point is integrated over Ω to give an average error) and that we have to strengthen the smoothness of u:

$$u \in H_E^1(\Omega) \cap H^2(\Omega) \quad . \qquad (1.3.7)$$

A useful consequence of (1.3.7) and S.E. (1.2.2) is that the interpolant $Iu \in S_E$ of u is now guaranteed to exist. (This is the function which has the same values as - "interpolates" - u at every node in the partition of Ω.) It has a central role in the derivation of our estimates.

Now, by (1.3.2) and (1.3.5),

$$\begin{aligned} &|Ru - u|_{1,\Omega}^2 \\ &= (\nabla(Ru - u) , \nabla(Ru - u))_\Omega \\ &= (\nabla(Iu - u) , \nabla(Ru - u))_\Omega \\ &= \Sigma_{k=1}^{k_{max}} F_k(u) \quad , \end{aligned} \qquad (1.3.8)$$

where the F_k are linear functionals on u defined by

$$F_k(u) = (\nabla(Iu - u) , \nabla\psi)_{A_k}$$

and we have set

$$\psi = Ru - u \in H^1(\Omega) \quad .$$

From S.E., (1.3.3) and the definition of S we have

$$\begin{aligned} & |Iu|_{1,A_k} \\ \leq\ & ch\ |Iu|_{1,\infty,A_k} \\ \leq\ & c\ ||Iu||_{L_\infty(A_k)} \\ \leq\ & c\ ||u||_{L_\infty(A_k)} \\ \leq\ & ch^{-1}\ ||u||_{2,A_k} \quad , \end{aligned}$$

whence

$$\begin{aligned} & |F_k(u)| \\ \leq\ & |Iu - u|_{1,A_k}\ |\psi|_{1,A_k} \\ \leq\ & \left[\ |Iu|_{1,A_k} + |u|_{1,A_k}\ \right] |\psi|_{1,A_k} \\ \leq\ & ch^{-1}\ ||u||_{2,A_k}\ |\psi|_{1,A_k} \quad . \end{aligned} \tag{1.3.9}$$

Further, it is clear that if u is linear on A_k then $Iu = u$ there; therefore $F_k(u) = 0$ for all linear u on A_k.

So, by (1.3.9) and B.H.,

$$|F_k(u)| \leq ch\ |u|_{2,A_k}\ |\psi|_{1,A_k} \quad .$$

(Note that both this and (1.3.9) are abstract error bounds: they hold for any u satisfying (1.3.7) and any $\psi \in H^1(\Omega)$, without reference to concrete externals, such as the differential equation.) We now return to (1.3.8) and, summing over k, apply Cauchy-Schwarz:

$$\begin{aligned} & |Ru - u|^2_{1,\Omega} \\ \leq\ & ch\ \Sigma_{k=1}^{k_{max}}\ |u|_{2,A_k}\ |\psi|_{1,A_k} \\ \leq\ & ch\ \left[\ \Sigma_k\ |u|^2_{2,A_k}\ \right]^{1/2}\ \left[\ \Sigma_k\ |\psi|^2_{1,A_k}\ \right]^{1/2} \\ =\ & ch\ |u|_{2,\Omega}\ |Ru - u|_{1,\Omega} \quad . \end{aligned} \tag{1.3.10}$$

We therefore arrive at (1.3.6) by dividing both sides of (1.3.10) by $|Ru - u|_{1,\Omega}$. (In the trivial event that $Ru = u$, (1.3.6) is obvious anyway.)

1.4 SUPERCONVERGENCE ON QUADRILATERAL ELEMENTS

In this section we give the full statement and proof of Zlámal's result for the bilinear elements introduced above. We note first that the $O(h)$ global result (1.3.6) does not make direct use of the shape of the elements or of the way that the nodes are connected to each other (the "mesh topology"). In our example each "internal" node (i.e. not on $\partial\Omega$) is connected by single edges to exactly four other nodes; equivalently each internal node is enclosed by exactly four elements. This property is a simple observation here, but on an apparently reasonable partition of a general region Ω into elements which cannot all be rectangles, it need not hold and for some superconvergence results it must be stipulated. (See the preamble to Theorem 5.1 of Lesaint & Zlámal, 1979.) When we move on to consider triangular elements, the mesh topology will have a greater significance; however for this example we stick to the sufficient condition that the elements are rectangles.

We write each element in the form of a Cartesian product of intervals

$$A_k = (x_k - \delta x_k/2 , x_k + \delta x_k/2) \times (y_k - \delta y_k/2 , y_k + \delta y_k/2)$$

($k = 1,\ldots,k_{max}$) and let $G_k = (x_k , y_k)$ be the centroid of each A_k. Now, if u is quadratic on A_k then, owing to the geometry of the elements,

$$[\nabla(Iu - u)]_{G_k} = 0 \qquad (1.4.1)$$

(where $[\cdot]_Q$ stands for sampling a value at Q). For if $u \in \{1,x,y,xy\}$ then $Iu = u$ throughout A_k. Also, if $u = x^2$ on A_k then

$$Iu = 2xx_k - x_k^2 + \delta x_k^2/4 \quad ;$$

hence

$$[\nabla Iu]_{G_k} \quad = \quad (2x_k , 0)^T \quad = \quad [\nabla u]_{G_k} \quad .$$

Similarly (1.4.1) holds if $u = y^2$ on A_k . So it holds for a basis of quadratics and thus for all quadratics (since $[\nabla(I - 1)\cdot]$ is a linear operator). Following the intuitive argument of the last section, we therefore hope that

$$| \, [\nabla(Ru - u)]_{G_k} \, | \quad = \quad O(h^2) \quad ,$$

$k = 1,\ldots,k_{max}$. (Note that (1.3.7) must be strengthened, even if only to guarantee that ∇u can be sampled at the points G_k .)

We now state the precise result. Let Ω be partitioned into rectangles, as above except that, for convenience, (1.3.3) is modified thus:

$$\left.\begin{aligned} & max_k \{ \delta x_k , \delta y_k \} = h \\ \text{and} \quad & min_k \{ \delta x_k , \delta y_k \} = ch \quad (c > 0) \quad . \end{aligned}\right\} \quad (1.4.2)$$

Let

$$u \quad \in \quad H_E^1(\Omega) \quad \cap \quad H^3(\Omega) \qquad (1.4.3)$$

and $Ru \in S_E$ satisfy (1.3.2) and (1.3.5) respectively.

Theorem 1.4 Under the above conditions,

$$h \left[\sum_k \left| \, [\nabla(Ru - u)]_{G_k} \, \right|^2 \right]^{1/2}$$
$$\leq \quad ch^2 \, |u|_{3,\Omega} \quad . \qquad (1.4.4)$$

Proof We follow the outline suggested by Table 1.3; our first task is to show that $|\nabla(I - R)u|$ is $O(h^2)$. We define the functionals

$$F_{k,\phi}(u) \quad = \quad (\nabla(Iu - u) , \nabla\phi)_{A_k} \quad , \qquad \phi \in S.$$

(These differ from the previous F_k only in the restriction on ϕ; the following derivation of (1.4.6) is similar to the proof of (1.3.6) above.) From (1.3.9) we have

$$|F_{k,\phi}(u)| \quad \leq \quad ch^{-1} \, ||u||_{3,A_k} \, |\phi|_{1,A_k} \quad . \qquad (1.4.5)$$

Also, $F_{k,\phi}$ vanishes if u is quadratic on A_k . As in the

demonstration of (1.4.1), we need only show that this holds when $u = x^2$. Let ϕ have the general form (1.3.4) on A_k. Then

$$\begin{aligned} F_{k,\phi}(x^2) &= (\nabla(2xx_k - x_k^2 + \delta x_k^2/4 - x^2) , \\ &\qquad \nabla(\alpha_1 + \alpha_2 x + \alpha_3 y + \alpha_4 xy))_{A_k} \\ &= 2 \left[\int_{x_k - \delta x_k/2}^{x_k + \delta x_k/2} (x_k - x)\, dx \right] \\ &\qquad \cdot \left[\int (\alpha_2 + \alpha_4 y)\, dy \right] \\ &= 0 \quad . \end{aligned}$$

So by (1.4.5) and B.H.,

$$|F_{k,\phi}(u)| \leq ch^2 |u|_{3,A_k} |\phi|_{1,A_k} .$$

Let us take $\phi = (I - R)u$ ($\in S$). Then by (1.3.2), (1.3.5) and Cauchy-Schwarz,

$$\begin{aligned} & |(I - R)u|_{1,\Omega}^2 \\ &= (\nabla(Iu - u) , \nabla\phi)_{1,\Omega} \\ &= \Sigma_k F_{k,\phi}(u) \\ &\leq ch^2 \Sigma_k |u|_{3,A_k} |\phi|_{1,A_k} \\ &\leq ch^2 |u|_{3,\Omega} |(I - R)u|_{1,\Omega} ; \end{aligned}$$

therefore

$$|(I - R)u|_{1,\Omega} \leq ch^2 |u|_{3,\Omega} . \qquad (1.4.6)$$

(Incidentally, one direct consequence of (1.4.6) is that the Finite Element solution is exact at the nodes - i.e. $Iu = Ru$ throughout Ω - for all quadratic u.) Now, in addition, for any $\phi \in S$ and any point $Q \in A_k$,

$$\begin{aligned} | [\nabla\phi]_Q | &\leq \max_{A_k} |\nabla\phi| \\ &\leq c |\phi|_{1,A_k} / (\text{meas } A_k)^{1/2} . \end{aligned}$$

So by (1.4.2) and (1.4.6),

$$\begin{aligned} & h \left[\Sigma_k \left| [\nabla(I - R)u]_{G_k} \right|^2 \right]^{1/2} \\ &\leq ch \left[\Sigma_k |(I - R)u|_{1,A_k}^2 / (\text{meas } A_k) \right]^{1/2} \end{aligned}$$

$$\leq \quad c\ |(I - R)u|_{1,\Omega}$$

$$\leq \quad ch^2\ |u|_{3,\Omega} \quad ; \qquad (1.4.7)$$

this completes the first stage of the proof.

For the second, we define a new set of functionals (or, to be precise, functional pairs):

$$F_k(u) \quad = \quad [\nabla(Iu - u)]_{G_k} \quad .$$

We have already shown – (1.4.1) – that these vanish when u is quadratic. But by S.E.,

$$|F_k(u)| \quad \leq \quad c\ (\ h^{-1}\ ||u||_{L_\infty(A_k)} \ + \ |u|_{1,\infty,A_k}\ )$$

$$\leq \quad ch^{-2}\ ||u||_{3,A_k} \quad .$$

So by B.H. we have

$$|F_k(u)| \quad \leq \quad ch\ |u|_{3,A_k}$$

whence

$$h\ \left[\ \Sigma_k\ \left|\ [\nabla(Iu - u)]_{G_k}\ \right|^2\ \right]^{1/2}$$

$$= \quad h\ \left[\ \Sigma_k\ |F_k(u)|^2\ \right]^{1/2}$$

$$\leq \quad ch^2\ |u|_{3,\Omega} \quad . \qquad (1.4.8)$$

Finally, we obtain (1.4.4) by squaring (1.4.7) and (1.4.8), applying "$(a + b)^2 \leq 2(a^2 + b^2)$" to each term and summing over k. ###

We remark that the result (1.4.4) is a bound on the ℓ_2 (i.e. root-mean-square) average error over the stress points G_k. This average is necessary to the proof if we are to derive (1.4.7) above – or any other bound on $|\nabla(I - R)u|$ – from the Galerkin equations (1.3.5) in a reasonably straightforward manner. An alternative approach, which involves Finite Element approximations to a Green's function, delivers a pointwise result; this will be the subject of Chapter 5. Incidentally, Zlámal's first results (1977) bounded the ℓ_1 average error. They

can be obtained from (1.4.4) by a simple application of the Cauchy-Schwarz inequality and (1.4.2).

1.5 SUPERCONVERGENCE ON TRIANGULAR ELEMENTS

It has been suggested (e.g. Moan, 1974) that the Galerkin least-squares approximation to gradients - i.e. (1.3.5) - is "almost local" and can therefore be analysed in one element in complete isolation from all others. Now, any non-local behaviour of a Finite Element approximation is entirely due to the inter-element continuity restriction in the definition of the approximation space S. (Indeed if this continuity were removed, $dim\ (S)$ would be increased by a factor of approximately four for bilinear elements and six for linear triangular elements.) Furthermore, it is only because $\phi \in S$ is continuous that an immediate consequence of (1.3.2) and (1.3.5) is

$$(\nabla Ru\ ,\ \nabla\phi\ )_\Omega \quad = \quad (\nabla u\ ,\ \nabla\phi\ )_\Omega \quad . \qquad (1.5.1)$$

If Ru and ϕ are assumed to behave as if S is not a space of continuous functions (so that the support of ϕ could be a single element) and if (1.5.1) is assumed nevertheless to hold, then it is indeed true that $|\nabla(Ru - u)| = O(h^2)$ at the centroid of each element. But neither of these assumptions is justified and the success on quadrilateral elements of their combination is entirely fortuitous. It does not work for triangles. In fact, stress points in the sense of Section 1.3 do not exist at all on these elements. We will pursue this line further in Chapter 3; for the time being we restrict ourselves to a very simple example of the sense in which stress points do exist.

As before let Ω be a rectangle with sides parallel to the

coordinate axes, partitioned this time into identical rectangles of dimension $\delta x \times \delta y$ such that

$$\left.\begin{aligned} \max\{\delta x, \delta y\} &= h, \\ \min\{\delta x, \delta y\} &= ch \quad (c > 0) \end{aligned}\right\} \quad (1.5.2)$$

and thence into triangular elements T_k, $k = 1,\ldots,K$ by means of a diagonal of positive slope in each rectangle. We redefine $S \in H^1(\Omega)$ now to be the space of continuous functions which are linear in each triangle, i.e. piecewise of the form

$$\alpha_1 + \alpha_2 x + \alpha_3 y .$$

We will employ later a grouping of the triangles T_k into triangle pairs with common edges parallel to the x-axis, denoting the resulting parallelograms by A_k, $k = 1,\ldots,K_A$. There will be a number of single triangles, whose edges parallel to the x-axis lie on $\partial\Omega$ and for which this pairing is therefore not possible; we denote these elements by B_k, $k = 1,\ldots,K_B$. So (see Figure 1.5.1),

$$\Omega = \bigcup^{K} T_k = \left(\bigcup^{K_A} A_k\right) \cup \left(\bigcup^{K_A} B_k\right) .$$

Note that the centroid of each pair A_k is the midpoint,

$$M_k = (x_k + \delta x/2, y_k) \quad (1.5.3)$$

say, of an elements edge. We call the two triangles which share that edge $T_{k\pm}$:

$$A_k = T_{k+} \cup T_{k-}, \quad k = 1,\ldots,K_A ;$$

$$T_{k\pm} = A_k \cap \{(x,y): \pm(y - y_k) > 0\} .$$

(See Figure 1.5.2.)

Now, "exceptional points for one stress component need not be exceptional for the others. The midpoints of an edge seem ... to be exceptional for derivatives along the edge but not for stresses in the direction of the normal." (Strang & Fix, 1973, page 169.)

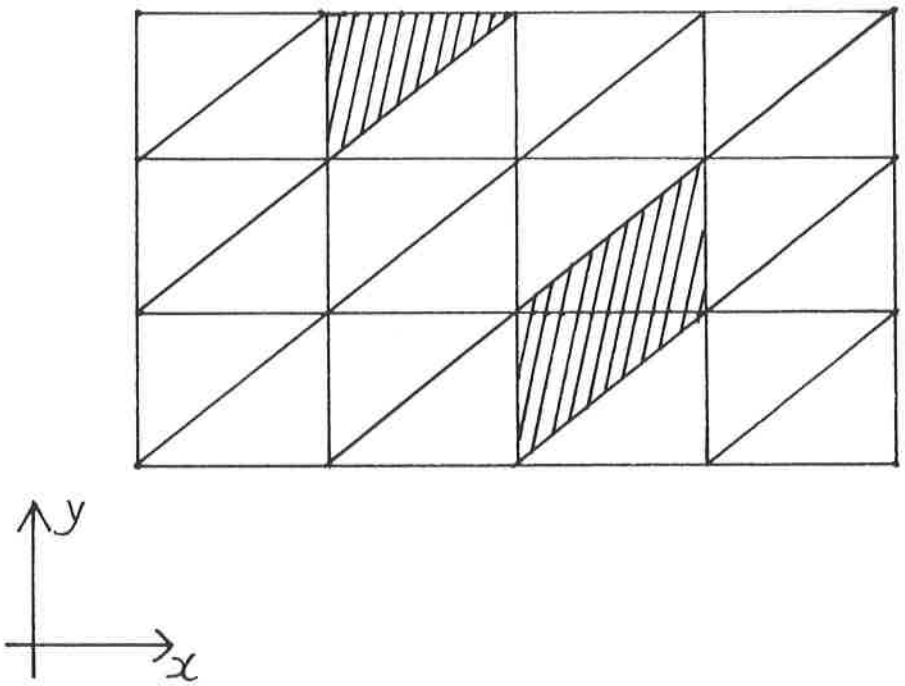

Figure 1.5.1

Grouping of elements

In this example $K_A = K_B = 8$. One of each of the triangle pairs A_k and the boundary elements B_k is shaded.

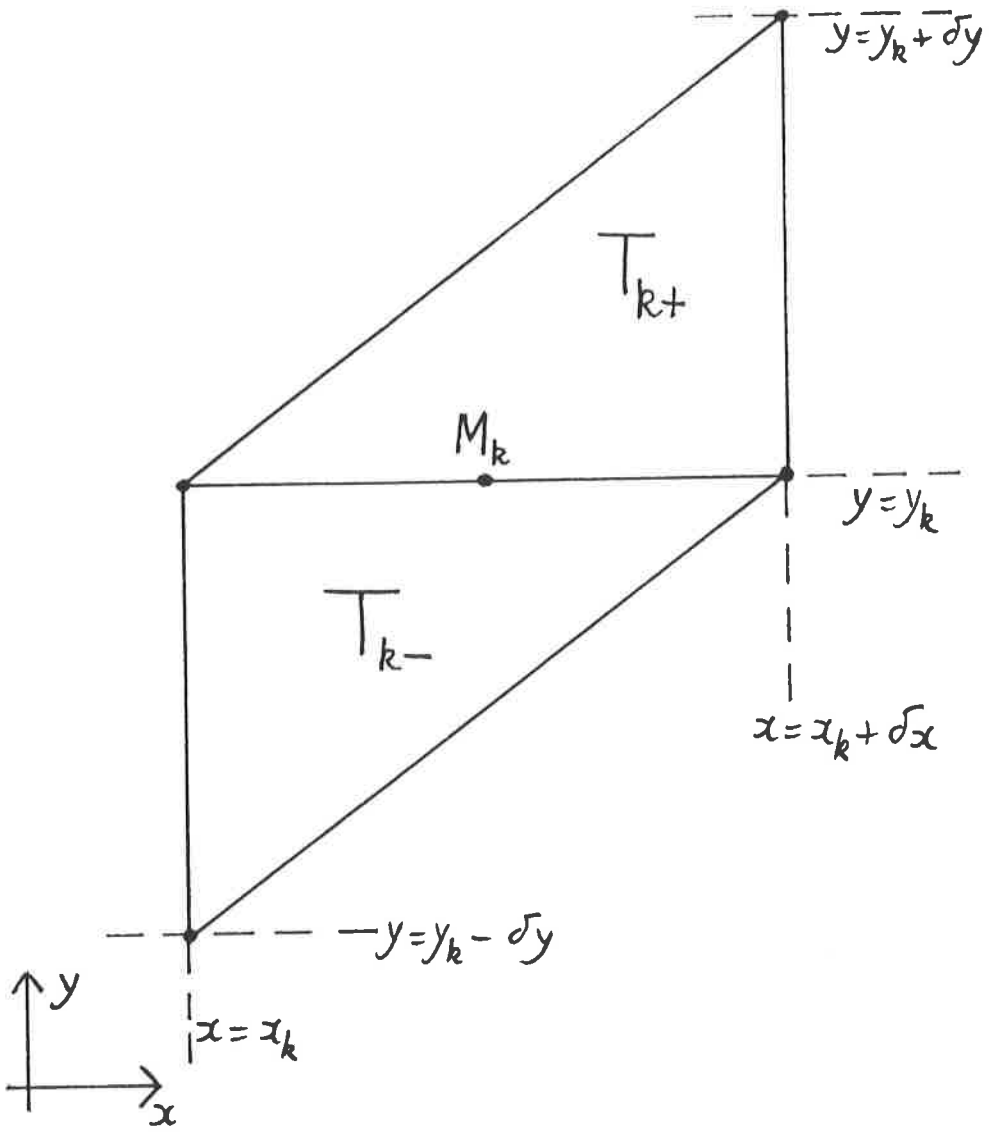

Figure 1.5.2

A triangle pair (A_k)

triangles analagous to Theorem 1.4. We note first the role of uniformity in the triangulation of Ω. The superconvergence result on quadrilaterals was derived by considering error contributions from each element in isolation. However, on triangles it is necessary to allow error terms to cancel between neighbouring elements (this is linked to Moan's mistake and the non-existence of stress points for the full gradient). The simplest way to achieve this is to require that the union of any two elements, which share a common edge, be a parallelogram (e.g., the A_k). Under this condition all the diagonals must have the same slope and, incidentally, each internal node is enclosed by exactly six elements. (See Chapter 2 for more general triangulations.)

Let u be a function known to satisfy (1.4.3) and (1.3.2). (For numerical evidence of the necessity of the smoothness condition (1.4.3), see Levine, 1982.) We define the subsets S_E and S_O of S as before and the Finite Element approximation $Ru \in S$ to u by the Galerkin equations (1.3.5). We claim that the M_k are x-derivative stress points:

Theorem 1.5 Under the above conditions,

$$h \left[\sum_{k=1}^{K_A} \left[\frac{\partial}{\partial x}(Ru - u) \right]^2_{M_k} \right]^{1/2} \leq ch^2 \, |u|_{3,\Omega} \, . \quad (1.5.6)$$

Proof We follow, in outline, the proof of Theorem 1.4, considering first the x-derivative term in

$$\begin{aligned} & |(I - R)u|^2_{1,\Omega} \\ &= \left(\nabla(Iu - u) \, , \, \nabla\phi \right)_\Omega \\ &= \left[\frac{\partial}{\partial x}(Iu - u) \, , \, \frac{\partial \phi}{\partial x} \right]_\Omega \\ &\quad + \left[\frac{\partial}{\partial y}(Iu - u) \, , \, \frac{\partial \phi}{\partial y} \right]_\Omega \, , \end{aligned} \quad (1.5.7)$$

where as before ϕ is taken to represent the function $(I - R)u \in S_O$. We observe first that if u is quadratic on A_k then, by (1.5.5), $\partial(Iu - u)/\partial x$ is linear there - and in particular

Indeed, suppose that (working with the piecewise linear elements introduced above) we define the functionals

$$F_k(u) = \left[\frac{\partial}{\partial x}(Iu - u) \right]_{M_k} , \quad k = 1,\ldots,K_A ,$$

where again $Iu \in S$ interpolates the nodal values of u. Then $F_k(u)$ vanishes when u is quadratic on A_k. For if u is linear then $Iu = u$ throughout A_k; therefore similarly to Section 1.4 it is sufficient to show that $F_k(u) = 0$ when $u \in \{x^2, xy, y^2\}$. But (recall Figure 1.5.2)

$$\text{if } u = x^2 \text{ in } A_k \text{ then } Iu = 2(x_k + \delta x/2)x - (x_k + \delta x)x_k \quad \text{in } A_k ;$$

$$\text{if } u = xy \text{ in } A_k \text{ then } Iu = xy_k + (x_k + \delta x/2 \pm \delta x/2) \cdot (y - y_k) \quad \text{in } T_{k\pm} ;$$

$$\text{if } u = y^2 \text{ in } A_k \text{ then } Iu = 2(y_k \pm \delta y/2)y - (y_k \pm \delta y)y_k \quad \text{in } T_{k\pm} .$$

So when $u = x^2$, xy or y^2 on A_k,

$$\left[\frac{\partial Iu}{\partial x} \right]_{A_k} = 2x_k + \delta x,\ y_k \text{ or } 0 \qquad (1.5.4)$$

respectively; note that it takes the same value in both T_{k+} and T_{k-}. In fact it is a key property of the space S of piecewise linears, as well as our motivation for considering the pairings A_k, that

$$\left[\frac{\partial \phi}{\partial x} \right]_{A_k} = \textit{constant over } A_k \qquad (1.5.5)$$

for all $\phi \in S$. Anyway, when $u = x^2$, xy or y^2, $\partial u/\partial x = 2x$, y or 0 respectively and so by (1.5.3) and (1.5.4) $F_k(u) = 0$. Hence $F_k(u)$ does indeed vanish for all quadratic u.

Therefore, if by "stress point" we mean, "a point on an element edge where the component of gradient tangential to that edge can be sampled to high accuracy," then according to the intuitive approach of Section 1.3, the midpoints M_k are indeed stress points. With this in mind, we construct below a result on

continuous - and so for the functionals F_k defined above,

$$\iint_{A_k} \frac{\partial}{\partial x}(Iu - u) \quad = \quad (meas\ A_k)\ F_k(u) \quad = \quad 0 \quad .$$

Now by (1.5.5), (1.5.2) and S.E.

$$\left| \left[\frac{\partial}{\partial x}(Iu - u) \ , \ \frac{\partial \phi}{\partial x} \right]_{A_k} \right|$$

$$= \quad \left| \iint_{A_k} \frac{\partial}{\partial x}(Iu - u) \right| \quad \left| \left[\frac{\partial \phi}{\partial x} \right]_{A_k} \right|$$

$$\leq \quad c\ ||u||_{3,A_k} \quad ch^{-1}\ |\phi|_{1,A_k} \ ;$$

therefore by B.H.

$$\left| \left[\frac{\partial}{\partial x}(Iu - u) \ , \ \frac{\partial \phi}{\partial x} \right]_{A_k} \right|$$

$$\leq \quad ch^2\ |u|_{3,A_k} \quad |\phi|_{1,A_k} \ . \qquad (1.5.8)$$

Also, $\phi \in S_0$ implies that

$$\left[\frac{\partial \phi}{\partial x} \right]_{B_k} \quad = \quad 0 \ , \quad k = 1,\ldots,K_B \ ;$$

from this, (1.5.8) and Cauchy-Schwarz we have

$$\left| \left[\frac{\partial}{\partial x}(Iu - u) \ , \ \frac{\partial \phi}{\partial x} \right]_{\Omega} \right|$$

$$\leq \quad \Sigma^{K_A} \left| \left[\frac{\partial}{\partial x}(Iu - u) \ , \ \frac{\partial \phi}{\partial x} \right]_{A_k} \right|$$

$$\leq \quad ch^2\ |u|_{3,\Omega} \quad |\phi|_{1,\Omega} \ .$$

(This intermediate result was also obtained - albeit with some difficulty - by Oganesjan & Ruchovec, 1969, but without the application to superconvergence.) Returning to (1.5.7), the y-derivative term is bounded similarly; we can now apply the method used to derive (1.4.6) and (1.4.7) to obtain

$$h \left[\Sigma^{K_A} \left[\frac{\partial}{\partial x}(I - R)u \right]^2_{M_k} \right]^{1/2} \quad \leq \quad ch^2\ |u|_{3,\Omega} \ . \qquad (1.5.9)$$

(Note again that $Iu = Ru$ throughout Ω when u is quadratic.) Finally, since $F_k(u)$ vanishes for quadratic u, S.E., B.H. and Cauchy-Schwarz imply

$$h \left[\Sigma^{K_A} \left[\frac{\partial}{\partial x}(Iu - u) \right]^2_{M_k} \right]^{1/2} \quad = \quad h \left[\Sigma^{K_A} F_k(u)^2 \right]^{1/2}$$

$$\leq \quad ch^2\ |u|_{3,\Omega} \ . \qquad (1.5.10)$$

The superconvergence result (1.5.6) now follows from (1.5.9) and

(1.5.10) as in the previous theorem. ###

Although we have bounded derivatives only on internal element edges parallel to the x-axis, we note that all edges can be included in the average; in particular (1.5.9) does not depend on the choice of sampling points.

1.6 NUMERICAL EVIDENCE

In the end, our interest lies not in unknown constants and asymptotic convergence rates as $h \to 0$ but in actual values of gradient errors when the mesh is computationally realistic or even rather coarse (e.g. less than a hundred nodes). We have shown (Levine, 1982) that theoretically optimal or near-optimal error bounds are difficult to obtain and tend to overestimate superconvergence errors to a significant extent: by a factor of h, for example. So, no matter how many theorems we prove about superconvergence algorithms, the final test is to try them out.

To construct our experimental estimates, we select a model function u on a given region Ω and set up a simple differential equation (Poisson's) of which u is the solution. We then approximate u by the Finite Element Method with various discretisation parameters h and examine the error with which ∇u is estimated from Ru. To be specific, we usually obtain Ru - via Poisson's equation - thus: $Ru \in S_E$ and

$$(\nabla Ru , \nabla \phi)_\Omega = (-\Delta u , \phi)^*_\Omega \qquad (1.6.1)$$

for all $\phi \in S_0$. The Laplacian Δu and the boundary values ($Ru = u_E$ at nodes on $\partial\Omega$) are obtained directly from the known function u. The inner product $(\cdot,\cdot)^*_\Omega$ denotes the use of the centroid rule in each element to approximate the integral $(\cdot,\cdot)_\Omega$; its effect,

which is neither asymptotically nor numerically significant, will be analysed in Chapter 4.

For example, let us compare our tangential derivative superconvergence bound on triangles (1.5.6) with Zlámal's $O(h^2)$ centroid result on quadrilaterals (1.4.4) and our $O(h)$ centroid sampling prediction on triangles. We denote these resulting errors (mean-square averaged over all possible sampling points) by E_{tgt}, E_{bilin} and E_{cent} respectively. Let us "define the unknown function" thus:

$$u = x\,(1-x)\,y\,(1-y)\,(1+2x+7y) \qquad (1.6.2)$$

on the unit square $\Omega = (0,1)^2$. We partition Ω into h^{-2} squares of side h and thence into $2h^{-2}$ triangles via diagonals of slope $+1$. Taking successively $h = 1/4,\ 1/6,\ 1/8,\ 1/10$, we calculate Ru from the equations (1.6.1); the errors E_{tgt}, E_{bilin} and E_{cent} are displayed in Table 1.6. (The calculations on bilinear elements are taken from Lesaint & Zlámal, 1979.)

An adequate summary of these figures is given by the asymptotic rates:

$$E_{tgt} \simeq 1.4h^2\ ,$$

$$E_{bilin} \simeq 0.9h^2$$

and $$E_{cent} \simeq 1.2h\ .$$

(We have found that errors are often within 10% - and frequently 5% or better - of asymptotic rates for $h \leq 1/8$; in almost every case this accuracy is sufficient for our purposes and we give these rates only, avoiding columns of unprocessed figures.) So, for this choice of u, Ω and method of partition, the order-of-h predictions in Sections 1.4 and 1.5 are confirmed. We also have a definite counter-example of the claim that $E_{cent} = O(h^2)$ and a strong indication that the constants c in the statements of

h	E_{tgt} $\times 10^2$	E_{bilin} $\times 10^2$	E_{cent} $\times 10^2$	E_{tgt} $\times h^{-2}$	E_{bilin} $\times h^{-2}$	E_{cent} $\times h^{-1}$
$\frac{1}{4}$	8.08	5.5	28.5	1.29	0.87	1.14
$\frac{1}{6}$	3.76	2.5	19.3	1.35	0.90	1.16
$\frac{1}{8}$	2.15	1.4	14.6	1.37	0.90	1.16
$\frac{1}{10}$	1.38	0.91	11.7	1.38	0.91	1.17

Table 1.6

Computed errors of various methods for estimating the gradient, with diminishing parameter h. The "unknown" u is given by (1.6.2).

Theorems 1.4 and 1.5 are reasonably small (because E_{tgt} and E_{bilin} are much smaller than E_{cent} even for the coarsest discretisation). Indeed, we can think of the above asymptotic value of $E_{tgt}h^{-2}$ (i.e. 1.4) as a rough yardstick against which to compare the results of other numerical experiments. Finally, it may be the case generally (but we would not regard the evidence as strong) that E_{bilin} is naturally smaller than E_{tgt} .

1.7 OVERVIEW

In summary: an unknown function satisfies Poisson's equation on a rectangle. We partition this rectangle into uniform elements in a prescribed manner and approximate the unknown via the Ritz projection. We do not permit numerical quadrature. We sample prescribed components of the approximation's gradient, at prescribed locations. Finally, we take a somewhat unpleasant global average of the error in these derivatives... This is the picture of superconvergence presented so far. Looked at one way it is a solution to the problem posed in Section 1.1: for it is a procedure "for obtaining gradients to the same degree of accuracy as the function values". Looked at another way, it is too special, too rigid, to be of any direct practical worth. We regard it therefore as the foundation stone of our work.

When we come to build upon this, one simple feature will be seen to appear again and again in our constructions: if the underlying unknown function (u) is quadratic, then key local functionals vanish completely. Later, when we introduce various perturbations to the result - such as curvature of the mesh - these key functionals will still occur in some (perturbed) form

and still vanish when the underlying function is quadratic. The general approach is as follows. Consider a functional which vanishes, in the absence of any perturbations, for all quadratic u. We express this as the sum of a related functional which is guaranteed to vanish when u is quadratic (perturbations or no) plus one or more perturbation functionals, which do not necessarilly vanish for quadratic u but are of high order anyway. It is the message of Chapter 4 that this approach works for our purposes: in that chapter we will prove our most general result with full rigour.

Before this we answer the more practical questions. We need a procedure for generating a triangulation conducive to superconvergence on a general domain and for recovering, from the Finite Element approximation on such a triangulation, a good estimate to the unknown gradient at any point. These "algorithms" will be the subjects of Chapters 2 and 3 respectively. At these stages we will be concerned mainly with practical choices; analysis will be kept to a minimum and in some places postponed. We will rely heavily on a search for functionals which vanish - in the absence of perturbations - when u is quadratic, knowing that Chapter 4 will take care of the perturbed case. Also in Chapter 4, we will examine the roles of numerical quadrature (in a sense this is another perturbation) and the cumbersome requirement for global averaging. In the final chapter (Chapter 5) we introduce a completely different approach to the mathematics of superconvergence which bypasses the need to take that average. The new analysis is neither simple nor complete; we are left at the end with the choice between generality and full rigour.

The work is arranged into two parts. The first, comprising this and the next two chapters, is presented at what we hope is a simpler level then the second. (The exceptions are the proof of Theorem 2.4 and the whole of Sections 1.2 and 3.2: all of these could be omitted on a first reading.)

We mention here the work of two research groups which are currently active in the same field as us: Lin Qun et al (1983) and Křížek and Neittaanmäki (1984). The result of the former parallels Section 5.1 of this work; however key properties of the Green's function are quoted entirely without proof. The others' result is based directly on Oganesjan and Ruchovec (1969) and concerns a full self-adjoint problem. It gives mean-square superconvergence for a nodal recovery scheme (see Figure 3.3.8 below) but only in an interior subregion of Ω. We remark on one other particular constraint which we consider unrealistic: the external boundary $\partial\Omega$ must be three times continuously differentiable. Incidentally, both sets of authors confine their study to fully uniform meshes (as in Chapter 1 here).

In summary: an unknown function satisfies any strongly elliptic self-adjoint differential equation on any well-defined region with the strong cone property. We partition this region, carefully, with certain general properties in mind. We then approximate the unknown by the Finite Element Method, using low-order numerical quadratures. We follow simple rules to construct $\hat{\Gamma}$ weighted averages of the approximate gradient vector over small patches of elements. This class of local averages can be used to approximate the unknown's gradient (both components) at every point in the domain. There is strong evidence that the presence of a global average in the analysis can usually be ignored.

CHAPTER TWO

THE GENERATION OF SUPERCONVERGENT APPROXIMATIONS

2.1 SUPERCONVERGENT MESHES

In this chapter we will enlarge upon the first stage of the scheme for obtaining superconvergent gradients, which was given in Table 1.3: the construction of a Finite Element approximation conducive to superconvergence. The most important aspect of such a construction for us to cover - unless Ω is the rectangle of Section 1.5 - is the choice of triangulation algorithm. Indeed, since superconvergence results are generally robust in the face of variational misdemeanor and other perturbations, the other aspects of generalising the model problem (1.3.1) are comparatively simple and we can safely postpone them to Chapter 4. This chapter, then, is about the generation of triangulations such that the gradients of the resulting Finite Element approximations and interpolants are "close". We assume for the time being that (1.3.2), (1.3.5) and (1.4.3) hold.

Let us start with a resumé of Section 1.5: superconvergence when Ω is a rectangle. The method given for triangulating Ω is to partition it into rectangles of dimension $\delta x \times \delta y$ and thence into triangles with hypotenuses of slope $\delta y / \delta x$. We then take S to be the space of continuous functions which are linear in each element. We define the discretisation parameter h by (1.5.2) and show that the ℓ_2 average error of the tangential derivatives at stress points is $O(h^2)$. The proof (of Theorem 1.5) is summarised in Table 2.1; it is important to note that properties of the triangulation are involved only in the first three stages. So, given (1.5.2) or an equivalent condition, for any series of triangulations (parametised by h) on any region Ω, tangential derivative superconvergence is equivalent to the bound

(1) Use B.H. and the shape of A_k to bound

$$\left| \left[\frac{\partial}{\partial x}(Iu - u) \ , \ \frac{\partial \phi}{\partial x}\right]_{A_k} \right| \ , \quad 1 \leq k \leq K_A \ , \quad \phi \in S.$$

(2) Use $\phi \in S_0$, (1) and the decomposition of Ω into the A_k and B_k to bound

$$\left| \left[\frac{\partial}{\partial x}(Iu - u) \ , \ \frac{\partial \phi}{\partial x}\right]_{\Omega} \right| \ .$$

(3) Similarly, bound

$$\left| \left[\frac{\partial}{\partial y}(Iu - u) \ , \ \frac{\partial \phi}{\partial y}\right]_{\Omega} \right| \ .$$

(4) From (2) and (3) bound

$$| \ (\ \nabla(Iu - u) \ , \ \nabla\phi \ )_{\Omega} \ |$$

and hence

$$| \ (I - R)u \ |_{1,\Omega}.$$

Now use $meas \ (A_k) \geq ch^2$, $1 \leq k \leq K_A$ (from (1.5.2)) to bound

$$h \left[\ \sum^{K_A} \left[\frac{\partial}{\partial x}(I - R)u\right]^2_{M_k} \ \right]^{1/2} \ .$$

(5) Bound

$$\left| \left[\frac{\partial}{\partial x}(Iu - u)\right]_{M_k} \right| \ , \quad 1 \leq k \leq K_A.$$

(By (1.5.5) this works independently of the shape of the A_k.)

(6) Combine (4) and (5) to bound

$$h \left[\ \sum^{K_A} \left[\frac{\partial}{\partial x}(Ru - u)\right]^2_{M_k} \ \right]^{1/2} \ .$$

Table 2.1

Superconvergence proof for the uniformly triangulated rectangle

Given (1.5.2), the positions and interconnections of nodes directly affect only the first three stages, in which the integral $(\ \nabla(Iu - u) \ , \ \nabla\phi \ )_{\Omega}$ is bounded.

$$| (I - R) u |_{1,\Omega} \leq c[u]h^2. \qquad (2.1.1)$$

Now in an application, it is unlikely that the resources will be available to triangulate Ω, solve the Finite Element equations (1.3.5) and extract results for a series of values of the discretisation parameter h. So our aim is to generate a mesh for a single value of h for which $| (I - R) u |_{1,\Omega}$ is reasonably small. But to define this quality - via (2.1.1) - we must hypothesise the existence of a series of meshes, even if we do not actually generate them. Therefore we define a mesh to be "superconvergent" if it is a natural member of a series for which (2.1.1) holds.

For example, consider the series of triangulations on a unit square shown in Figure 2.1.1. Taken without mesh (a), the series is clearly such that (2.1.1) holds; therefore meshes (b),(c),(d),... are superconvergent. Now mesh (a) is by definition a formal member of the series, but it is not a natural one. If it is taken as the starting point for any natural series of refinements, (2.1.1) will not hold (see Section 2.4 below); therefore mesh (a) is not superconvergent.

We wish to generate superconvergent meshes on regions other than rectangles. For example, let Ω be a parallelogram and let us triangulate it as in Figure 2.1.2. We claim that this mesh is superconvergent. For it is still possible to decompose Ω into pairs A_k of triangles whose common edge is parallel to the x-axis (note that in this example there are no leftover triangles B_k) and the first two stages of the superconvergence proof (Table 2.1) proceed as usual. We then decompose Ω into triangle pairs with common edge parallel to the y-axis for stage three (this time there do exist leftover triangles on $\partial\Omega$); the rest of the proof is exactly as before.

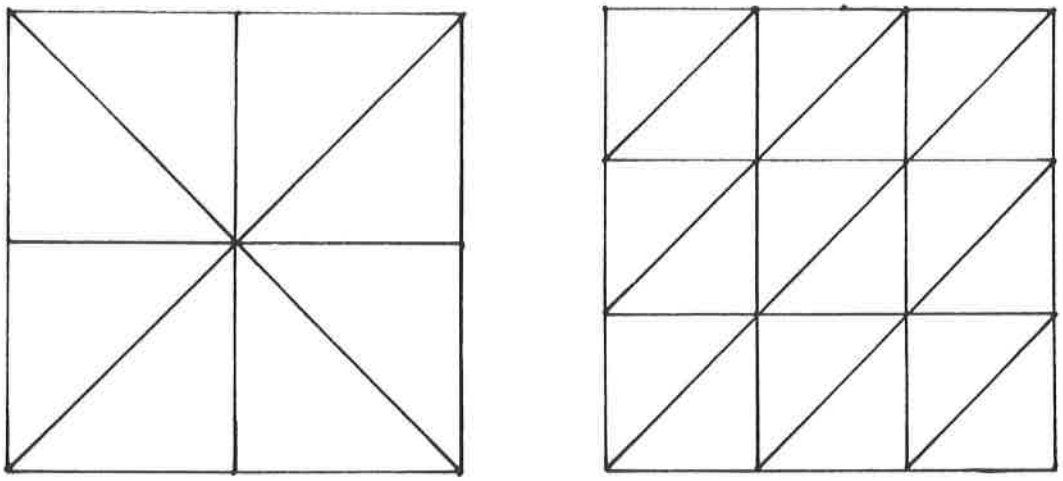

Figure 2.1.1

Series of triangulations of a unit square

All but the first mesh are superconvergent.

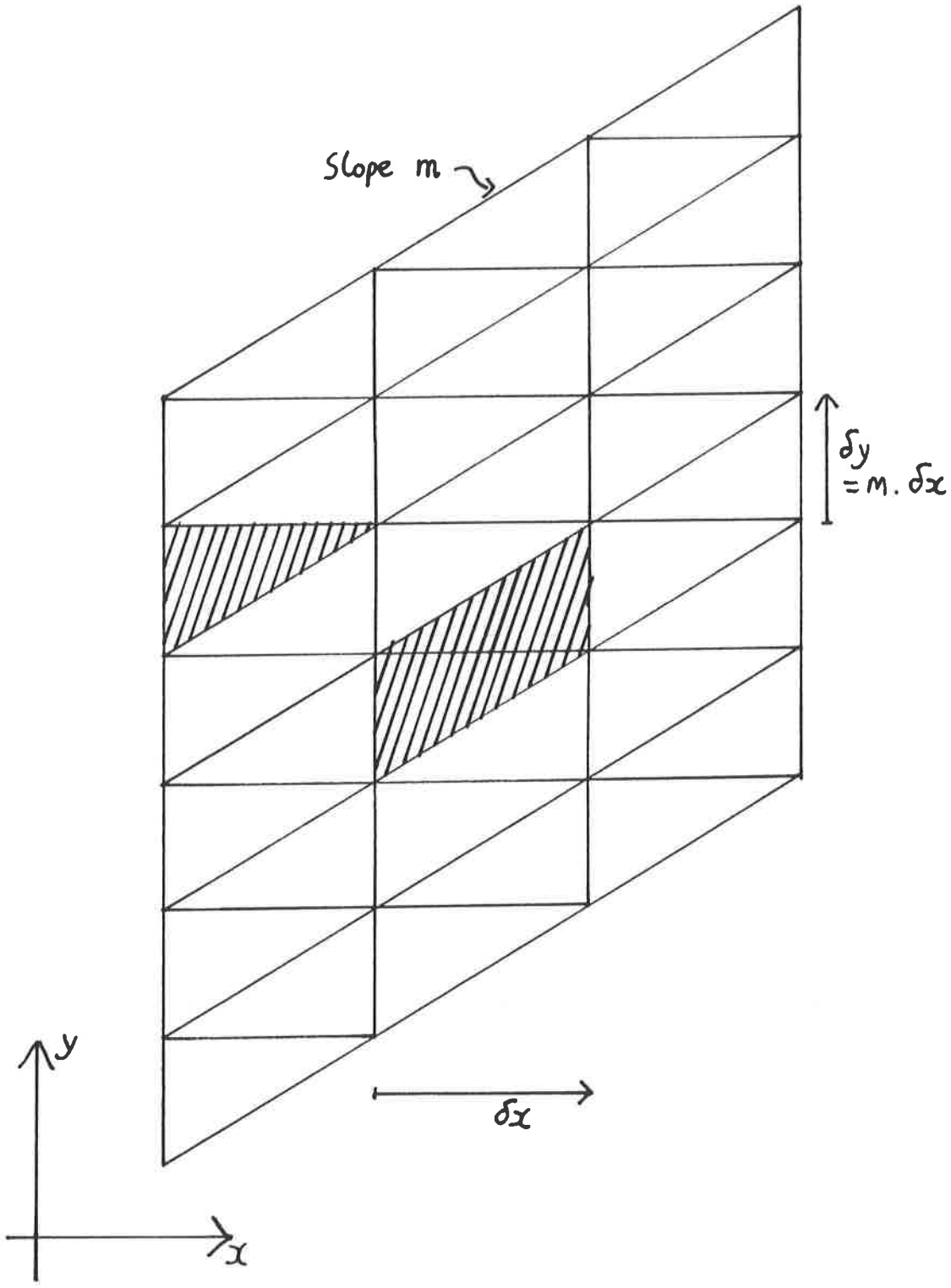

Figure 2.1.2

A superconvergent triangulation for a parallelogram

A triangle pair for stage (2), and a leftover boundary triangle for stage (3), of the proof summary in Table 2.1 are shaded.

So if Ω is a parallelogram, we can triangulate it as in Figure 2.1.2 and the resulting mesh will be superconvergent. But this scheme is not a good idea if $|m|$ is very small, because δy will also be very small and the number of nodes very large, without any useful refinement taking place ($h = \delta x$ remains constant). We give below a more general triangulation scheme for the parallelogram and show that it, too, leads to superconvergence.

2.2 DIRECTIONS AND DECOMPOSITIONS

Let Ω be the parallelogram considered above, triangulated now as in Figure 2.2.1. The difference is that the element edges now have slopes m, $m + \delta y/\delta x$ and ∞. So in general there are no element edges parallel to the x-axis and the decomposition of

$$(\nabla(Iu - u) , \nabla\phi)_{\Omega}$$

into x- and y-derivative terms no longer leads to superconvergence (see stages (2) and (3) of Table 2.1 and the discussion on (1.5.5)).

However this triangulation is superconvergent. To prove this we group the elements into pairs A_k with common edge of slope m. As before, there is a component of $\nabla\phi$ ($\phi \in S_0$) which is constant over each A_k:

$$\frac{\partial\phi}{\partial x} + m\frac{\partial\phi}{\partial y}$$

So we replace (1.5.7) with

$$\left.\begin{aligned} &(\nabla(Iu - u) , \nabla\phi)_{\Omega} \\ &= \left[\frac{\partial}{\partial x}(Iu - u) , \left[\frac{\partial}{\partial x} + m\frac{\partial}{\partial y}\right]\phi \right]_{\Omega} \\ &+ \left[\left[-m\frac{\partial}{\partial x} + \frac{\partial}{\partial y}\right](Iu - u) , \frac{\partial\phi}{\partial y} \right]_{\Omega} . \end{aligned}\right\} \quad (2.2.1)$$

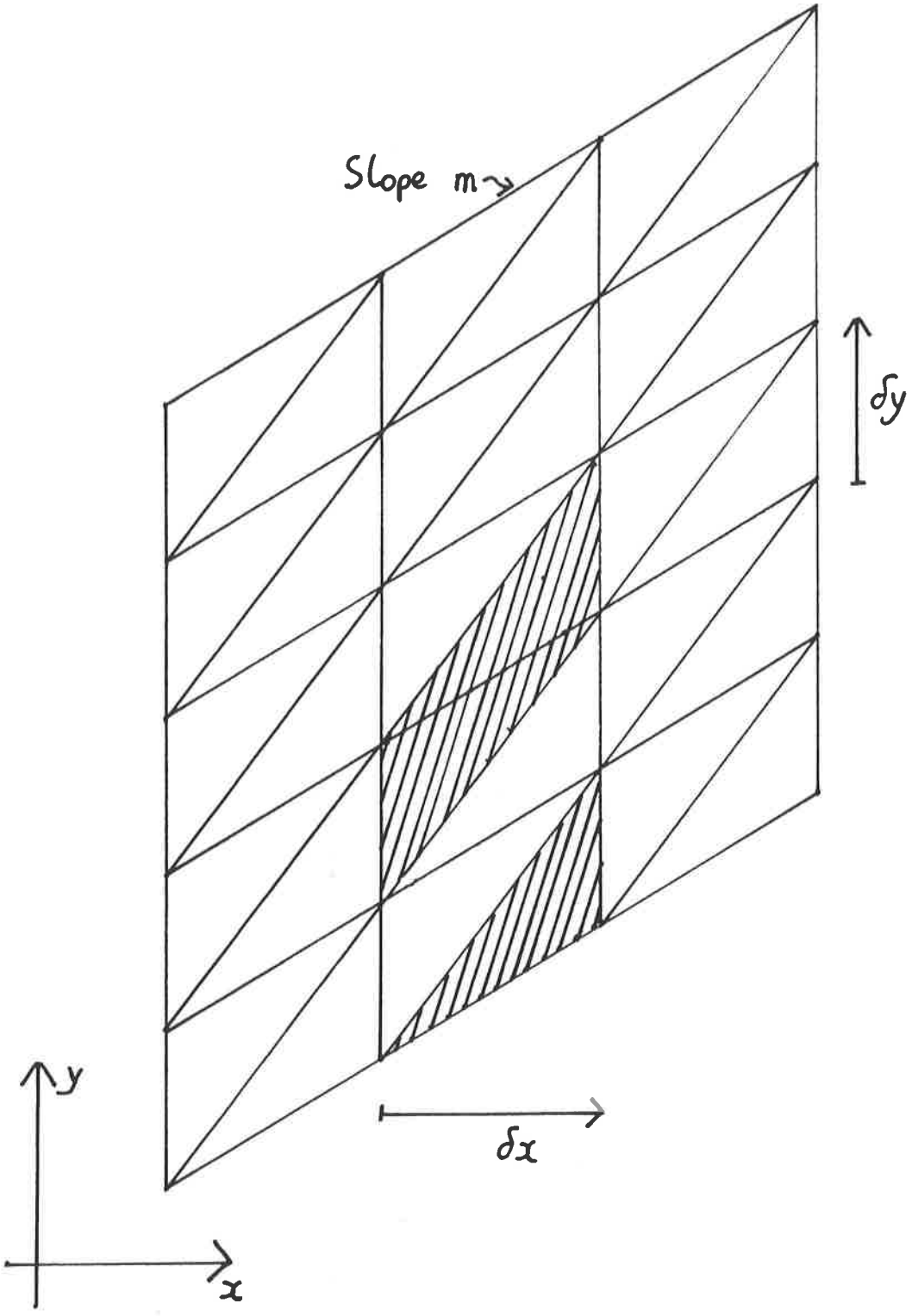

Figure 2.2.1

A modified superconvergent triangulation for the parallelogram

We no longer constrain $\delta y = m\delta x$. A triangle pair (A_k) and an unpaired triangle (B_k) on $\partial\Omega$ are shaded.

We write the first term as a sum of integrals over the A_k; note that there are zero contributions from a number of unpaired triangles B_k on the boundary segment of slope m (recall $\phi = 0$ on $\partial\Omega$). We follow the derivation of (1.5.8); we need therefore to show that

$$\iint_{A_k} \frac{\partial}{\partial x} (Iu - u) = 0$$

for all quadratic u. For the second term of (2.2.1) we regroup the elements into pairs with common edge parallel to the y-axis; the derivative of ϕ constant over each pair is now $\partial\phi/\partial y$. Again we must show that when u is quadratic the integral over such a pair of the appropriate component of ∇u (namely $\partial/\partial y - m\partial/\partial x$) vanishes. Therefore the following result is more than sufficient to prove that the triangulation of Ω is superconvergent.

Lemma 2.2 Let A be any parallelogram formed by two neighbouring elements in the triangulation of some region Ω, let u be quadratic on A and let $Iu \in S$ interpolate u there. Then

$$\iint_A \nabla(Iu - u) = 0. \qquad (2.2.2)$$

Proof For simplicity we let (ξ,η) be an affine transformation of (x,y) such that the ξ-axis coincides with the edge common to the two triangles and the nodes on this edge are at $(0,0)$ and $(1,0)$. We denote by $T_\pm$ the triangle in $\pm\eta>0$ and by $(\xi_\pm,\eta_\pm)$ the remaining node in $T_\pm$. (See Figure 2.2.2.) Because the transformation is affine and ∇u linear, (2.2.2) is equivalent to

$$\begin{aligned} F(u) &= meas(T_+)[\ \nabla(Iu - u)\ ]_{G_+} \\ &\quad + meas(T_-)[\ \nabla(Iu - u)\ ]_{G_-} \\ &= 0, \end{aligned} \qquad (2.2.3)$$

where $G_\pm$ are the centroids $(\ (1 + \xi_\pm)/3\ ,\ \eta_\pm/3\ )$ of $T_\pm$ and by ∇ we now mean $(\ \partial/\partial\xi\ ,\ \partial/\partial\eta\ )$.

Now,

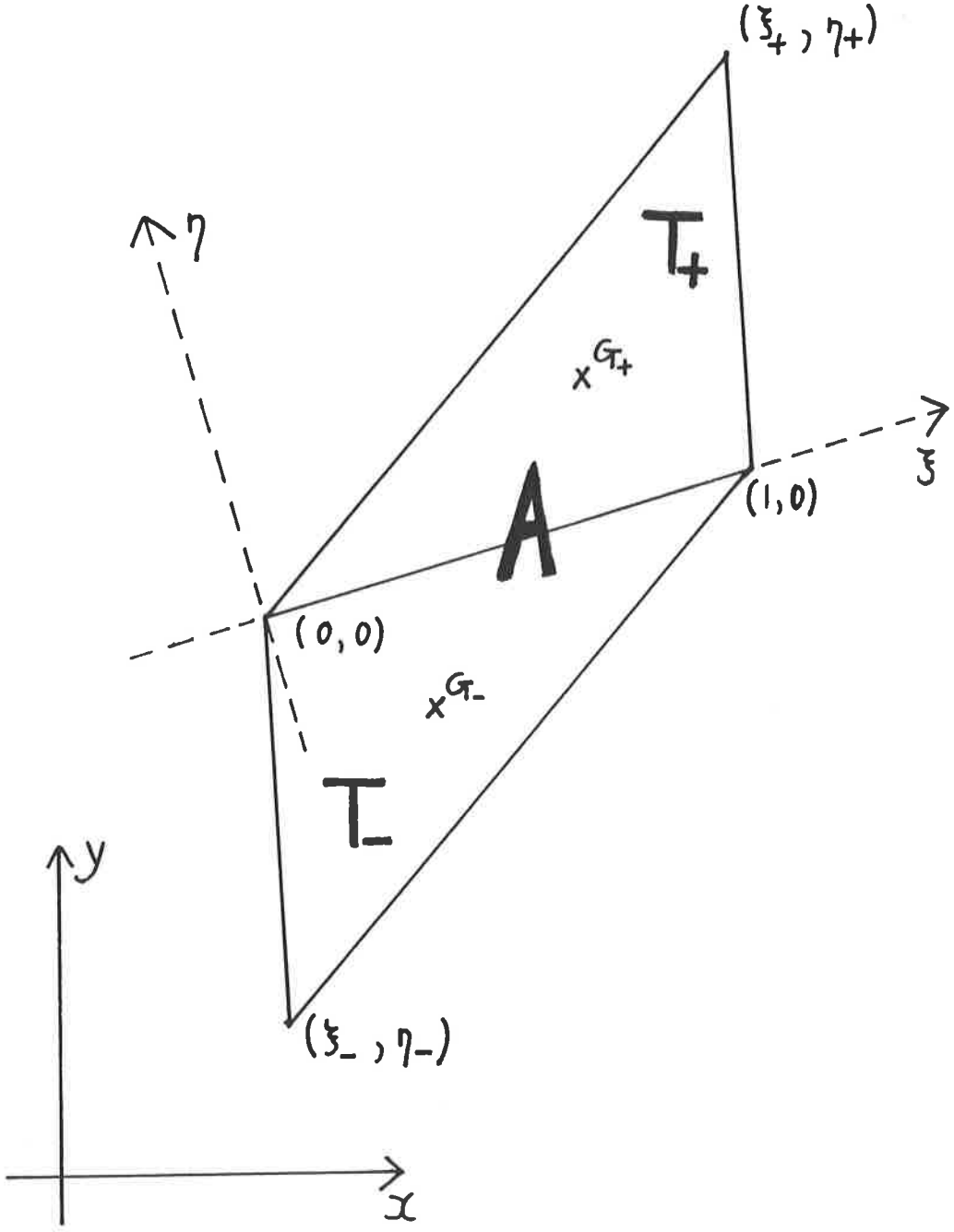

Figure 2.2.2

The local coordinate transformation

Note that A is a parallelogram and that in consequence its diagonals bisect each other.

if $u = \xi^2$ in A then $Iu = \xi + \eta(\xi_\pm^2 - \xi_\pm)/\eta_\pm$ in $T_\pm$;

if $u = \xi\eta$ in A then $Iu = \eta\xi_\pm$ in $T_\pm$;

if $u = \eta^2$ in A then $Iu = \eta\eta_\pm$ in $T_\pm$.

So

$$\left.\begin{aligned}
F(\xi^2) &= \frac{\eta_+}{2}\left[\begin{bmatrix} 1 \\ (\xi_+^2 - \xi_+)/\eta_+ \end{bmatrix} - \begin{bmatrix} (2 + 2\xi_+)/3 \\ 0 \end{bmatrix}\right] \\
&\quad - \frac{\eta_-}{2}\left[\begin{bmatrix} 1 \\ (\xi_-^2 - \xi_-)/\eta_- \end{bmatrix} - \begin{bmatrix} (2 + 2\xi_-)/3 \\ 0 \end{bmatrix}\right] \\
&= \begin{bmatrix} ((1 - 2\xi_+)\eta_+ - (1 - 2\xi_-)\eta_-)/6 \\ ((\xi_+ - 1)\xi_+ - (\xi_- - 1)\xi_-)/2 \end{bmatrix}; \\
F(\xi\eta) &= \frac{\eta_+}{2}\left[\begin{bmatrix} 0 \\ \xi_+ \end{bmatrix} - \begin{bmatrix} \eta_+/3 \\ (1 + \xi_+)/3 \end{bmatrix}\right] \\
&\quad - \frac{\eta_-}{2}\left[\begin{bmatrix} 0 \\ \xi_- \end{bmatrix} - \begin{bmatrix} \eta_-/3 \\ (1 + \xi_-)/3 \end{bmatrix}\right] \\
&= \begin{bmatrix} (-\eta_+^2 + \eta_-^2)/6 \\ ((2\xi_+ - 1)\eta_+ - (2\xi_- - 1)\eta_-)/6 \end{bmatrix}; \\
F(\eta^2) &= \frac{\eta_+}{2}\left[\begin{bmatrix} 0 \\ \eta_+ \end{bmatrix} - \begin{bmatrix} 0 \\ 2\eta_+/3 \end{bmatrix}\right] \\
&\quad - \frac{\eta_+}{2}\left[\begin{bmatrix} 0 \\ \eta_- \end{bmatrix} - \begin{bmatrix} 0 \\ 2\eta_-/3 \end{bmatrix}\right] \\
&= \begin{bmatrix} 0 \\ (\eta_+^2 - \eta_-^2)/6 \end{bmatrix}.
\end{aligned}\right\} \qquad (2.2.4)$$

As in Sections 1.4 and 1.5, if F vanishes for these three choices of u then (2.2.3) holds for all quadratic u. But A is a parallelogram and so its diagonals bisect each other:

$$\xi_+ + \xi_- = 1 \quad \text{and} \quad \eta_+ + \eta_- = 0. \qquad (2.2.5)$$

Therefore by (2.2.4) $F = 0$ when $u \in \{\xi^2, \xi\eta, \eta^2\}$ and the lemma is proved. ###

We have now shown that the triangulation of the parallelogram

Ω is indeed superconvergent, for any m. In particular, if

$$m = -1/\sqrt{3}, \quad \delta x = (\sqrt{3}/2)\delta y$$

then we have a superconvergent partition into equilateral triangles. If $m = 0$ then Ω is a rectangle, triangulated exactly as in Chapter 1; the superconvergence proof is essentially unchanged. On the other hand, if

$$m = -\delta y/\delta x$$

we have a triangulation related - or identical under the transformation $y \to -y$ - to that given in the last section but a different proof of superconvergence based on a different decomposition of $(\nabla(Iu - u) , \nabla\phi)_\Omega$ and a different pairing of elements.

In fact for all values of m there exist precisely three different ways of pairing elements, each corresponding to one of the three directions of triangle edges and each leading to a different proof of superconvergence. For, writing $s = \delta y/\delta x$, we have the three distinct decompositions

$$\left.\begin{aligned}
&(\nabla(Iu - u) , \nabla\phi)_\Omega \\
&= \left[\frac{\partial}{\partial x}(Iu - u) , \left[\frac{\partial}{\partial x} + m\frac{\partial}{\partial y}\right]\phi \right]_\Omega \\
&\quad + \left[\left[-m\frac{\partial}{\partial x} + \frac{\partial}{\partial y}\right](Iu - u) , \frac{\partial\phi}{\partial y} \right]_\Omega \qquad \text{(a)} \\
&= \left[\frac{\partial}{\partial x}(Iu - u) , \left[\frac{\partial}{\partial x} + (m + s)\frac{\partial}{\partial y}\right]\phi \right]_\Omega \\
&\quad + \left[\left[-(m + s)\frac{\partial}{\partial x} + \frac{\partial}{\partial y}\right](Iu - u) , \frac{\partial\phi}{\partial y} \right]_\Omega \qquad \text{(b)} \\
&= \left[\left[\left[\frac{m + s}{s}\right]\frac{\partial}{\partial x} - \frac{1}{s}\frac{\partial}{\partial y}\right](Iu - u) , \left[\frac{\partial}{\partial x} + m\frac{\partial}{\partial y}\right]\phi \right]_\Omega \\
&\quad + \left[\left[\frac{-m}{s}\frac{\partial}{\partial x} + \frac{1}{s}\frac{\partial}{\partial y}\right](Iu - u) , \left[\frac{\partial}{\partial x} + (m + s)\frac{\partial}{\partial y}\right]\phi \right]_\Omega . \qquad \text{(c)}
\end{aligned}\right\} \qquad (2.2.6)$$

Now, the components of $\nabla\phi$ constant across shared element edges with slopes m and ∞ are

$$\left[\frac{\partial}{\partial x} + m\frac{\partial}{\partial y}\right]\phi \quad \text{and} \quad \frac{\partial \phi}{\partial y}$$

respectively. Therefore with the first decomposition above (used before in (2.2.1)) triangles in the first set of pairings need common edges of slope m and those in the second need common edges of slope ∞. We say that the "primary directions" of this decomposition are m and ∞. There is of course a third direction for element edges (given by the slope $m + s$). We call this the "secondary direction" of the decomposition. The reason for making this distinction is that, although all three directions can in general be present as segments of the boundary $\partial\Omega$, the leftover triangles (B_k above) for which it is required that

$$\phi = 0 \text{ on } \partial\Omega \tag{2.2.7}$$

only appear on segments given by the primary directions.

For example, see Figure 2.2.3. There, the triangulation is based on the three directions D_1, D_2 and D_3. In (a), D_1 has been chosen as a primary direction for the superconvergence proof and the fourteen triangle pairings are shaded. There are four leftover triangles with edges on $\partial\Omega$. The segments of $\partial\Omega$ on which they lie are precisely those which have direction D_1; the boundary condition (2.2.7) must be taken up on these segments.

The other primary direction chosen for the proof is D_2. In (b) the twelve resulting pairings are shaded; for this stage of the superconvergence proof we require that $\phi = 0$ on all the segments of $\partial\Omega$ with direction D_2. D_3 is therefore the secondary direction of the triangulation (as far as this proof of superconvergence is concerned); $\phi = 0$ is not necessary on the segments of $\partial\Omega$ with direction D_3.

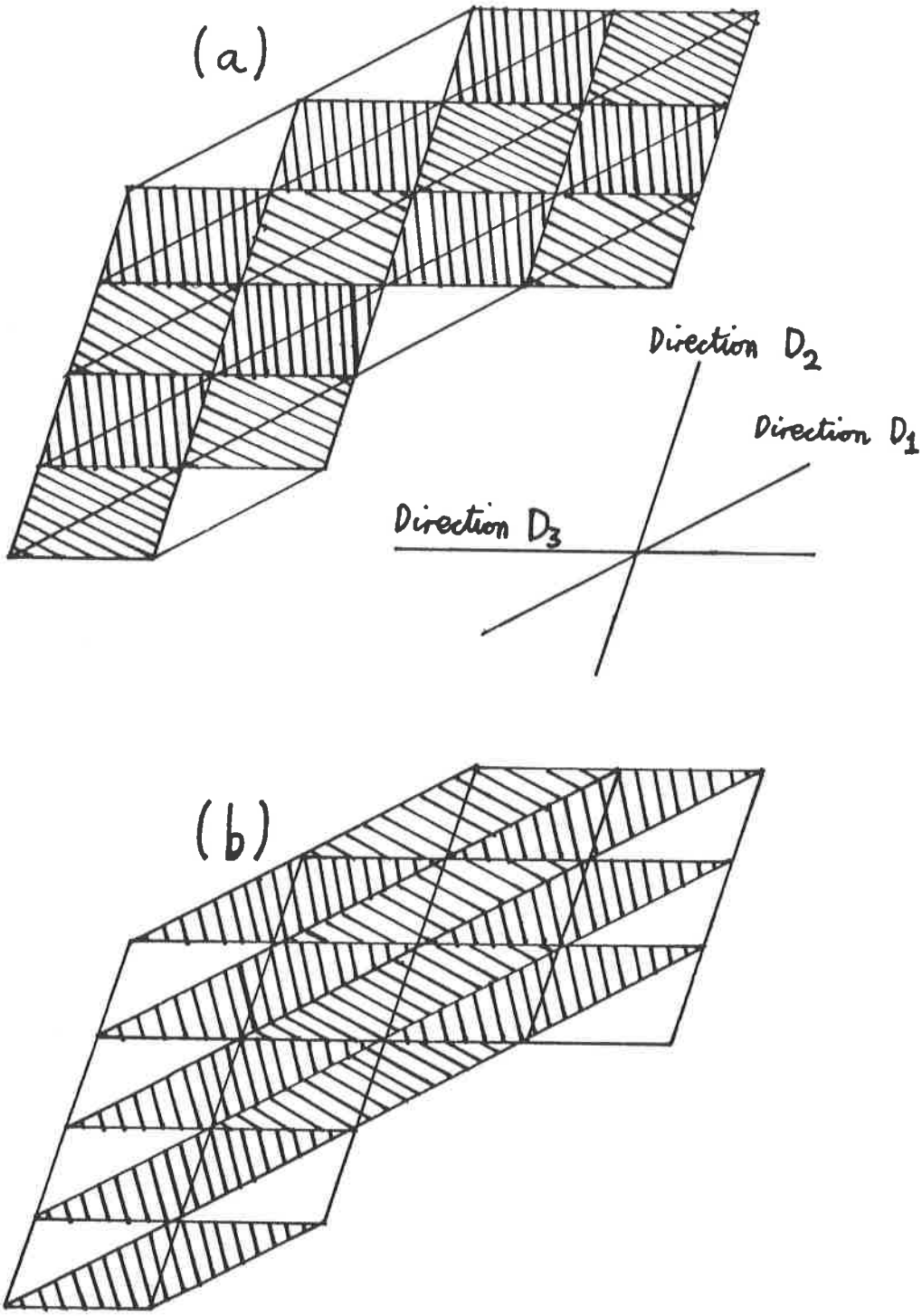

Figure 2.2.3

Primary and secondary directions of a uniform triangulation

Returning to (2.2.6), the primary directions for decomposition (b) (used in Section 2.1 with $m = -s$) are $m + s$ and ∞; therefore condition (2.2.7) is not exploited on any boundary segments of slope m (the secondary direction). Similarly for decomposition (c): the secondary direction now has slope ∞. (See Figure 2.2.4 for another example.)

We have now arrived at a more flexible approach to the superconvergence proof. We summarise it in Table 2.2 and move on to its applications in the next section.

2.3 TRIANGULATION BANDS

Let a polygonal region Ω be divided into subdomains by means of a number of parallel lines of direction D. We call these subdomains "bands"; they enable us to expand greatly the class of regions Ω for which there exist superconvergent triangulations. (See Figure 2.3.1 for an example.)

Theorem 2.3 Suppose there exists a partition of a banded region Ω into triangles which meet only in entire common sides or vertices such that

(i) each of the dividing lines between bands is made up of triangle sides, of direction D

and (ii) the triangulation of each band, when viewed as a problem domain in isolation from the rest of Ω, is uniform and superconvergent.

Then the triangulation of Ω is superconvergent.

Proof By (i), D must be a direction of the triangulation in each band; let it be secondary throughout. Then the condition $\phi = 0$ is not required on any of the dividing lines which separate the

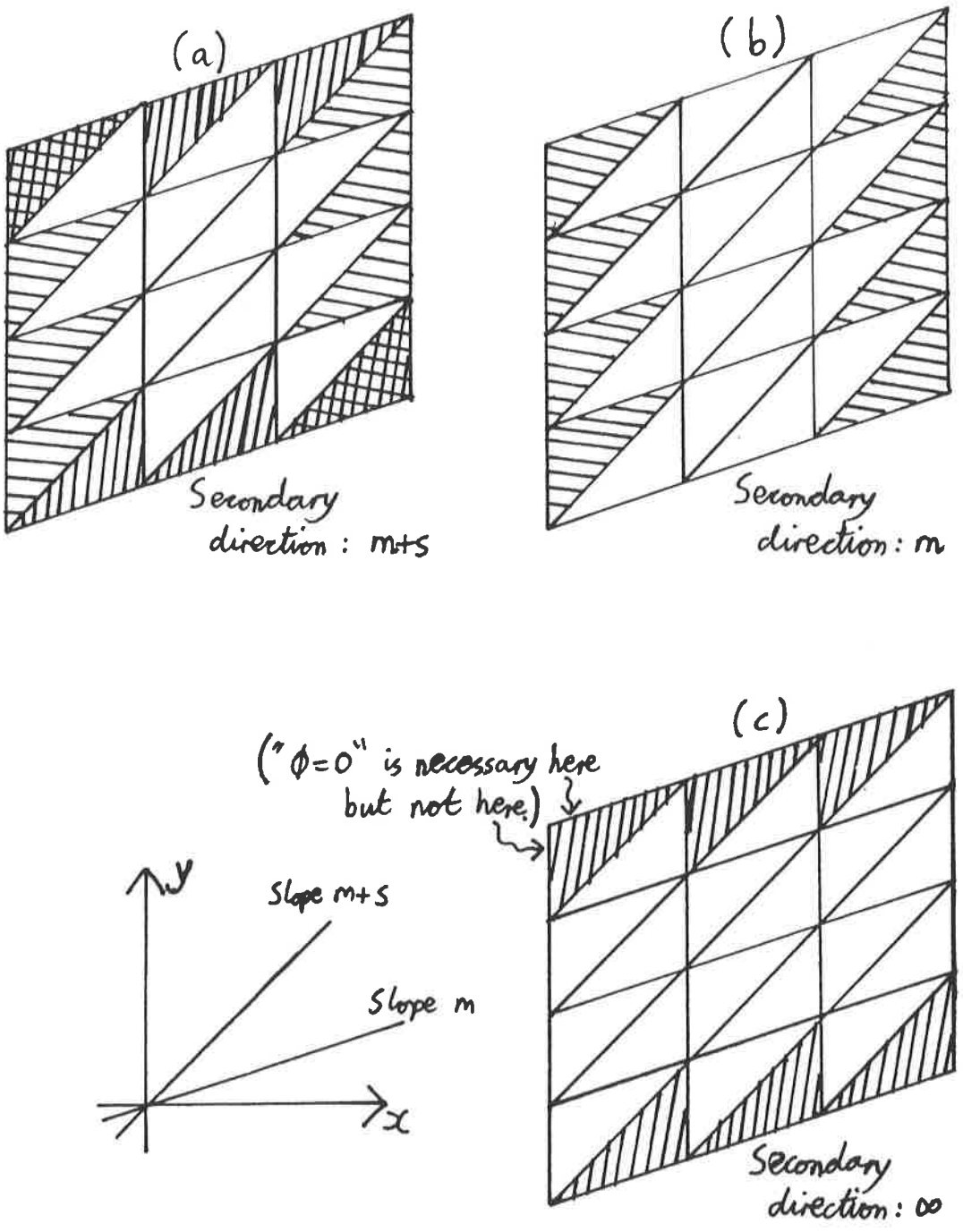

Figure 2.2.4

Unpaired triangles on ∂Ω for the three choices of decomposition (2.2.6)

The two shadings denote triangles unpaired after consideration of each of the two primary directions. On any segments of ∂Ω given by the secondary direction, "$\phi = 0$" is not used.

(1) Lemma 2.2.1.

(2) Use (1) and (if necessary) "$\phi = 0$ on $\partial\Omega$" to bound the contribution to $(\nabla(Iu - u) , \nabla\phi)_{\Omega}$ ($\phi \in S_0$) associated with the first primary direction.

(3) Repeat (2) for the second primary direction.

(4) Combine (2) and (3) via one of the decompositions (2.2.6). Hence bound the point sampling difference of ∇Iu and ∇Ru.

(5) Bound the point sampling error in ∇Iu.

(6) Combine (4) and (5) to bound the point samping error in ∇Ru.

Table 2.2

Superconvergence proof on a uniformly triangulated polygon

This is a step by step generalisation of Table 2.1.

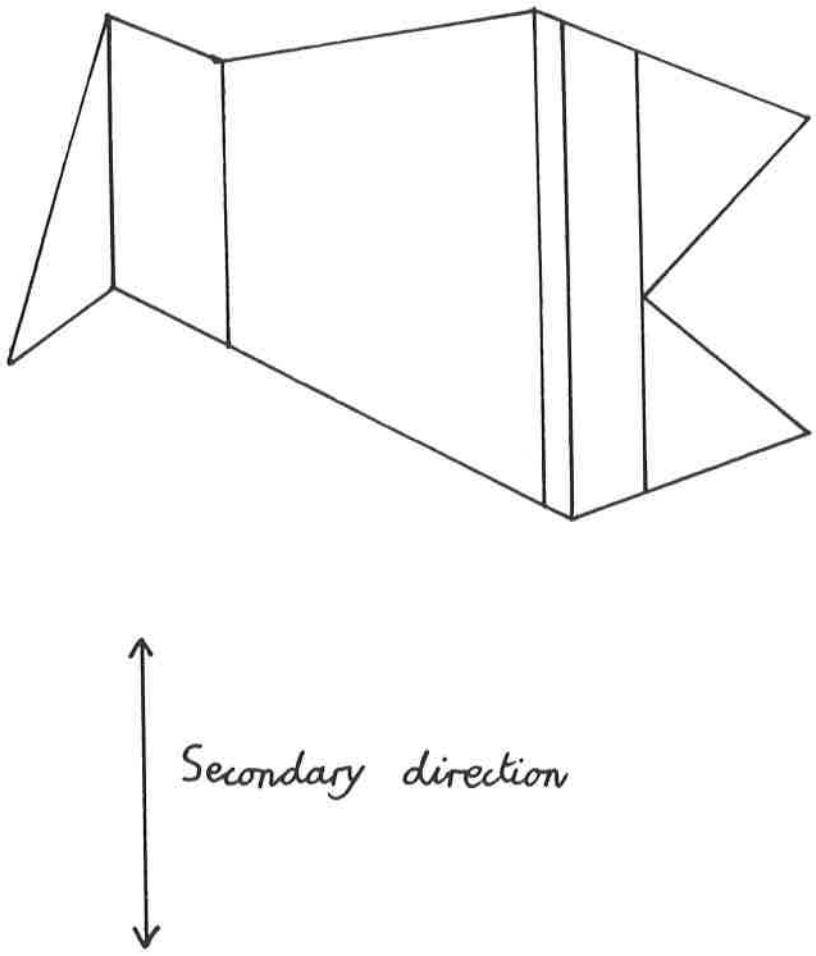

Figure 2.3.1

A general polygon reduced to bands

Four of the bands are trapezia and three are triangles.

bands (i.e. the band boundaries internal to Ω). So the contribution to $(\nabla(Iu - u) , \nabla\phi)_\Omega$ from any band β would be unchanged if β were a complete problem domain, isolated from the rest of Ω. By (ii) therefore, this contribution from β is bounded by

$$ch^2 \; | u |_{3,\beta} \; | \phi |_{1,\beta} ;$$

it is irrelevant that ϕ may be non-zero on the parts of $\partial\beta$ with direction D. (Here and henceforth we take h to be a typical element edge length of the triangulation; we assume that the maximum element diameter is bounded above by ch for some $c > 0$). To deduce that the triangulation is superconvergent, we simply sum these contributions over all the bands. ###

For example, consider the "chevron" mesh used to triangulate the square in Figure 2.3.2. The five band boundaries are parallel to the x-axis. If we take the secondary direction to have slope 0 and the primary direction to have slopes ± 1 (in alternate bands) and ∞, then this triangulation is superconvergent by the above theorem. The octagon in Figure 2.3.3 also has a superconvergent triangulation. Again the secondary direction has slope 0; the primary directions have slopes $1/2$ and ∞ in the central band, $+1$ and -1 in both of the others. (Note that, unlike the square, the octagon cannot be triangulated without the use of some subtlety. There is an alternative to a decomposition into bands: the "block" triangulation of Figure 2.4.3 below. But we expect that this will generate unacceptable errors in the centre of the domain - see Section 2.4 for discussion.)

Now if we take a sufficient number of bands, we can reduce any polygon to a series of trapezia and triangles (see Figure 2.3.1). To triangulate the triangular subdomains we can take the primary

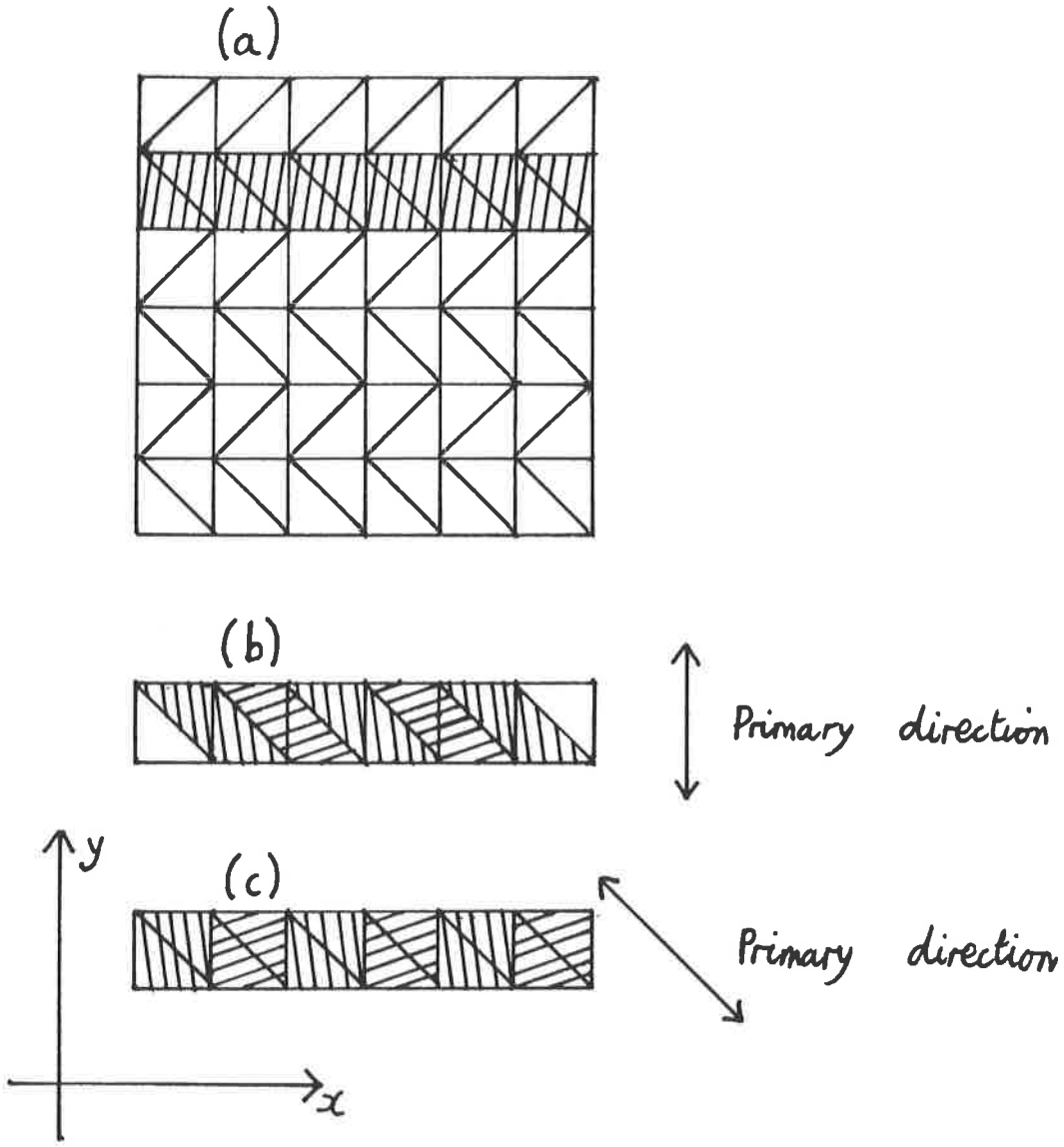

Figure 2.3.2

A chevron mesh on the unit square

(a) The triangulation. One band, β, is shaded.

(b) & (c) The band is considered in isolation. The triangle pairings are shaded; the unshaded triangles in (b) indicate that we need to use "$\phi = 0$" on $\partial\beta \cap \partial\Omega$ in order to prove superconvergence.

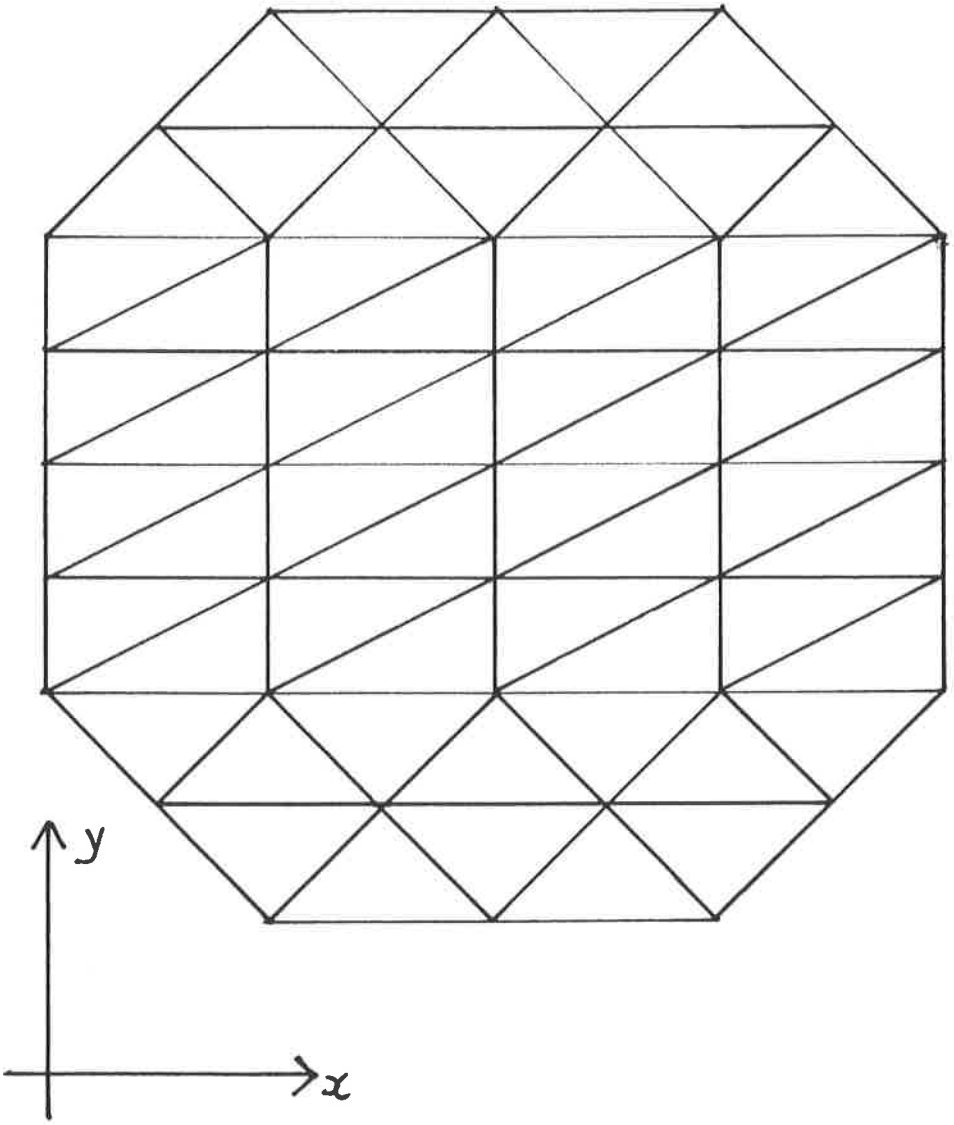

Figure 2.3.3

Superconvergent triangulation of a regular octagon

directions to be parallel to their external boundaries (i.e. the edges on $\partial\Omega$) and the resulting band triangulations are clearly superconvergent. We can attempt to do the same for the trapezia: the triangulation will again - if it exists - be superconvergent. However, (see Figure 2.3.4) we cannot partition the general trapezium into a uniform mesh (nor will it help to insert extra band boundaries). Also, the triangulations of two neighbouring bands may not be compatible unless the mesh is impractically fine. For if the triangulation of band β_1 requires at least n_1 equal element edges on its boundary with band β_2 and β_2 requires at least n_2 edges there, then a triangulation compatible to both bands requires at least $l.c.m.(n_1,n_2)$ element edges on this boundary. If there are several bands, even the coarsest possible triangulation may have far too many nodes for practical computation.

More general triangulation techniques are necessary for the general polygon and, indeed, for regions whose boundaries include curved segments; we will discuss these in Section 2.5. In the next section we digress a little to examine the topology of superconvergent triangulations.

2.4 THE SIX ELEMENT PROPERTY

Our purpose in this chapter is to formulate generic triangulations which can be applied to yield superconvergence on a wide variety of problem domains. When we have found a successful triangulation for a given region Ω, we move on to a more "general" domain and attempt to extend our methods. We feel there is little use in remaining behind with the same Ω and

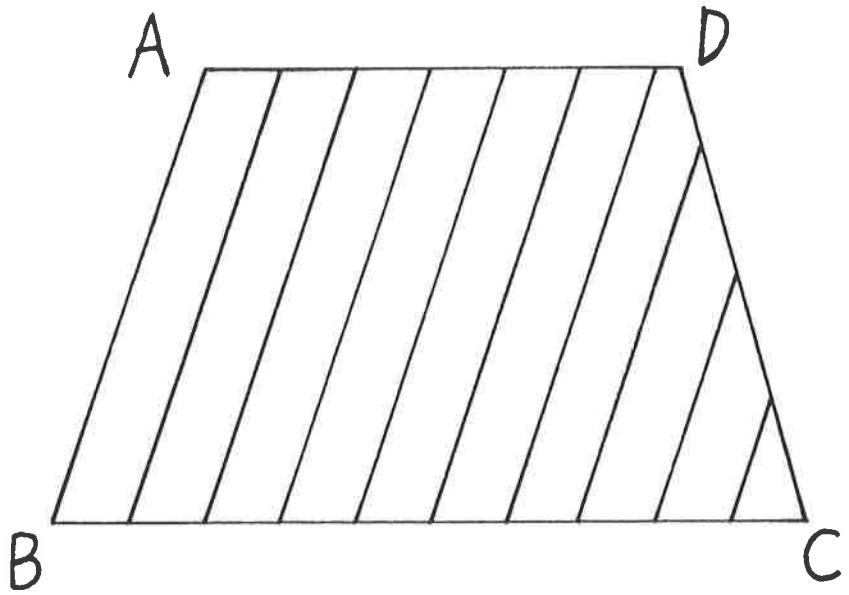

Figure 2.3.4

The general trapezium does not have a uniform triangulation

The triangulation lines drawn parallel to *AB* have identical spacing along *AD* and *BC*. Each of the four vertices must lie on one such line. This is possible only if *AD/BC* is rational, which is not the case here.

searching for the whole class of superconvergent triangulations. Also, we see even less use in a classification of non-superconvergent triangulations.

There is however a general property of superconvergent triangulations which we highlight because it can be particularly helpful when distinguishing them from the rest. We recall that for the triangulation of the rectangle given in Section 1.5, each internal node is enclosed by exactly six elements. This property is obviously retained for the triangulations which we have given for parallelograms; therefore it applies to the interior of any band in a superconvergent triangulation. Similarly, it is clear that each boundary node of such a band is either placed at a vertex of the boundary or enclosed by exactly three elements plus the exterior of the band. So a node on a band boundary but internal to Ω is met by three elements on each side of the band boundary, i.e. is enclosed by six elements altogether.

Therefore all the superconvergent meshes discussed so far have the "six element property": precisely six elements meet at each internal node. Now in the following sections we will introduce mesh distortions and pseudo-vertices, neither of which affect this property. We stress the following point: that

> together with banded triangulations, these techniques are powerful enough to triangulate any domain which satisfies the cone condition and whose boundary is a finite union of smooth curves.

So we regard the six element property as a practical requirement in the construction of superconvergent meshes. We will now discuss the extent to which this property can be mathematically identified with the superconvergence of gradient errors.

Consider the "criss-cross" mesh shown in Figure 2.4.1. Although this configuration was necessary for high order derivative convergence in the mixed method of Fix et al (1981), it does not lead to superconvergence in our sense. It is clearly not amenable to a superconvergence proof via a partition into bands: for a start there are four triangulation directions everywhere. Moreover, while the global combination of bands, choice of secondary direction, etc. are aspects only of the construction of a proof, the local combination of elements and cancellation of errors (and, to an extent, the six element property which this triangulation lacks) are fundamental to the superconvergence phenomenon. So indeed we do not expect this mesh to be superconvergent.

A numerical test confirms this. We solve (1.6.1) on the unit square $\Omega = (0,1)^2$ with u given by (1.6.2) and $h = 1/4,\ldots,1/12$. With the criss-cross mesh we obtain the asymptotic error rates

$$| (I - R)u |_{1,\Omega} \simeq 5.4\, h$$

and $$E_{tgt} \simeq 3.1\, h;$$

with the superconvergent uniform triangulation we have

$$| (I - R)u |_{1,\Omega} \simeq 1.2\, h^2$$

and $$E_{tgt} \simeq 1.4\, h^2.$$

Hence there exists a function u, satisfying (1.4.3), such that (2.1.1) fails for the criss-cross mesh; this triangulation is not superconvergent. From the viewpoint of regularity, this example of the link between the six element property and superconvergence is a particularly simple one and thus a strong argument for treating the property as a practical necessity.

We must now admit that both this topological uniformity and the geometric uniformity (congruence of triangles within a band)

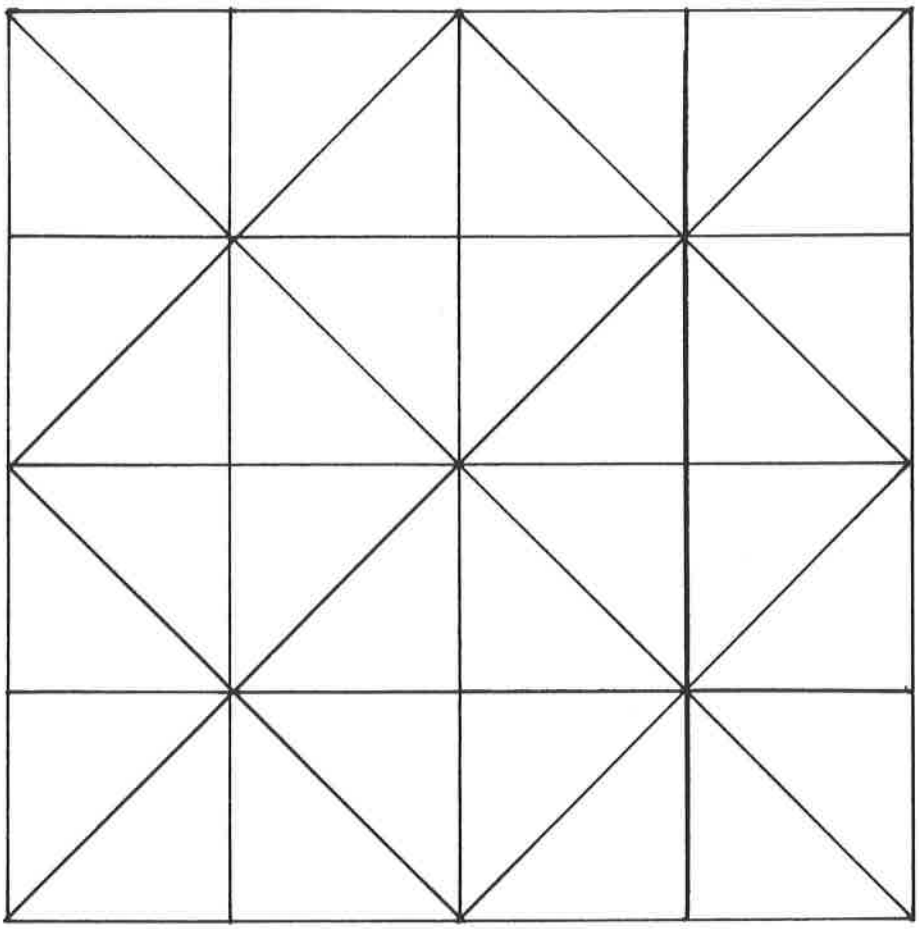

Figure 2.4.1

A uniform criss-cross mesh on the unit square

This triangulation is not superconvergent.

can in fact be dropped, at a bounded number of nodes, and are therefore not strict mathematical necessities. Superconvergence is retained but, as we shall see, there are reasons for avoiding such constructions.

Theorem 2.4 Suppose there exists a partition of a polygon Ω into triangles (which meet only in entire common sides or vertices) via a finite number of triangular subdomains, each of which is uniformly triangulated with the three directions given by its sides. Then this triangulation is superconvergent.

Proof We refer to the triangular subdomains as "blocks" (see Figure 2.4.2(a)). To prove superconvergence we consider separately the contributions to

$$(\nabla(Iu - u) , \nabla\phi)_{\Omega}$$

from the neighbourhood of each block vertex internal to Ω. We then add contributions from the neighbourhoods of members of a number of sets of nodes, each set being associated with the boundary between two blocks. It is convenient to assign sets to the nodes at block vertices too; therefore let the sets $v_1,\ldots,v_n$ each contain one of the n block vertices internal to Ω. To arrange the remaining nodes into sets we proceed thus (see Figure 2.4.2(b)). For each interblock boundary internal to Ω, let the set of nodes on that boundary (excluding the block vertices in $v_1,\ldots,v_n$) be placed in one of the $N - n$ sets $v_{n+1},\ldots,v_N$. (Note that the number of blocks is finite and so N is bounded as $h \to 0$.) Let each remaining node of the triangulation then be placed in one of $v_{n+1},\ldots,v_N$, according to which interblock boundary is closest; any consistent proceedure can be adopted in the case of nodes equidistant from two (or three) boundaries.

All the vertices in the triangulation are now distributed

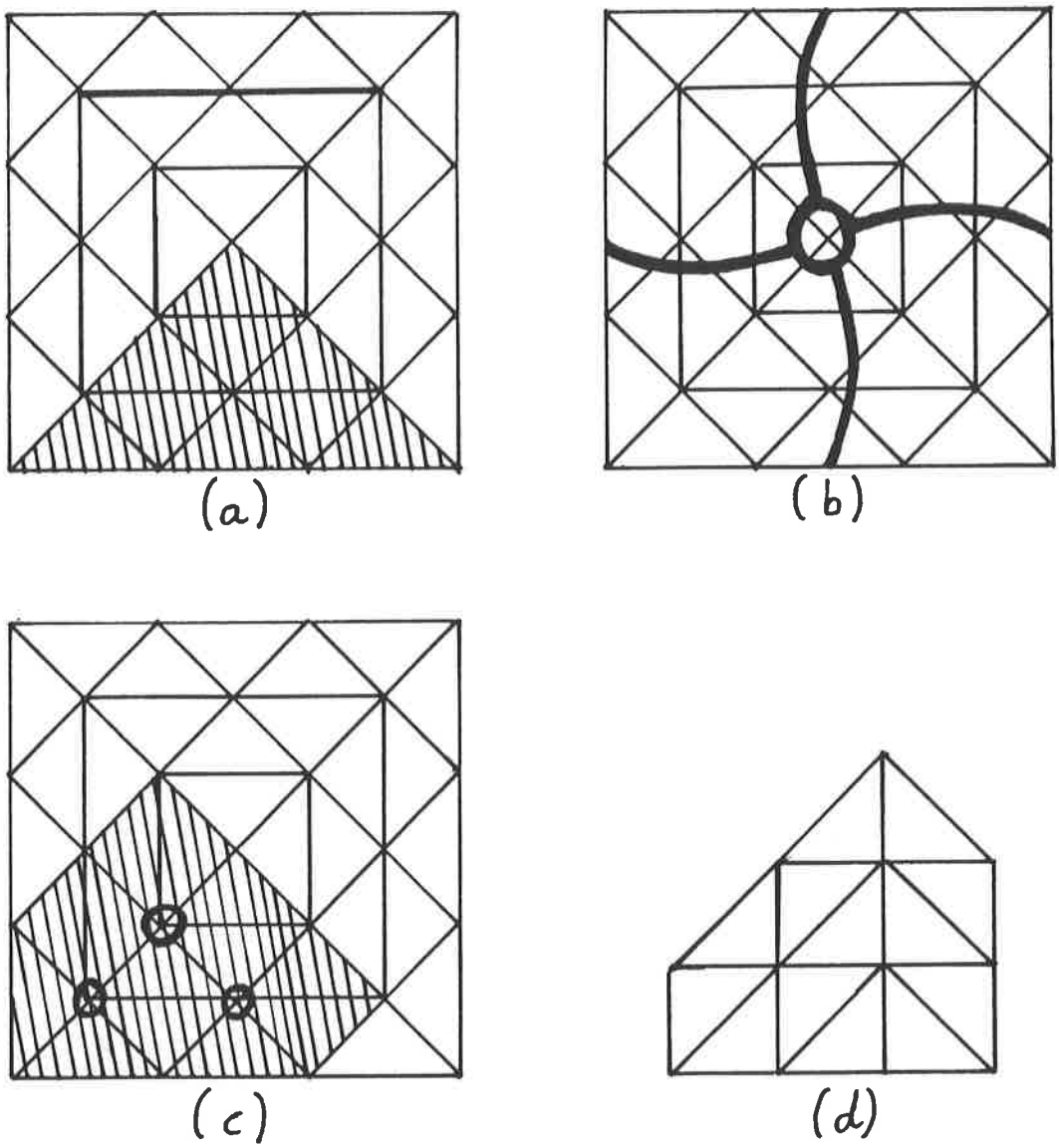

Figure 2.4.2

A block triangulated square

(a) One of the four blocks is shaded.

(b) The divisions indicate the five sets v_k (one block vertex internal to Ω, plus four interblock boundaries).

(c) The support V_k of one of the $\phi_{(k)}$ $(k > 1)$. Nodes internal to V_k are marked.

(d) V_k behaves as a banded domain.

between N sets: one set for each internal block vertex (with one member - that vertex) and one for each interblock boundary (with $O(h^{-2})$ members). For $k = 1,\ldots,N$, let V_k be the union of supports of the basis functions in S_O which are centred on the nodes in v_k. Given any $\phi \in S_O$, let $\phi_{(1)},\ldots,\phi_{(N)}$ satisfy

$$\left.\begin{aligned} &supp\ \phi_{(k)} \subseteq V_k\ , \quad k = 1,\ldots,N \\ \text{and} \quad &\Sigma_{k=1}^{N}\ \phi_{(k)} = \phi. \end{aligned}\right\} \quad (2.4.1)$$

(See Figure 2.4.2(c).)

Let $\phi \in S_O$. By (2.4.1)

$$(\nabla(Iu - u)\ ,\ \nabla\phi\ )_\Omega = \Sigma_{k=1}^{N}\ (\nabla(Iu - u)\ ,\ \nabla\phi_{(k)}\ )_{V_k}\ ;$$

we bound each of these terms separately. First, let $1 \leq k \leq n$ (i.e. there is only one node internal to V_k) and let us make the mild additional assumption (recall (1.4.3))

$$u \in H_E^1(\Omega) \cap W_{2+\delta}^{3+\epsilon}(\Omega), \quad (2.4.2)$$

where one of δ and ϵ is positive and the other non-negative. There is absolutely no guarantee that any superconvergence properties will hold in V_k and so the best we can do is (by S.E., B.H. and $meas\ (V_k) \leq ch^2$)

$$\begin{aligned} &(\nabla(Iu - u)\ ,\ \nabla\phi_{(k)}\ )_{V_k} \\ &\leq\ |\ (Iu - u)\ |_{1,V_k}\ |\ \phi_{(k)}\ |_{1,V_k} \\ &\leq\ ch\ |\ u\ |_{2,V_k}\ |\ \phi_{(k)}\ |_{1,V_k} \\ &\leq\ ch^2\ |\ u\ |_{2,\infty,V_k}\ |\ \phi_{(k)}\ |_{1,V_k} \\ &\leq\ ch^2\ |\ u\ |_{3+\epsilon,2+\delta,\Omega}\ |\ \phi_{(k)}\ |_{1,V_k}. \end{aligned} \quad (2.4.3)$$

Now let $n + 1 \leq k \leq N$. Since the support V_k of $\phi_{(k)}$ lies within two neighbouring uniformly triangulated blocks, we can regard V_k as a pair of bands (see Figure 2.4.2(d)) and by Theorem 2.3

$$\begin{aligned} &(\nabla(Iu - u)\ ,\ \nabla\phi_{(k)}\ )_{V_k} \\ &\leq\ ch^2\ |\ u\ |_{3,V_k}\ |\ \phi_{(k)}\ |_{1,V_k}. \end{aligned} \quad (2.4.4)$$

Hence by (2.4.3) and (2.4.4)

$$
\begin{aligned}
&(\nabla(Iu - u) , \nabla\phi)_{\Omega} \\
&\leq ch^2 \; | u |_{3+\epsilon,2+\delta,\Omega} \; \Sigma_{k=1}^{N} \; | \phi_{(k)} |_{1,\nabla_k} \\
&\leq cNh^2 \; | u |_{3+\epsilon,2+\delta,\Omega} \; | \phi |_{1,\Omega}.
\end{aligned}
$$

But N is finite; therefore the triangulation is indeed superconvergent (for functions u satisfying (2.4.2)). ###

We do not greatly recommend the use of block triangulations. For although they may simplify a programmer's task somewhat (compare Figures 2.4.3 and 2.3.3), asymptotic accuracy will be lost in the vicinities of internal block vertices. There the contribution to $(\nabla(Iu - u) , \nabla\phi)_{\Omega}$ from a small (i.e. diameter $O(h)$) patch of elements ∇_k ($k \leq n$) is $O(h^2)$ instead of the usual $O(h^3)$. (See (1.5.8); on global averaging, $| u |_{3,\bar{A}_k} = O(h)$.) Now this additional error does not change the order of the average gradient difference $| (I - R)u |_{1,\Omega}$ but it may still produce a significant numerical increase. In particular, the spreading effect of the Galerkin equations is sufficiently weak that the increased (non superconvergent) contribution to the error will be concentrated around the vertex. (This may however be acceptable if the gradient is not going to be sampled near the vertex - see Chapter 5.)

For example, consider the unit square $\Omega = (0,1)^2$, triangulated as in Figure 2.4.4. (This is related to the meshes in Figures 2.4.2 and 2.4.3.) In a numerical test, we solve (1.6.1) with (1.6.2) as usual, taking $h = 1/4,\ldots,1/12$. As predicted above, $| (I - R)u |_{1,\Omega}$ is larger than it is on the uniform triangulation (by over 50%) and the pointwise difference $| (I - R)u |_{1,\infty,\Omega}$ is an order of magnitude larger. With the block triangulation we obtain

$$
| (I - R)u |_{1,\Omega} \simeq 1.9 \, h^2
$$

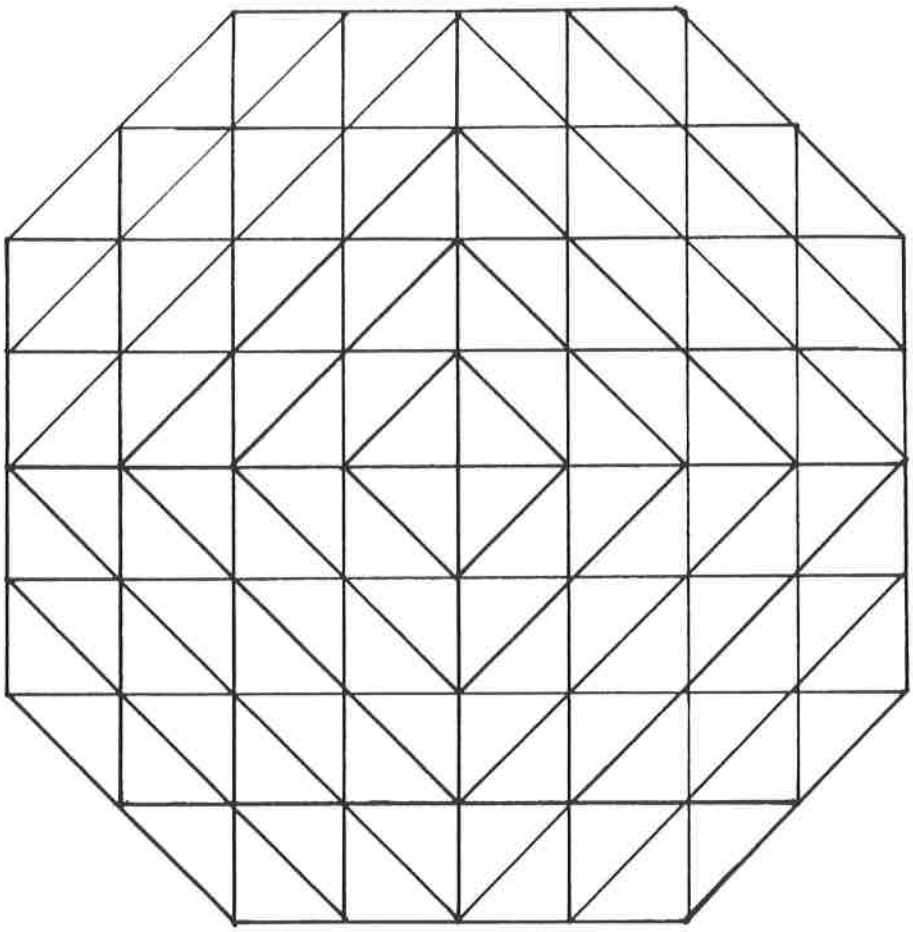

Figure 2.4.3

A block triangulation (without the six element property) on the octagon

Accuracy will be lost near the centre.

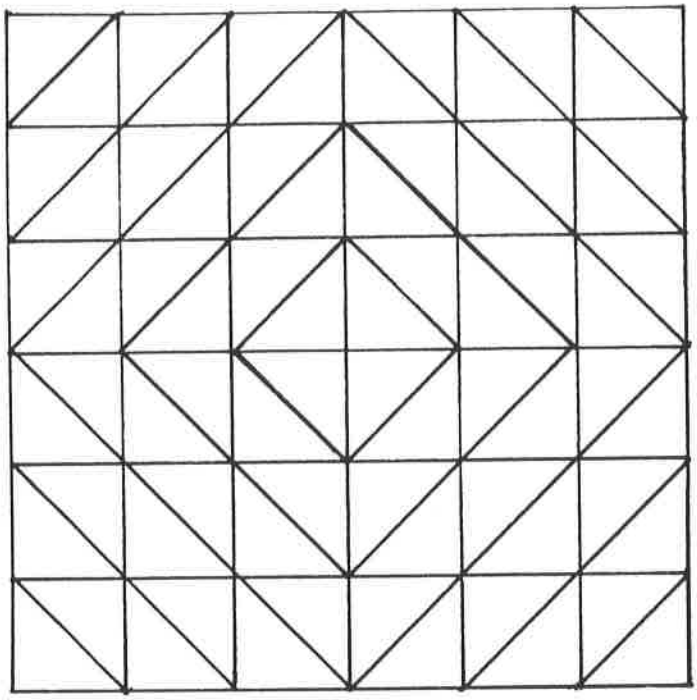

Figure 2.4.4

A block triangulation on the unit square

We expect that $| \nabla(I - R)u |$ will be higher on average and much higher pointwise than it would be if the triangulation were uniform throughout Ω.

and $| (I - R)u |_{1,\infty,\Omega} \simeq 0.7\, h$

whereas with the uniform triangulation

$$| (I - R)u |_{1,\Omega} \simeq 1.2\, h^2$$

and $| (I - R)u |_{1,\infty,\Omega} \simeq 3\, h^2.$

2.5 GLOBAL DISTORTIONS

We turn now to a triangulation technique which can be used to generate superconvergent meshes on regions with curved or general polygonal boundaries - a smooth distortion of the positions of the nodes. The mathematical effect of such a transformation is to add a number of perturbation terms to the superconvergence error bound. A simple example indicates that moderate distortions are not numerically significant, but the asymptotic analysis is a little tricky and we postpone it to Chapter 4.

Suppose we are given a triangulation with the six element property on some domain Ω. We define a "path" across Ω to be a union of triangle sides with the property that, at each internal node along its route, exactly three elements meet on each side of the path. (See Figure 2.5.1.) We partition the set of all paths across Ω into three families such that, if two different paths meet at any node of Ω, then they belong to different families. Also, we divide the boundary of the triangulation into (a minimum number of) segments such that each one can be included naturally in one of the families of paths. Now, if the mesh were uniform, each family would consist of straight lines in one of the triangulation directions. So for the general mesh, it is natural to define these three "directions" by associating them with the three families of paths. Further, for each direction there is a

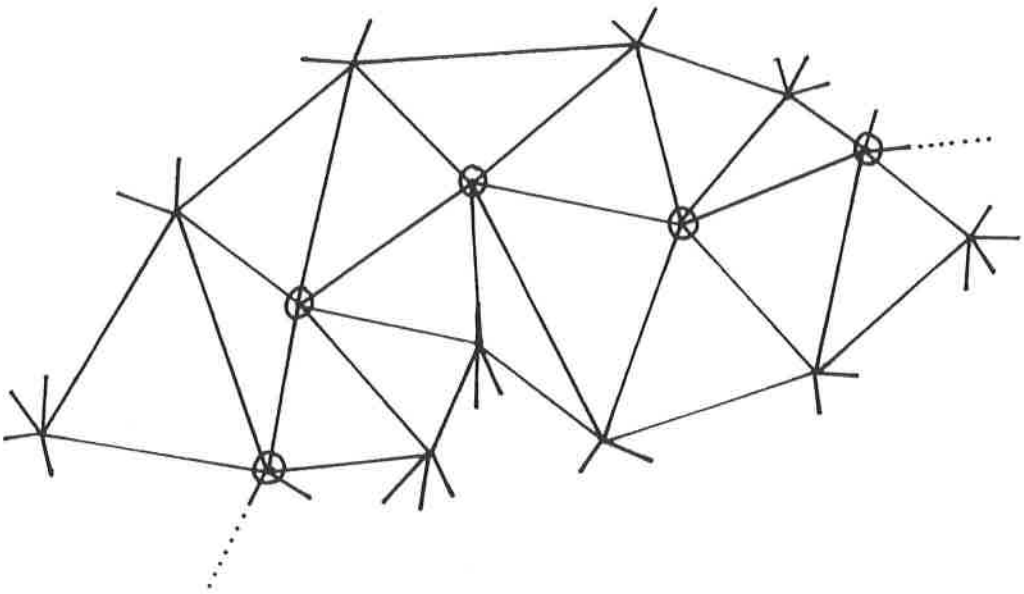

Figure 2.5.1

A path through a mesh with the six element property

Nodes along the path are circled.

(unique) partition of Ω into triangle pairs (A_k) with - as usual - a number of left-over triangles (B_k) on $\partial\Omega$. If, again, the triangulation were uniform, each A_k would be a parallelogram; we recall that this leads us to Lemma 2.2 - the heart of superconvergence on uniform meshes.

Let us consider now a mesh with the six element property. Let it be smoothly distorted from uniformity (see, for example, Figure 2.5.2) in such a way that for two (primary) directions, the A_k are "almost" parallelograms. By this we mean the following:

$$\left.\begin{array}{l}\text{the midpoints of the diagonals of the}\\ \text{quadrilateral } A_k \text{ have separation } O(h^2),\end{array}\right\} \quad (2.5.1)$$

$k = 1,\ldots,K_A$. Equivalently, under the local transformation $(x,y) \to (\xi,\eta)$ of Lemma 2.2,

$$\left.\begin{array}{ll} |\ \xi_+ + \xi_- - 1\ | & = O(h)\\ \text{and} \quad |\ \eta_+ + \eta_-\ | & = O(h).\end{array}\right\} \quad (2.5.2)$$

(See (2.2.5) and Figure 2.5.3.) In Chapter 4 we will define this property exactly and prove, via a modification of Lemma 2.2, that such a triangulation is indeed superconvergent and that the boundary condition

$$\phi = 0 \quad \text{for } \phi \in S_0$$

is not necessary on the boundary segments which follow the secondary direction. If, therefore, a mesh consists of a number of bands such that the secondary direction and mesh spacing in that direction are consistent across each band boundary, then this triangulation too is superconvergent. Similarly, though we still do not recommend this application, the above constructions can be combined with the block triangulations of Section 2.4 above.

We are now in a position to return to the problem of

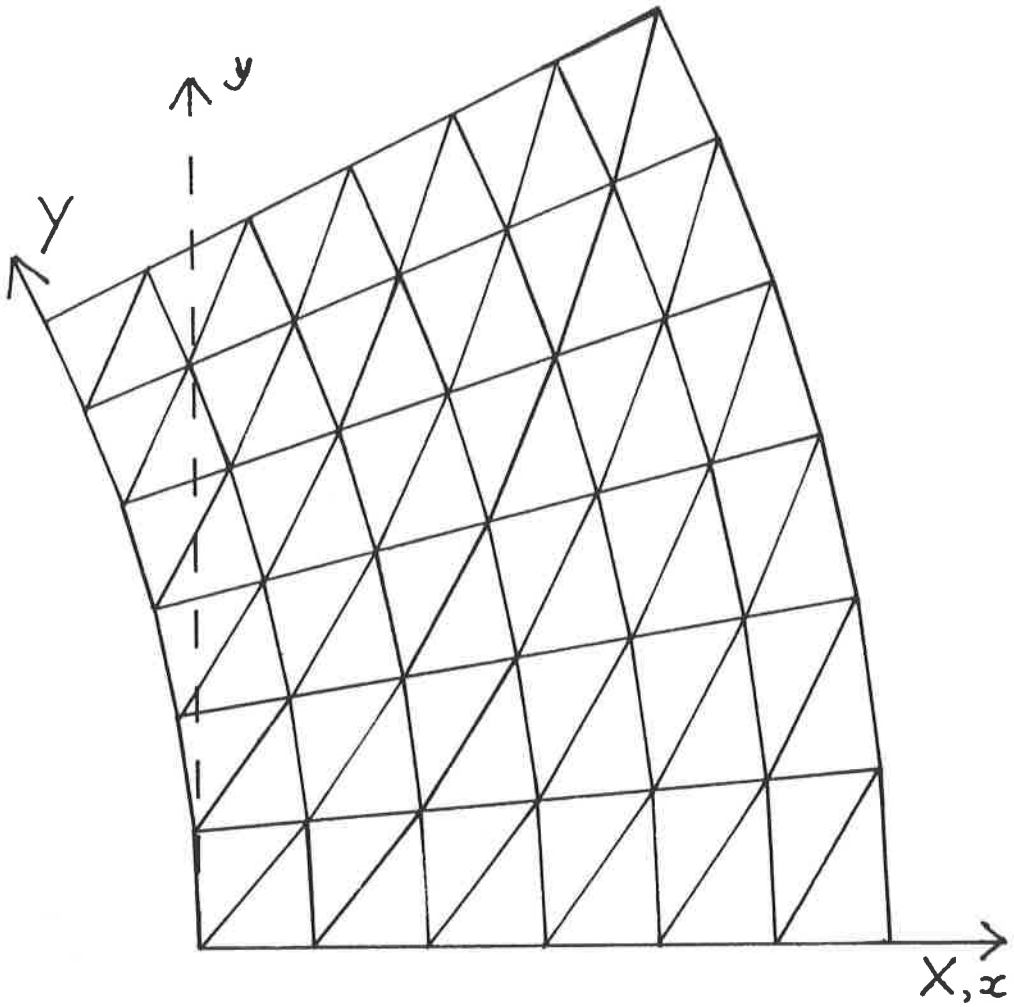

Figure 2.5.2

Superconvergent mesh on a distortion of the uniformly triangulated unit square $(X,Y) \in (0,1)^2$

The transformation of nodal positions is given by:

$$x = (X + 2) / (1 + Y^2/4)^{1/2} - 2 \quad ,$$

$$y = (X + 2)Y / 2(1 + Y^2/4)^{1/2} \quad .$$

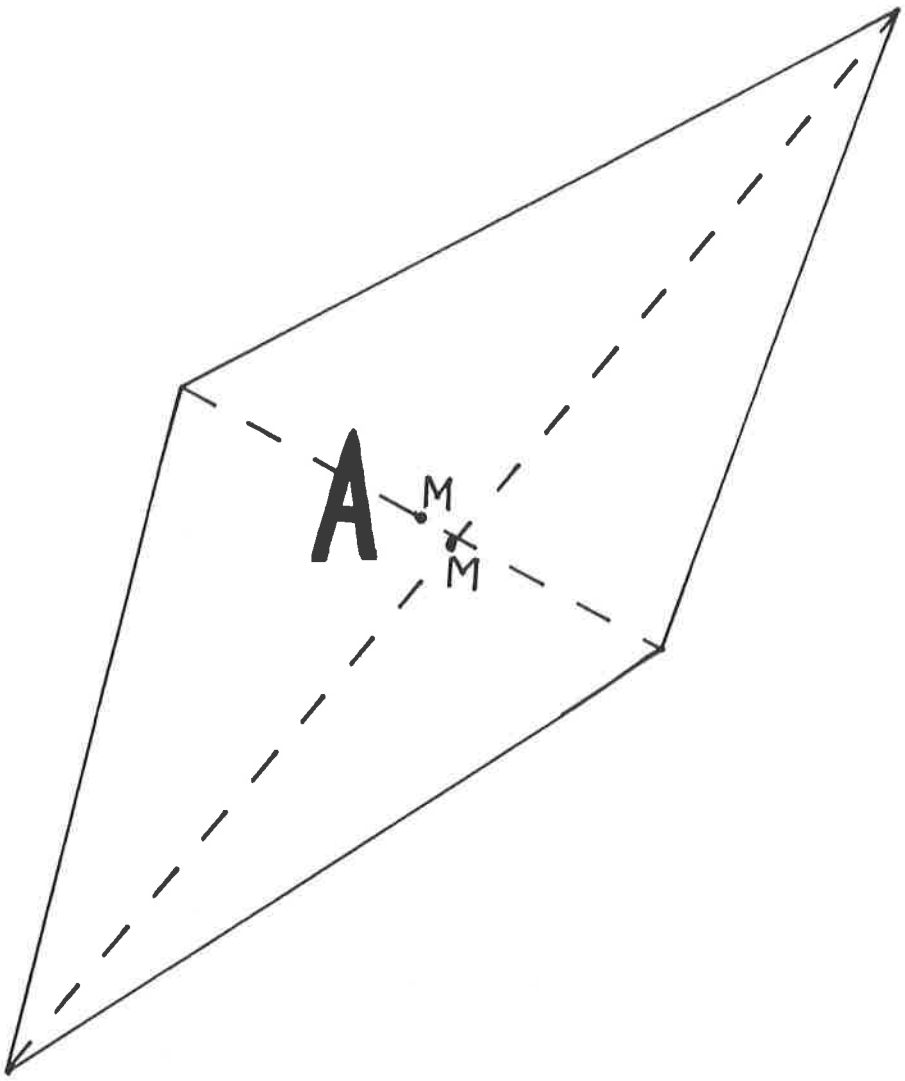

Figure 2.5.3

"Almost" a parallelogram

The two points M are the midpoints of the diagonals of A; $diam\ (A) = O(h)$. We require $MM = O(h^2)$ as $h \to 0$, i.e. the shape of A tends to that of a parallelogram.

triangulating a general polygon. We abandoned this in Section 2.3 because of the problems raised by the general trapezium. However with distorted meshes this becomes a simple region to triangulate. (Recall Figure 2.3.4.) In Figure 2.5.4, mesh (a) is a distortion of a uniform mesh on a rectangle and mesh (b) is a distortion of a uniformly triangulated trapezium. The main advantage of (a) is its simplicity: in particular the nodes are equispaced along each of the four boundary segments. Meshes such as (b) can be used to effect a change across a band in the number of nodes on the interband boundary.

When we move on to less simple regions and require a division into bands, we no longer have the constraint, that the band boundaries must be parallel. (They must, however, lie in the same mesh direction: AB and CD could be band boundaries in mesh (a) of Figure 2.5.4 but not in mesh (b).) So, for example, the band boundaries for the polygon shown in Figure 2.3.1 above could be as given by Figure 2.5.5. Finally, just as paths internal to bands need not be straight lines, the boundaries of bands can also be curved (whether or not they are internal to Ω).

We conclude this section with a numerical example: we solve (1.6.1) with u given by (1.6.2), where Ω is the triangulation for a truncated sector shown in Figure 2.5.2. (Incidentally, this is the first example we have met with non-homogeneous boundary conditions.) We write Ω_h for the union of elements ($\neq \Omega$) and h for the mesh spacing along the x-axis. We obtain

$$| (I - R)u |_{1,\Omega_h} \simeq 0.98\, h^2;$$

we recall that

$$| (I - R)u |_{1,\Omega_h} \simeq 1.2\, h^2$$

when Ω is the undistorted square. The change in u due to the

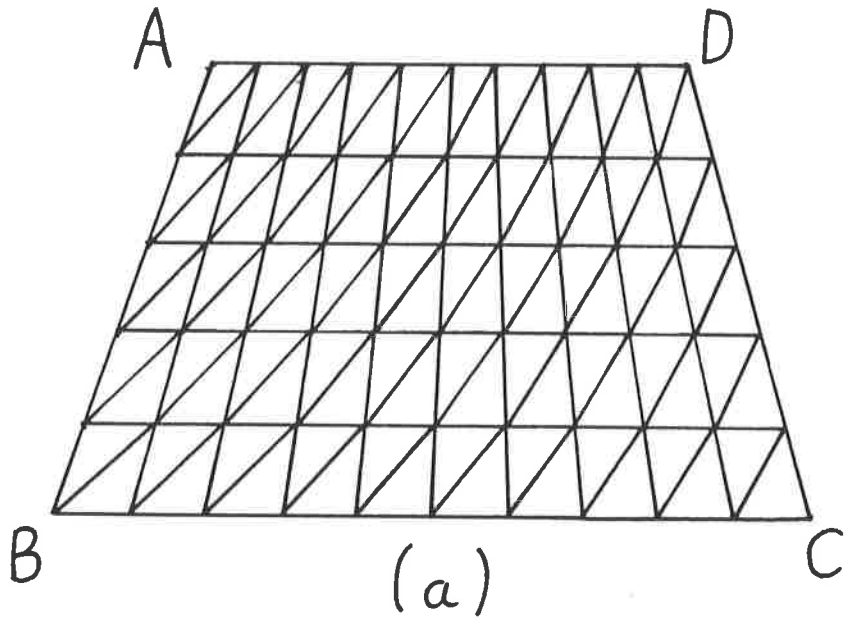

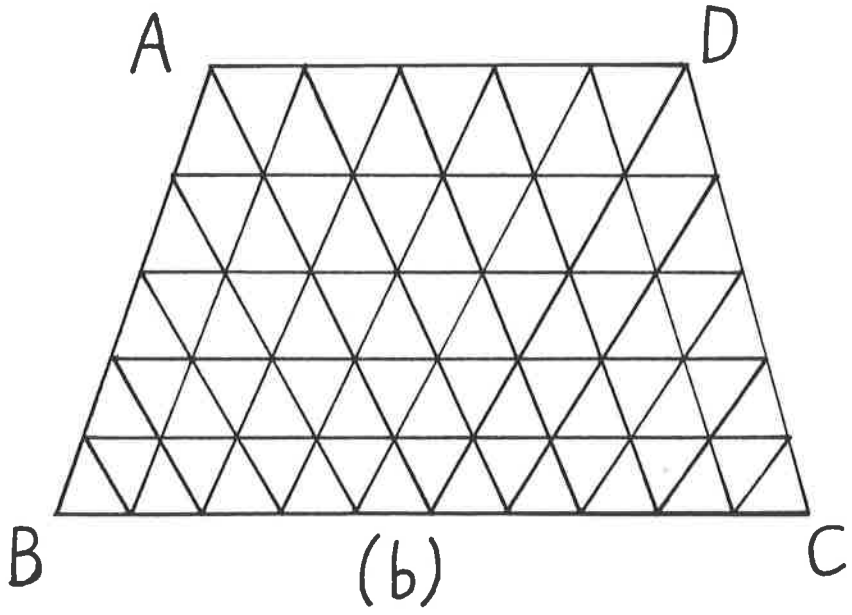

Figure 2.5.4

Two of the possible superconvergent triangulations for the general trapezium

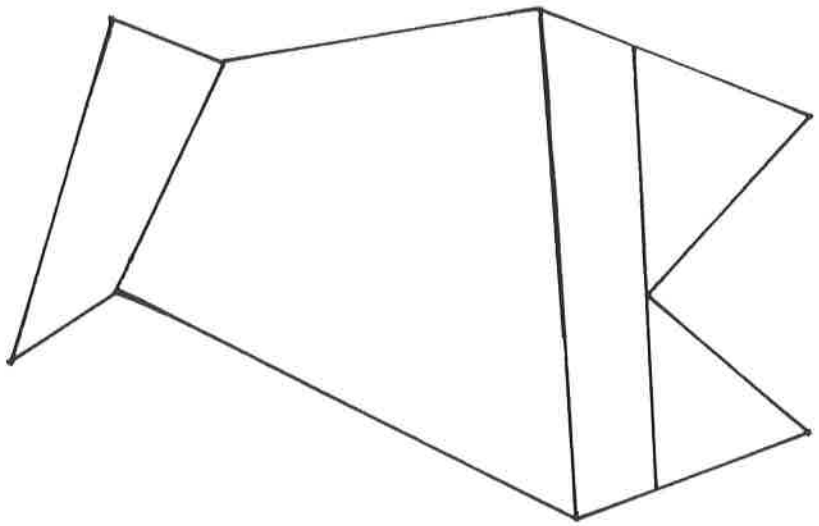

Figure 2.5.5

An irregular polygon reduced to bands for a distorted triangulation

It may well be possible to construct a triangulation which is uniform across some of these band boundaries, thus reducing still further the number of bands. This is however not a simple task; it may not be worthwhile.

change of Ω dominates the variation in the error; this has swamped any increase caused by the failure of any element pairs to (quite) form parallelograms.

2.6 PSEUDO - VERTICES

In the last section we saw that the mesh in each band of a superconvergent triangulation can be a smooth distortion of some uniform mesh. In particular the boundary of each band is a smooth distortion of a polygon (consisting of segments in the three triangulation directions). Now, let Ω be a simply-connected region whose boundary $\partial\Omega$ has no vertices: $\partial\Omega \in C^1$. If we partition it into bands, there will be at least two which have only two vertices (see Figure 2.6.1). So we have the problem of finding a smooth transformation from a region with less than three vertices onto a polygon (i.e. a region with no less than three). In effect we need to introduce the topological behaviour of at least one additional vertex to the triangulation. We call it a "pseudo-vertex" - the meeting point of two paths which follow different mesh directions but together form a smooth segment of the boundary. (See Figure 2.6.2.)

As an example, let us introduce to the neighbourhood of a straight boundary segment a suitable distortion of the mesh near the vertex shown in Figure 2.6.3(a): a corner of a uniform square triangulation. Using the axes marked we define a transformation for the nodes from mesh (a) to mesh (b). (We then complete the triangulation of mesh (b) with straight lines topologically corresponding to the links in mesh (a).) We require the mapping to take the vertex and the mesh boundary in its neighbourhood to

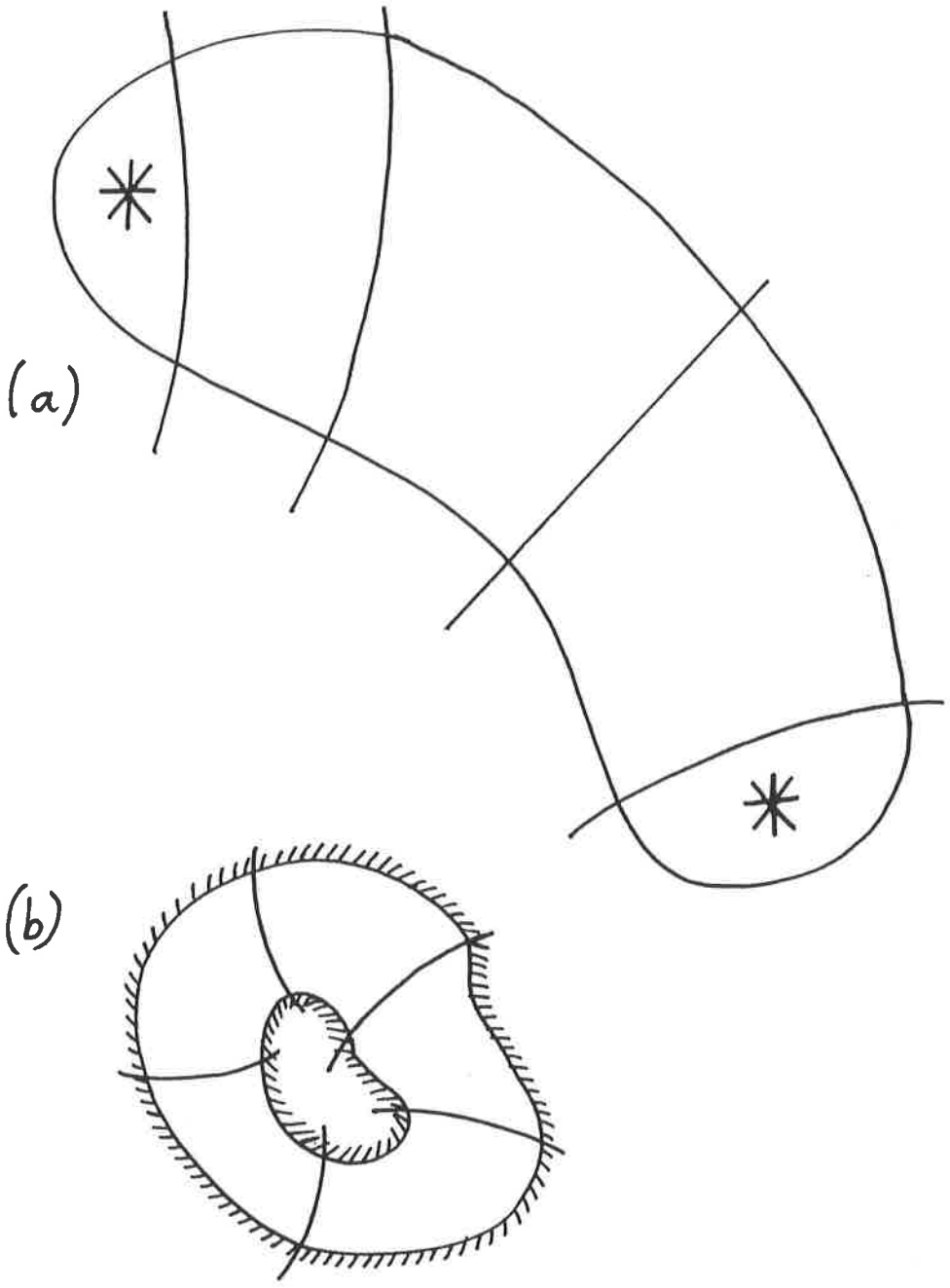

Figure 2.6.1

Triangulating a region with no vertices

(a) Even after a partition into bands, we still have to triangulate regions * with less than three vertices.

(b) This problem does not, however, apply to doubly connected domains.

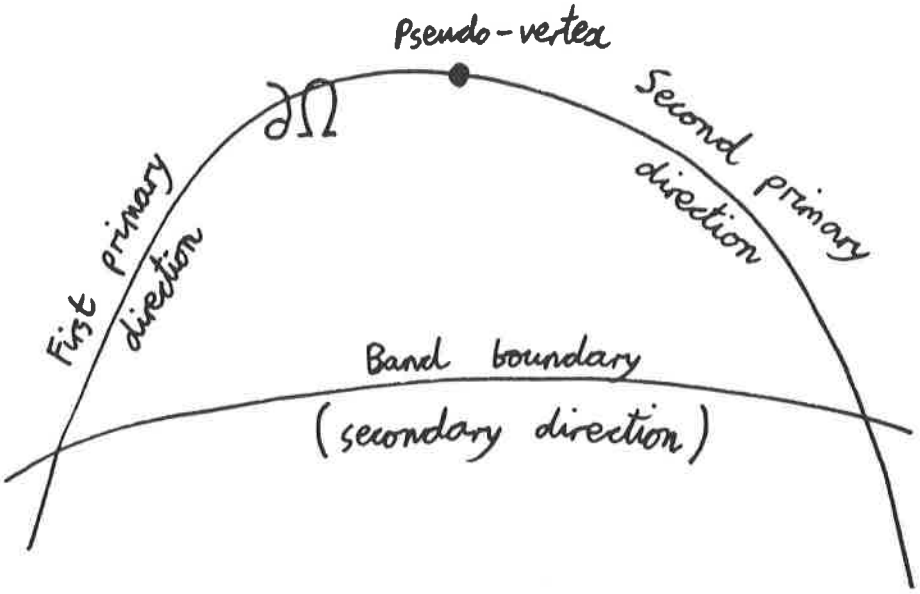

Figure 2.6.2

A band with a pseudo-vertex

The boundary of this band consists of three paths, even though it only has two true vertices.

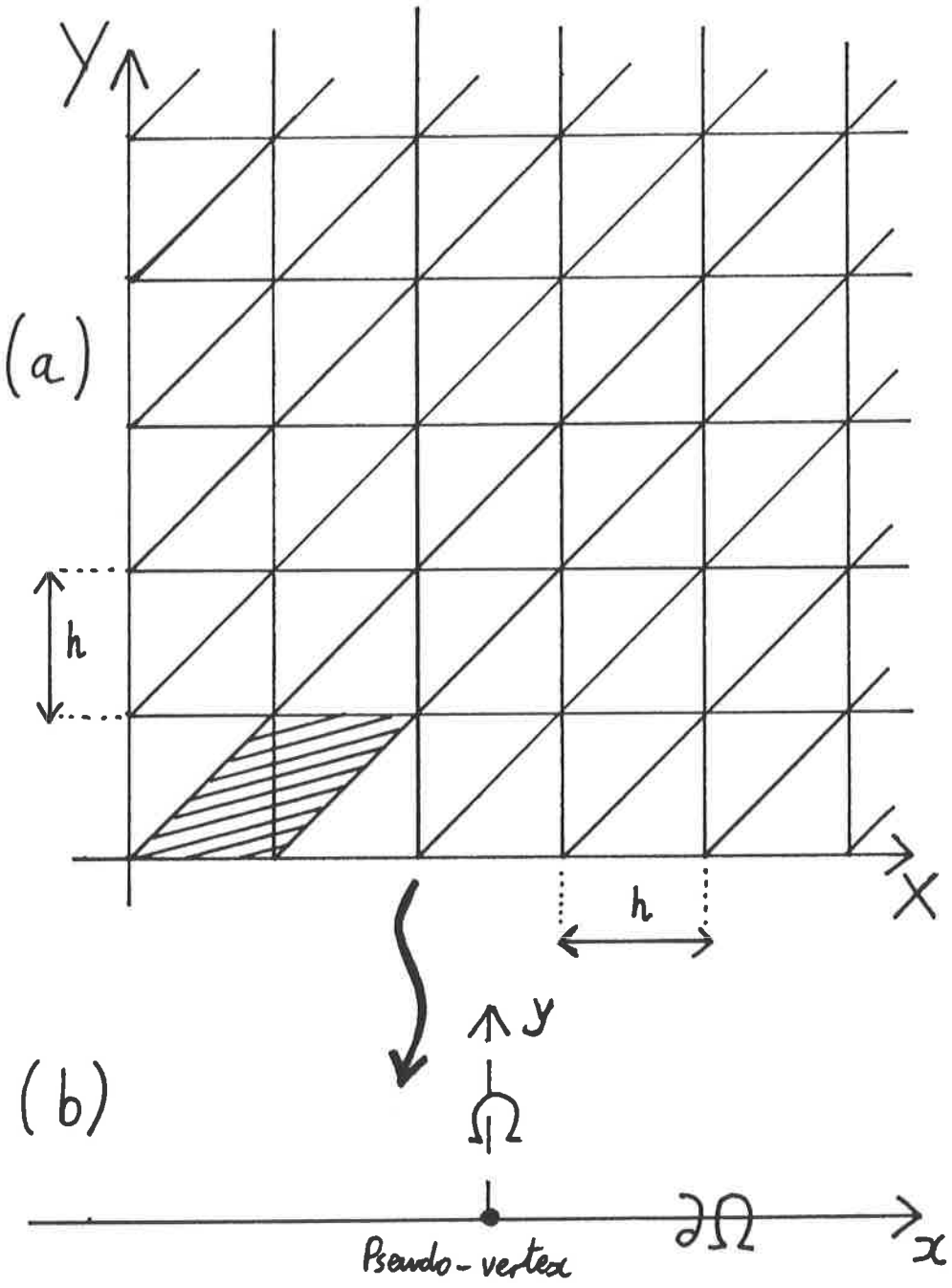

Figure 2.6.3

Transformation of a square mesh to create a pseudo-vertex

The vertex in (a) is mapped to the pseudo-vertex in (b); the X- and Y- axes go to the positive and negative directions of the x-axis.

the pseudo-vertex and the mesh boundary in its neighbourhood.

For instance, let us consider the relations

$$x = (X^2 - Y^2)/(X^2 + Y^2)^{1/2}$$

and $$y = 2XY/(X^2 + Y^2)^{1/2}.$$

In polar coordinates ((R,Θ) for the (X,Y)-plane, (r,θ) for the (x,y)-plane) these are

$$r = R \quad \text{and} \quad \theta = 2\Theta;$$

they correspond therefore to leaving distance from the origin unchanged but doubling the angle subtended at the X-axis. They lead to the mesh shown in Figure 2.6.4 which has the correct topological behaviour but is not superconvergent: for triangle pairs near the pseudo-vertex do not approximate parallelograms in the sense of (2.5.1). (Consider, say, the pair shaded in Figures 2.6.3(a) and 2.6.4. The latter quadrilateral has vertices $(0,0)$, $(h,0)$, $(3h/\sqrt{5},4h/\sqrt{5})$, $(0,h)$; the midpoints of its diagonals are at $(3h/2\sqrt{5},2h/\sqrt{5})$ and $(h/2,h/2)$ and thus have separation $O(h)$.)

To obtain a superconvergent mesh while retaining the property $\Theta \to \theta = 2\Theta$, we can map $R \to r = R^2$:

$$x = (X^2 - Y^2) \quad \text{and} \quad y = 2XY. \qquad (2.6.1)$$

The mesh resulting from this transformation is shown in Figure 2.6.5; the midpoints of the diagonals of the shaded quadrilateral are now at $(3h^2/2,2h^2)$ and $(h^2/2,h^2/2)$. Even though the shape of the triangle pair is very far from that of a parallelogram, it is "close" in the sense of (2.5.1): the separation of the midpoints of its diagonals is $O(h^2)$. Indeed the transformation shrinks the diameters of all the elements near the pseudo-vertex to $O(h^2)$. However it does retain the non-degeneracy property that

$$\left.\begin{array}{l}\text{every triangle } T_k \text{ contains a circle of} \\ \text{diameter } c.diam(T_k) \text{ (for some fixed } c > 0).\end{array}\right\} (2.6.2)$$

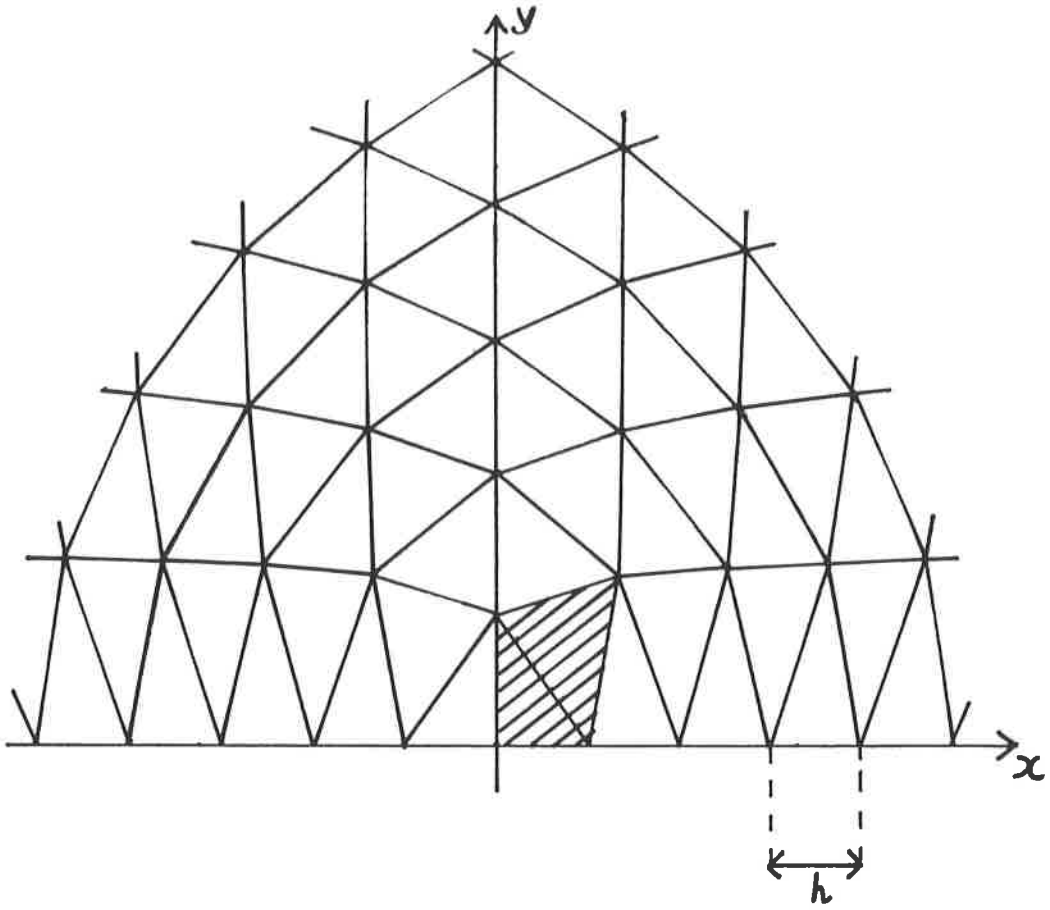

Figure 2.6.4

A non-superconvergent mesh in the vicinity of a pseudo-vertex

The shaded triangle pair is the "image" of the shaded pair in Figure 2.6.3(a).

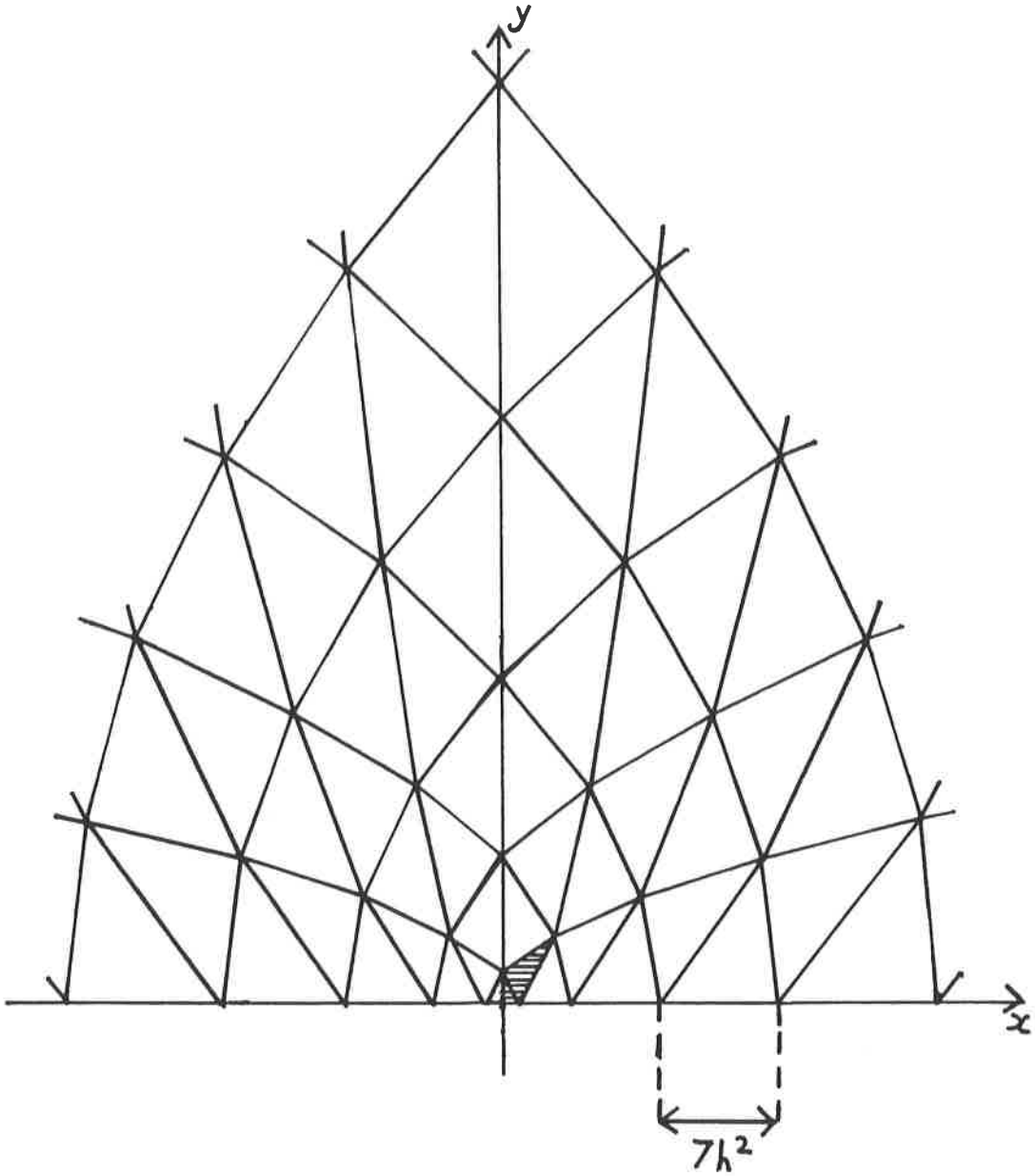

Figure 2.6.5

A superconvergent triangulation near a pseudo-vertex

The shaded triangle pair is again the "image" of the shaded pair in Figure 2.6.3(a).

It also retains the six element property and sufficient regularity away from the pseudo-vertex for the mesh to be superconvergent. We note that (2.6.1) can be regarded as a member of the family of conformal transformations (in which $Z = X + iY$ - $x + iy = z$):

$$z = Z^{\gamma}; \qquad (2.6.3)$$

in Chapter 4 we will prove that (2.6.3) leads to a superconvergent mesh for all $\gamma \geq 2$.

We look now at an application of pseudo-vertices: the triangulation of a circle. In this example we use four pseudo-vertices; we show their locations and the triangulation directions in their vicinities in Figure 2.6.6. The transformation used to create each pseudo-vertex is given locally by (2.6.1); the mesh is therefore a smooth transformation of a uniformly triangulated polygon with four right-angled vertices: (w.l.o.g) a square. Clearly we need to alter (2.6.1) to take account of the curvature of $\partial\Omega$ near each pseudo-vertex; we must also link the triangulations between pseudo-vertices to obtain a mesh which is globally smooth. We perform these modifications in an ad hoc manner and check our mesh generating algorithm by visual observations of refinements of the mesh beyond the computational range in which we are interested (i.e. we take very small values of h). Our criterion is that the over-refined meshes should not have any noticeably sharp distortions. In Figure 2.6.7 we display a mesh thus generated for the first quadrant of the circle; the triangulation is designed to be compatible with the scheme of Figure 2.6.6. (For the other quadrants, we rotate node positions about the centre.)

As a numerical test, we solve (1.6.1), (1.6.2) on the quadrant

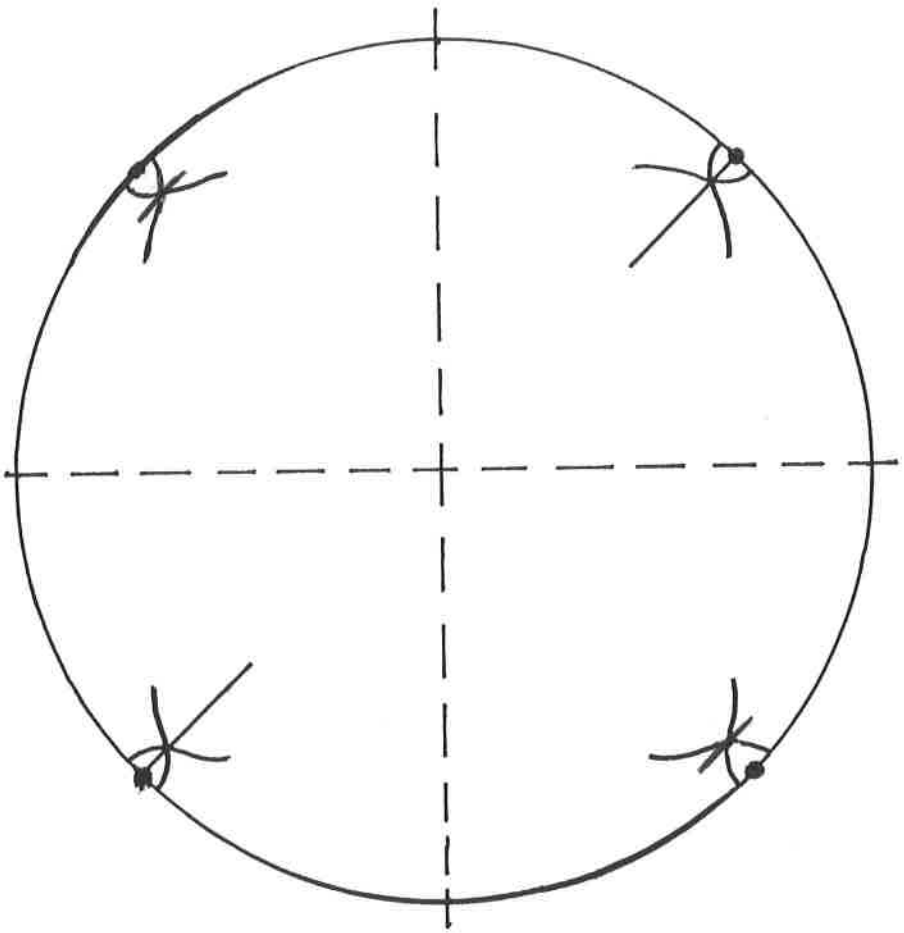

Figure 2.6.6

Triangulating the circle

The three mesh directions are indicated in the vicinity of each of the four pseudo-vertices.

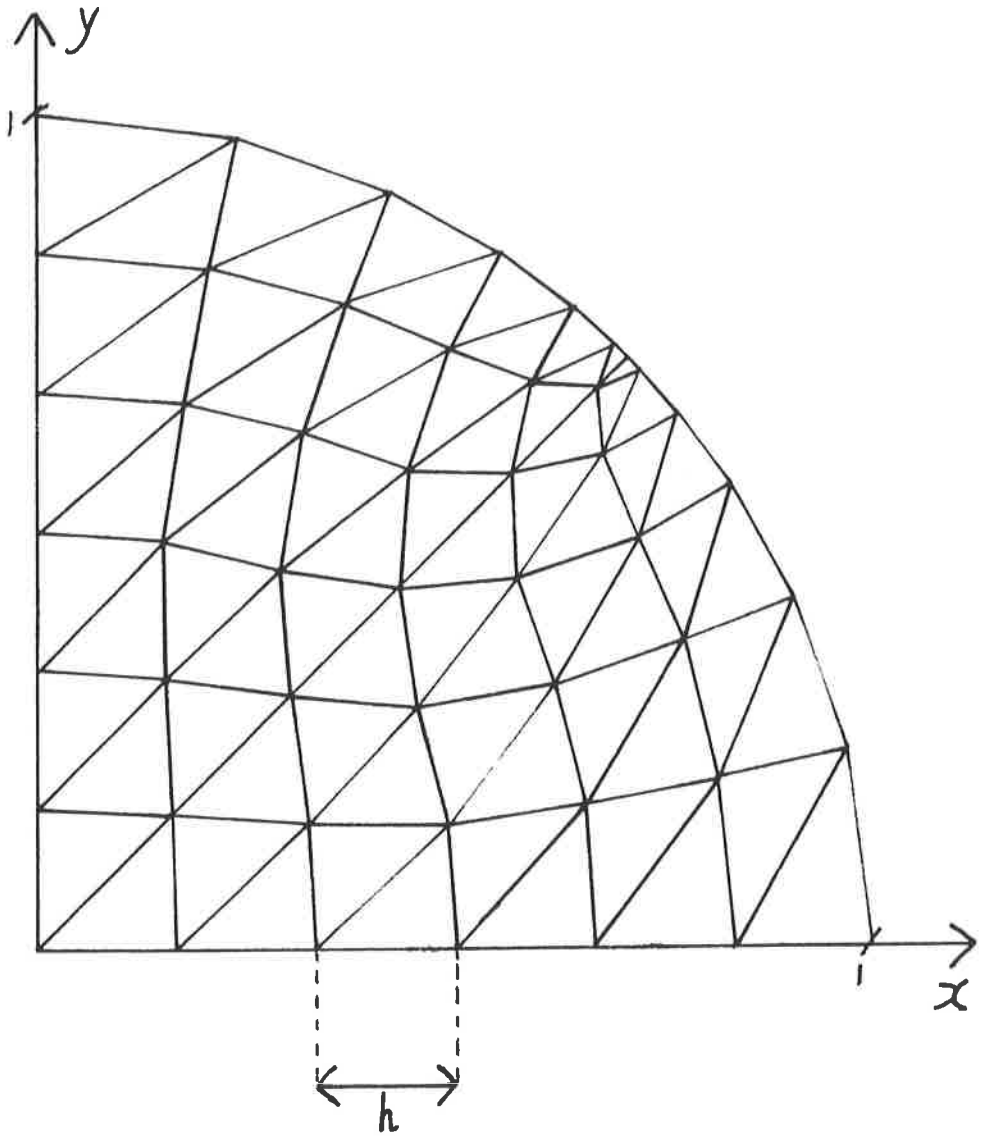

Figure 2.6.7

A superconvergent mesh on a quadrant

This mesh would be suitable for use in the triangulation of the circle (Figure 2.6.6).

with axes placed as shown in the figure. Writing h for the node separation along the axes, we obtain

$$| (I - R)u |_{1,\Omega_h} \simeq 1.3\, h^2$$

and $$E_{tgt} \simeq 1.4\, h^2.$$

For comparison, we repeat the calculation on the mesh shown in Figure 2.6.8 and obtain

$$| (I - R)u |_{1,\Omega_h} \simeq 1.5\, h^2;$$

again $$E_{tgt} \simeq 1.4\, h^2.$$

The latter triangulation falls into the class of meshes which are "not-recommended" – the six element property and (2.6.2) both fail – but the averaged errors are similar to those of the former mesh and the ease of generating it may be considered to be adequate compensation. We note however that the simpler mesh is not superconvergent in the neighbourhood of the origin.

The choice of triangulations for the circle is not limited to the two possibilities given by Figures 2.6.7 and 2.6.8. At the cost of greater complexity in chosing mesh points, though probably with a gain in accuracy due to the greater contraction, we can instead map acute angles onto the boundary of the circle. Further, it may turn out that the topology of the square is less suited to this transformation than, say, those of the octagon – recall Figure 2.3.3 – or hexagon. (For obtuse-angled regions such as these, we retain $\gamma \geq 2$ in (2.6.3) by applying first a suitable sheqring transformation in the vicinity of each vertex – see Figure 2.6.9.) In fact we can start from any convex polygon, using a different value of γ in (2.6.3) for the transformation in the neighbourhood of each vertex (although there seems to be little to be gained from such a process).

Now in a genuine application we would not be able to conduct a

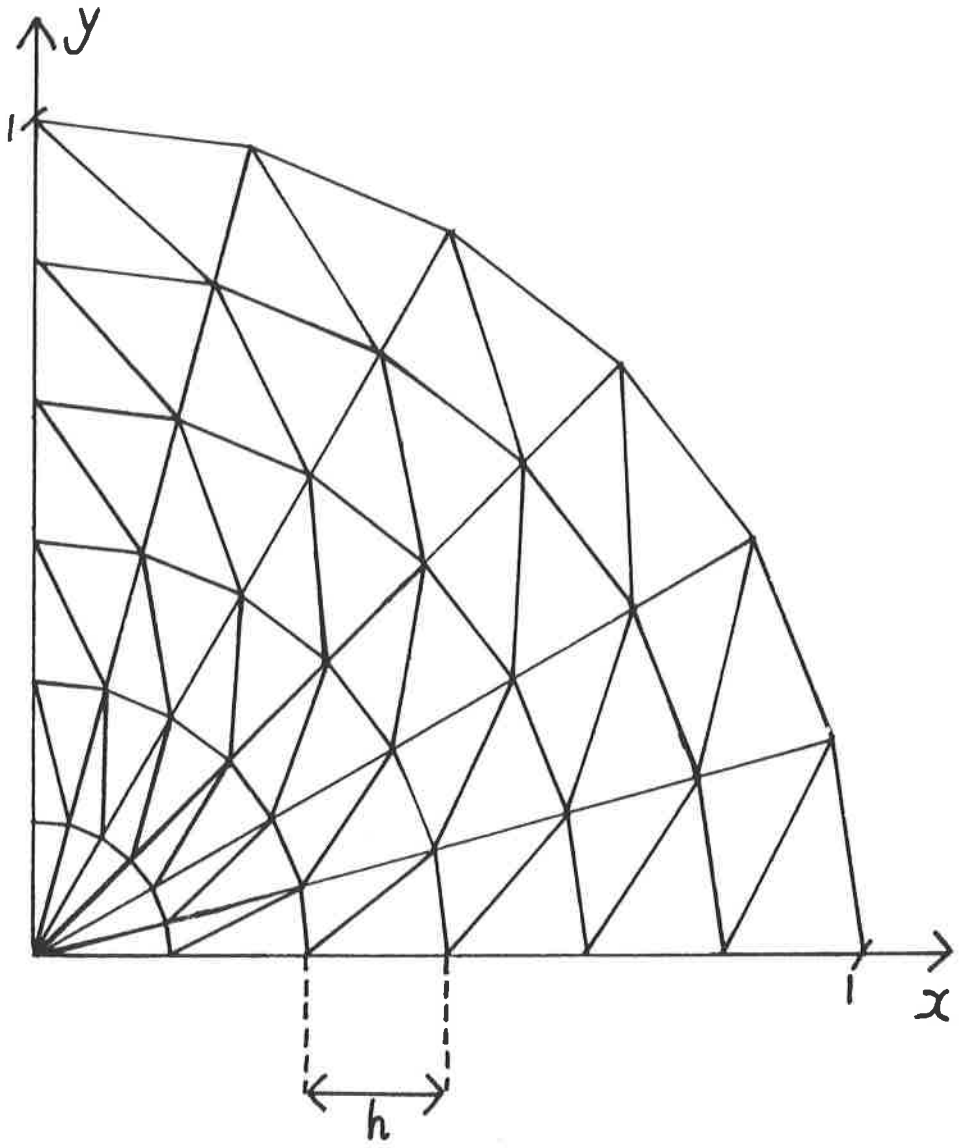

Figure 2.6.8

An alternative triangulation of the quadrant

This is superconvergent only in the sense of Theorem 2.4 – the geometric conditions of superconvergence fail near the origin.

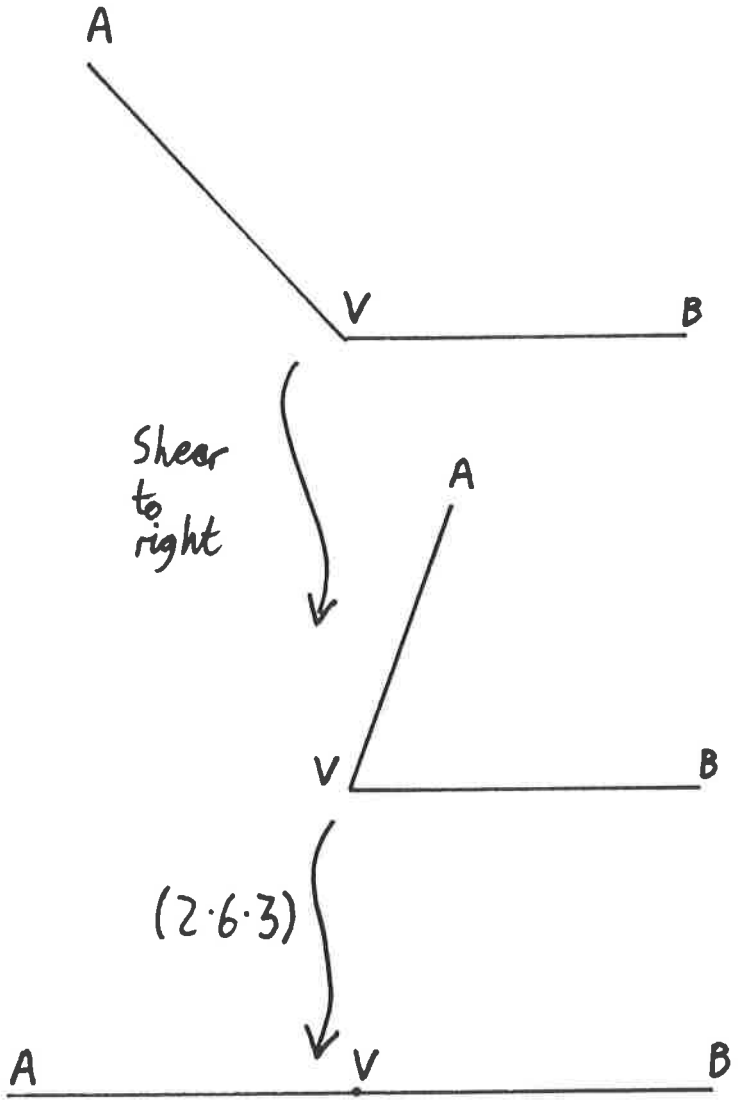

Figure 2.6.9

Combined transformation from obtuse angle to pseudo-vertex

series of experiments to compare the options for triangulation; neither the true solution u nor the resources for such experimentation would be available. We feel therefore that the ideas introduced in this chapter deserve a more detailed investigation. A balance must be sought: between the time of a programmer and that of a computer: the complexity of generating a mesh versus its efficency.

CHAPTER THREE

GRADIENT ESTIMATION FROM SUPERCONVERGENT APPROXIMATIONS

3.1 SAMPLING ONE COMPONENT

Suppose we are given a superconvergent triangulation of some domain Ω and a Finite Element approximation Ru to u on that mesh. How do we use Ru to obtain approximations to ∇u? This is the question to which we now turn. We assume that the first stage of the scheme of Table 1.3 has been successful and concentrate upon the second: a generalisation of the "location of the interpolant's stress points". For, once we have found an accurate method for estimating ∇u from Iu, we can complete the approximation process by applying precisely the same method to Ru. (As in the earlier derivation of (1.4.7) and (1.4.4) from (1.4.6) and (1.4.8), it is a simple matter to confirm the validity of the third step. See also Section 4.2.)

So the main subjects of this chapter are the methods and theory of gradient approximation from interpolants in the space S of piece-wise linears. Our starting point is the characterisation of stress points in Section 1.5: they are

> locations at which there exists a component of $\nabla(Iu - u)$ which vanishes when u is quadratic in a suitable neighbourhood. (3.1.1)

In this section we will examine the possibilities of sites and sampling directions other than those already found (i.e. tangential derivatives at element edge midpoints). The following result concerns the set of points which satisfy the description (3.1.1) given above.

Lemma 3.1 In every non-degenerate triangle there are precisely three points at which (3.1.1) holds and precisely one sampling direction at each point: these are the midpoints of the edges and

the tangential derivatives there.

Proof We prove this by chosing an arbitrary point and requiring it to satisfy (3.1.1). As in Lemma 2.2, we simplify our working with an affine transformation $(x,y) \to (\xi,\eta)$ which maps any element T onto the triangle T_+ with vertices $(\xi,\eta) \in \{(0,0), (1,0), (\xi_+,\eta_+)\}$. (Clearly, for each T there are - including reflections - six such transformations; the choice is arbitrary. Note however that for any such choice and with any definition of "non-degenerate triangles", we have $\eta_+ \neq 0$.) As before, we have the following correspondance between u and Iu on T_+ when u is quadratic:

$$\left.\begin{aligned} &\text{if } u = \xi^2 \text{ then } Iu = \xi + \eta(\xi_+^2 - \xi_+)/\eta_+ \ ; \\ &\text{if } u = \xi\eta \text{ then } Iu = \eta\xi_+ \ ; \\ &\text{if } u = \eta^2 \text{ then } Iu = \eta\eta_+ \ ; \\ &\text{if } u \text{ is linear then } Iu = u \ . \end{aligned}\right\} \quad (3.1.2)$$

Let (ξ,η) be a stress point for the derivative in the direction which subtends angle θ from the ξ-axis (see Figure 3.1.1):

$$[\partial_\theta (Iu - u)]_{(\xi,\eta)} = 0 \quad \text{for all quadratic } u, \quad (3.1.3)$$

where

$$\partial_\theta = \cos\theta \frac{\partial}{\partial\xi} + \sin\theta \frac{\partial}{\partial\eta} \ .$$

Equivalently, by (3.1.2),

$$\left.\begin{aligned} &2\,\xi\cos\theta = \cos\theta + (\xi_+^2 - \xi_+)\,\eta_+^{-1}\sin\theta \ , \\ &\eta\cos\theta + \xi\sin\theta = \xi_+\sin\theta \\ &\text{and} \qquad 2\,\eta\sin\theta = \eta_+\sin\theta \ . \end{aligned}\right\} \quad (3.1.4)$$

Now, by the third of these identities,

$$\text{either } 2\eta = \eta_+ \quad \text{or} \quad \sin\theta = 0. \quad (3.1.5)$$

Clearly, this is very limiting. With the first option, writing

$$C = \cot\theta,$$

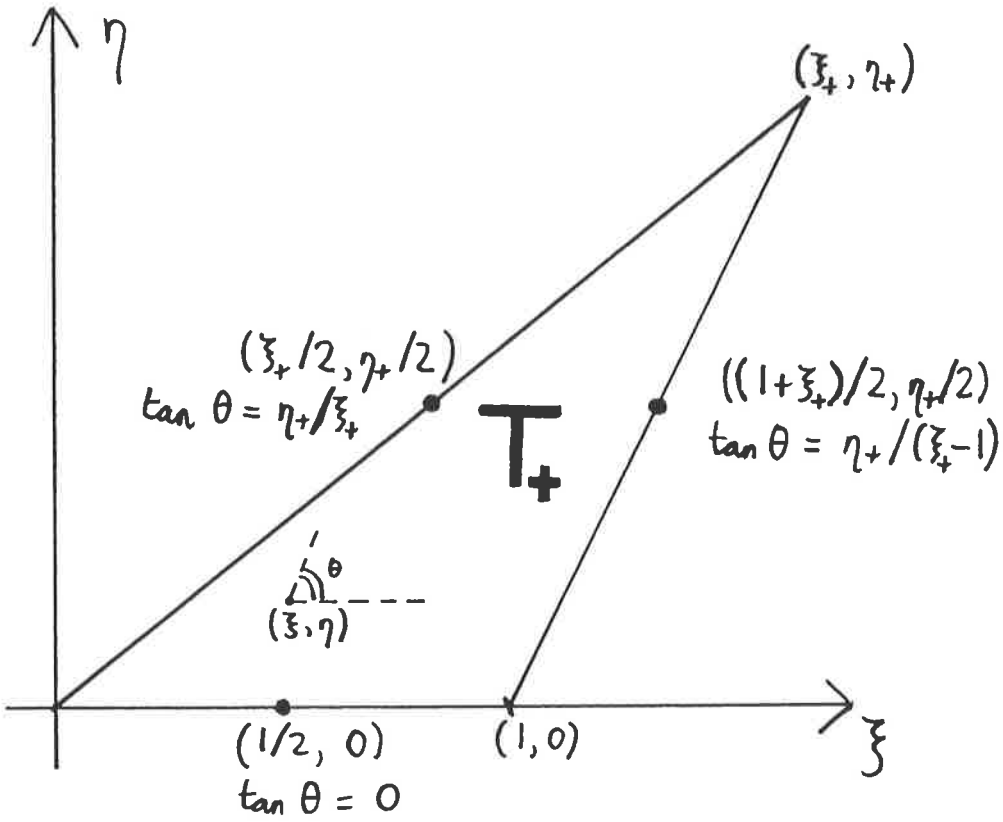

Figure 3.1.1

Stress Points

They are located at the midpoints of each edge and are applicable only for tangential derivative sampling, i.e. in the directions whose tangents are given here.

the first two of the identities (3.1.4) become

$$\left.\begin{aligned} 2\eta\,(2\xi - 1)\,C &= \xi_+^2 - \xi_+ \\ \text{and} \qquad \eta\,C + \xi &= \xi_+ \,. \end{aligned}\right\} \quad (3.1.6)$$

Eliminating C from (3.1.6),

$$2\,(\xi_+ - \xi)\,(2\xi - 1) = \xi_+^2 - \xi_+ \,;$$

this rearranges to

$$(\xi_+ - 2\xi)\,(\xi_+ - 2\xi + 1) = 0 \,. \qquad (3.1.7)$$

Now by (3.1.5) and (3.1.6),

either $2\eta = \eta_+$, $\tan\theta = C^{-1} = \eta\,/\,(\xi_+ - \xi)$ and (3.1.7) holds

or $\sin\theta = 0$.

Hence either (taking the first option in (3.1.7))

$$\left.\begin{aligned} (\xi,\eta) &= (\,\xi_+/2\,,\,\eta_+/2\,) \\ \text{and} \qquad \tan\theta &= \eta_+/\xi_+ \end{aligned}\right\}$$

or (the second option)

$$\left.\begin{aligned} (\xi,\eta) &= (\,(\xi_+ + 1)/2\,,\,\eta_+/2\,) \\ \text{and} \qquad \tan\theta &= \eta_+/(\xi_+ - 1) \end{aligned}\right\}$$

or (using (3.1.4) and the second option in (3.1.5))

$$\left.\begin{aligned} \tan\theta &= 0 \\ \text{and} \qquad (\xi,\eta) &= (\,1/2\,,\,0\,) \,. \end{aligned}\right\}$$

So the three stress points found in Chapter 1 are the only points in the triangle T satisfying (3.1.3) for any θ (see Figure 3.1.1); in particular there are no points (ξ,η) in any triangle of any shape at which (3.1.3) holds for all θ, i.e. for the full gradient. ###

Now, there are two reasons why this lemma is not mathematically equivalent to the statement that there are no points at which ∇Ru estimates ∇u to $O(h^2)$. There might exist new triangulation configurations in which ∇Ru is close to some member $\hat{I}$ of S with sampling properties different from those of the

interpolant and there does exist a modification to our results (see Section 3.4) in which it is sufficient merely that

$$[\partial_\Theta (Iu - u)]_{(\xi,\eta)} = O(h^2) \qquad (3.1.8)$$

for all quadratic u. We regard these possibilities as inadequacies in the description (3.1.1) and will return to this matter later (especially in Section 3.2).

We examine now a strong, though somewhat informal, alternative justification for the "tangential derivative at midpoints" sampling policy. Hitherto we have considered the success of the sampling scheme only in terms which are open to direct measurement: the optimal sampling location is specified (albeit with the approximation properties of quadratics - i.e. Lemma 3.1. - in mind) and the error there bounded or measured experimentally. An altogether different approach is to specify an "ideal" error (zero!) and then locate experimentally the sampling points which yield this error.

To be specific, for each element edge we locate the "zero point" - that point where the tangential component of $\nabla(Ru - u)$ is zero. We note that there may well exist edges which do not contain a zero point for the triangulation and unknown u under consideration; in the table that follows we classify such points under the heading "out of range". (Incidentally, by Rolle's Theorem, every edge does contain a zero point for the interpolant.) On the other hand the function u, whose approximation we consider in the following examples, does not have any inflections and so there can be no more than one zero point on each edge.

Let us denote the ratio of a zero point's distance from the midpoint to the half-length of the edge by d (see Figure 3.1.2).

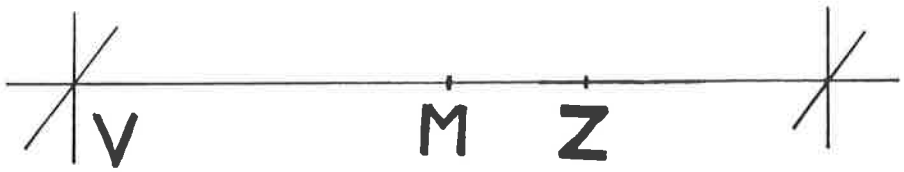

Figure 3.1.2

A Zero Point

V is a vertex of the edge, *M* is the midpoint and *Z* is the zero point. The ratio *d* is given by:

$$d = \frac{MZ}{MV} .$$

We divide the range $0 \leq d \leq 1$ into (twenty) smaller subintervals and tabulate against d the number N of zero points found in each interval, searching through the set of element edges. (We exclude edges which link two boundary nodes.) We expect the distribution N/d to be clustered around $d=0$ (zero points should tend to the midpoints as $h \to 0$) with a weaker grouping for non-superconvergent meshes.

We define u by (1.6.2) and approximate it by (1.6.1) as usual, taking (a) $h = 1/6$ and (b) $h = 1/8$ on the following regions:

(1) Ω is the unit square; uniform triangulation as in Figure 1.5.1. (Superconvergent.)

(2) Ω is the unit square; criss-cross triangulation as in Figure 2.4.1. (Nowhere superconvergent.)

(3) Ω is the "truncated" unit square, triangulated as in Figure 3.1.3. (Superconvergence improves towards the origin. Globally $|(I - R)u|_{1,\Omega} = O(h^{3/2})$ - the derivation of this bound is closely related to Theorem 2.4. See also Křížek & Neittaanmäki (1984).)

Our results are displayed in Table 3.1 and the above predictions on the distribution of d readily confirmed. (For further examples see Levine, 1982.) We note that the distribution is reasonably well clustered about the midpoints in case (1) and in case (3) where the dominant error contributions come from a small subregion of Ω. Indeed, even in the total absence of superconvergence - case (2) - the zero points show a marked grouping about the stress points: for the coarser mesh, zero points of over half the element edges are within a distance of less than 10% of the edge length from the midpoint. We note also that for all three cases the grouping becomes tighter when the

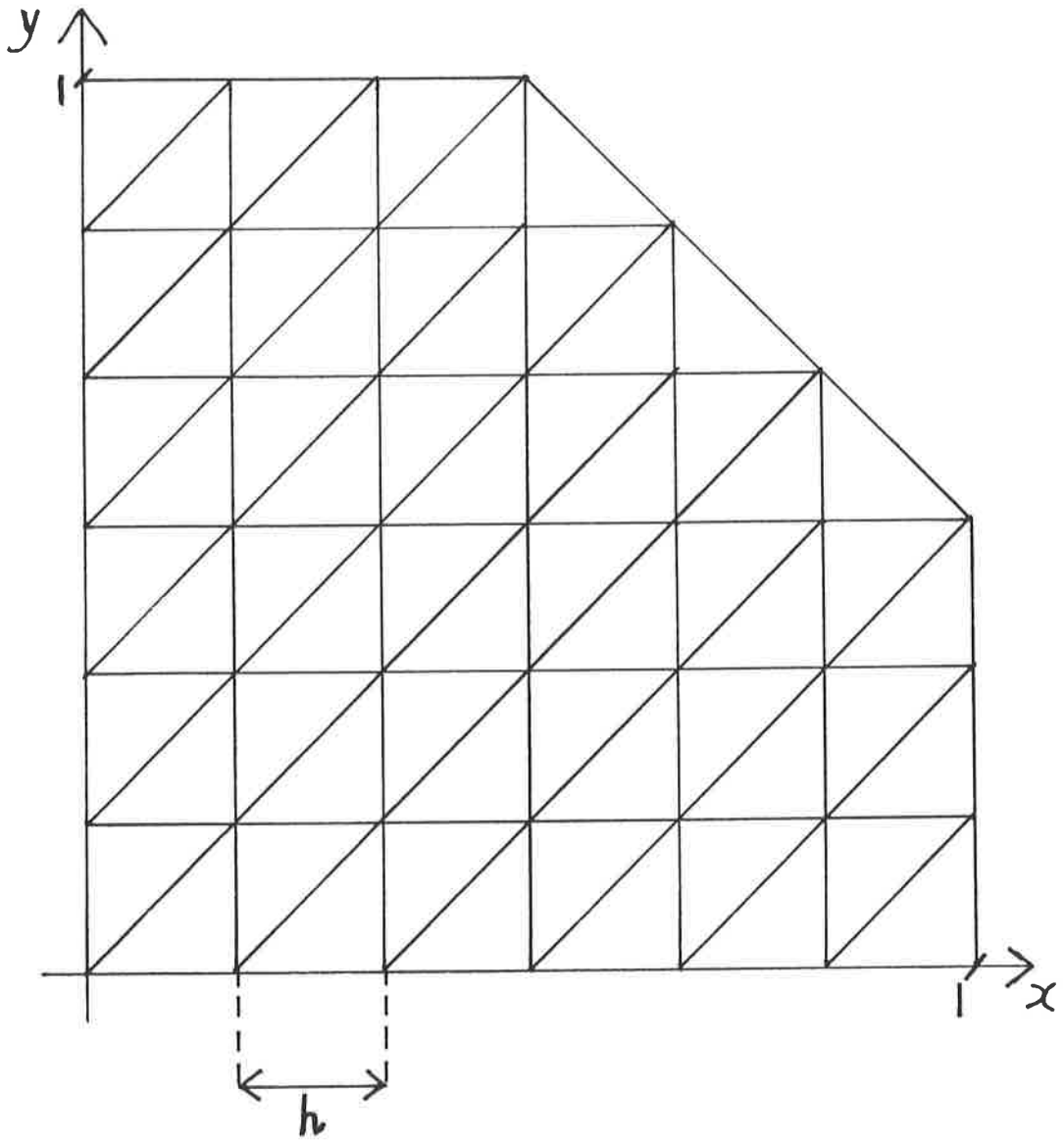

Figure 3.1.3

The truncated square

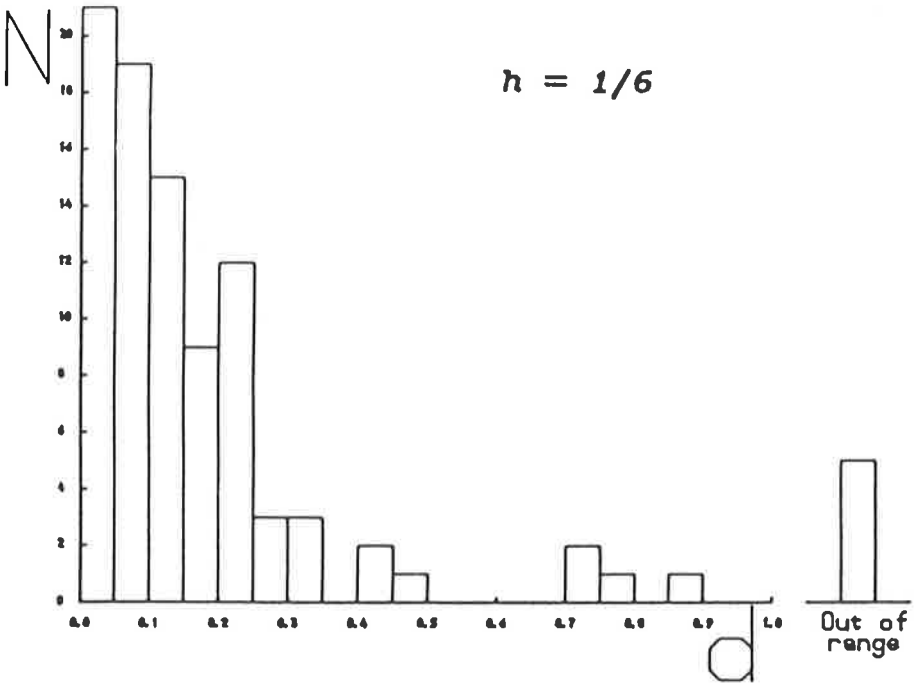

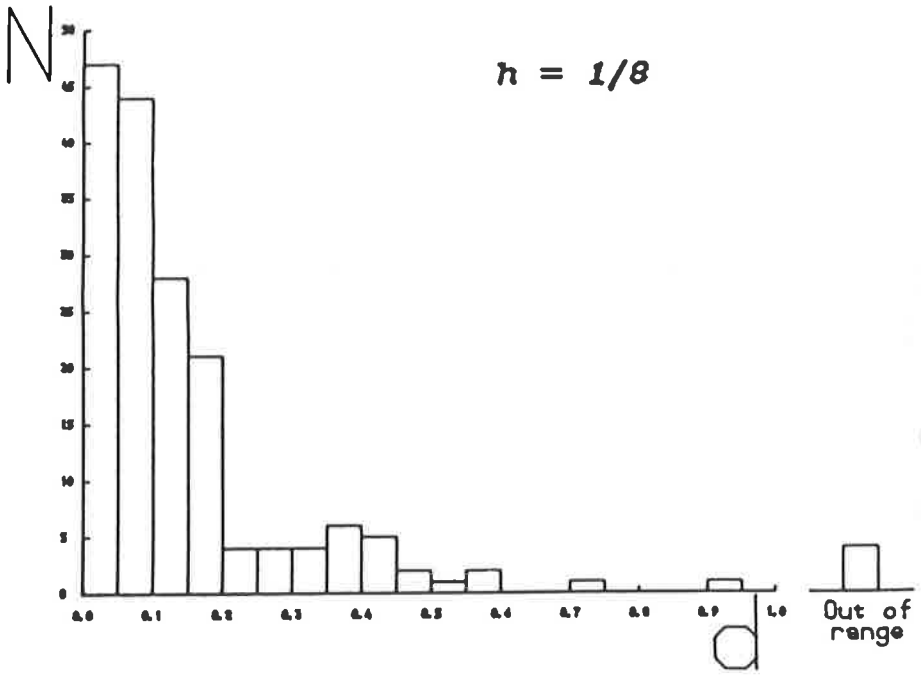

Table 3.1

Distribution of zero points

Mesh (1) - see Figure 1.5.1.

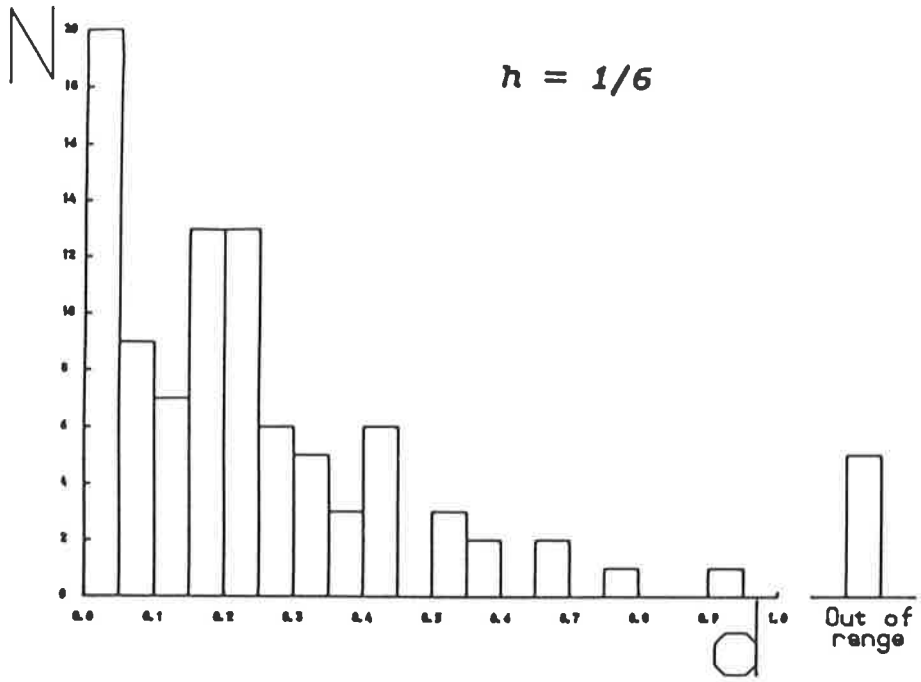

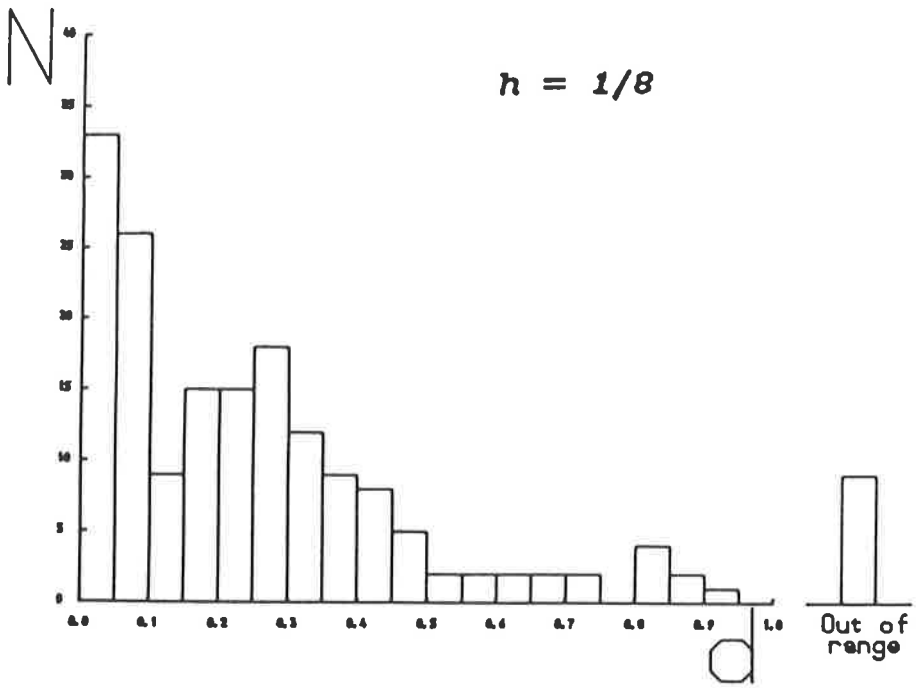

Table 3.1 (continued)

Mesh (2) - see Figure 2.4.1.

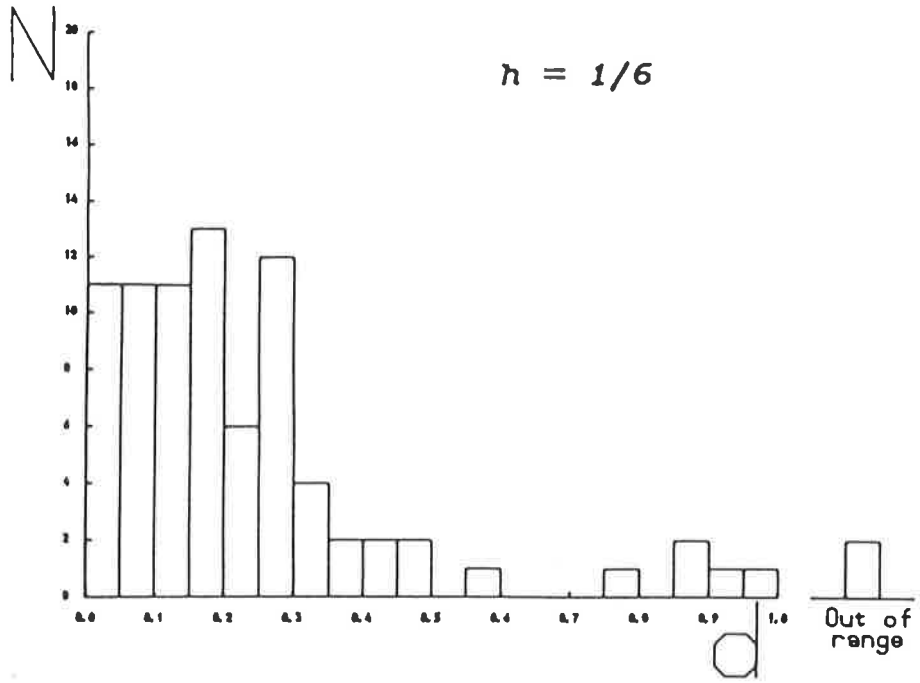

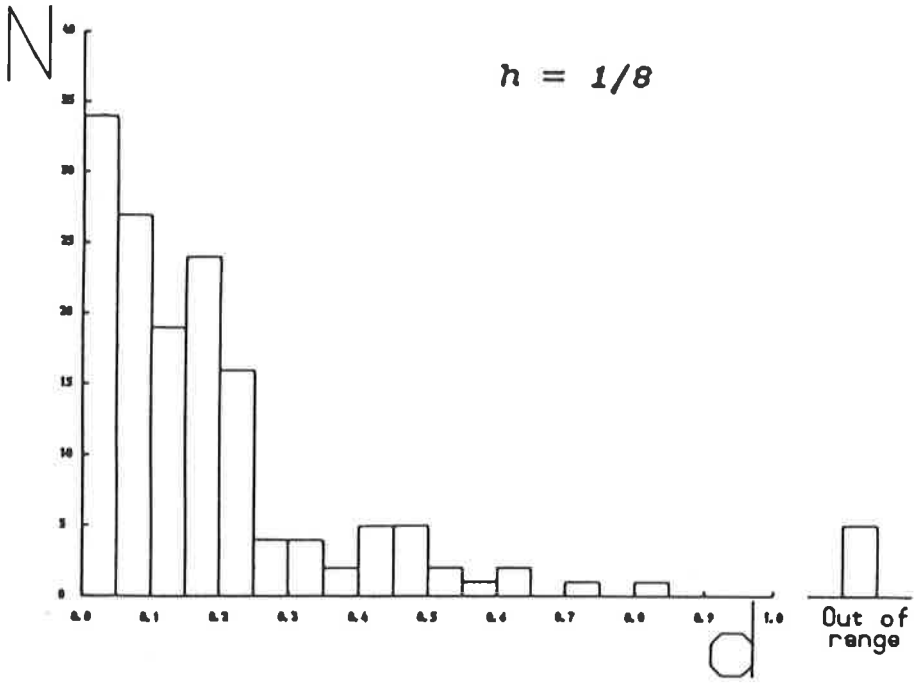

Table 3.1 (continued)

Mesh (3) - see Figure 3.1.3.

mesh is refined.

These examples therefore lend strong weight to a policy of selecting edge midpoints as stress sampling points, even when the mesh is not superconvergent. For, on average and irrespective of the value of $|(I-R)u|_{1,\Omega}$, the interpolant error is minimised by such a procedure. What our examples demonstrate is that this minimisation is significant.

3.2 SAMPLING BOTH COMPONENTS

As noted above, stress points for the full gradient do not exist. Lemma 3.1, although not a formal proof, should be seen as sufficient indication of this. However, against the once popular cause of centroid stress points, it is worth taking the argument further. The following "inability to approximate" theorem links some ideas from the last section with remarks in Section 1.5 on centroid results and the continuity of the approximation space S. It is based on the more general characterisation (3.1.8) for stress points.

We start by introducing the notion of a "reasonable triangulation" with mesh parameter h. This is a member of a series of mesh refinements such that the non-degeneracy property (2.6.2) holds, h is the longest element edge and the following "limiting patch" property holds for all but at most $o(h^{-2})$ of the internal nodes. As $h \to 0$ the number J of elements (T_j, $j = 1,\ldots,J$) in the patch surrounding each node tends to some limit (particular to that node) and the positions ((x_j,y_j), $j = 1,\ldots,J$) of the J nodes which define the patch can be expressed as functions of h (see Figure 3.2.1).

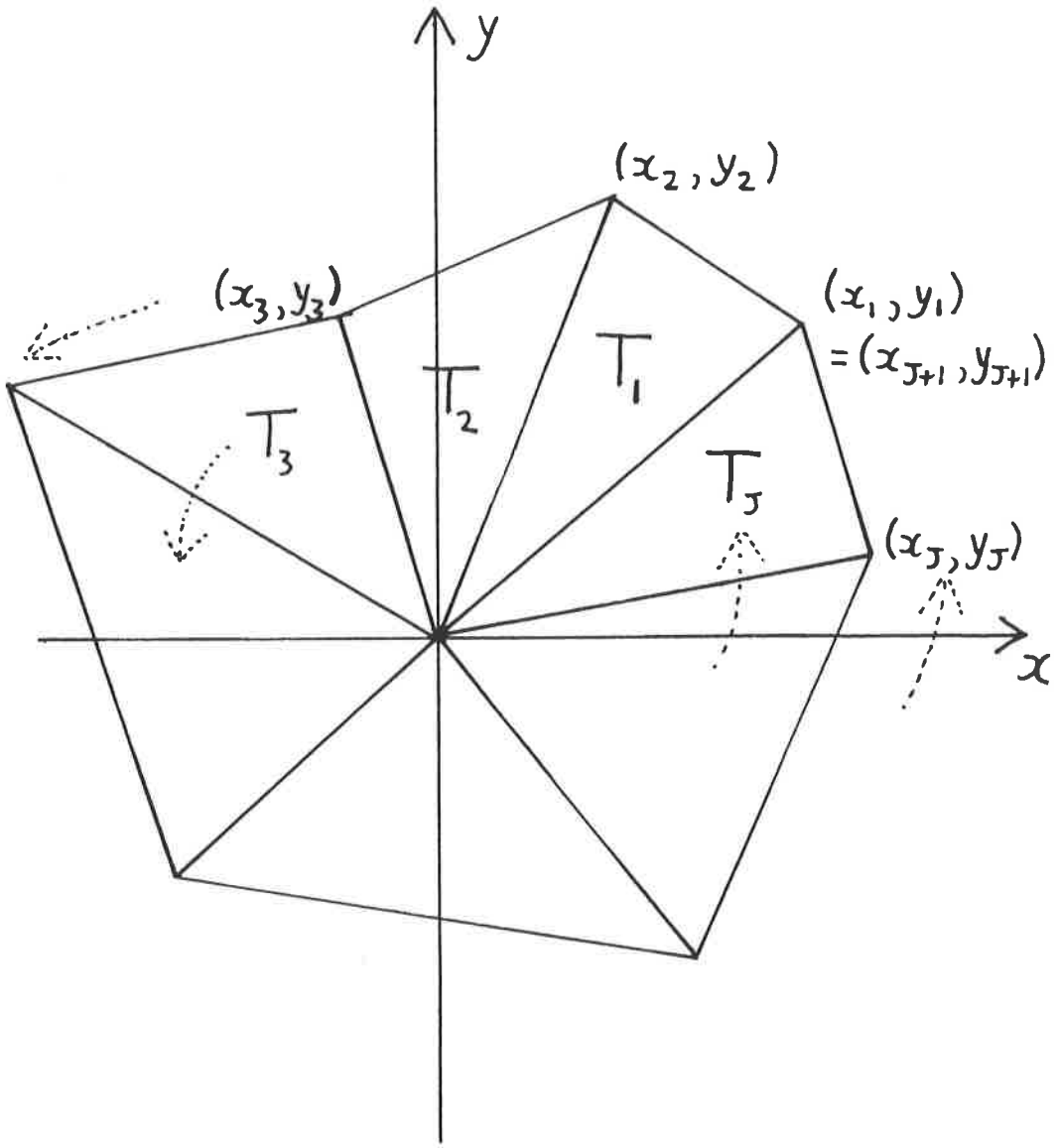

Figure 3.2.1

Notation for a patch of elements

If the patch has the limiting property then (x_j, y_j) are functions of h, $j = 1, \ldots, J$ and J is fixed for sufficiently small h. Note that the path of nodes $(x_1, y_1) - (x_2, y_2) - \ldots - (x_J, y_J) - (x_1, y_1)$ encloses the origin, once, moving strictly anti-clockwise.

We expect all computer-generated meshes to be reasonable; certainly all the triangulations of Chapter 2 - superconvergent or otherwise - satisfy this property.

Let us consider the patch surrounding an internal node with the limiting patch property. W.l.o.g. we take the coordinates of that node to be the (x,y)-origin, for all h. We then label the surrounding nodes and elements as in Figure 3.2.1. Note that J must be finite and that the average of J over the whole triangulation tends to 6 (given by *2π/(the average internal angle in the triangulation)*). We note further that, as a particular consequence of (2.6.2) and the bound on J, for every element T_j in a patch with the limiting property,

$$meas\ (T_j) \ > \ ch_*^2 \quad \text{for some fixed } c > 0,$$

where h_* is the maximum edge length in the patch.

The result that follows is asymptotic in nature; on coarse meshes we resort to the numerical indications of Section 1.6. Note also that the proof fills the gap in Lemma 3.1 due to the weakness of (3.1.1), and that the methods used here could be applied to prove a stronger version of that lemma in which stress points would be characterised by (3.1.8).

Theorem 3.2 Let the set of elements in a reasonable triangulation of Ω be $\{T_k, \ k = 1,\ldots,K\}$. Let G_k be the centroid and h_k be the greatest edge length of each T_k. Then there exists a quadratic u on Ω such that, for all members ϕ of the space S of piecewise linears,

$$| \ [\nabla(u - \phi)]_{G_k} \ | \ > \ O(h_k^2) \qquad (3.2.1)$$

for at least ch^{-2} elements, $c > 0$.

Proof We suppose the result to be false (and derive a contradiction).

Then for all quadratic u, there exists $\phi = \phi(u) \in S$ for which

$$| [\nabla(u - \phi(u))]_{G_k} | = O(h_k^2) \qquad (3.2.2)$$

in all but at most $o(h^{-2})$ elements. So given sufficiently small h, there must exist (many times over) a pair of neighbouring internal nodes, both enclosed by a patch of elements with the limiting property, such that (3.2.2) holds in every element in the pair of patches when $u \in \{x^2, xy, y^2\}$. Further, if we set

$$\phi(\lambda x^2 + \mu xy + \nu y^2) = \lambda\phi(x^2) + \mu\phi(xy) + \nu\phi(y^2)$$

for all λ,μ,ν then (3.2.2) must hold in every element in the pair of patches for all quadratic u.

Let us concentrate on one of the patches. We use the notation of Figure 3.2.1, (w.l.o.g.) rotating the axes so that the node central to the second patch is on the x-axis (e.g. see Figure 3.2.3(b) below). We set

$$u = x^2 \quad \text{on} \quad \Omega.$$

Then by hypothesis there exists $\phi = \phi(u) \in S$ such that

$$[\nabla\phi]_{T_j} = [\nabla u]_{G_j} + O(h_j^2)$$

in each of the J elements of the patch. So

$$[\nabla\phi]_{T_j} = \left(\tfrac{2}{3}(x_j + x_{j+1}) , 0 \right)^T + O(h_j^2) , \qquad (3.2.3)$$

$j = 1,\ldots,J$. (The notations $\cdot_{J+j}$ and $\cdot_j$ are equivalent, for all j.)

Now ϕ is continuous and piece-wise linear; if we impose the continuity at the origin we can write

$$[\phi]_{T_j} = \alpha + \beta_j x + \gamma_j y ,$$

$j = 1,\ldots,J$. Then by (3.2.3)

$$\beta_j = \tfrac{2}{3}(x_j + x_{j+1}) + O(h_j^2)$$

and $$\gamma_j = O(h_j^2).$$

So

$$[\phi]_{T_j} = \alpha + \tfrac{2}{3}(x_j + x_{j+1})x + O(h_j^3) ,$$

$j = 1,\ldots,J$. Hence by continuity of ϕ at the nodes (x_j,y_j)

$$(x_j + x_{j+1})x_j + O(h_j^3) = (x_{j-1} + x_j)x_j + O(h_{j-1}^3) ,$$

$j = 1,\ldots,J$. Therefore (we recall that $h_* = max_j\ (h_j)$)

$$x_j(x_{j+1} - x_{j-1}) = O(h_*^3) , \qquad (3.2.4)$$

$j = 1,\ldots,J$.

We use (3.2.4) to set up some contradictions. We start by making a hypothesis: that for some $c > 0$ and all $j = 1,\ldots,J$,

$$|x_j| \geq ch_* . \qquad (3.2.5)$$

(In other words, there is no nearly vertical edge connected to the origin.) Then (3.2.4) implies that

$$|x_{j+1} - x_{j-1}| = O(h_*^3)/|x_j| = O(h_*^2) , \qquad (3.2.6)$$

$j = 1,\ldots,J$. Now either $x_1x_2 > 0$ or $x_1x_2 < 0$ (recall (3.2.5)). In the first case, (3.2.5) and (3.2.6) imply that $x_1,\ldots,x_J$ are all of the same sign; in the second case $x_1,\ldots,x_J$ must be of alternating signs and J therefore even. Hence the ordered path of nodes $(x_1,y_1) \rightarrow (x_2,y_2) \rightarrow \ldots \rightarrow (x_J,y_J) \rightarrow (x_1,y_1)$ crosses the y-axis either not at all or more than twice (in fact: J times, where $J \geq 4$). Both these deductions lead to a geometric contradiction with the notion of a patch of elements (see Figure 3.2.2); we deduce that hypothesis (3.2.5) is false.

We have shown that at least one of the nodes is distance $o(h_*)$ from the y-axis; w.l.o.g let this be the first in our numbering:

$$x_1 = o(h_*).$$

Now, the measure of element T_1 is given by

$$2\ meas\ (T_1) = x_1y_2 - x_2y_1 ;$$

as already noted, this quantity is greater than $o(h_*^2)$. But

$$x_1y_2 = o(h_*^2) \quad \text{and} \quad y_1 = O(h_*).$$

Therefore

$$|x_2| > o(h_*).$$

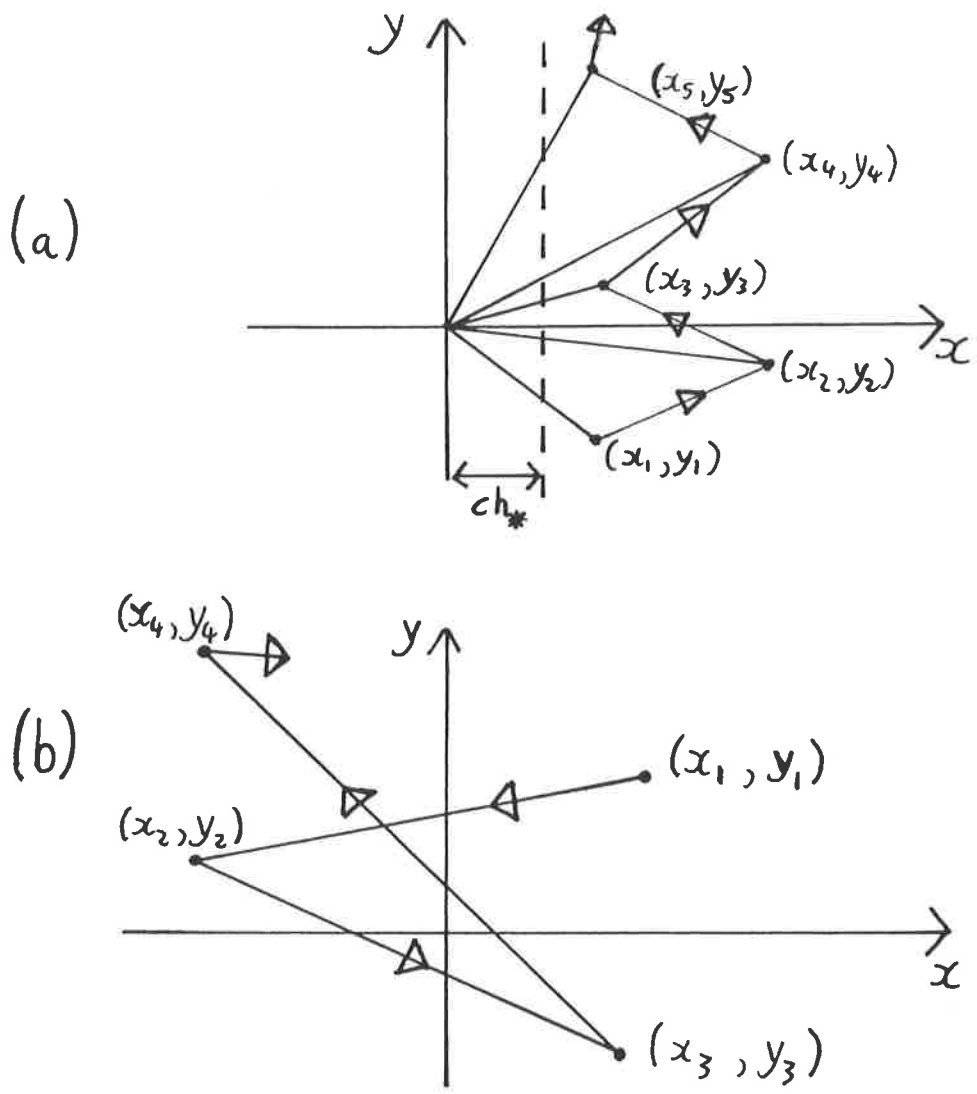

Figure 3.2.2

Possibilities under the assumption that (3.2.5) holds

(a) x_1 and x_2 have the same sign. Then by (3.2.6) all x_j have the same sign and the elements T_j fail to enclose the origin.

(b) x_1 and x_2 have different signs. By (3.2.6) all x_j and x_{j+2} have the same sign; therefore in particular J is even. It must be greater than 2. So as in the diagram, the path between nodes crosses the y-axis at least four times. The obvious requirement (recall Figure 3.2.1) that this path should enclose the origin "once, moving strictly anti-clockwise" is not met.

Hence, using (3.2.4) , $|x_3 - x_1| = o(h_*^2)$, i.e.

$$x_3 = o(h_*).$$

Continuing with a simple induction process,

$$\left.\begin{aligned} |x_j| &> o(h_*) \quad \text{for all even } j \\ \text{and} \qquad x_j &= o(h_*) \quad \text{for all odd } j \ . \end{aligned}\right]$$

So in particular J must be even. Further (see Figure 3.2.3(a)) if $J > 4$ we arrive at another geometric contradiction. Therefore

$$\left.\begin{aligned} J &= 4 \\ x_1, x_3 &= o(h_*^2) \\ \text{and} \qquad |x_2|, |x_4| &> o(h_*^2) \ . \end{aligned}\right] \quad (3.2.7)$$

Now, we recall that there exists a second patch of elements, with the limiting property, partly overlapping the first patch $\{T_1,\ldots,T_4\}$ and centred about a node on the x-axis. W.l.o.g. we can take this node to be (x_2,y_2). Further (3.2.2) holds at every centroid in this patch. Therefore by the above argument, the second patch also consists of four elements. (See Figure 3.2.3(b): the four nodes which define the boundary of the patch are at $(0,0)$, (x_1,y_1), (x_*,y_*) and (x_3,y_3).) Again using our earlier reasoning, two of the four nodes which define the patch have x-coordinates which differ from x_2 by $o(h_*)$. But these two coordinates must be x_1 and x_3 and so (3.2.7) is contradicted:

$$|x_1 - x_2| = o(h_*) \quad \text{and yet} \quad |x_1 - x_2| > o(h_*).$$

Thus we are forced to the conclusion that our central supposition is false; the theorem is proved. ###

Let us now interpret the statement of the theorem: for any (reasonable) triangulation and any method of approximation (whatsoever) by members of S, a very large number of centroids fail to be full derivative stress points for the estimation of even the simplest of gradients. We note that the centroid of a

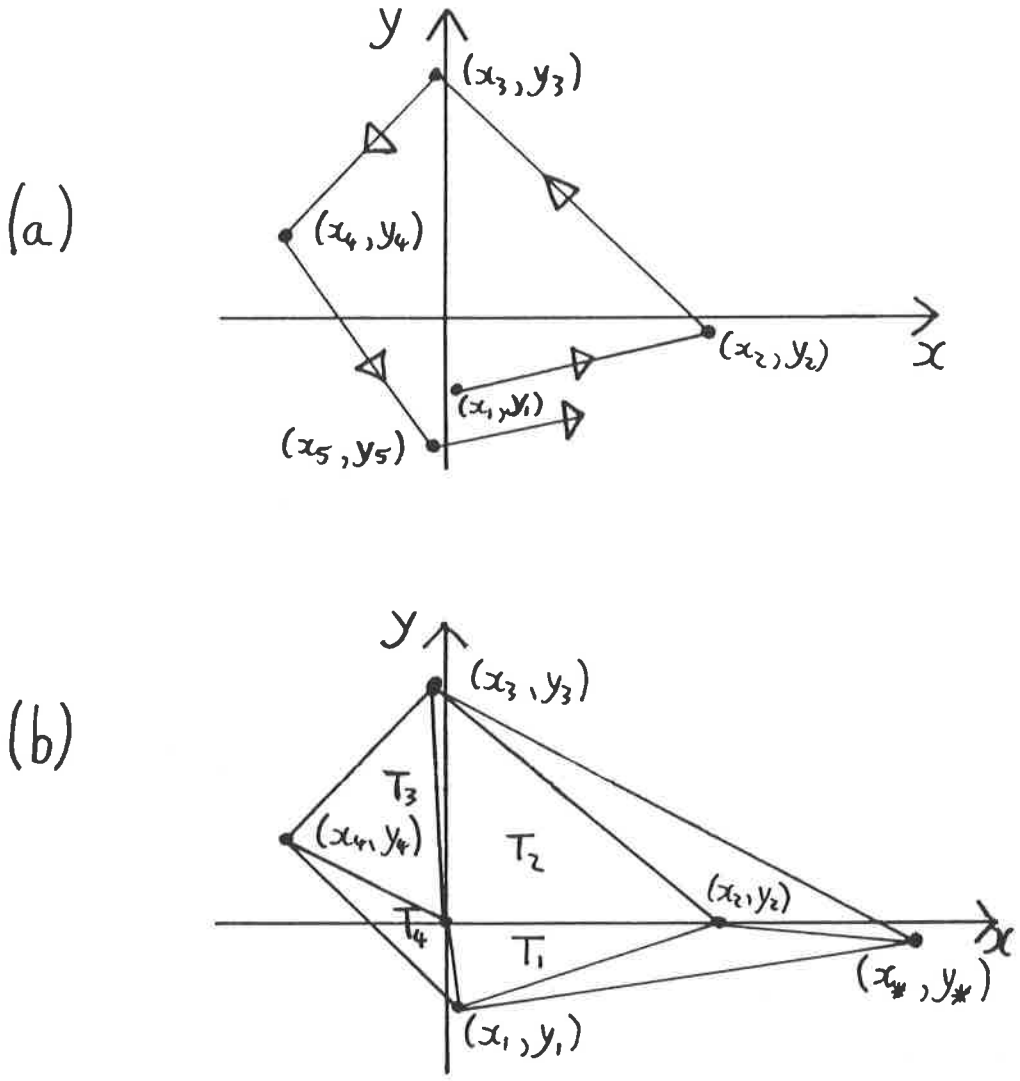

Figure 3.2.3

Possibilities, given that (3.2.5) does not hold

(a) $J \geq 6$. The presence of a third node close to the y-axis, followed by another away from the axis, contradicts the "once, moving strictly anti-clockwise" requirement of Figure 3.2.1.

(b) $J = 4$. By consideration of a second patch of elements, namely that centred about (x_2, y_2), we reach a contradiction of (3.2.7).

triangle cannot be associated with any naturally preferred single direction (unlike points on element edges - for example these can be naturally associated with either the normal or the tangent). So centroids are not stress points for single stress components either. While we are on the subject of natural choice, if a full derivative stress point exists anywhere else in a triangle (i.e. not at the centroid) then there must exist at least three such points. But because approximating gradients are constant in the triangle, these points must lie within a distance $O(h^2)$ of each other just to satisfy the generalised requirement (3.1.8). If their locations are to be naturally chosen this then means that all three points lie within a distance $O(h^2)$ of the centroid. So, almost exactly as in the theorem, none of the points is a full derivative stress point after all. We conclude instead that there is no such thing as a full derivative stress point. Yet a method for obtaining both components of ∇u (at special points or, ideally, anywhere) is clearly desirable. We need a stronger "post-processor" than point sampling; such a technique is commonly called "recovery". We will start in Section 3.3 with recovery methods which apply to uniform (banded) triangulations.

We note finally that Theorem 3.2 is of greater generality than the outline of superconvergence presented in Table 1.3: it is independent of the role of the interpolant and hence of the notion of superconvergent triangulations. It may well be possible that with different modes of smooth triangulation - globally curved criss-cross meshes for example - there still exist functions $\hat{I}u \in S$ which satisfy

$$|(\hat{I} - R)u|_{1,\Omega} \leq ch^2|u|_{3,\Omega}$$

and whose properties can thus be substituted for those of the interpolant in the construction of sampling/recovery schemes. But we do not expect to simplify our task with such a procedure; in particular we have proved that no choice of triangulation and $\hat{I}$ will allow us to sample, to superconvergent accuracy, both components of the gradient at a single point.

3.3 RECOVERY OF BOTH COMPONENTS

We have seen that no method of approximation by members of the space S - and in particular no Finite Element projection or interpolant into S, on any mesh - is suitable for superconvergent sampling of the full gradient. However there exists a very straightforward method for "recovering" from $\nabla I u$ a superconvergent estimate of ∇u at each stress point (in the interior of a band): we simply average $\nabla I u$ between the two neighbouring elements. We say that this is a "local" recovery scheme - it is the (bounded) weighted average of the values of $\nabla I u$ in a bounded number of neighbouring elements. From this we will construct later other local schemes for recovery at any point in any superconvergent triangulation.

Now, as in in derivations of (1.4.8) and (1.5.10), a sufficient condition for a local scheme to recover ∇u from $\nabla I u$ to superconvergent accuracy is that there should be no error when u is quadratic. Also, as noted in Section 3.1, any local scheme which recovers to superconvergent accuracy from $\nabla I u$ will have the same effect on $\nabla R u$. So, given a superconvergent triangulation, sufficient conditions for a scheme to lead to superconvergence are simply that it is local (this will obviously apply to all the

schemes in this and the next section) and that it recovers exactly the gradients of all quadratics from the gradients of their interpolants.

Let β be a band in a superconvergent triangulation of some region Ω. Let us denote by A_k, $k = 1,\ldots,K_A$ the element pairs associated with one of the three mesh directions of β. (We only consider uniformly triangulated bands in this section; therefore the A_k are parallelograms.) As in Section 1.5, we call the internal stress point and two constituent triangles of each pair M_k and $T_{k\pm}$. We write ∂_k for the local recovery operator at M_k introduced above:

$$\partial_k\phi = ([\nabla\phi]_{T_{k+}} + [\nabla\phi]_{T_{k-}})/2 , \quad \phi \in S. \qquad (3.3.1)$$

Finally, for fixed $k \leq K_A$, we denote by the subscripts $\cdot_{T;k}$ and $\cdot_{N;k}$ the components of any gradient tangential and normal to the edge on which the stress point M_k lies (example: $\partial_{T;k}u$).

Now, let us recall (1.5.5): if $\phi \in S$ then the tangential component $\nabla_{T;k}\phi$ of $\nabla\phi$ is a constant throughout A_k. So this component of a recovered gradient is identical to the sampled derivative and

$$\partial_{T;k}Iu = [\nabla_{T;k}u]_{M_k} \qquad (3.3.2)$$

for all quadratics u on A_k. (Note that, unlike the result (3.3.3) below for the normal component, (3.3.2) is independent of the shape of the quadrilateral A_k.) Therefore the following lemma is sufficient to prove superconvergence of the full recovered gradient, i.e. that

$$h \left[\sum_{k=1}^{K_A} \left| \partial_k Ru - [\nabla u]_{M_k} \right|^2 \right]^{1/2} \leq ch^2|u|_{3,\Omega} .$$

Lemma 3.3 Let u be quadratic on A_k for some $k \leq K_A$. Then

$$\partial_{N;k}Iu = [\nabla_{N;k}u]_{M_k} . \qquad (3.3.3)$$

Proof We reintroduce the transformation $(x,y) \to (\xi,\eta)$ of Lemma

2.2; we denote the recovery error by the functional

$$F(u) = \frac{1}{2}\left[\left[\frac{\partial Iu}{\partial \eta}\right]_{T_{k+}} + \left[\frac{\partial Iu}{\partial \eta}\right]_{T_{k-}} \right] - \left[\frac{\partial u}{\partial \eta}\right]_{(1/2,0)} .$$

Then (compare with (2.2.4))

$$F(\xi^2) = (\xi_+^2 - \xi_+)/2\eta_+ + (\xi_-^2 - \xi_-)/2\eta_- ;$$

$$F(\xi\eta) = (\xi_+ + \xi_- - 1)/2 ;$$

$$F(\eta^2) = (\eta_+ + \eta_-)/2.$$

But A is a parallelogram; the result now follows directly from (2.2.5). ###

For an indication of the numerical performance of the recovery scheme, we solve (1.6.1) with (1.6.2) on the usual uniformly triangulated unit square $\Omega = (0,1)^2$; we denote by E_{mid} the difference between the recovered and true (full) gradients, root-mean-square averaged over all stress points internal to Ω. We obtain

$$E_{mid} \simeq 3.0\, h^2 .$$

Since

$$E_{tgt} \simeq 1.4\, h^2 \qquad (3.3.4)$$

the (averaged) normal component of the error is given by

$$E_{norm} \simeq \sqrt{(3.0^2 - 1.4^2)}\, h^2 \simeq 2.7\, h^2 . \qquad (3.3.5)$$

So the recovery process (3.3.1) for the normal component can result in a noticeably greater error than sampling for the tangential component; we will discuss later an approach by which we may be able to avoid this significant loss of accuracy.

We turn now to recovery schemes for stress points which are not internal to their band (see also Section 3.5). We describe the schemes diagramatically: for an example see the representation of (3.3.1) in Figure 3.3.1.

The scheme shown in Figure 3.3.2(a) is suitable for a recovery point on $\partial\Omega$; we can prove this by a simple extension of Lemma

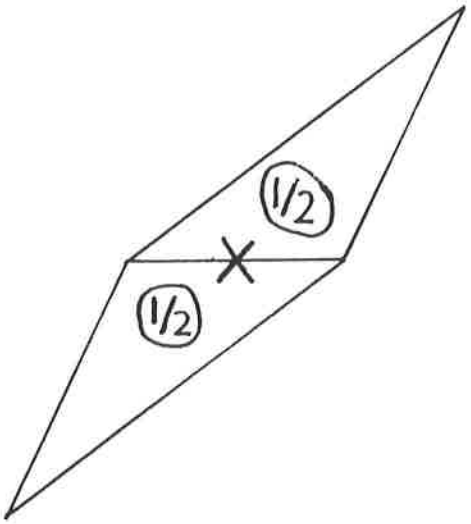

Figure 3.3.1

Graphical representation of the recovery scheme (3.3.1)

The weights in each element and the "recovery point" (the location at which the true gradient is estimated by the recovered gradient, to superconvergent accuracy) are indicated.

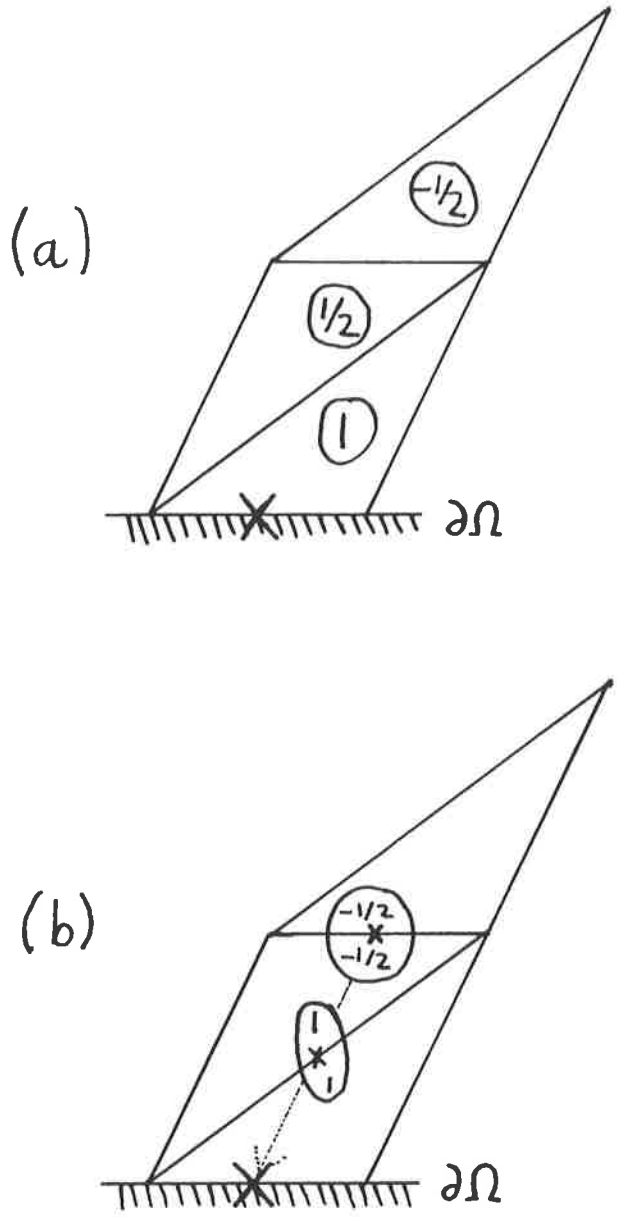

Figure 3.3.2

Recovery point on $\partial\Omega$

(a) A scheme which uses values of ∇Ru in three elements.

(b) The scheme is decomposed into recoveries at two other stress points and reassembled by linear extrapolation.

3.3. Less formally, we regard the scheme as the combination of recoveries at two other stress points, using the $O(h^2)$ accurate linear interpolation

$$\nabla w(z + \delta z) \simeq 2\nabla w(z) - \nabla w(z - \delta z) .$$

(See Figure 3.3.2(b); note that the above interpolation scheme is exact when w is quadratic.) By an identical argument, the scheme in Figure 3.3.3(a) also leads to superconvergence. Indeed any linear combination of the two schemes (such that the sum of weights is equal to one) will do this - see Figure 3.3.3(b) for an example.

On an internal band boundary, we can use any of the above schemes for $\partial\Omega$, taking values of ∇Ru from either side of the boundary. Alternatively we can combine schemes across the boundary, as in Figure 3.3.4. We can, however, find simpler schemes than this! For, so long as the sum of weights is equal to one, recovery is exact for all linear u (both components). We then require that (3.3.3) holds for all quadratic u; this gives us three additional conditions on the set of weights (i.e. a total of four). So no more than four elements are strictly necessary in the construction of a local recovery scheme for the normal component of the gradient.

Let us take as an example the band boundaries of the octagon triangulated in Figure 2.3.3. We work in the usual (ξ,η) coordinate system and select the four elements shown in Figure 3.3.5(a), with weights $\omega_1,\ldots,\omega_4$ as marked. Then the values in each triangle of $\partial Iu/\partial\eta$ $(=\partial_N Iu)$ for $u \in \{\xi^2,\xi\eta,\eta^2\}$ are as shown in Figure 3.3.5(b) and the conditions on the weights are thus

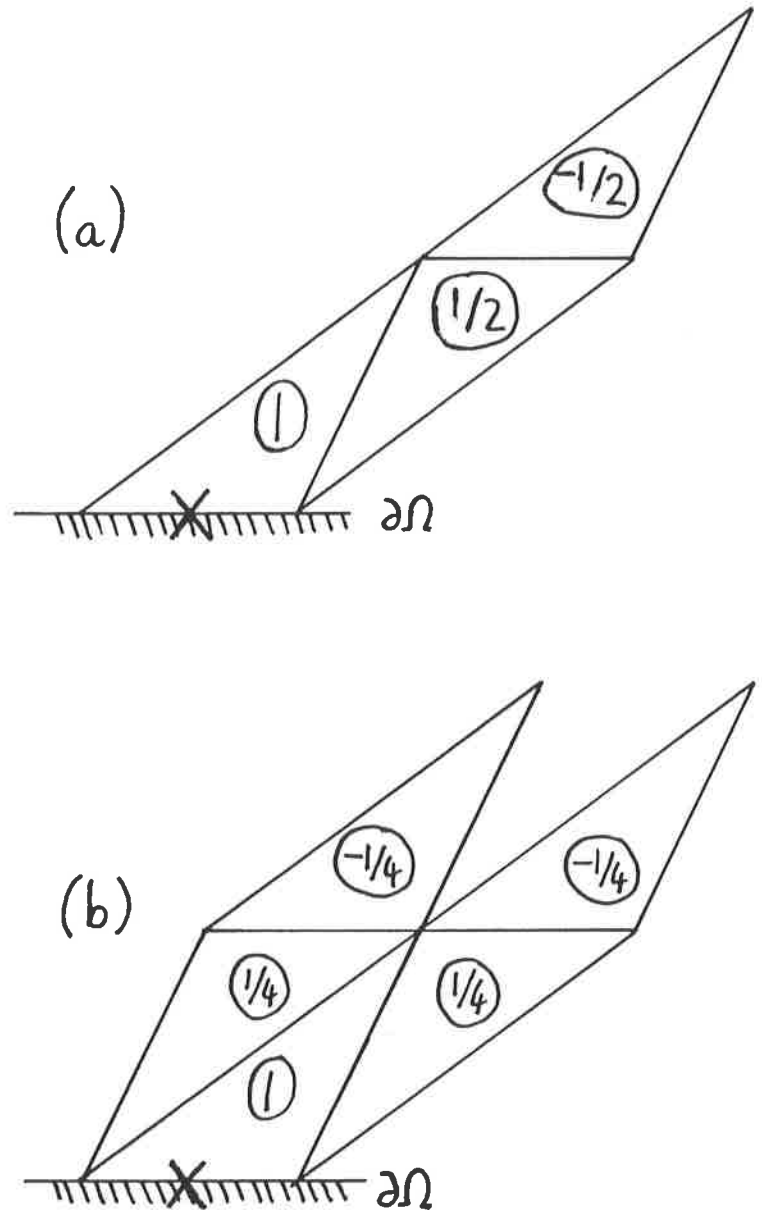

Figure 3.3.3

Alternatives for recovery on $\partial\Omega$

(a) The other three-element scheme (c.f. Figure 3.3.2(a)).

(b) A natural - though not necessarily useful - combination of the two: this is a five-element scheme.

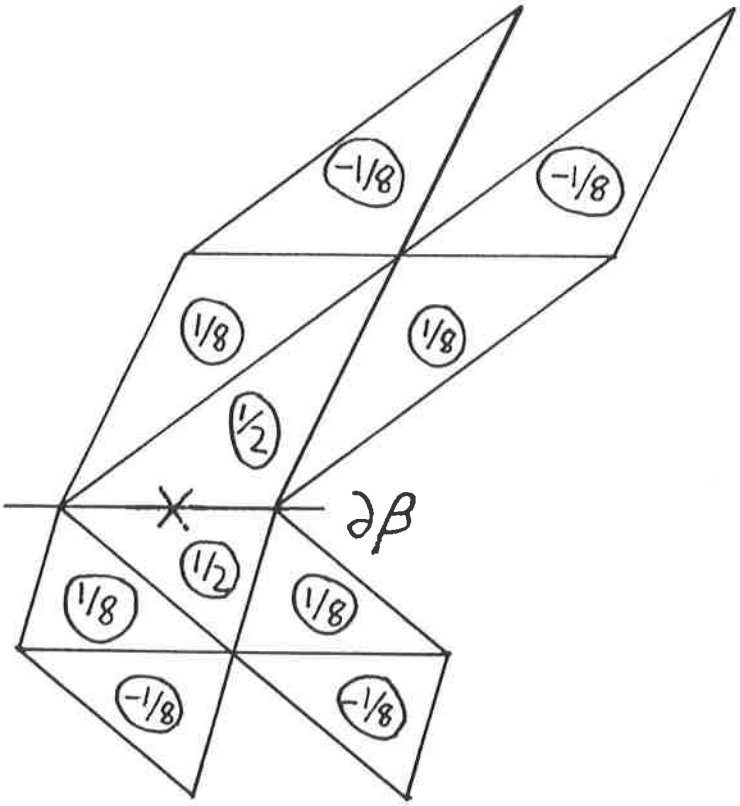

Figure 3.3.4

A cumbersome ten-element scheme for use on a band boundary

Note that (3.3.1) cannot be used at this recovery point: A_k is not (close to) a parallelogram.

(a)

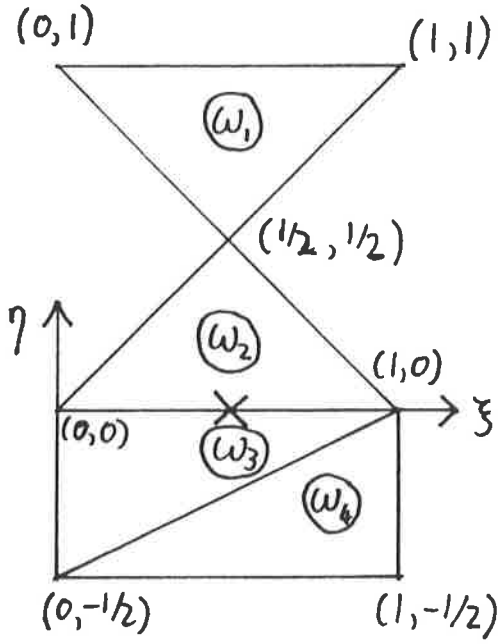

(b)

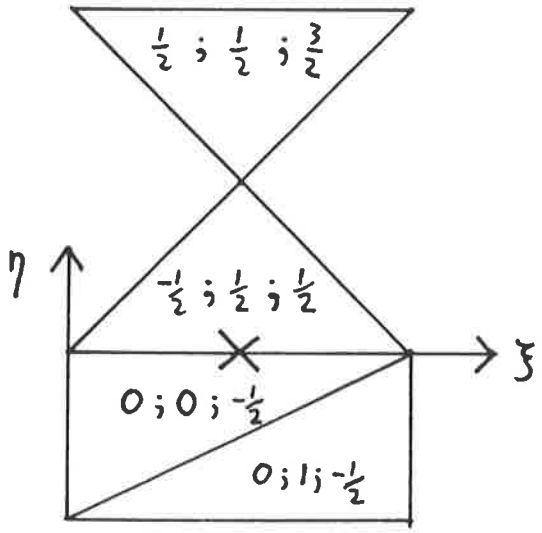

Figure 3.3.5

Recovery for the band boundaries of Figure 2.3.3

(a) Weights in four elements. Note that - for the purposes of asymptotic accuracy - the choice of elements is arbitrary.

(b) Values in each element of $\frac{\partial}{\partial \eta} I(\xi^2)$; $\frac{\partial}{\partial \eta} I(\xi\eta)$; $\frac{\partial}{\partial \eta} I(\eta^2)$.

$$\left.\begin{aligned} &\omega_1 + \omega_2 + \omega_3 + \omega_4 = 1 \ , \\ &(\omega_1 - \omega_2)/2 = 0 \ , \\ &(\omega_1 + \omega_2 + 2\omega_4)/2 = 1/2 \\ \text{and} \quad &(3\omega_1 + \omega_2 - \omega_3 - \omega_4)/2 = 0 \ ; \end{aligned}\right\} \quad (3.3.6)$$

therefore

$$\left.\begin{aligned} &\omega_1 = \omega_2 = 1/6 \\ \text{and} \quad &\omega_3 = \omega_4 = 1/3 \ . \end{aligned}\right\}$$

Note that, as with the other schemes proposed so far, this one preserves the property (3.3.2):

$$\partial_T Iu = \left[\frac{\partial u}{\partial \xi}\right]_{(1/2,0)} \quad \text{for all quadratic } u.$$

We could however employ a different scheme (e.g. direct sampling) for the tangential derivative: indeed it is conceivable that with some recovery schemes we might have to.

Any of the schemes in Figures 3.3.2 – 3.3.4 (or any local scheme satisfying (3.3.2) and (3.3.3)) can be used equally well for recovery points internal to a band. We are thus always faced with a wide choice when constructing a recovery algorithm.

We consider next recovery at points other than stress points. Our first remark is that for the recovery of any component of the gradient at any point, we can construct a system of equations similar to (3.3.6) linking the appropriate weights in four elements (and occasionally less). In particular, for both components at the centroid of an element clear of any band boundaries, the scheme shown in Figure 3.3.6(a) leads to superconvergence. As in Figure 3.3.2(b), we can examine the centroid scheme informally as a linear interpolation of the full gradient between the three stress points for that element (see Figure (3.3.6(b)):

$$[\nabla w]_G = \frac{1}{3} \Sigma_{j=1}^{3} [\nabla w]_{M_j} + O(h^2) \ .$$

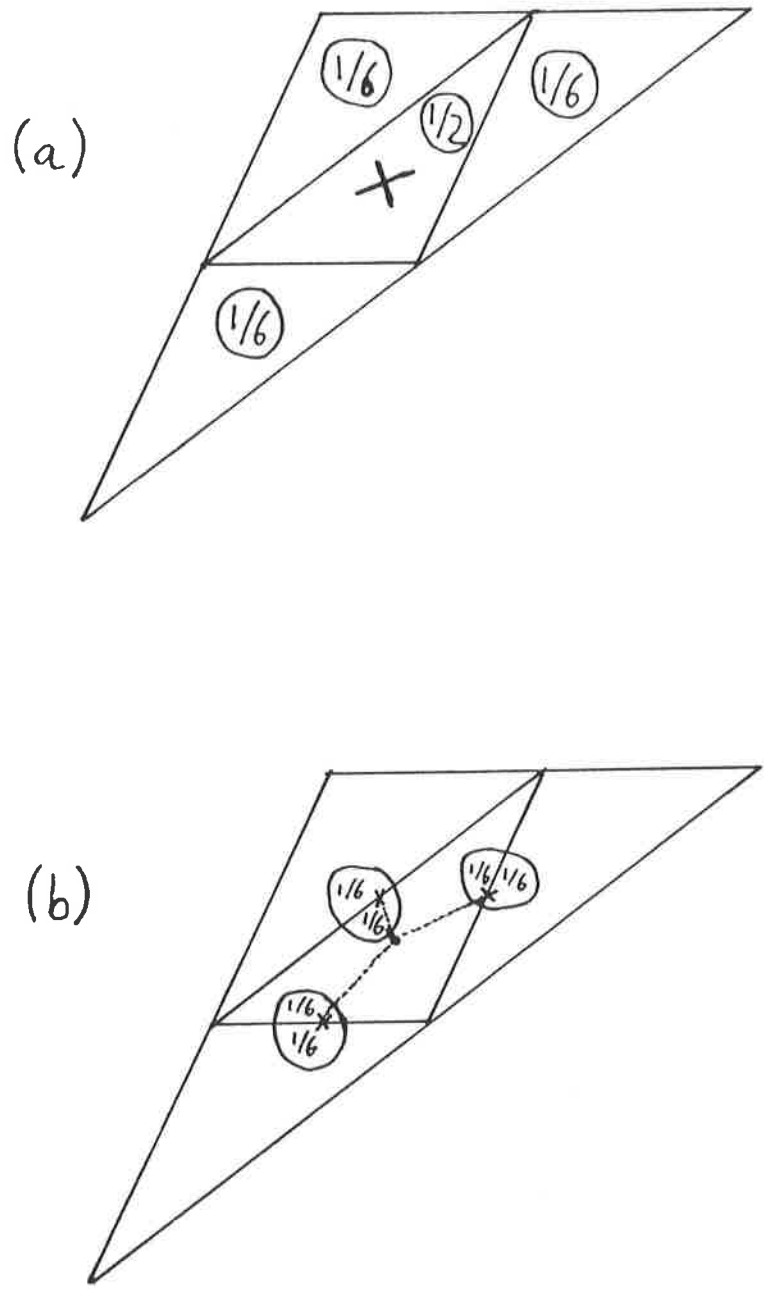

Figure 3.3.6

Scheme for recovery of the full gradient at the centroid

(a) Weights in the four elements.

(b) The scheme is decomposed into recoveries at three stress points and reassembled by interpolation (i.e. averaging).

Note that this attitude leads us to the scheme given in Figure 3.3.7 for recovery at the centroid of an element on $\partial\Omega$ (or a band boundary).

The numerical behaviour of the centroid scheme is satisfactory. Let us denote by E_{rec} the root-mean-square averaged error in the full recovered gradient at centroids of elements. (We exclude from this average those elements which have an edge tangential to $\partial\Omega$). Solving, as usual, (1.6.1) with u given by (1.6.2), we obtain

$$E_{rec} \simeq 3.0\, h^2 ;$$

we recall

$$E_{mid} \simeq 3.0\, h^2$$

and the centroid sampling result from Chapter 1:

$$E_{cent} \simeq 1.2\, h .$$

Interpolation between stress points in each element gives us a piece-wise linear function which, though discontinuous between elements, estimates the true gradient to $O(h^2)$ everywhere. To obtain a continuous approximation we devise a nodal recovery scheme (see Figure 3.3.8) and interpolate in the interior of each element. (The nodal scheme must be modified when the recovery point is on $\partial\Omega$ and there are several ways of doing this, two of which are illustrated in Figure 3.3.9.)

We end this section with the remark that interpolation between recovery points is essentially an intuitive attitude. It is however always a simple matter to prove that a scheme thus constructed does lead to superconvergence: we merely verify that

$$\partial Iu - \nabla u$$

vanishes at all required points for all quadratic u.

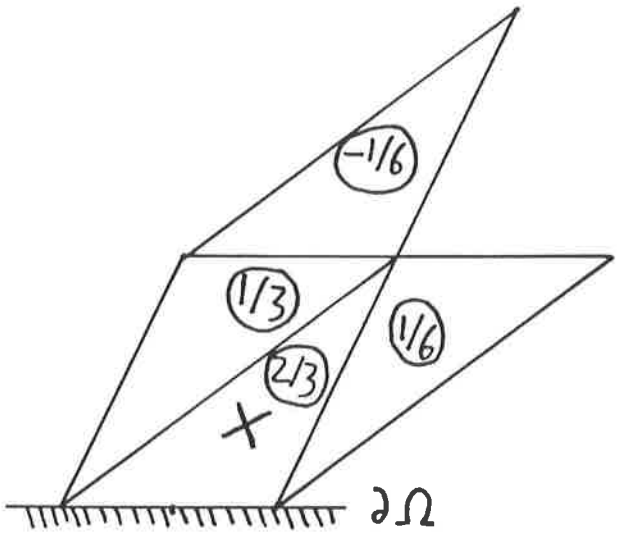

Figure 3.3.7

Recovery at the centroid of a boundary element

This scheme is derived from Figures 3.3.6 and 3.3.2.

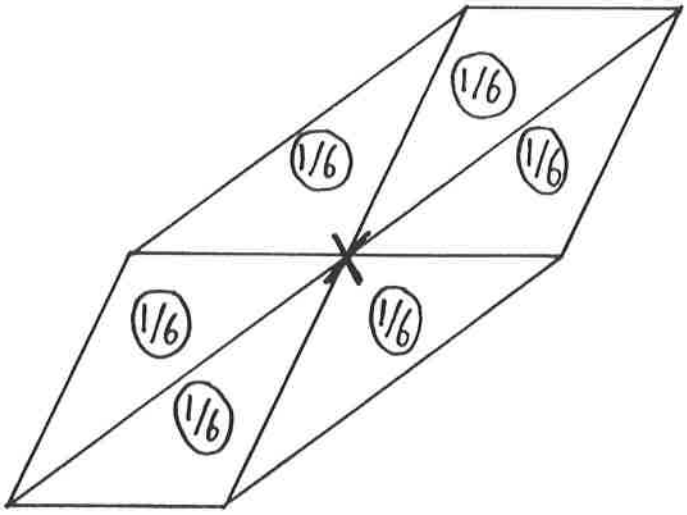

Figure 3.3.8

Recovery of the full gradient at the nodes of the triangulation

This natural six-point scheme for a node internal to a band can be used to generate a continuous, superconvergent piece-wise linear approximation to ∇u. (It has also been suggested by Křižek and Neittaanmäki (1984).)

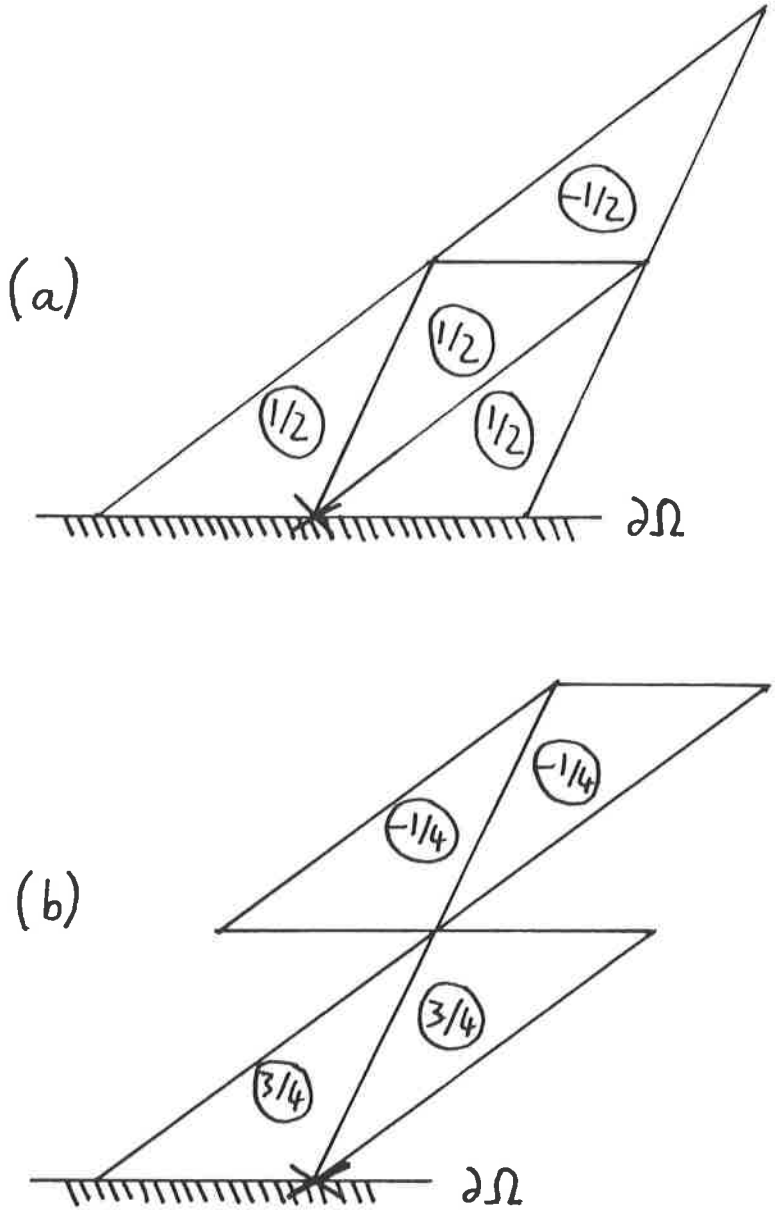

Figure 3.3.9

Recovery at boundary nodes

These two examples of schemes for nodes on $\partial\Omega$ (or a band boundary) are intuitive combinations by linear interpolation of previous schemes; as already noted they can be checked formally by adapting Lemma 3.3. A numerical example of the use of (b) is given in Section 3.5.

3.4 RECOVERY ON DISTORTED MESHES

In the last section we discussed recovery schemes for triangulations which are banded but otherwise uniform. We consider here the effect of mesh distortions on the recovery process, starting with recovery at stress points internal to a band. As before, our concern is with the normal component of gradient; the tangential component can always be sampled, to superconvergent accuracy, irrespective of the mesh geometry (recall (3.3.2) and the discussion on Table 2.1).

Let A_k be a pair of neighbouring triangles $T_{k\pm}$ internal to a band and let M_k be the midpoint of the shared element edge. We seek a recovery operator $\partial_{N;k}$ for estimation of the normal derivative $[\nabla_{N;k} u]_{M_k}$. We show first that no weighted average of $[\nabla_{N;k} Iu]_{T_{k\pm}}$ (i.e. the normal derivative in the two constituent triangles $T_{k\pm}$) can match exactly the gradients of quadratics (recall (3.3.3)) unless A_k is a parallelogram - i.e. the mesh is locally undistorted.

As in previous sections we will simplify the discussion by dropping the $\cdot_k$ subscripts and adopting the transformation $(x,y) \rightarrow (\xi,\eta)$ of Lemma 2.2. Let the weights in $T_\pm$ be $\omega_\pm$. Then for (3.3.3) to hold we require (recall (2.2.4))

$$\omega_+ + \omega_- = 1 \qquad (u \text{ linear}),$$

$$\omega_+(\xi_+^2 - \xi_+)/\eta_+ + \omega_-(\xi_-^2 - \xi_-)/\eta_- = 0 \qquad (u = \xi^2),$$

$$\omega_+\xi_+ + \omega_-\xi_- = 1/2 \qquad (u = \xi\eta)$$

and

$$\omega_+\eta_+ + \omega_-\eta_- = 0 \qquad (u = \eta^2).$$

The last two equations imply that

$$\xi_+\eta_- - \xi_-\eta_+ \neq 0$$

and

$$\omega_\pm = \pm\eta_\mp/2(\xi_+\eta_- - \xi_-\eta_+) \ ;$$

substitution into the first two yields

$$\eta_+(2\xi_- - 1) = \eta_-(2\xi_+ - 1)$$

and $$\eta_+^2((2\xi_- - 1)^2 - 1) = \eta_-^2((2\xi_+ - 1)^2 - 1)$$

respectively, whence

$$\eta_+^2 = \eta_-^2.$$

So, since $\pm\eta_\pm > 0$,

$$\eta_+ + \eta_- = 0 \quad \text{and} \quad \xi_+ + \xi_- = 1$$

(this is (2.2.5)) and A is indeed a parallelogram.

Now, as noted in the last section, if we are prepared to combine values of $\partial_{N;k} Iu$ from a sufficient number of elements (four) then a set of weights can be found such that (3.3.3) is satisfied. Whether such a procedure is worthwhile is an open question, for (3.3.3) is not in fact necessary to superconvergence. We will now prove that the scheme (3.3.1), in which $[\nabla u]_{M_k}$ is recovered from $[\nabla Iu]_{T_{k\pm}}$ with weights

$$\omega_+ = \omega_- = 1/2 ,$$

estimates the gradients of quadratics - and hence of any $u \in H^3$ - to full superconvergent accuracy (recall (3.1.8)).

<u>Theorem 3.4</u> Let A_k be a pair of neighbouring elements $T_{k\pm}$ in the triangulation of a band β, such that

$$diam\,(A_k) = h_k$$

and $$max_\beta\,(h_k) \leq ch$$

for some $c > 0$. Suppose that (2.5.1) and (2.6.2) are satisfied. Let $u \in H^3(A_k)$, let $Iu \in S$ interpolate u there and let $\partial_{N;k}$ be the standard recovery operator for the normal component at M_k (the midpoint of the edge common to $T_{k\pm}$):

$$\partial_{N;k}\phi = ([\nabla_{N;k}\phi]_{T_{k+}} + [\nabla_{N;k}\phi]_{T_{k-}})/2 , \qquad \phi \in S.$$

Then

$$\left| \partial_{N;k}(Iu) - [\nabla_{N;k}u]_{M_k} \right| \leq ch^2 h_k^{-1} ||u||_{3,A_k} . \quad (3.4.1)$$

Proof For convenience we drop the $\cdot_k$ subscript, the exception being h_k which we must distinguish from h. As before, we can simplify our working with a transformation to a different coordinate system. This time we choose an (affine) mapping $(x,y) \to (\xi,\eta) = (\xi_k,\eta_k)$ which does not rescale any lengths. The vertices common to the two elements $T_\pm$ are mapped to $(0,0)$ and $(\xi_1,0)$, the others to $(\xi_\pm,\eta_\pm) \in T_\pm$; see Figure 3.4.1. Note that $|\xi_1|$, $|\xi_\pm|$ and $|\eta_\pm|$ are all bounded above by ch_k; by (2.6.2) $\sqrt{meas(T_\pm)}$ and hence $|\eta_\pm|$ are bounded below by ch_k ($c > 0$). We express (2.5.1) in the following form:

$$\left.\begin{aligned} &|\xi_+ + \xi_- - \xi_1| \leq \kappa h \\ \text{and} \quad &|\eta_+ + \eta_-| \leq \kappa h \end{aligned}\right\} \quad (3.4.2)$$

where

$$\kappa \leq ch. \quad (3.4.3)$$

(The κ notation and perhaps bizzare form (3.4.2) are used for compatibilty with the more formal treatment of mesh distortions in Chapter 4.) The recovery error which we wish to bound is given by

$$F(u) = \frac{1}{2}\left[\left[\frac{\partial Iu}{\partial \eta}\right]_{T_+} + \left[\frac{\partial Iu}{\partial \eta}\right]_{T_-} \right] - \left[\frac{\partial u}{\partial \eta}\right]_{(\xi_1/2,0)} .$$

Now,

$$\left.\begin{aligned} &\text{if } u = \xi^2 \text{ in } A \text{ then } Iu = \xi\xi_1 + \eta(\xi_\pm^2 - \xi_\pm\xi_1)/\eta_\pm \text{ in } T_\pm; \\ &\text{if } u = \xi\eta \text{ in } A \text{ then } Iu = \eta\xi_\pm \text{ in } T_\pm ; \\ &\text{if } u = \eta^2 \text{ in } A \text{ then } Iu = \eta\eta_\pm \text{ in } T_\pm . \end{aligned}\right\} \quad (3.4.4)$$

So

$$\begin{aligned} F(\xi^2) &= (\xi_+^2 - \xi_+\xi_1)/2\eta_+ + (\xi_-^2 - \xi_-\xi_1)/2\eta_- ; \\ F(\xi\eta) &= (\xi_+ + \xi_- - \xi_1)/2 ; \\ F(\eta^2) &= (\eta_+ + \eta_-)/2. \end{aligned}$$

(Compare this with Lemma 3.3; there $\xi_1 = 1$.) Now (3.4.2) implies immediately that

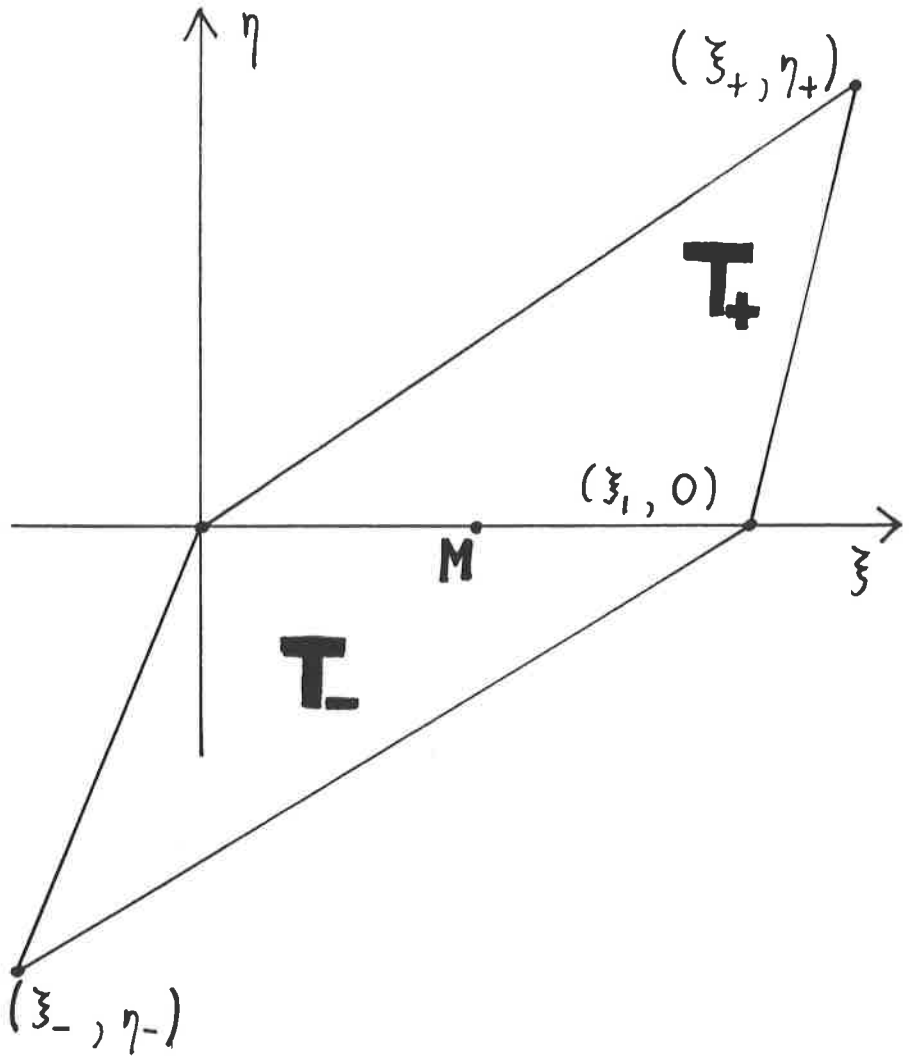

Figure 3.4.1

The coordinate transformation for Lemma 3.4

The coordinate system (ξ,η) is a rotation and translation of (x,y). The recovery point M is at $(\xi_1/2,0)$.

$$|F(\xi\eta)| \leq c\kappa h \quad \text{and} \quad |F(\eta^2)| \leq c\kappa h .$$

Further, on rearranging,

$$|F(\xi^2)| = (\xi_+ + \xi_- - \xi_1)(\xi_+ - \xi_-)/2\eta_+ + (\eta_+ + \eta_+)\xi_-(\xi_- - \xi_1)/2\eta_+\eta_- ;$$

by (3.4.2) and the upper and lower bounds on the ξ's and η's

$$|F(\xi^2)| \leq c\kappa h$$

too.

These bounds lead straight to (3.4.1) for quadratic u, but not for general $u \in H^3$. To obtain the full result we apply the lemmas S.E. and B.H. of Section 1.2; this must be done with some care. (Recall that the functional F does not vanish for all quadratic u.)

We use a projection method. Let Π be the projection onto the span of $\{\xi^2, \xi\eta, \eta^2\}$ defined on $W_1^2(A)$ by

$$\Pi u = \frac{1}{2meas(A)}\left[\xi^2 \iint_A \frac{\partial^2 u}{\partial \xi^2} + 2\xi\eta \iint_A \frac{\partial^2 u}{\partial \xi \partial \eta} + \eta^2 \iint_A \frac{\partial^2 u}{\partial \eta^2} \right]. \tag{3.4.5}$$

We write

$$F(u) = F(\Pi u) + F(u - \Pi u)$$

and bound the two terms separately. First,

$$\begin{aligned} |F(\Pi u)| &\leq \frac{c}{meas(A)}\left[|F(\xi^2)| \left| \iint_A \frac{\partial^2 u}{\partial \xi^2} \right| \right. \\ &\quad + |F(\xi\eta)| \left| \iint_A \frac{\partial^2 u}{\partial \xi \partial \eta} \right| \\ &\quad \left. + |F(\eta^2)| \left| \iint_A \frac{\partial^2 u}{\partial \eta^2} \right| \right] \\ &\leq c(meas(A))^{-1} . c\kappa h . (meas(A))^{1/2} |u|_{2,A} \\ &\leq c\kappa h h_k^{-1} |u|_{2,A} . \end{aligned} \tag{3.4.6}$$

Now when u is linear, both $F(u)$ and Πu vanish; when u belongs to the span of $\{\xi^2, \xi\eta, \eta^2\}$, u is equal to Πu. So for all quadratic u, $F(u - \Pi u) = 0$. Further by S.E. and (3.4.6), we have

$$|F(u - \Pi u)| \leq |F(u)| + |F(\Pi u)|$$
$$\leq ch_k^{-2} ||u||_{3,A} + c\kappa h h_k^{-1} |u|_{2,A}$$
$$\leq c(h_k^2 + \kappa h h_k^3) h_k^{-4} ||u||_{3,A} .$$

We can now apply B.H. (Note that since $h_k \leq diam(\Omega) = c$, we can drop the h_k^3 factor inside the brackets!)

$$|F(u - \Pi u)| \leq c(h_k^2 + \kappa h) h_k^{-1} |u|_{3,A} .$$

Hence by (3.4.6) and (3.4.3)

$$|F(u)| \leq c(h_k^2 + \kappa h) h_k^{-1} ||u||_{3,A} \qquad (3.4.7)$$
$$\leq ch^2 h_k^{-1} ||u||_{3,A}$$

as desired, for any $u \in H^3(A)$. ###

We remarked before that any scheme which recovers exactly from ∇Iu leads to superconvergence for ∇Ru. With more generality: any scheme which satisfies (3.4.1) above has this property. (See also Section 4.2.) We note also that $O(h^2)$ convergence is not apparent in (3.4.1) until - as on previous occasions (e.g. Theorem 1.5) - we average over all recovery points in Ω.

We have shown that smooth mesh distortions can be ignored when schemes are constructed for recovery at stress points in the interior of a band - we regard this as one of our more significant findings. By a similar (though slightly lengthier) argument the same applies to stress points on band boundaries or $\partial\Omega$ and hence to any recovery points in any region Ω with a superconvergent triangulation.

We conclude our treatment of local recovery with a simple numerical example. We recall the distortion of the unit square, illustrated in Figure 2.5.2. Denoting as usual the averaged errors in the solution of (1.6.1),(1.6.2) by E_{tgt}, E_{mid} and E_{rec} for midpoint (tangential) sampling, midpoint (full) recovery and centroid recovery, we obtain

$$E_{tgt} \simeq 1.2\, h^2,$$

$$E_{mid} \simeq 3.2\, h^2$$

and $$E_{rec} \simeq 3.0\, h^2.$$

(Here h is the mesh spacing on the x-axis.) For comparison, recall that on the undistorted square,

$$E_{tgt} \simeq 1.4\, h^2,$$

$$E_{mid} \simeq 3.0\, h^2$$

and $$E_{rec} \simeq 3.0\, h^2.$$

So, as in Section 2.5, the numerical effect of a realistic mesh distortion is seen to be negligible.

3.5 GALERKIN RECOVERY

We conclude this chapter with a brief introduction to a different, non-local approach to recovery; it was originally proposed by Wheeler (1973) for use with the heat equation and boundary fluxes. We recall (1.3.2): it is a special case of Green's Theorem

$$(\nabla u , \nabla v)_\Omega = (f , v)_\Omega + \langle u_\nu , v \rangle_{\partial\Omega} , \quad (3.5.1)$$

where $\langle \cdot, \cdot \rangle_{\partial\Omega}$ is the inner product in $L_2(\partial\Omega)$ and u_ν is the outward normal derivative on the Dirichlet boundary $\partial\Omega$. Note that (3.5.1) holds for any $v \in H^1(\Omega)$ and is not restricted to H^1_0. By analogy, let us define an approximation $\gamma \in S$ to u_ν thus:

$$(\nabla Ru , \nabla \phi)_\Omega = (f , \phi)_\Omega + \langle \gamma , \phi \rangle_{\partial\Omega} , \quad (3.5.2)$$

for all $\phi \in S$. (Note that we have only defined $-$ and are only interested in $-$ values of γ on $\partial\Omega$.)

According to Douglas, Dupont and Wheeler (1974), $[\gamma]_{\partial\Omega}$ is a superconvergent approximation to u_ν, provided that the elements are undistorted rectangles and their approximation is of a higher

order than linear. (Their proof cannot be applied to bilinear elements.) We give below an analysis, for a superconvergent mesh of triangular elements, which avoids both restrictions. (A similar result holds for bilinears.) Following that we give an example of the application of (3.5.2.). Incidentally, our result derives superconvergence for the product

$$< \gamma , \phi_Z >_{\partial\Omega}/h$$

(defined below and obtained by (3.5.7)), as opposed to the computationally less accessible quantity $[\gamma]_{\partial\Omega}$.

We must quote here a pointwise version of (2.1.1):

$$| (I - R)u |_{1,\infty,\Omega} \leq C_1[u]H^2 , \qquad (3.5.3)$$

where

$$H = max_{K\in\mathcal{K}} (diam (T_K))$$

and

$$C_1[u] = c ||u||_{3+\epsilon,\infty,\Omega}$$

for some $c > 0$ and fixed $\epsilon > 0$. We will discuss this bound in Chapter 5.

Let Γ be a pair of adjacent element edges on $\partial\Omega$. If the node Z internal to Γ is on a band boundary then superconvergence of γ fails there; the best we can do is to absorb the non-superconvergent error into a superconvergent average along $\partial\Omega$ (in the manner of Theorem 2.4) or resort to the recovery techniques of Section 3.3. If on the other hand this node is a vertex of $\partial\Omega$ then u_ν is given there anyway (by the Dirichlet boundary conditions on u). So we can assume here that neither of these circumstances apply.

We define $\phi_Z \in S$ to have the values 1 at Z and zero at all other nodes (see Figure 3.5.1) and set $\int_\Gamma \phi_Z = h$ ($\leq H$). Finally, we assume that the elements in $supp\ \phi_Z$ satisfy the non-degeneracy

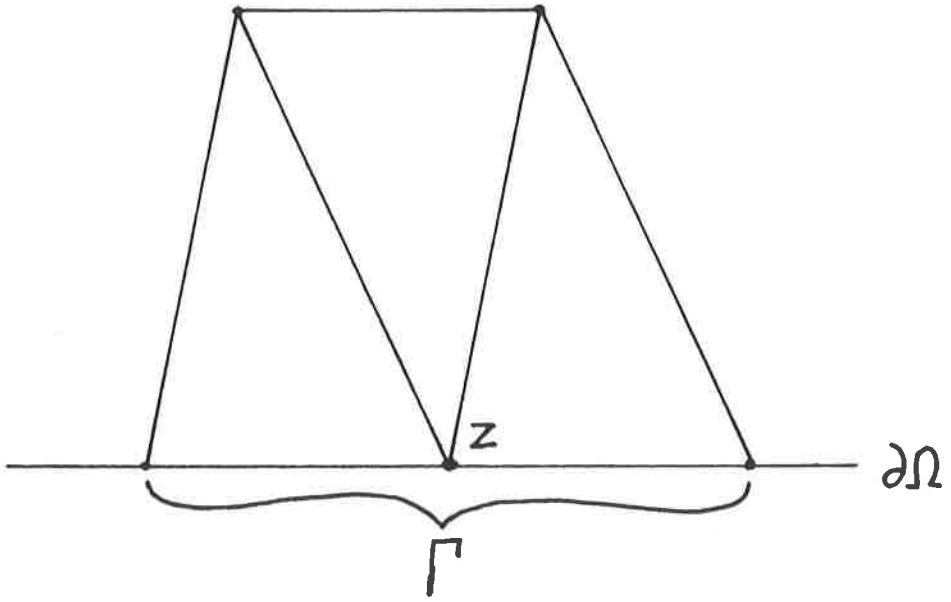

Figure 3.5.1

The support of the boundary basis function ϕ_z

condition (2.6.2); this implies that $H \leq ch$ and so

$$| \phi_Z |_{1,1,\Omega} \leq ch \quad . \tag{3.5.4}$$

Lemma 3.5 Under the above definitions,

$$| \langle \gamma , \phi_Z \rangle_\Gamma / h - [u_\nu]_Z | \leq cC_1[u]H^2 \quad . \tag{3.5.5}$$

Proof By (3.5.1) and (3.5.2),

$$\begin{aligned} & | \langle \gamma - u_\nu , \phi_Z \rangle_\Gamma | \\ = \; & | (\nabla(Ru - u) , \nabla\phi_Z)_\Omega | \\ \leq \; & | (\nabla(I - R)u , \nabla\phi_Z)_\Omega | \\ + \; & | (\nabla(Iu - u) , \nabla\phi_Z)_\Omega | \quad . \end{aligned} \tag{3.5.6}$$

Now by the Hölder inequality, (3.5.3) and (3.5.4),

$$\begin{aligned} & | (\nabla(I - R)u , \nabla\phi_Z)_\Omega | \\ \leq \; & | (I - R)u |_{1,\infty,\Omega} \; | \phi_Z |_{1,1,\Omega} \\ \leq \; & cC_1[u]H^2 h \quad . \end{aligned}$$

Also, by (3.5.4) and S.E.,

$$\begin{aligned} & | (\nabla(Iu - u) , \nabla\phi_Z)_\Omega | \\ \leq \; & ch \; | (Iu - u) |_{1,\infty,supp\ \phi_Z} \\ \leq \; & c \; ||u||_{3,\infty,supp\ \phi_Z} \quad . \end{aligned}$$

But this product vanishes if the mesh is uniform and u quadratic on $supp\ \phi_Z$. (This is easily verified, in the manner of Lemma 2.2, etc.) Therefore by B.H.

$$\begin{aligned} & | (\nabla(Iu - u) , \nabla\phi_Z)_\Omega | \\ \leq \; & ch^3 \; |u|_{3,\infty,supp\ \phi_Z} \\ \leq \; & cC_1[u]H^2 h \quad ; \end{aligned}$$

in the event of a smooth local distortion we apply the techniques of Theorem 3.4 and obtain the same result. So, substituting back into (3.5.6),

$$| \langle \gamma - u_\nu , \phi_Z \rangle_\Gamma | \leq cC_1[u]H^2 h \quad .$$

Finally by S.E. and B.H.,

$$
\begin{aligned}
&| \langle u_\nu - [u_\nu]_Z , \phi_Z \rangle_\Gamma | \\
&\leq ch^2 |u_\nu|_{2,\infty,\Gamma} \cdot h \\
&\leq cC_1[u]H^2h
\end{aligned}
$$

and so

$$
| \langle \gamma - [u_\nu]_Z , \phi_Z \rangle_\Gamma |/h \leq cC_1[u]H^2
$$

as required. ###

We have shown that the Galerkin recovery method does indeed yield a superconvergent approximation to u_ν; however we do not recommend its use. Our main criticism is its inflexibility: it is only suitable for estimation of a single stress component (in the normal direction) at a node on a smooth boundary segment. It fails altogether at band boundaries and cannot be adapted to them. Also it is less simple to program than the schemes of Section 3.3. On the other hand we have not yet given any reason to suspect that it is generally less accurate than the more direct methods.

We turn once more to a numerical test, solving (1.6.1), (1.6.2) on the usual uniformly triangulated unit square $\Omega = [0,1]^2$. For each node Z on the boundary segment $x = 0$, we estimate $[u_\nu]$ by

$$
((\nabla Ru , \nabla \phi_Z)_\Omega - (f , \phi_Z)_\Omega)/h \qquad (3.5.7)
$$

(recall (3.5.5) and (3.5.2)). We denote the mean-square error in this approximation - over all the nodes on $x = 0$ excepting those at the corners $(0,0)$ and $(0,1)$ - by E_{gal}. For comparison we use the four-element boundary node recovery scheme of Figure 3.3.9(b), which in effect reduces on this triangulation to a three-point linear combination of values of Ru (see Figure 3.5.2); we denote the mean-square error associated with this method by E_{node}.

We obtain the following rates of convergence:

$$E_{gal} \simeq 2.4\, h^2$$

and $$E_{node} \simeq 0.9\, h^2;$$

this experiment therefore serves to confirm that there is no strong reason to favour the use of Galerkin recovery methods.

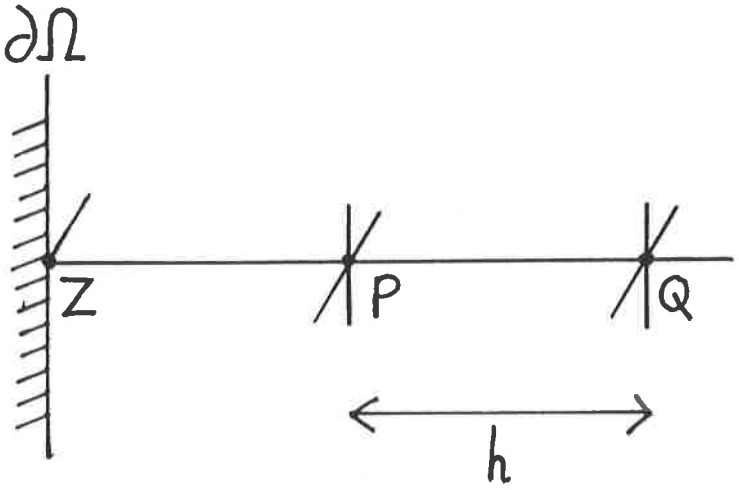

Figure 3.5.2

Direct recovery of u_v at a boundary node

On this undistorted mesh, the scheme of Figure 3.3.9(b) approximates the component of $[\nabla u]_Z$ directed along QZ. It reduces to the following estimate:

$$(3[Ru]_Z - 4[Ru]_P + [Ru]_Q)/2h \quad ,$$

where h is the distance PQ ($=ZP$).

CHAPTER FOUR

THE MEAN-SQUARE ERROR

4.1 THE TRIANGULATION

In Chapter 2 we introduced, "a mesh with the six element property which is smoothly distorted from uniformity." Our first goal in this chapter is a formal definition of that mesh and the derivation of its essential properties.

Let the problem domain Ω be a bounded open region with the strong cone property and let the problem and the unknown u be defined in terms of rectangular Cartesian coordinates (x,y) on Ω. Let the discretisation parameter h, as before, be a length typical of the required nodal separation.

We partition Ω into "bands": open regions with the strong cone property which do not intersect; their boundaries may depend - smoothly - on the value of h but their number may not. We will triangulate each band separately, subject to the requirements below.

Let β be one of the bands. Let $(X,Y) = (X_\beta, Y_\beta)$ be a second coordinate system on β and its neighbourhood, such that (see Figure 4.1.1 for an example)

> the (X,Y)-slope of every segment of the boundary $\partial\beta$ is 1 if the segment is internal to Ω and either 0, 1 or ∞ for segments on the external boundary $\partial\Omega$; the X- and Y-coordinates of each vertex are integer multiples of h. (4.1.1)

We form a grid on the closure β^C of β by placing nodes at all the points

$$(k_X h , k_Y h) \in \beta^C ,$$

where k_X and k_Y are integers. We triangulate the region in the

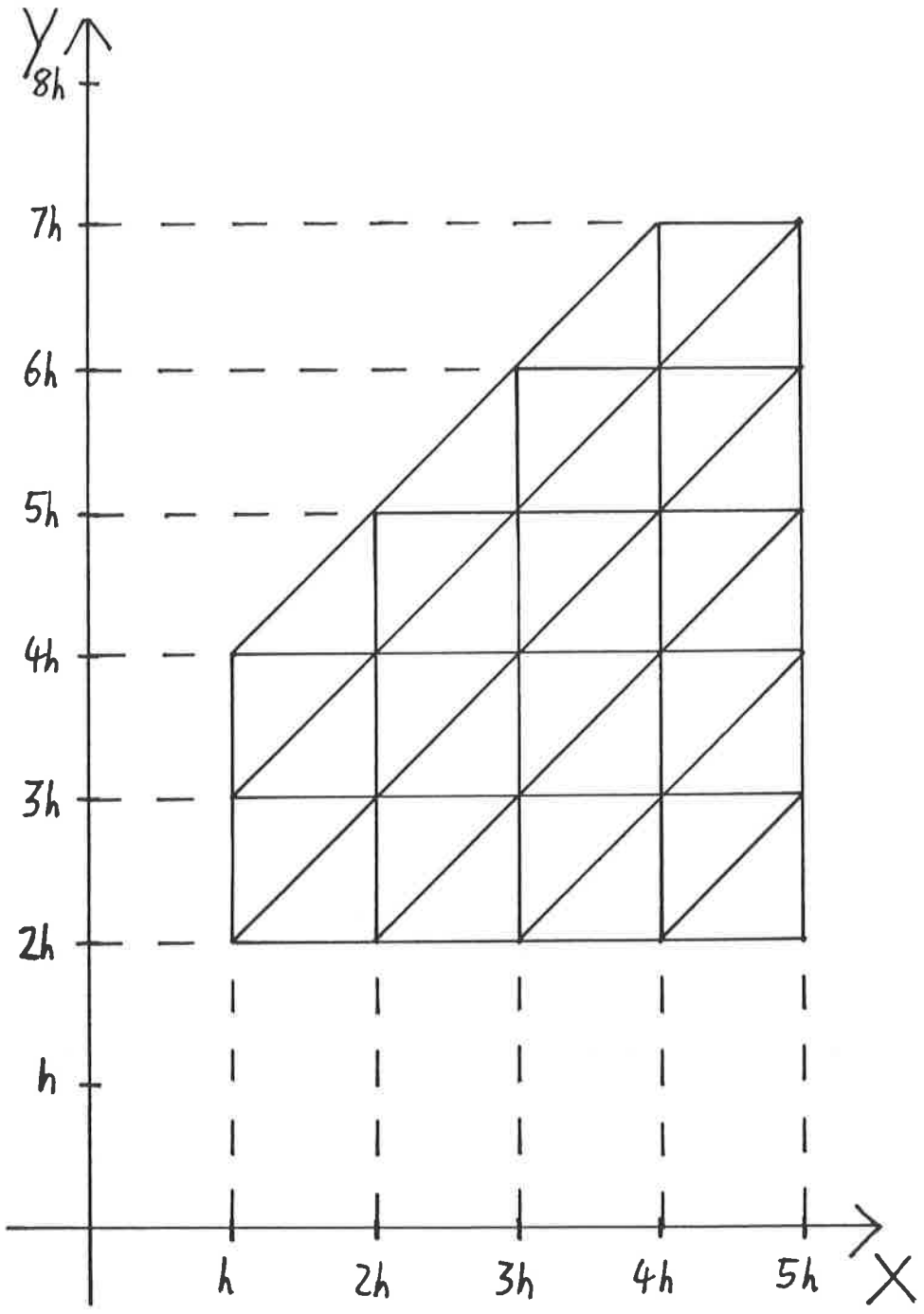

Figure 4.1.1

(X,Y)-representation of a band

The horizontal and vertical boundary segments must lie on an external boundary (i.e. on $\partial\Omega$); other segments may but need not.

(X,Y)-plane by means of horizontals, verticals and diagonals of slope $+1$ between the grid points and then in the (x,y)-plane with straight lines between these points, topologically corresponding to the (X,Y)-links. (See Figure 4.1.2.) When we refer to "elements" we will usually mean the (non-curved) triangles in the (x,y)-plane. (As in Chapter 2, members of the approximation space S are piecewise linear with respect to the (x,y)- coordinates and elements. They can be piecewise linear in the (X,Y)-plane only if the triangulation is locally uniform.) We call the union of elements in this band β_h and the union over all bands Ω_h. Although $\partial\beta_h$ and $\partial\beta$ do not in general coincide the former is a good approximation to the latter in the sense that all the nodes on $\partial\beta_h$ also lie on $\partial\beta$. (This follows immediately from (4.1.1).)

Now, regarding the rectangular coordinates (x,y) as functions of (X,Y) and if necessary of h, we require

$$(x,y) \in \left[W^2_{2+\epsilon}(\beta_h) \right]^2 \qquad (4.1.2)$$

(for some $\epsilon > 0$, for all h) and

$$|\nabla x|^2 + |\nabla y|^2 \leq c\, |\partial(x,y)/\partial(X,Y)| \qquad (4.1.3)$$

throughout β. Given the three above conditions on the "mesh functions" (X,Y) and (4.1.4) below (a compatibility condition between the bands), the approximation space S is well defined and all the properties of the triangulation that we will require can be derived.

The final condition on the triangulation is that

> the locations of nodes are consistent across each interband boundary. (4.1.4)

For an alternative, more formal approach, we use a single pair (X,Y) of mesh functions over the entire triangulation of Ω. Viewing (x,y) as functions of (X,Y) (and of h) we then locate

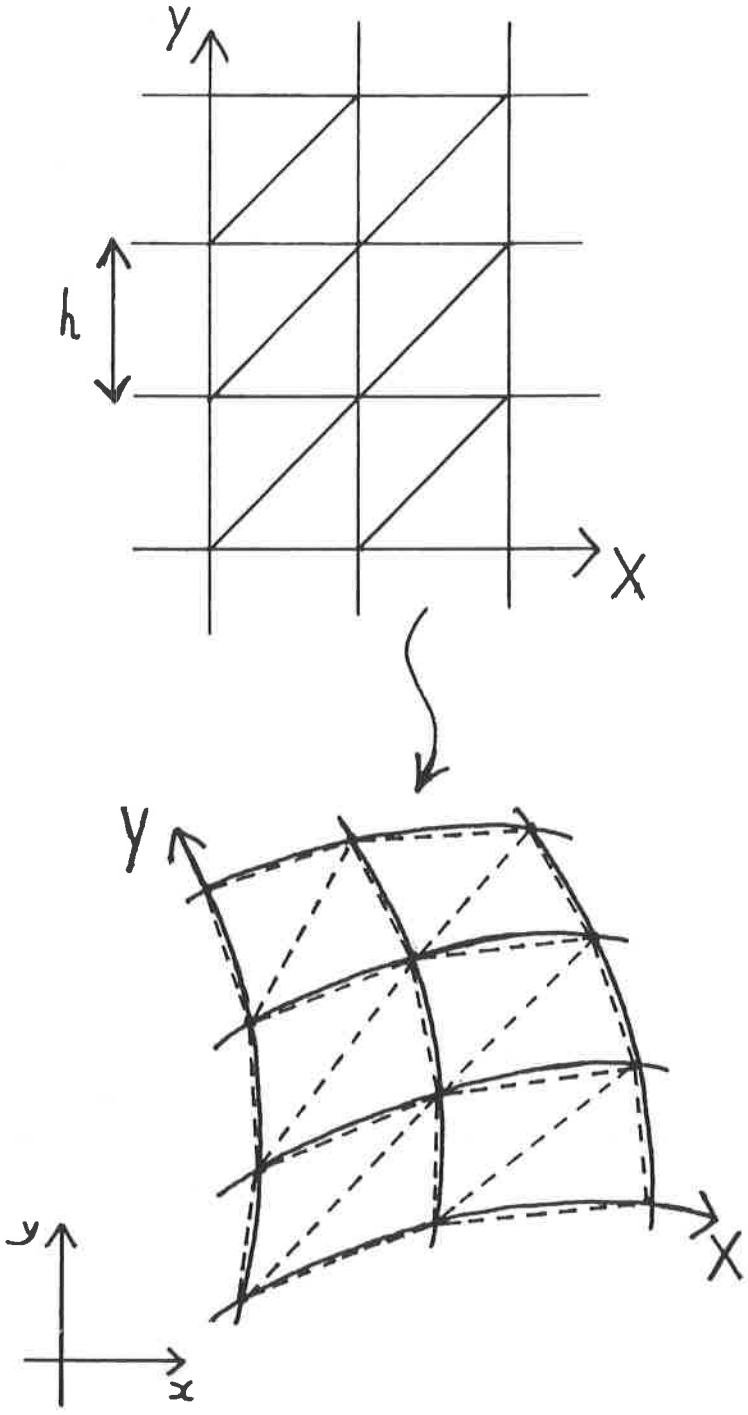

Figure 4.1.2

The global transformation (X,Y) → (x,y)

band boundaries as lines of discontinuity in the derivatives of x and y. We require (4.1.1), (4.1.2) and (4.1.3) to hold for each band as before and (x,y) to be continuous throughout; (4.1.4) is now a consequence of that continuity. When reading this chapter, either approach to bands may be adopted; the statements and proofs of superconvergence apply equally well to both.

We obtain smoothness properties for the mesh from (4.1.2). Let the triangulation of a band consist of elements T_k , $k = 1,\ldots,K$ with diameters h_k. Then for all k

$$diam\ (T_k) \;=\; h_k \;\leq\; c\ |(x,y)|_{1,T_k} \;\leq\; cC_\Omega h\ , \qquad (4.1.5)$$

where

$$C_\Omega \;=\; ||(x,y)||_{2,2+\epsilon,\Omega} \;>\; 0 \quad .$$

(Note that norms of coordinate functions such as x, y and - as above - the vector field (x,y) are with respect to (X,Y) and over the (X,Y)-regions which transform to the elements T_k . All other norms are with respect to the Cartesian coordinates (x,y) and over regions described in the (x,y)-plane.)

To prove (4.1.5), we consider a single element T_k . Let $N_{k0} = (\ X_k\ ,\ Y_k\ )$ and $N_{k1} = (\ X_k+h\ ,\ Y_k\ )$ be the nodes with the same Y-coordinate (see Figure 4.1.3); let N_{k2} be the third node (either $(\ X_k\ ,\ Y_k-h\ )$ or $(\ X_k+h\ \ ,\ \ Y_k+h\ ))$. The x-coordinate difference between N_{k0} and N_{k1} is

$$|\ x(\ X_k+h\ ,\ Y_k\ ) - x(\ X_k\ ,\ Y_k\ )\ |\ ;$$

by the lemmas S.E. and B.H. this is bounded by

$$c\ |x|_{1,T_k}\ .$$

The y-coordinate difference is bounded similarly and so the distance between N_{k0} and N_{k1} is bounded thus (using (4.1.2) and S.E.):

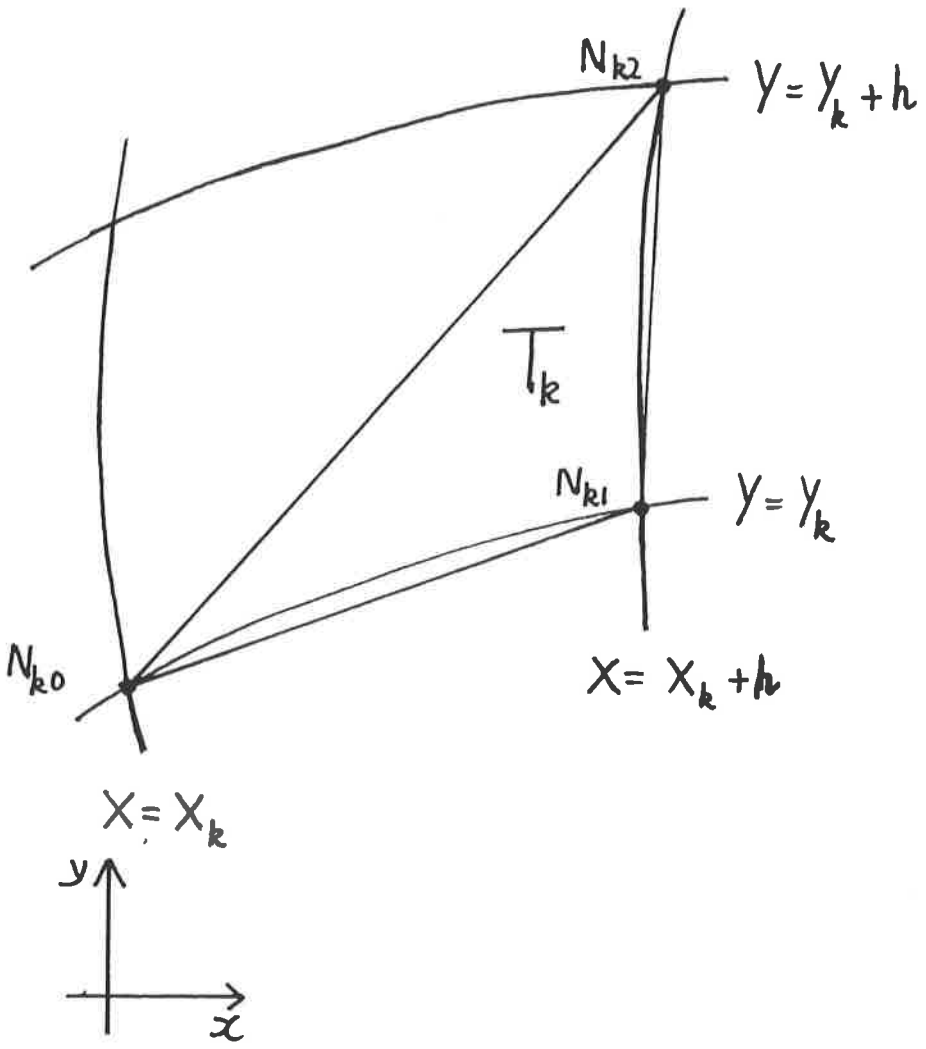

Figure 4.1.3

Labelling an element

In this example N_{k2} is at ($X_k + h$, $Y_k + h$).

$$
\begin{aligned}
| N_{k0}N_{k1} | &\leq c\, |(x,y)|_{1,T_k} \\
&\leq c \sqrt{meas_{(X,Y)}(T_k)}\ |(x,y)|_{1,\infty,T_k} \\
&\leq c \sqrt{(h^2/2)}\ |(x,y)|_{1,\infty,\beta} \\
&\leq cC_\Omega h \quad .
\end{aligned}
$$

The other sides of T_k are bounded identically, whence (4.1.5).

There usually exists another triangle $T_{k'}$ with the nodes N_{k0} and N_{k1} in common with T_k ; we refer to the union of T_k and $T_{k'}$ as A_k (see Figure 4.1.4). If such a $T_{k'}$ does not exist then N_{k0} and N_{k1} must lie on $\partial\Omega$ (to be precise: on a segment of $\partial\Omega$ with (X,Y)-slope 0) and we denote T_k by B_k (see Figure 4.1.5). This grouping of the elements has already been introduced (in Section 1.5); its role was discussed in detail in Chapter 2. As before, we can group the elements in two other ways. In one the triangles in each pair share two nodes with the same X-coordinate; any unpaired triangles will lie on segments of $\partial\Omega_h$ with (X,Y)-slope ∞ (i.e. X-contours). In the other grouping the shared nodes in each pair have the value of $Y-X$ in common; alternatively the shared edges have slope 1. Any unpaired elements which lie on segments of $\partial\beta_h$ with this slope are not necessarily on $\partial\Omega_h$; we therefore take the slope 1 to be the secondary direction of the triangulation and will make no use of the third way of grouping the triangles.

We can now turn to another consequence of (4.1.2), which links the triangulation conditions to the superconvergence results that follow: the "almost parallelograms" property (2.5.1). Let $k \leq K_A$ be fixed. (K_A is the number of triangle pairs A_k in β.) Adopting from Theorem 3.4 the transformation $(x,y) \rightarrow (\xi,\eta)$ (see Figure 4.1.4), we obtain the mathematical form of (2.5.1):

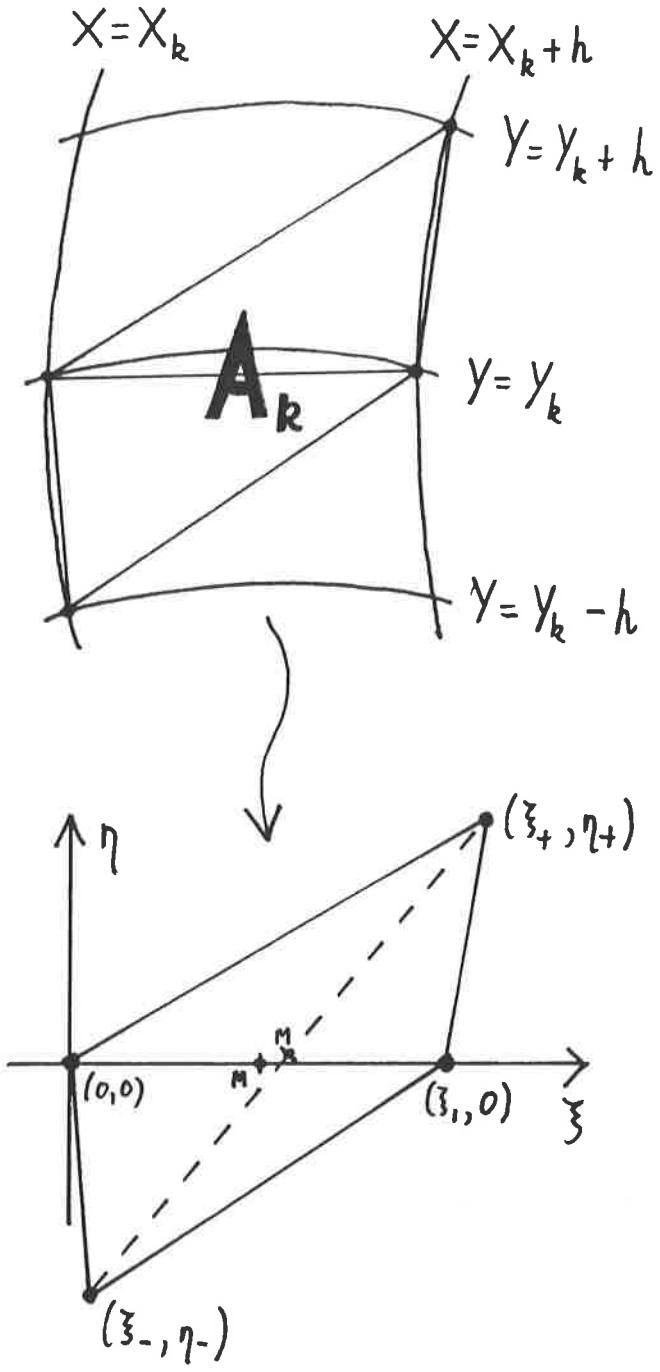

Figure 4.1.4

The transformation of an element pair

The two triangles share nodes with a common Y-coordinate. In the (ξ,η) system the midpoints M of the diagonals of the quadrilaterals are at

$$(\xi_1/2 , 0) \text{ and } ((\xi_+ + \xi_-)/2 , (\eta_+ + \eta_-)/2) ;$$

their separation is $O(h^2)$.

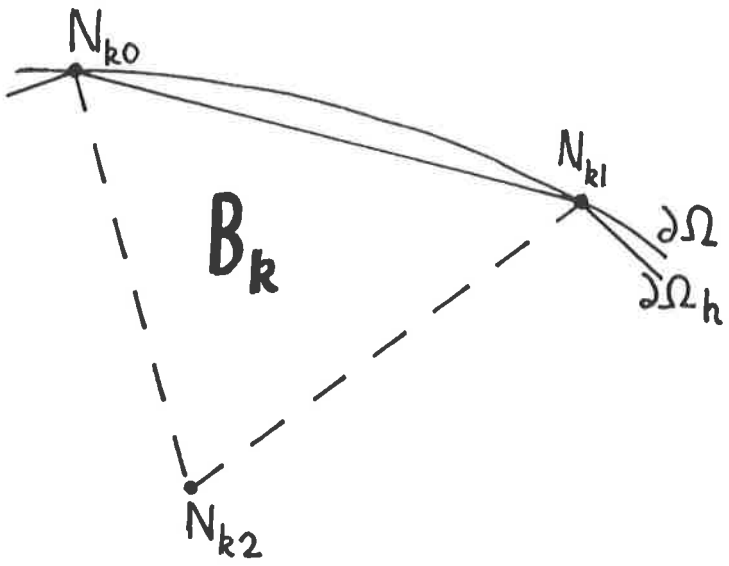

Figure 4.1.5

A boundary triangle

$\partial\Omega$ is locally a contour of Y.

Lemma 4.1

$$\left.\begin{aligned} &|\xi_+ + \xi_- - \xi_1| \leq \kappa h \\ \text{and} \quad &|\eta_+ + \eta_-| \leq \kappa h \end{aligned}\right\} \quad (4.1.6)$$

where, for some $c > 0$,

$$\kappa \ (= \kappa_k) = c\,|(x,y)|_{2,\mathbb{A}_k} \ . \qquad (4.1.7)$$

(Recall (3.4.2) and (3.4.3).)

Proof We view ξ as a function of (X,Y) and consider the functional

$$\xi(X_k+h,Y_k+h) + \xi(X_k,Y_k-h) - \xi(X_k+h,Y_k) - \xi(X_k,Y_k) \ .$$

It vanishes for linear ξ and is thus bounded - via the lemmas S.E. and B.H. of Section 1.2 and the linearity of (ξ,η) w.r.t. (x,y) - by

$$ch\,|\xi|_{2,\mathbb{A}_k} \leq ch\,|(x,y)|_{2,\mathbb{A}_k} = \kappa h \ .$$

(Note that this defines the constant c in (4.1.7).)

Now the above functional is precisely equal to $\xi_+ + \xi_- - \xi_1$; we have therefore obtained the first part of (4.1.6). The second is derived identically. ###

One further property that we require is non-degeneracy of the elements:

$$h_k^2 \leq c\ meas\ (T_k) \ ; \qquad (4.1.8)$$

this is equivalent to (2.6.2). It is a consequence of (4.1.5) and (4.1.3). For

$$\begin{aligned} h_k^2 &\leq c\,|(x,y)|^2_{1,T_k} \\ &= c \iint_{T_k} \left[\ |\nabla x|^2 + |\nabla y|^2\ \right] dX\,dY \\ &\leq c \iint_{T_k} |\partial(x,y)/\partial(X,Y)|\ dX\,dY \\ &= c \iint_{T_k} dx\,dy \ . \end{aligned}$$

As already stated, mesh functions which satisfy (4.1.1) -

(4.1.4) are a prerequisite for superconvergence. If it is not possible to satisfy these conditions then the number of bands must be increased, pseudo-vertices introduced or h decreased, as appropriate. Alternatively (recall Theorem 2.4) superconvergence can be allowed to fail in certain subregions of Ω - see also Section 5.3. Incidentally, there may be difficulties if any curved segments of $\partial\Omega$ are highly concave. We will see why this is a problem in the next section; we note here that one way round it is to refine the mesh further (if possible in the neighbourhood of the boundary only).

We have shown that the triangulation is smooth and non-degenerate. We can easily verify that it is reasonable; in particular the six element property holds throughout. Our main interest is of course to show that the mesh is superconvergent; we will devote the remaining sections of the chapter to that.

We conclude this section with an example of a mesh-function pair (X,Y): we demonstrate that the general pseudo-vertex transformation (2.6.3) satisfies (4.1.2) and (4.1.3). The transformation can be written thus:

$$\left.\begin{array}{l} x = R^{\gamma} \cos \gamma\Theta \quad \text{and} \quad y = R^{\gamma} \sin \gamma\Theta \\ \text{where} \quad R^2 = X^2 + Y^2 , \quad \tan \Theta = Y/X \quad \text{and} \quad \gamma \geq 2 . \end{array}\right\} (4.1.9)$$

Expanding,

$$x = (X^2 + Y^2)^{\gamma/2} \cos (\gamma \tan^{-1}(Y/X)) \ ;$$

on differentiating we obtain

$$\frac{\partial x}{\partial X} = \gamma (X^2 + Y^2)^{(\gamma/2)-1} \left[X \cos (\gamma \tan^{-1} \frac{Y}{X}) + Y \sin (\gamma \tan^{-1} \frac{Y}{X}) \right] .$$

So

$$\partial x/\partial X = \gamma R^{\gamma-2} (X \cos \gamma\Theta + Y \sin \gamma\Theta) \ ;$$

similarly

$$\partial x/\partial Y = \gamma R^{\gamma-2} (Y \cos \gamma\Theta - X \sin \gamma\Theta) ,$$

$$\partial y/\partial X = \gamma R^{\gamma-2} (X \sin \gamma\Theta - Y \cos \gamma\Theta)$$

and $$\partial y/\partial Y = \gamma R^{\gamma-2} (Y \sin \gamma\Theta + X \cos \gamma\Theta) .$$

Hence

$$|\nabla x|^2 = |\nabla y|^2 = |\partial(x,y)/\partial(X,Y)| = \gamma^2 R^{2\gamma-2}$$

and (4.1.3) is verified.

Now, by further differentiation, the second derivatives of (x,y) are $O(R^{\gamma-2})$. So

$$\begin{aligned} |(x,y)|^{2+\epsilon}_{2,2+\epsilon} &\leq c \int \left[R^{\gamma-2} \right]^{2+\epsilon} R \, dR \\ &\leq c \left[R^{2\gamma - 2 - 2\epsilon + \gamma\epsilon} \right]_0^{diam\ (\Omega)} \\ &\leq c , \end{aligned}$$

so long as $2\gamma - 2 - 2\epsilon + \gamma\epsilon > 0$. Therefore (x,y) will be in $\left[W^2_{2+\epsilon}(\beta_h) \right]^2$ provided either

$$\gamma \geq 2 \qquad (4.1.10)$$

or

$$\gamma > 1 \quad \text{and} \quad \epsilon < \frac{2\gamma-2}{2-\gamma} .$$

So in fact (4.1.2) can hold for all $\gamma > 1$. However, we shall see in the next section that superconvergence breaks down in the vicinity of the pseudo-vertex when $\gamma < 2$; therefore we recommend that γ should always satisfy (4.1.10). As already noted, this does not limit us from transforming obtuse angles into pseudo-vertices: the transformation (4.1.9) can be preceded by a shear. (Recall Figure 2.6.9 - the restriction is on the radial scaling.)

4.2 THE SUPERCONVERGENCE RESULT

We are now in a position to state the problem, its approximation and the mean-square superconvergence result in their general forms. Let Ω satisfy the usual conditions (Section

4.1). We take u to be the (unknown) solution to the self-adjoint Dirichlet problem:

$$\left.\begin{aligned} Lu &= f \quad \text{in } \Omega \\ \text{and} \qquad u &= u_E \quad \text{on } \partial\Omega. \end{aligned}\right\} \tag{4.2.1}$$

Here

$$\begin{aligned} &Lu \\ &= -\frac{\partial}{\partial x}\left[a_{11}\frac{\partial u}{\partial x} + a_{12}\frac{\partial u}{\partial y}\right] - \frac{\partial}{\partial y}\left[a_{21}\frac{\partial u}{\partial x} - a_{22}\frac{\partial u}{\partial y}\right] \end{aligned} \tag{4.2.2}$$

satisfies the classical ellipticity condition (see inequality (4.1.2) of Ciarlet, 1978) and $a_{12} = a_{21}$. We note that we can add the term

$$a_0 u \quad \text{where} \quad a_0 \geq 0\,, \quad a_0 \in W^2_{2+\epsilon}(\Omega)$$

to L with only a straightforward supplementary analysis. Also, the Dirichlet boundary data can be replaced on part or all of $\partial\Omega$ by a Neumann condition in which the conormal u_ν is given as a linear function of u. Again, there is a straightforward supplementary analysis (see Zlámal, 1976). For simplicity we assume that neither of these conditions occur here.

Let us associate with (4.2.2) a bilinear form on $\left[H^1(\Omega)\right]^2$:

$$\left.\begin{aligned} a_\Omega(w,v) = \iint_\Omega \Bigg[& a_{11}\frac{\partial w}{\partial x}\frac{\partial v}{\partial x} \\ & + a_{12}\left[\frac{\partial w}{\partial x}\frac{\partial v}{\partial y} + \frac{\partial w}{\partial y}\frac{\partial v}{\partial x}\right] \\ & + a_{22}\frac{\partial w}{\partial y}\frac{\partial v}{\partial y}\Bigg]\, dx\, dy\,. \end{aligned}\right\} \tag{4.2.3}$$

Then (compare with (1.3.2)) the weak solution of (4.2.1) is a function $u \in H^1_E(\Omega)$ satisfying

$$a_\Omega(\,u\,,\,v\,) = (\,f\,,\,v\,)_\Omega \quad \text{for all } v \in H^1_0(\Omega). \tag{4.2.4}$$

In fact we require additional smoothness as follows:

$$\left.\begin{aligned} & u \in H^1_E(\Omega) \cap H^3(\Omega)\,; \\ \text{further} \quad & a_{ij} \in W^2_{2+\epsilon}(\Omega) \quad (i,j = 1,2) \quad \text{for some } \epsilon > 0 \\ \text{and} \quad & f \in H^2(\Omega)\,. \end{aligned}\right\} \tag{4.2.5}$$

(Note that f has one more derivative than is implicit in (4.2.1).

This is necessary to ensure that the effects of numerical quadrature do not swamp the superconvergence effect.)

The first stage in the approximation process is the triangulation of Ω (Section 4.1). All piecewise linears - including the Finite Element solution Ru which we reintroduce below - are defined on Ω_h. However Ω_h is not necessarily contained in Ω and although Ru is computed using values of functions on Ω, it will simplify our analysis to extend the domains of these functions to Ω_h. Since Ω has the strong cone property we can apply Calderon's theorem (Calderon, 1961, Theorem 12; see also Babich, 1953) and extend u and a_{ij} $(i,j = 1,2)$, in the Sobolev spaces of (4.2.5), to $\mathbb{R}^2$ (as opposed to Ω). The restriction back to Ω of the extension operator yields the identity and so without ambiguity we can use a single symbol for both a function and its extension. By Calderon's Theorem, we have

$$\left.\begin{aligned} &||u||_{3,\Omega_h} \leq c\,||u||_{3,\Omega} \\ \text{and}\quad &||a_{ij}||_{2,2+\epsilon,\Omega_h} \leq c\,||a_{ij}||_{2,2+\epsilon,\Omega} \end{aligned}\right\} \quad (4.2.6)$$

$(i,j = 1,2)$. We use these Calderon extensions to extend f, as follows:

$$f = Lu \in H^1(\Omega_h) \cap H^2(\Omega)\,, \qquad (4.2.7)$$

where L is the elliptic operator of (4.2.1). Then by Green's Theorem,

$$a_{\Omega_h}(u, v) = (f, v)_{\Omega_h} \qquad (4.2.8)$$

for all $v \in H_0^1(\Omega_h)$, where $a_{\Omega_h}(\cdot,\cdot)$ corresponds to the form (4.2.3) with integration over Ω_h. Note that the Finite Element equations (4.2.12) below approximate the function $u \in H_E^1(\Omega_h)$ defined by (4.2.8) and not the original unknown $u \in H_E^1(\Omega)$ defined by (4.2.4). We are thus committing (with - as we shall see - impunity) two of the variational crimes described by Strang and

Fix (1973): interpolation of boundary arcs and interpolation of the boundary data u_E.

In practical computations, $a_{\Omega_h}(\cdot,\cdot)$ and $(\cdot,\cdot)_{\Omega_h}$ will be evaluated by numerical quadrature (recall (1.6.1)). The centroid rule is sufficient for our purposes; its use is denoted thus: $a^*_{\Omega_h}(\cdot,\cdot)$, $(\cdot,\cdot)^*_{\Omega_h}$. Our results can easily be modified to apply to any other rule, provided it integrates linear functions exactly in each element. However numerical evidence, presented in the next section, indicates that the error introduced by the use of the centroid rule is not numerically significant.

No quadrature rule will be practical if the functions, whose integrals we wish to approximate, have to be evaluated with explicit (non-trivial) recourse to the Calderon extensions (4.2.6). We therefore require that the centroid of every element be contained in Ω ($\neq \Omega_h$). Now by (4.1.8), each element T_k contains an open disk, T_k^* say, such that

$$meas\ (T_k) \leq c\ meas\ (T_k^*) \tag{4.2.9}$$

for some c independent of k. (See Figure 4.2.1 for the derivation of (4.2.9).) We combine this bound with the above centroid condition and make the following requirement (which is a little stronger): for each element T_k there exists an open disk T_k^* satisfying (4.2.9) such that

$$G_k \in T_k^* \subset T_k \cap \Omega . \tag{4.2.10}$$

Given (4.2.9), this condition is trivial unless T_k lies on a segment of $\partial\Omega$ which has a strong concave curvature. (See Figure 4.2.2.) If a triangulation fails to satisfy (4.2.10) there are two remedies: we refine the mesh (as noted previously) or use a different quadrature scheme for the offending elements. Ideally, such a scheme will integrate linear functions exactly; in each

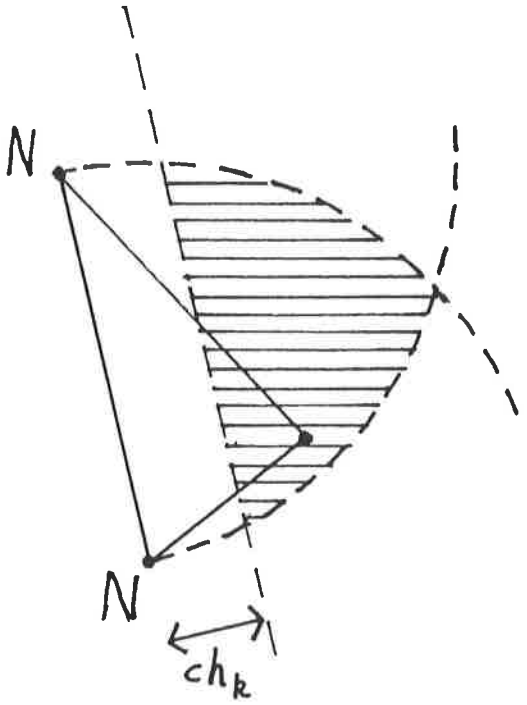

Figure 4.2.1

(4.2.9) follows from (4.1.8)

Let the longest side of an element T_k be the line NN shown here. Then the third node must lie within the two arcs. But by (4.1.8) this node must also be at least ch_k ($c > 0$) away from the base line NN; therefore it lies in the shaded region. It is now seen that T_k is sufficiently undistorted for a disk $T_k^* \subset T_k$ satisfying (4.2.9) to exist.

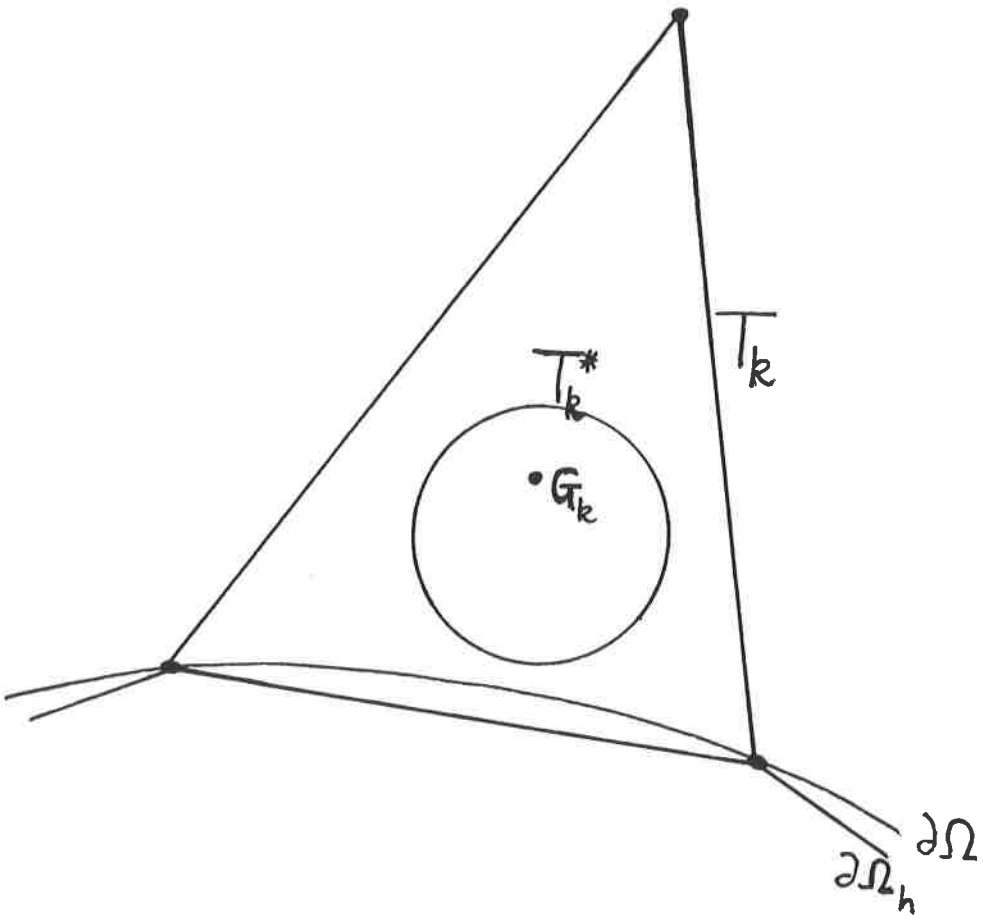

Figure 4.2.2

Condition on boundary elements

The centroid of each element is inside Ω and isolated from $\partial\Omega$. (T_k^* is open.)

element the quadrature points must lie in some open disk T_k^* ($\subset T_k \cap \Omega$) which satisfies (4.2.9).

Now if h is sufficiently small, the ellipticity of L is passed onto its extension and so (Ciarlet, 1978, Theorem 4.1.2 – this result remains valid on regions with curved boundaries) there exists an $\alpha > 0$ independent of h such that

$$\alpha \, |\phi|^2_{1,\Omega_h} \leq a^*_{\Omega_h}(\phi, \phi) \quad \text{for all } \phi \in S. \qquad (4.2.11)$$

This discrete coercivity condition implies the existence and uniqueness of the Finite Element approximation which we now define. Let S_E and S_0 be the subsets of S defined in Section 1.3: members of S_E interpolate values of u_E between boundary nodes and members of S_0 vanish there. (Note incidentally that S_E is now a subset of $H^1_E(\Omega_h)$.) Then – recall (1.3.5) – we take Ru to be the member of S_E which solves

$$a^*_{\Omega_h}(Ru, \phi) = (f, \phi)^*_{\Omega_h} \qquad (4.2.12)$$

for all $\phi \in S_0$.

The following result holds equally well for any class of local recovery schemes satisfying error bounds of the form (3.4.7); in particular it applies to all schemes which are exact when used on the interpolants of quadratics on undistorted meshes. For ease of notation, we present our result in terms of the standard recovery scheme (Figure 3.3.1) for the midpoints M_k of the shared element edge internal to each triangle pair A_k. We denote the use of this scheme by the operator D_k.

<u>Theorem 4.2</u> Let $||u||_3$, $|f|_2$ and $||a||_2$ stand for $||u||_{3,\Omega_h}$, $|f|_{2,\Omega}$ and $\Sigma_{ij}||a_{ij}||_{2,2+\epsilon,\Omega}$ respectively and let the norm $||u||_\kappa$ be given by

$$||u||^2_\kappa = \Sigma_k \, (C^2_\Omega + \kappa_k h^{-1})^2 \, ||u||^2_{3,T_k},$$

where C_Ω and κ_k are as defined by (4.1.5) and (4.1.7) above. Then

the following weighted mean-square superconvergence bound holds:

$$\left[\Sigma_k \, h_k^2 \left| D_k Ru - [\nabla u]_{M_k} \right|^2 \right]^{1/2}$$

$$\leq \; c \, h^2 \alpha^{-1} \left[(\alpha + ||a||_2)||u||_\kappa + C_\Omega^2 \, |f|_2 \right] . \quad (4.2.13)$$

Proof (Recall Theorem 1.5. See also the "first Strang Lemma" - Theorem 4.1.1 of Ciarlet, 1978 - and Zlámal, 1978.)

We substitute $v = \phi = (I - R)u \in S_0$ into (4.2.8), (4.2.11) and (4.2.12):

$$\alpha \, |(I - R)u|^2_{1,\Omega_h}$$

$$\leq \; a^*_{\Omega_h}(\, (I - R)u \, , \, (I - R)u \,)$$

$$\leq \; |a^*_{\Omega_h}(\, Iu - u \, , \, (I - R)u \,)|$$

$$+ \; |a^*_{\Omega_h}(\, u \, , \, (I - R)u \,) - a_{\Omega_h}(\, u \, , \, (I - R)u \,)|$$

$$+ \; |(\, f \, , \, (I - R)u \,)_{\Omega_h} - (\, f \, , \, (I - R)u \,)^*_{\Omega_h}| \quad .$$

We show in the next two sections that the following bounds apply, for any $\phi \in S_0$:

$$\left. \begin{aligned} & |a^*_{\Omega_h}(\, Iu - u \, , \, \phi \,)| \\ & \leq \; ch^2 \, ||a||_2 \, ||u||_\kappa \, |\phi|_{1,\Omega_h} \, , \end{aligned} \right\} (4.2.14)$$

$$\left. \begin{aligned} & |a^*_{\Omega_h}(\, u \, , \, \phi \,) - a_{\Omega_h}(\, u \, , \, \phi \,)| \\ & \leq \; cC_\Omega^2 h^2 \, ||a||_2 \, ||u||_3 \, |\phi|_{1,\Omega_h} \end{aligned} \right\} (4.2.15)$$

and

$$\left. \begin{aligned} & |(\, f \, , \, \phi \,)_{\Omega_h} - (\, f \, , \, \phi \,)^*_{\Omega_h}| \\ & \leq \; cC_\Omega^2 h^2 \, (|f|_2 + ||a||_2 \, ||u||_3) \, |\phi|_{1,\Omega_h} \, . \end{aligned} \right\} (4.2.16)$$

Hence

$$\alpha \, |(I - R)u|^2_{1,\Omega_h}$$

$$\leq \; ch^2 \left[\, ||a||_2 (||u||_\kappa + C_\Omega^2 \, ||u||_3) + C_\Omega^2 \, |f|_2 \, \right]$$

$$\cdot \; |(I - R)u|_{1,\Omega_h}$$

and so (note that $||u||_3 \leq cC_\Omega^{-2} \, ||u||_\kappa$)

$$\left. \begin{aligned} & |(I - R)u|_{1,\Omega_h} \\ & \leq \; ch^2 \alpha^{-1} \left[\, ||a||_2 \, ||u||_\kappa + C_\Omega^2 \, |f|_2 \, \right] \quad . \end{aligned} \right\} (4.2.17)$$

Now the recovery scheme is local. So by (4.1.8)

$$\begin{aligned} & \Sigma\, h_k^2 \left| D_k(I - R)u \right|^2 \\ \leq\ & c\, \Sigma\, h_k^2 \left| [\nabla(I - R)u]_{T_k} \right|^2 \\ \leq\ & c\, \Sigma \left| [\nabla(I - R)u]_{T_k} \right|^2 meas\ (T_k) \\ =\ & c\, |(I - R)u|^2_{1,\Omega_h} \quad . \end{aligned} \tag{4.2.18}$$

Further, by (3.4.7) and (4.1.5)

$$\begin{aligned} & \Sigma\, h_k^2 \left| D_k Iu - [\nabla u]_{M_k} \right|^2 \\ \leq\ & c\, \Sigma \left[h_k^2 + \kappa_k h \right]^2 ||u||^2_{3,A_k} \\ \leq\ & c\, \Sigma \left[C_\Omega^2 h^2 + \kappa_k h \right]^2 ||u||^2_{3,T_k} \\ =\ & c \left[h^2\, ||u||_\kappa \right]^2 \quad . \end{aligned} \tag{4.2.19}$$

We now obtain the required result by adding (4.2.18) and (4.2.19), substituting from (4.2.17) and taking the square-root. ###

We conclude this section with brief examples of the relation between (4.2.13) and practical triangulations. We consider first a mesh which has no degeneracies:

$$h_k \geq ch \quad \text{for some } c > 0 \text{ independent of } k$$

and $$(x,y) \in \left[W_\infty^2 \right]^2 \quad .$$

The second condition implies, via (4.1.7) that

$$\kappa_k \leq ch \quad \text{for all } k$$

whence by (4.2.6)

$$||u||_\kappa \leq cC_\Omega^2\, ||u||_{3,\Omega_h} \leq cC_\Omega^2\, ||u||_{3,\Omega} \ .$$

The superconvergence result now reduces to a more familiar form (recall (1.5.10)):

$$\begin{aligned} & h \left[\Sigma_k \left| D_k Ru - [\nabla u]_{M_k} \right|^2 \right]^{1/2} \\ \leq\ & cC_\Omega^2 h^2 \alpha^{-1} \left[(\alpha + ||a||_2)||u||_{3,\Omega} + |f|_2 \right] \\ =\ & O(h^2) \quad . \end{aligned} \tag{4.2.20}$$

If, on the other hand, the triangulation contains any pseudo-vertices, we cannot simplify the left-hand side of (4.2.13). Let us make the mild assumption, however, that $u \in W_\infty^3(\Omega_h)$. Then

$$\begin{aligned} ||u||_\kappa^2 &\leq c[u;C_\Omega]\left[\, 1 + \Sigma(\kappa_k h_k h^{-1})^2 \,\right] \\ &\leq c[u;C_\Omega]\left[\, 1 + \Sigma\, \kappa_k^2 \,\right] \\ &\leq c[u;C_\Omega]\left[\, 1 + |(x,y)|_2^2 \,\right] \quad ; \end{aligned}$$

therefore the right-hand side of (4.2.13) remains $O(h^2)$ and mean-square superconvergence is retained. But, as already noted, this does not imply superconvergence right up to a pseudo-vertex. For in the notation of (4.1.9),

$$\begin{aligned} \kappa_k &= O(R^{\gamma-2})h \\ &= O(h^{\gamma-1}) \end{aligned}$$

in elements immediately neighbouring the psuodo-vertex. So in that neighbourhood,

$$\begin{aligned} |D_k Iu - [\nabla u]_{M_k}| &\leq c\left[\, h_k^2 + \kappa_k h \,\right] h_k^{-1}\, ||u||_{3,A_k} \qquad (4.2.21) \\ &= c[u]\left[\, O(h^{2\gamma}) + O(h^\gamma) \,\right] \quad ; \end{aligned}$$

this will be $O(h^2)$ only if $\gamma \geq 2$. (Recall the proof of Lemma 3.4: the bound (4.2.21) is sharp when u is quadratic.) Now, we have not proved that "$\gamma < 2$" implies

$$|D_k Ru - [\nabla u]_{M_k}| \neq O(h^2) \quad . \qquad (4.2.22)$$

However, we do believe that (4.2.22) is true under these circumstances. Further, as discussed in other sections, it is always possible to avoid triangulations for which $\gamma < 2$; we therefore recommend that this be done in practice.

As a final remark, we recall the scheme noted in Section 3.3 (derived from the nodal recoveries given in Figures 3.3.8 and 3.3.9) for recovering ∇u at all points in Ω_h: on any triangulation the left-hand side of (4.2.13) now takes the elegant, natural form $||\, DRu - \nabla u \,||_{L_2(\Omega_h)}$.

4.3 NUMERICAL QUADRATURE

In this section we will demonstrate, both analytically and numerically, that the effects of numerical quadrature by the centroid rule are not significant to the superconvergence phenomenon. They can in consequence be ignored in the construction of triangulation and recovery schemes. We will see that mesh geometry (i.e. Lemma 4.1) and topology play no part in the following analysis. Therefore the effect on energy error, due to use of the centroid rule, is second order even in the total absence of superconvergence.

The numerical approximation to the integral

$$\iint_{\Omega_h} w \, dx \, dy$$

is

$$\sum_{k=1}^{K} [w]_{G_k} \, meas \, (T_k) \quad ,$$

where G_k is the centroid of element T_k ($k = 1,\ldots,K$). We define a local error functional over each T_k:

$$E_k(w) \quad = \quad \iint_{T_k} w \, dx \, dy \; - \; [w]_{G_k} \, meas \, (T_k)$$

and bound it using the lemmas S.E. and B.H. of Section 1.2.

Lemma 4.3 The following abstract estimates hold in every element:

(i) $|E_k(w)| \leq ch_k^3 \, |w|_{2,T_k}$ for all $w \in H^2(T_k)$

(ii) $|E_k(w)| \leq ch_k^2 \left[\, |w|_{1,T_k} + |w|_{2,T_k \cap \Omega} \, \right]$ for all $w \in H^1(T_k) \cap H^2(\Omega)$.

Proof Suppose $w \in H^2(T_k)$. Then by S.E.,

$$|E_k(w)| \quad \leq \quad ch_k \, ||w||_{2,T_k} \quad .$$

But when w is linear on T_k the centroid rule is exact and so E_k vanishes. Thus by B.H.,

$$|E_k(w)| \quad \leq \quad ch_k^3 \, |w|_{2,T_k}$$

and (i) is proved.

Part (ii) will be applied later to elements which lie on the boundary $\partial\Omega$. It is less straightforward to establish and we proceed with caution. We recall (4.2.9) and (4.2.10) and, as in Lemma 3.4, introduce a projection operator. (For convenience we will assume here that k is fixed; without ambiguity we can drop the suffix $\cdot_k$ from any symbol apart from h_k.) Let the projection be

$$\Pi w = \begin{cases} meas\ (T^*)^{-1} \iint_{T^*} w\ dx\ dy & \text{in } T^* \\ w & \text{in } T \setminus T^* . \end{cases}$$

Then

$$E(\Pi w) = \iint_T w\ dx\ dy - \frac{meas\ (T)}{meas\ (T^*)} \iint_{T^*} w\ dx\ dy ;$$

by (4.2.9) this is bounded by $ch_k\ ||w||_{1,T}$. But the functional $E(\Pi w)$ vanishes whenever w is a constant over T; therefore by B.H.

$$|E(\Pi w)| \leq ch_k^2\ |w|_{1,T} . \qquad (4.3.1)$$

Now

$$E(w - \Pi w) = \frac{meas\ (T)}{meas\ (T^*)} \iint_{T^*} w\ dx\ dy - [w]_G\ meas\ (T).$$

This remainder is bounded in $L_\infty(T^*)$ and hence by S.E. in $W^1_{2+\epsilon}(T^*)$ for any fixed $\epsilon > 0$:

$$|E(w - \Pi w)| \leq ch_k^{(2+2\epsilon)/(2+\epsilon)}\ ||w||_{1,2+\epsilon,T^*} .$$

(Note that by (4.2.9) $h_k \leq c\ diam\ (T^*)$.) Again when w is a constant over T^* this vanishes. So by B.H.

$$|E(w - \Pi w)| \leq ch_k^{(4+3\epsilon)/(2+\epsilon)}\ |w|_{1,2+\epsilon,T^*} .$$

We now apply S.E. again:

$$||v||_{L_{2+\epsilon}(T^*)} \leq ch_k^{-\epsilon/2+\epsilon}\ ||v||_{1,T^*}$$

for all $v \in H^1(T^*)$; substituting $v = \nabla w$ we arrive at

$$|E(w - \Pi w)| \leq ch_k^2 \left[|w|_{1,T^*} + |w|_{2,T^*} \right] . \qquad (4.3.2)$$

To obtain (ii) we now add (4.3.1) to (4.3.2) and recall (4.2.10). ###

$$\left.\begin{aligned} &|(f , \phi)_{\Omega_h} - (f , \phi)^*_{\Omega_h}| \\ &\leq \Sigma_K \left| E_K\left[f[\phi]_{G_K} \right] \right| \\ &\quad + \Sigma_K \left| E_K\left[f(\phi - [\phi]_{G_K}) \right] \right| . \end{aligned}\right\} \quad (4.3.4)$$

To bound the first term for an element T_K wholly contained in Ω (for which $f \in H^2(T_K)$) we note first that by (4.1.8)

$$\sup_{T_K} |\phi| \leq c h_K^{-1} \|\phi\|_{1,T_K} \quad \text{for all } \phi \in S. \quad (4.3.5)$$

Then by Lemma 4.3(i) and (4.3.5),

$$\begin{aligned} &\left| E_K\left[f[\phi]_{G_K} \right] \right| \\ &\leq |E_K(f)| \, |[\phi]_{G_K}| \\ &\leq c h_K^2 |f|_{2,T_K} \|\phi\|_{1,T_K} \\ &= c h_K^2 |f|_{2,T_K \cap \Omega} \|\phi\|_{1,T_K} . \end{aligned} \quad (4.3.6)$$

Alternatively if T_K is a boundary element then (recall (4.2.7)) we can do no better than (Lemma 4.3(ii))

$$\begin{aligned} &\left| E_K\left[f[\phi]_{G_K} \right] \right| \\ &\leq c h_K^2 \left[|f|_{1,T_K} + |f|_{2,T_K \cap \Omega} \right] |[\phi]_{G_K}| . \end{aligned}$$

We cannot use (4.3.5) here without losing a power of h_K. But since $\phi = 0$ on $\partial\Omega$ (recall Theorem 4.2) and $\nabla\phi$ is constant on T_K,

$$|[\phi]_{G_K}| \leq c h_K \|\nabla\phi\|_{L_\infty(T_K)} \leq c |\phi|_{1,T_K} . \quad (4.3.7)$$

So for all T_K,

$$\begin{aligned} &\left| E_K\left[f[\phi]_{G_K} \right] \right| \\ &\leq c h_K^2 \left[|f|_{1,T_K} + |f|_{2,T_K \cap \Omega} \right] \|\phi\|_{1,T_K} . \end{aligned}$$

To bound the other term in (4.3.4) we note that $f(\phi - [\phi]_{G_K})$ vanishes at the centroid G_K and write

$$\begin{aligned} &\left| E_K\left[f(\phi - [\phi]_{G_K}) \right] \right| \\ &= \left| \iint_{T_K} \left[f(\phi - [\phi]_{G_K}) \right] \right| \quad (4.3.8) \\ &\leq c h_K \|f\|_{1,T_K} \|\phi - [\phi]_{G_K}\|_{L_\infty(T_K)} . \end{aligned}$$

The ϕ term is bounded by $c |\phi|_{1,T_K}$ (as in (4.3.7)). Further, since the integral (4.3.8) vanishes when f is a constant on T_K,

We turn next to the derivations of (4.2.15) and (4.2.16) and start by bounding the error in the numerical quadrature of the term

$$a_{11}\,\frac{\partial u}{\partial x}\,\frac{\partial \phi}{\partial x}\ .$$

By the above lemma and the Liebnitz differentiation rule - recall $\partial\phi/\partial x$ is constant in the triangle T_k -

$$\begin{aligned}
&\left| E_k\left[\, a_{11}\,\frac{\partial u}{\partial x}\,\frac{\partial \phi}{\partial x}\,\right]\right| \\
&\leq\ ch_k^3 \left| a_{11}\,\frac{\partial u}{\partial x}\,\frac{\partial \phi}{\partial x}\right|_{2,T_k} \\
&=\ ch_k^3 \left| a_{11}\,\frac{\partial u}{\partial x}\right|_{2,T_k} \left|\left[\frac{\partial \phi}{\partial x}\right]_{T_k}\right| \\
&\leq\ ch_k^2 \left| a_{11}\,\frac{\partial u}{\partial x}\right|_{2,T_k} |\phi|_{1,T_k} \\
&\leq\ ch_k^2 \Big[\, |a_{11}|_{2,T_k}\, \|\partial u/\partial x\|_{L_\infty(T_k)} \\
&\qquad +\ |a_{11}|_{1,\infty,T_k}\, |\partial u/\partial x|_{1,T_k} \\
&\qquad +\ \|a_{11}\|_{L_\infty(T_k)}\, |\partial u/\partial x|_{2,T_k}\,\Big]\, |\phi|_{1,T_k} \\
&\leq\ ch_k^2 \Big[\, \|a_{11}\|_{2,T_k}\, \|u\|_{3,\Omega_h} \\
&\qquad +\ \|a_{11}\|_{2,2+\epsilon,\Omega_h}\, \|u\|_{3,T_k}\,\Big]\, |\phi|_{1,T_k}\ .
\end{aligned}$$

The total error over all the elements is bounded - by Cauchy-Schwarz, (4.1.5) and (4.2.6) - thus:

$$\begin{aligned}
&\Sigma_k \left| E_k\left[\, a_{11}\,\frac{\partial u}{\partial x}\,\frac{\partial \phi}{\partial x}\,\right]\right| \\
&\leq\ c\left[\, \Sigma_k\, h_k^4 \Big[\, \|a_{11}\|_{2,T_k}^2\, \|u\|_{3,\Omega_h}^2 \right. \\
&\qquad\qquad \left. +\ \|a_{11}\|_{2,2+\epsilon,\Omega_h}^2\, \|u\|_{3,T_k}^2\,\Big]\,\right]^{1/2} |\phi|_{1,\Omega_h} \\
&\leq\ cC_\Omega^2 h^2\, \|a_{11}\|_{2,2+\epsilon,\Omega_h}\, \|u\|_{3,\Omega_h}\, |\phi|_{1,\Omega_h} \\
&\leq\ cC_\Omega^2 h^2\, \|a\|_2\, \|u\|_3\, |\phi|_{1,\Omega_h} \qquad (4.3.3)
\end{aligned}$$

in the notation of Theorem 4.2. The other terms in (4.2.15) are bounded identically.

In effect we use another projection to obtain (4.2.16), writing

B.H. yields

$$\left| E_k\left[f(\phi - [\phi]_{G_k}) \right] \right|$$
$$\leq \quad c h_k^2 \, |f|_{1,T_k} \, |\phi|_{1,T_k} \quad . \qquad (4.3.9)$$

We substitute (4.3.6) and (4.3.9) into (4.3.4):

$$|(f , \phi)_{\Omega_h} - (f , \phi)^*_{\Omega_h}|$$
$$\leq \quad c \left[\Sigma_k \, h_k^4 \, (|f|^2_{1,T_k} + |f|^2_{2,T_k \cap \Omega}) \right]^{1/2} \, ||\phi||_{1,\Omega_h} \; ;$$

by (4.1.5) and Friedrich's inequality (recall $\phi = 0$ on $\partial\Omega_h$), this is bounded by

$$c C_\Omega^2 h^2 \, (|f|_{1,\Omega_h} + |f|_{2,\Omega_h}) \, |\phi|_{1,\Omega_h} \quad .$$

Finally, we can bound $|f|_{1,\Omega_h}$ by (4.2.7). For

$$\left| - \frac{\partial}{\partial x}\left[a_{11} \, \frac{\partial u}{\partial x} \right] \right|_{1,\Omega_h} \quad \leq \quad \left| a_{11} \frac{\partial u}{\partial x} \right|_{2,\Omega_h} \; ,$$

etc. and so (this is almost identical to the derivation of (4.3.3))

$$|f|_{1,\Omega_h} \quad = \quad |Lu|_{1,\Omega_h} \quad \leq \quad ||a||_2 \;\; ||u||_3 \quad .$$

We have now established (4.2.16).

We end this section with a simple numerical example. We consider the standard uniform mesh on the unit square and note that, solving (1.6.1) with (1.6.2),

$$E_{rec} \quad \simeq \quad 3.0 h^2 \quad .$$

(This was given in Section 3.3. E_{rec} is the average error for recovery at centroids.) Alternatively we replace (1.6.1) with

$$(\nabla R u \; , \; \nabla \phi \;)_\Omega \quad = \quad (\; -\Delta u \; , \; \phi \;)_\Omega \qquad (4.3.10)$$

for all $\phi \in S_0$ (i.e. exact quadrature); we now obtain

$$E_{rec} \quad \simeq \quad 2.8 h^2 \quad .$$

This is only a very minor improvement. We assume therefore that the cost of using high-order quadrature, involving many extra function evaluations, will not in general be justified by its effect on gradient errors.

4.4 CURVATURE, COEFFICIENTS AND CANCELLATION

Theorem 4.4 Under the conditions of Section 4.2 (in particular, $u \in H^3(\Omega_h)$ and $\phi \in S_0$),

$$\left| a^*_{\Omega_h}(Iu - u , \phi) \right| \leq ch^2 \, ||a||_2 \, ||u||_K \, |\phi|_{1,\Omega_h} .$$

Proof We consider the contribution from a single band β:

$$a^*_{\beta_h}(Iu - u , \phi) = \Sigma_k [\nabla e^T . a . \nabla \phi]_{G_k} \, meas\,(T_K) , \qquad (4.4.1)$$

where

$$e = Iu - u$$

and a is the matrix $(a)_{ij} = a_{ij}$.

The first stage is to decompose $\nabla\phi$ (as in Section 2.2). We note that the primary triangulation directions are given by discretised X- and Y- parallels; because the mesh is curved the decomposition will therefore vary from element to element.

For example, let us consider a triangle T_+ with nodes given by (X,Y) coordinates (X_0,Y_0), (X_0+h,Y_0) and (X_0+h,Y_0+h) for some (X_0,Y_0). Let these nodes be $N_0 = (x_0,y_0)$, $N_1 = (x_1,y_1)$ and $N_+ = (x_+,y_+)$ respectively in the (x,y)-plane (see Figure 4.4.1); let ϕ ($\in S_0$) take the values ϕ_0, ϕ_1 and ϕ_+ at the three nodes.

We note that

$$2\, meas\,(T_+) = x_0(y_1 - y_+) + x_1(y_+ - y_0) + x_+(y_0 - y_1) ;$$

it can then be verified from the appropriate simultaneous equations that

$$[\phi]_{T_+} = \lambda + \mu x + \nu y ,$$

where λ, μ and ν are given by

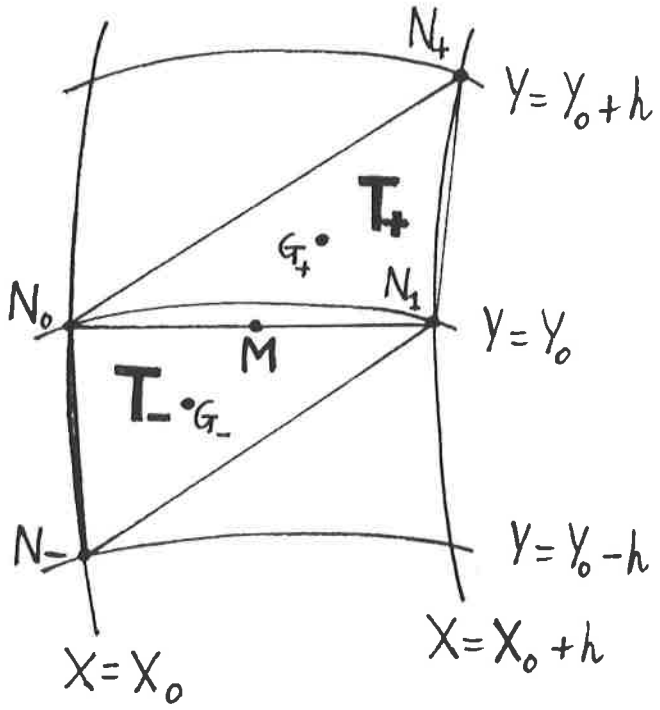

Figure 4.4.1

Labelling of nodes for Theorem 4.4

$N_j = (x_j, y_j)$ for each symbol $j \in \{0,1,+,-\}$.

$$
\left.
\begin{aligned}
&2\,meas\,(T_+)\;\lambda \\
&= \phi_0(x_1y_+ - x_+y_1) + \phi_1(x_+y_0 - x_0y_+) \\
&\qquad\qquad + \phi_+(x_0y_1 - x_1y_0) \quad , \\
&2\,meas\,(T_+)\;\mu \\
&= \phi_0(y_1 - y_+) + \phi_1(y_+ - y_0) + \phi_+(y_0 - y_1) \\
\text{and}\quad &2\,meas\,(T_+)\;\nu \\
&= \phi_0(x_+ - x_1) + \phi_1(x_0 - x_+) + \phi_+(x_1 - x_0) \quad .
\end{aligned}
\right]
$$

We choose to write

$$
[\nabla\phi]_{T_+} = \begin{bmatrix} \mu \\ \nu \end{bmatrix}
$$

in the following form:

$$
[\nabla\phi]_{T_+} = D_X\phi + D_Y\phi \quad , \tag{4.4.2}
$$

where

$$
\left.
\begin{aligned}
D_X\phi &= \frac{1}{2\,meas\,(T_+)} \begin{bmatrix} y_1 - y_+ \\ x_+ - x_1 \end{bmatrix} (\phi_0 - \phi_1) \\
\text{and}\quad D_Y\phi &= \frac{1}{2\,meas\,(T_+)} \begin{bmatrix} y_1 - y_0 \\ x_0 - x_1 \end{bmatrix} (\phi_1 - \phi_+) \quad .
\end{aligned}
\right\} \tag{4.4.3}
$$

This variable decomposition is essential to our result; as far as we know it does not appear elsewhere in the literature. Note that, for instance, $D_X\phi$ is perpendicular to N_1N_+ (the element edge given by the triangulation direction associated with X-parallels); this vector will not in general be parallel to N_0N_1. More crucially, however, the ϕ-dependence of $D_X\phi$ is precisely that component of $\nabla\phi$ which is constant across N_0N_1 (the edge associated with Y-parallels). We now recall (2.2.6) and the subsequent discussion and see that the decompositions used in Section 2.2 are all special cases of the above.

The situation is very similar in the triangle T_- with nodes N_0, N_1 and N_-, where $N_- = (x_-,y_-)$ is the image of (X_0,Y_0-h) and $\phi = \phi_-$ there. We use the decomposition (4.4.2) again:

$$
[\nabla\phi]_{T_-} = D_X\phi + D_Y\phi \quad .
$$

This time however, insted of (4.4.3), we obtain

$$\left.\begin{aligned} D_X\phi &= \frac{1}{2\ meas\ (T_-)} \begin{bmatrix} y_- - y_0 \\ x_0 - x_- \end{bmatrix} (\phi_0 - \phi_1) \\ \text{and} \qquad D_Y\phi &= \frac{1}{2\ meas\ (T_-)} \begin{bmatrix} y_1 - y_0 \\ x_0 - x_1 \end{bmatrix} (\phi_- - \phi_0) \quad . \end{aligned}\right\} (4.4.4)$$

Now, since all elements have one of the two forms $T_\pm$, we can write (4.4.1) in the form

$$\begin{aligned} & a^*_{\beta_h}(e, \phi) \\ &= \Sigma_k \left[\nabla e^T \cdot a \right]_{G_k} \left[D_X\phi + D_Y\phi \right]_{T_k} meas\ (T_k) \quad ; \end{aligned}$$

we interpret D_X and D_Y by (4.4.3) or (4.4.4) as appropriate to each element T_k. We will examine in detail the "X-derivative" term, rewriting it thus:

$$\left.\begin{aligned} & \Sigma_k \left[\nabla e^T \cdot a \right]_{G_k} \left[D_X\phi \right]_{T_k} meas\ (T_k) \\ &= \Sigma_k \left[\nabla e^T \cdot a \right]_{G_k} \delta_{k\pm} (\phi_{k0} - \phi_{k1})/2 \quad . \end{aligned}\right\} (4.4.5)$$

By ϕ_{k0} we mean the value of ϕ_0 in the element T_k, and so on; from (4.4.3) and (4.4.4) we have

$$\delta_{k+} = \begin{bmatrix} y_{k1} - y_{k+} \\ x_{k+} - x_{k1} \end{bmatrix}$$

$$\text{and} \qquad \delta_{k-} = \begin{bmatrix} y_{k-} - y_{k0} \\ x_{k0} - x_{k-} \end{bmatrix} .$$

We set

$$\begin{aligned} \delta_k &= (\delta_{k+} + \delta_{k-})/2 \\ &= \begin{bmatrix} (y_{k1} - y_{k+} + y_{k-} - y_{k0})/2 \\ (x_{k+} - x_{k1} + x_{k0} - x_{k-})/2 \end{bmatrix} . \end{aligned}$$

We then split the sum (4.4.5) thus:

$$\begin{aligned} & \left| \Sigma_k \left[\nabla e^T \cdot a \right]_{G_k} \left[D_X\phi \right]_{T_k} meas\ (T_k) \right| \\ &\leq \frac{1}{2} \left[|s_1| + |s_2| + |s_3| \right] \end{aligned}$$

where (recall that M_k is the midpoint of the shared edge N_0N_1)

$$\begin{aligned} s_1 &= \Sigma_k \left[\nabla e^T \cdot a \right]_{G_k} (\delta_{k\pm} - \delta_k) (\phi_{k0} - \phi_{k1}) \quad , \\ s_2 &= \Sigma_k \left[\nabla e^T \right]_{G_k} ([a]_{G_k} - [a]_{M_k}) \delta_k (\phi_{k0} - \phi_{k1}) \end{aligned}$$

and $s_3 = \Sigma_k [\nabla e^T]_{G_k} [a]_{M_k} \delta_k (\phi_{k0} - \phi_{k1})$.

The purpose behind our decomposition now becomes clear. For $[a]_{M_k}$, δ_k and $(\phi_{k0} - \phi_{k1})$ take identical values in the two triangles T_{k+} and T_{k-} , for every k. We can therefore rearrange s_3 thus:

$$s_3 = \Sigma_k ([\nabla e^T]_{G_{k+}} + [\nabla e^T]_{G_{k-}}) [a]_{M_k} \delta_k (\phi_{k0} - \phi_{k1}) ;$$

this summation is now over the triangle pairs $A_k = T_{k+} \cup T_{k-}$ - see Figure 4.1.4. Note that contributions to s_3 from the elements B_k , which cannot be paired off, vanish. For - recall (4.1.1) and the discussion on Figure 4.1.5 - N_{k0} and N_{k1} lie on a segment of $\partial\beta_h$ with (X,Y)-slope (almost) zero and hence on $\partial\Omega_h$; therefore $\phi_{k0} = \phi_{k1} = 0$. Note also that the three sums s_1 , s_2 and s_3 represent the effects of curvature of the mesh, local variation of the coefficients a_{ij} and - at the core of superconvergence - cancellation of the dominant error term between neighbouring elements. Incidentally, as with the bounds of Section 4.3, the bound for s_2 that follows is not dependent on the triangulation being superconvergent.

We consider in turn the factors which make up the three summands. By (4.1.8),

$$\begin{aligned} & | \phi_{k0} - \phi_{k1} | \\ & \leq |N_{k0}N_{k1}| \; | [\nabla\phi]_{T_k} | \\ & \leq h_k \, |\phi|_{1,T_k} \, (meas\ (T_k))^{-1/2} \\ & \leq c \, |\phi|_{1,T_k} . \end{aligned} \qquad (4.4.6)$$

Next

$$\begin{aligned} & \delta_k - \delta_{k\pm} \\ & = \begin{bmatrix} (y_{k+} + y_{k-} - y_{k1} - y_{k0})/2 \\ (x_{k1} + x_{k0} - x_{k+} - x_{k-})/2 \end{bmatrix} ; \end{aligned}$$

by (4.1.6)

$$| \delta_k - \delta_{k\pm} | \leq \kappa_k h/2 \ . \qquad (4.4.7)$$

In addition,

$$| \delta_k | \leq c \ diam \ (A_k) = ch_k \ . \qquad (4.4.8)$$

Now by S.E.,

$$| [a]_{G_k} - [a]_{M_k} | \leq c \ ||a||_{1,\infty,T_k} \ ;$$

therefore by B.H. and S.E. again

$$\begin{aligned} | [a]_{G_k} - [a]_{M_k} | &\leq ch_k \ |a|_{1,\infty,T_k} \\ &\leq ch_k \ ||a||_2 \ . \end{aligned} \qquad (4.4.9)$$

Also, by S.E.,

$$| [a]_{G_k} | \leq c \ ||a||_2 \ ; \qquad (4.4.10)$$

$| [a]_{M_k} |$ is bounded identically.

The ∇e factors are less simple. To bound the "cancellation" factor

$$F(u) = [\nabla e]_{G_+} + [\nabla e]_{G_-}$$

(once again, the $\cdot_k$ has been dropped from all symbols except h_k), we move back to the (ξ,η)-coordinate system of Lemma 3.4. The centroids $G_\pm$ have coordinates $((\xi_1 + \xi_\pm)/3 \ , \ \eta_\pm/3)$. We note that (3.4.4) still holds; for quadratic u we obtain

$$F(\xi^2) = \begin{bmatrix} 2(\xi_1 - \xi_+ - \xi_-)/3 \\ (\xi_+^2 - \xi_+\xi_1)/\eta_+ + (\xi_-^2 - \xi_-\xi_1)/\eta_- \end{bmatrix}$$

$$F(\xi\eta) = \begin{bmatrix} -(\eta_+ + \eta_-)/3 \\ 2(\xi_+ + \xi_- - \xi_1)/3 \end{bmatrix}$$

and $$F(\eta^2) = \begin{bmatrix} 0 \\ (\eta_+ + \eta_-)/3 \end{bmatrix} \ .$$

We now proceed exactly as in the earlier lemma. By means of the projection (3.4.5) we obtain the general bound - c.f. (3.4.7) -

$$\begin{aligned} &| F_k(u) | \\ &\leq c(h_k^2 + \kappa_k h) \ h_k^{-1} \ ||u||_{3,A_k} \ . \end{aligned} \qquad (4.4.11)$$

Finally, by S.E.,

$$| [\nabla e^T]_{G_k} | \leq ch^{-(4+\epsilon)/(2+\epsilon)} ||u||_{2,2+\epsilon,T_k}$$

for any fixed $\epsilon > 0$. Since ∇e vanishes in T_k when u is linear, B.H. implies

$$| [\nabla e^T]_{G_k} | \leq ch^{\epsilon/(2+\epsilon)} |u|_{2,2+\epsilon,T_k} ;$$

by S.E again we obtain

$$| [\nabla e^T]_{G_k} | \leq c ||u||_{3,T_k} . \qquad (4.4.12)$$

We substitute (4.4.6),...,(4.4.12) into s_1 , s_2 and s_3 :

$$| s_1 |$$
$$\leq c \Sigma ||u||_{3,T_k} \cdot ||a||_2 \cdot \kappa_k h \cdot |\phi|_{1,T_k}$$
$$\leq ch ||a||_2 \left[\Sigma \kappa_k^2 ||u||^2_{3,T_k} \right]^{1/2} |\phi|_{1,\beta_h}$$
$$\leq ch^2 ||a||_2 \left[\Sigma (\kappa_k h^{-1})^2 ||u||^2_{3,T_k} \right]^{1/2} |\phi|_{1,\beta_h} ;$$
$$| s_2 |$$
$$\leq c \Sigma ||u||_{3,T_k} \cdot h_k ||a||_2 \cdot h_k \cdot |\phi|_{1,T_k}$$
$$\leq cC_\Omega^2 h^2 ||a||_2 ||u||_{3,\Omega_h} |\phi|_{1,\beta_h} ;$$
$$| s_3 |$$
$$\leq c \Sigma (h_k^2 + \kappa_\kappa h) h_k^{-1} ||u||_{3,A_k} \cdot ||a||_2 \cdot h_k \cdot |\phi|_{1,A_k}$$
$$\leq ch^2 ||a||_2 \left[\Sigma (C_\Omega^2 + \kappa_k h^{-1})^2 ||u||^2_{3,A_k} \right]^{1/2}$$
$$\cdot |\phi|_{1,\beta_h} .$$

We then substitute these bounds back into (4.4.5) and obtain

$$\Sigma_k [\nabla e^T \cdot a]_{G_k} [D_X \phi]_{T_k} \, meas\,(T_k)$$
$$\leq ch^2 ||a||_2 \left[\Sigma (C_\Omega^2 + \kappa_k h^{-1})^2 ||u||^2_{3,A_k} \right]^{1/2}$$
$$\cdot |\phi|_{1,\beta_h} .$$

We now bound the $D_Y \phi$ term. This process is identical to the above, except that the contributions to s_3 from unpaired triangles B_k now vanish because N_{k0} and N_{k1} are on a segment of $\partial\beta_h$ with (X,Y)-slope (almost) infinity.

To complete the superconvergence proof, we substitute the D_X and D_Y estimates back into

CHAPTER FIVE

THE POINTWISE ERROR

$$a^{*}_{\beta_h}(\theta, \phi)$$

and sum over the bands β which constitute Ω. Note that, as required, the condition "$\phi = 0$ on $\partial\beta_h$" is only taken up on segments of $\partial\Omega_h$ and not on interband boundaries. ###

5.1 INTRODUCTION

The superconvergence results given so far (in particular Theorems 1.5 and 4.2) are all encumbered by the presence of a mean-square average. It is due to the substitution $\phi = (I - R)u$ into bounds on

$$| \ (\ \nabla(Iu - u) \ , \ \nabla\phi \ )_{\Omega} \ | \qquad\qquad (\phi \in S_0);$$

this leads directly to a bound on $||\nabla(I - R)u||$ in $L_2(\Omega)$ (whence, for example, the form of (1.5.9) et.seq.). However a different choice of $\phi \in S_0$ - see (5.1.11) below - can avoid the $L_2(\Omega)$ norm altogether. The subject of this chapter is the link between the mean-square average and the superconvergence phenomenon; we start with an interpretation of the norms of error bounds given so far.

We consider (4.2.20):

$$\left[\ \Sigma_k \ \left| D_k Ru - [\nabla u]_{M_k} \right|^2 \ \right]^{1/2} \quad = \quad O(h) \quad .$$

It implies that the number of recovery points M_k (out of the total $O(h^{-2})$ in Ω_h) at which the convergence rate is no better than $O(h^s)$ cannot be greater than $O(h^{2(1-s)})$, for any fixed s. So the number of recovery points at which second order convergence (i.e. superconvergence) does not occur is $o(h^{-2})$; the proportion of such points out of the total is $o(1)$. We therefore expect that as $h \to 0$ the subregions of Ω in which pointwise superconvergence fails will decrease in total measure. Further, we expect that there will be some natural connection between any absence of pointwise superconvergence on one hand and local properties of the problem and our approximation to it on the other.

Now the only natural locations for such a limited number of recovery points are in a layer close to the boundary $\partial\Omega$ (recall, for example, (4.2.21)) or in narrow regions in the interior of Ω

where the smoothness of the problem or mesh may be open to question. If all such aspects are sufficiently regular in the interior, we can assume that superconvergence will be pointwise (away from $\partial\Omega$). Further, if the boundary and conditions imposed there are sufficently smooth and well represented then there is no intuitive reason why superconvergence should not occur "pointwise", i.e. individually at every recovery point.

We aim to give some meaning to such terms as "sufficiently regular" and "narrow regions". In this section we will give a model pointwise result corresponding to Theorem 1.5; later we will use this as a framework for discussing more general problems. However in the later cases there are great technical difficulties and we will not be able to justify all our hypotheses rigorously.

The technicalities which arise throughout are connected with a derivative Green's function and its Finite Element approximation; we will introduce these below. (Nitsche (1978) has discussed other approaches to L_∞ error bounds; the principal alternative - using carefully chosen weighted norms - is closely related to the Green's function method and we do not expect it to yield results which are either stronger or simpler.)

Let Ω be a rectangle, partitioned as in Section 1.5 (and satisfying (1.5.2)). We group the elements into pairs A_k with common edges parallel to the x-axis and denote the midpoints of these edges by M_k. In particular, we concentrate on a fixed element pair A_0 and the corresponding midpoint $M_0 = (x_0, y_0)$. We associate with them a distance ρ and a $C_0^\infty(A_0)$ function $\delta = \delta(\rho)$ such that

$$\left.\begin{aligned} \rho^2 &= \xi^2 + \eta^2 \ , \ \xi = x - x_0 \ , \ \eta = y - y_0 \ , \\ \iint_{A_0} \delta(\rho)\, dx\, dy &= 1 \quad \text{and} \quad 0 \leq \delta \leq ch^{-2} \end{aligned}\right\} \tag{5.1.1}$$

(See Figure 5.1.1.) Then by construction,

$$\left[\frac{\partial \phi}{\partial x} \right]_Q = \left[\frac{\partial \phi}{\partial x} \ , \ \delta \right]_\Omega \ , \quad \text{for all } \phi \in S \tag{5.1.2}$$

and for any $Q \in A_0$ (in particular the point M_0). Corresponding to δ, let us define

$$g = g(x,y;x_0,y_0) = g(\xi,\eta) \in H_0^1(\Omega)$$

by

$$(\nabla g \ , \ \nabla v \ )_\Omega = \left[\frac{\partial v}{\partial x} \ , \ \delta \right]_\Omega \tag{5.1.3}$$

for all $v \in H_0^1(\Omega)$; g is a smoothed x-derivative Green's function for the Laplacian on Ω. (See (5.1.27) below.) The Finite Element approximation $Rg \in S_0$ to g is given by

$$(\nabla Rg \ , \ \nabla \phi \ )_\Omega = \left[\frac{\partial \phi}{\partial x} \ , \ \delta \right]_\Omega \tag{5.1.4}$$

for all $\phi \in S_0$.

The functions δ, g and Rg were introduced in this form by Rannacher and Scott (1982). They proved (for the less simplified case of general triangulations on any convex polygonal region Ω) that

$$| Rg - g |_{1,1,\Omega} \leq c \ , \tag{5.1.5}$$

whence incidentally their W_∞^1 estimate

$$| Ru - u |_{1,\infty,\Omega} \leq ch \, |u|_{2,\infty,\Omega} \ . \tag{5.1.6}$$

Note that g and Rg both vanish on $\partial\Omega$ but that - as in previous chapters - u need not. In the derivation of (5.1.10) below we will require $(I - R)u = 0$ on $\partial\Omega$; this is of course satisfied without any special restrictions on u.

We remark that (5.1.5) appears to lack one order of h; this is due to the singularity in g at M_0 (albeit smoothed). Another consequence of the singularity is that

$$| g |_{1,1,\Omega} \leq c \, |\log h| \ ; \tag{5.1.7}$$

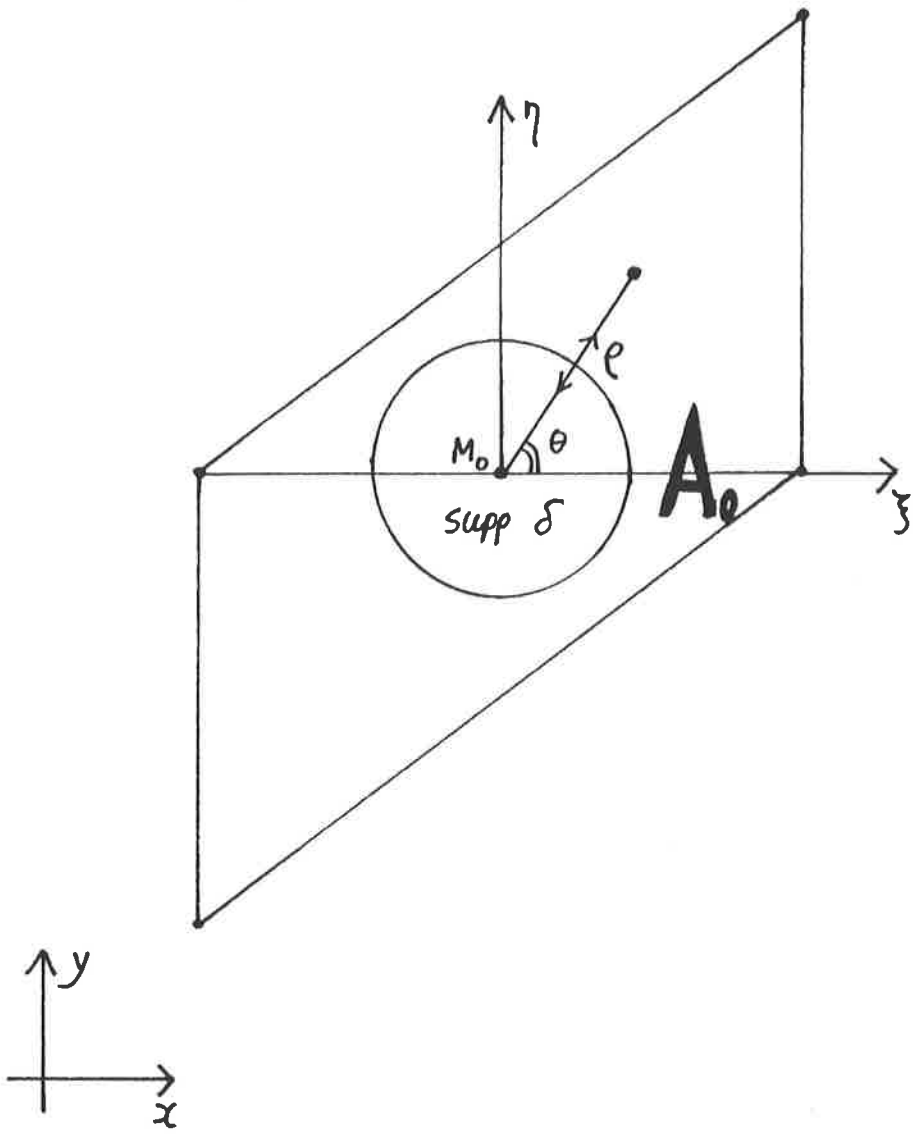

Figure 5.1.1

Coordinate notation

Any point (x,y) in Ω can also be given in terms of the local coordinates (ξ,η) - or the local polars (ρ,θ) - as shown. (Note that the ξ-axis - eqivalently the radius $\theta = 0$ - indicates the direction for differentiation of the error $(Ru - u)$ in (5.1.14).)

we shall derive this inequality in the lemma at the end of the section. We take (5.1.5) and (5.1.7) together thus:

$$| Rg |_{1,1,\Omega} \leq c\,|\log h| \quad . \tag{5.1.8}$$

We use the Green's function to estimate the error in the x-derivative of Ru at the stress point M_0 - without the need for averaging. Let

$$u \in H_0^1(\Omega) \cap W_\infty^3(\Omega) \tag{5.1.9}$$

and $Ru \in S_0$ satisfy (1.3.2) and (1.3.5) respectively. By (5.1.2), (5.1.4) and (1.5.1), for any $Q \in A_0$,

$$\begin{aligned}
&\left[\frac{\partial}{\partial x}(I - R)u \right]_Q \\
&= \left[\frac{\partial}{\partial x}(I - R)u \ , \ \delta \right]_\Omega \\
&= (\nabla(I - R)u \ , \ \nabla Rg)_\Omega \\
&= (\nabla(Iu - u) \ , \ \nabla Rg)_\Omega \\
&= \left[\frac{\partial}{\partial x}(Iu - u) \ , \ \frac{\partial Rg}{\partial x} \right]_\Omega \\
&\quad + \left[\frac{\partial}{\partial y}(Iu - u) \ , \ \frac{\partial Rg}{\partial y} \right]_\Omega \quad .
\end{aligned} \tag{5.1.10}$$

We consider the x-derivative term. It can be expanded thus:

$$\Sigma_k \, F_{k,Rg}(u) \quad ,$$

where the sum is over the triangle pairs A_k. The functionals $F_{k,Rg}$ are defined by

$$F_{k,\phi}(u) \quad = \quad \left[\frac{\partial}{\partial x}(Iu - u) \ , \ \frac{\partial \phi}{\partial x} \right]_{A_k} \quad ,$$

where ϕ can be any member of S. (Recall that $Rg = 0$ on $\partial\Omega$; as usual this implies the vanishing of contributions to the sum from all unpaired triangles B_k.) Now if u is quadratic on A_k then $F_{k,\phi}$ vanishes by (1.5.4) and (1.5.5). But by S.E.

$$\left| F_{k,\phi}(u) \right| \leq ch^{-1} \, |||u|||_{3,\infty,A_k} \left|\left| \frac{\partial \phi}{\partial x} \right|\right|_{L_1(A_k)}$$

for all $u \in W_\infty^3(A_k)$. Hence by B.H. (compare with (1.5.8)),

$$\left| F_{k,\phi}(u) \right| \leq ch^2 \, |u|_{3,\infty,A_k} \left|\left| \frac{\partial \phi}{\partial x} \right|\right|_{L_1(A_k)} \quad .$$

Substituting

$$\phi \quad = \quad Rg \tag{5.1.11}$$

into this bound and summing over k, we get

$$\left| \left[\frac{\partial}{\partial x}(Iu - u) \, , \, \frac{\partial Rq}{\partial x} \right]_{\Omega} \right|$$
$$\leq \quad ch^2 \, |u|_{3,\infty,\Omega} \left\| \frac{\partial Rq}{\partial x} \right\|_{L_1(\Omega)} .$$

The y-derivative term in (5.1.10) is now bounded identically and by (5.1.8),

$$\left| \left[\frac{\partial}{\partial x}(I - R)u \right]_{Q} \right|$$
$$\leq \quad ch^2 \, |u|_{3,\infty,\Omega} \, |Rq|_{1,1,\Omega}$$
$$\leq \quad ch^2 |\log h| \quad |u|_{3,\infty,\Omega} . \qquad (5.1.12)$$

But by S.E. and B.H. (recall that M_0 is an x-derivative stress-point)

$$\left| \left[\frac{\partial}{\partial x}(Iu - u) \right]_{M_0} \right|$$
$$\leq \quad ch^2 \, |u|_{3,\infty,\Omega} \; ; \qquad (5.1.13)$$

adding (5.1.12) with $Q = M_0$ to (5.1.13) we arrive at the pointwise superconvergence result

$$\left| \left[\frac{\partial}{\partial x}(Ru - u) \right]_{M_0} \right|$$
$$\leq \quad ch^2 |\log h| \quad |u|_{3,\infty,\Omega} . \qquad (5.1.14)$$

We remark that we can bound the y-component of $\nabla(I - R)u$ in exactly the same way as the x-component. So in fact

$$| \, (I - R)u \, |_{1,\infty,\Omega} \quad \leq \quad ch^2 |\log h| \quad |u|_{3,\infty,\Omega}$$

and (5.1.14) can be extended at once to cover any superconvergent recovery schemes for the full gradient at any point in Ω (recall Section 3.3).

We note the $|\log h|$ term in (5.1.12) and (5.1.14). It implies that there may exist a limited number of stress points M at which

$$\left| \left[\frac{\partial}{\partial x}(I - R)u \right]_{M} \right| \quad = \quad O(h^{2-\epsilon}) \qquad (0 < \epsilon << 1) ,$$

i.e. superconvergence "just fails". We will discuss this phenomenon in detail in the next section and explain why it does not in general occur. Therefore in practice we simply ignore the logarithm and say that the (recovered) gradient is indeed

superconverent in a pointwise sense.

Numerically, the maximum error over all stress (or recovery) points tends to exceed the averaged error by an empirical factor of between two and five. For example, we recall (from Section 1.6) that the averaged tangential derivative error at stress points, when u satisfies (1.6.2) and is approximated by (1.6.1), is

$$E_{tgt} \simeq 1.4h^2 .$$

The corresponding maximum error (over all stress points in Ω) is found to be

$$E_{tgt[max]} \simeq 5.6h^2 .$$

(For other examples see Levine, 1982.)

We turn finally to the proof of (5.1.7), considering the result in a slightly more general form which will be useful to us in the next section. For simplicity of presentation we consider only the Green's function corresponding to the x-derivative in (5.1.3), (5.1.14), etc. (The result and proof are identical for all other derivatives.)

Lemma 5.1 Let $\epsilon \geq 0$ be a constant and let

$$\beta = \beta(\epsilon) = \begin{cases} 1 & \text{when } \epsilon = 0 \\ 0 & \text{when } \epsilon > 0 . \end{cases} \qquad (5.1.15)$$

Let $g = g(\xi,\eta) \in H_0^1(\Omega)$ be defined by (5.1.3) Then

$$|| \rho^{\epsilon} \nabla g ||_{L_1(\Omega)} \leq c \, |\log h|^{\beta} . \qquad (5.1.16)$$

In particular, if $\epsilon = 0$ then we have (5.1.7).

Proof Let us define the function $g_\delta = g_\delta(\xi,\eta)$ - recall (5.1.1) and Figure 5.1.1 - by

$$g_\delta = \frac{\xi}{\rho^2} \int_0^\rho \delta(s) \, s \, ds . \qquad (5.1.17)$$

We show first that g_δ satisfies a bound identical to (5.1.16) and then examine the connection between g_δ and g.

We express g_δ in the form

$$g_\delta = \frac{\cos\theta}{\rho}\int_0^\rho \delta(s)\, s\, ds \quad , \tag{5.1.18}$$

where (ρ,θ) are the polar coordinates corresponding to (ξ,η) (recall Figure 5.1.1), and substitute this into the differential identity

$$\left| \nabla g_\delta \right|^2 = \left[\frac{\partial}{\partial\rho} g_\delta \right]^2 + \frac{1}{\rho^2}\left[\frac{\partial}{\partial\theta} g_\delta \right]^2 \quad .$$

Then, since

$$\frac{\partial g_\delta}{\partial\rho} = -\frac{\cos\theta}{\rho^2}\int_0^\rho \delta(s)\, s\, ds + \delta(\rho)\cos\theta \quad ,$$

we have

$$\left| \nabla g_\delta \right| \leq \frac{1}{\rho^2}\int_0^\rho \delta(s)\, s\, ds + \delta(\rho) \quad . \tag{5.1.19}$$

Now, suppose that $(x,y) \notin A_0$. Then $\delta(\rho) = 0$ and

$$2\pi\int_0^\rho \delta(s)\, s\, ds = \iint_{A_0} \delta\, dx\, dy = 1 \tag{5.1.20}$$

and so (5.1.19) reduces to

$$\left| \nabla g_\delta \right| \leq \frac{1}{2\pi\rho^2} \quad . \tag{5.1.21}$$

Therefore the contribution to the integral $|| \rho^\epsilon \nabla g_\delta ||_{L_1}$ from $\Omega\backslash A_0$ is

$$\begin{aligned}
&|| \rho^\epsilon \nabla g_\delta ||_{L_1(\Omega\backslash A_0)} \\
&\leq \int_{ch}^{c}\int_0^{2\pi} \rho^\epsilon \left| \nabla g_\delta \right| \rho\, d\theta\, d\rho \\
&\leq \int_{ch}^{c} \rho^{\epsilon-1}\, d\rho \\
&\leq c\left[\rho^\epsilon\, (\log\rho)^\beta \right]_{ch}^{c} \\
&\leq c\,|\log h|^\beta + c \\
&\leq c\,|\log h|^\beta \quad .
\end{aligned} \tag{5.1.22}$$

Alternatively suppose that $(x,y) \in A_0$: we must now work directly from (5.1.19) because we are too close to the singularity at M_0 (i.e. $\rho = 0$) to use (5.1.21). If $\epsilon > 0$, (5.1.1) implies the following bound:

$$\int_0^{ch} \int_0^{\rho} \rho^{\epsilon-1} \, \delta(s) \, s \, ds \, d\rho$$

$$\leq \frac{1}{2\pi} \int_0^{ch} \rho^{\epsilon-1} \, d\rho$$

$$\leq \frac{1}{2\pi\epsilon} \left[\rho^{\epsilon} \right]_0^{ch}$$

$$\leq ch^{\epsilon}$$

$$\leq c \quad . \tag{5.1.23}$$

Or if $\epsilon = 0$, we must resort to the asymptotic bound on δ in (5.1.1), to obtain

$$\int_0^{ch} \int_0^{\rho} \rho^{-1} \, \delta(s) \, s \, ds \, d\rho$$

$$\leq ch^{-2} \int_0^{ch} \int_0^{\rho} \rho^{-1} \, s \, ds \, d\rho$$

$$\leq ch^{-2} \int_0^{ch} \rho \, d\rho$$

$$\leq c \quad . \tag{5.1.24}$$

Hence by (5.1.19), and (5.1.23) or (5.1.24) as appropriate,

$$\| \rho^{\epsilon} \nabla g_{\delta} \|_{L_1(A_0)}$$

$$\leq \int_0^{ch} \int_0^{2\pi} \rho^{\epsilon} \left| \nabla g_{\delta} \right| \rho \, d\theta \, d\rho$$

$$\leq 2\pi \int_0^{ch} \int_0^{\rho} \rho^{\epsilon-1} \, \delta(s) \, s \, ds \, d\rho + \iint_{\Omega} \rho^{\epsilon} \, \delta(\rho)$$

$$\leq c \, .$$

Adding this to (5.1.22), we therefore obtain

$$\| \rho^{\epsilon} \nabla g_{\delta} \|_{L_1(\Omega)}$$

$$\leq c \, |\log h|^{\beta} \tag{5.1.25}$$

as desired.

In the remainder of this proof we will show that g_δ and the Green's function g are sufficiently similar for the property (5.1.25) of g_δ to carry over to g. We note that g_δ is the smoothed x-derivative of the (better known, undifferentiated) free-space Green's function $(2\pi)^{-1} \log \rho$; indeed if $(x,y) \notin A_0$ then, by (5.1.20) and (5.1.1) the form (5.1.17) reduces to

$$g_\delta = \frac{1}{2\pi} \frac{\xi}{\rho^2} = \frac{1}{2\pi} \frac{\partial}{\partial x} \log \rho \quad . \tag{5.1.26}$$

In fact, for any $\rho > 0$, g_δ is a fundamental solution of the differential equation corresponding to (5.1.3). For (from (5.1.18))

$$\frac{1}{\rho} \frac{\partial}{\partial \rho} \left[\rho \frac{\partial g_\delta}{\partial \rho} \right] = \frac{\cos \theta}{\rho^3} \int_0^\rho \delta(s)\, s\, ds + \cos \theta \frac{\partial \delta}{\partial \rho}$$

and

$$\frac{1}{\rho^2} \frac{\partial^2}{\partial \theta^2} g_\delta = - \frac{\cos \theta}{\rho^3} \int_0^\rho \delta(s)\, s\, ds \quad .$$

So by the chain rule and (5.1.1),

$$\Delta g_\delta = \cos \theta \frac{\partial \delta}{\partial \rho} = \frac{\partial \delta}{\partial \xi} = \frac{\partial \delta}{\partial x} \quad . \tag{5.1.27}$$

We investigate the case $\rho = 0$ (i.e. $(x,y) = M_0$) separately, by expanding (5.1.18) for small ρ – recall $\delta \in C^\infty$ –

$$g_\delta \sim \cos \theta \left[\delta(0) \frac{\rho}{2} + \frac{\partial \delta}{\partial \rho}(0) \frac{\rho^2}{3} + O(\rho^3) \right]$$

$$\sim \delta(0) \frac{\xi}{2} + \cos \theta \left[\frac{\partial \delta}{\partial \rho}(0) \frac{\rho^2}{3} + O(\rho^3) \right] \quad .$$

Although $|\cos \theta|$ is undefined at the origin, it is bounded; furthermore since $\delta \in C^\infty$, $\partial\delta/\partial\rho$ vanishes at the origin $\rho = 0$. So $|\Delta g_\delta|$ vanishes there as well:

$$\left| \left[\Delta g_\delta \right]_{\rho=0} \right| \leq \left| \left[\frac{\partial \delta}{\partial \rho} \right]_{\rho=0} \right| = 0 \quad .$$

Now, let $v \in H_0^1(\Omega)$. Then by (5.1.27) and integration by parts twice,

$$\begin{aligned} (\nabla g_\delta , \nabla v)_\Omega &= - (\Delta g_\delta , v)_\Omega \\ &= - \left[\frac{\partial \delta}{\partial x} , v \right]_\Omega \\ &= \left[\delta , \frac{\partial v}{\partial x} \right]_\Omega \quad . \end{aligned}$$

So $g_\delta \in H^1(\Omega)$ satisfies the weak equation (5.1.3). However it is not the same function as g because the latter vanishes on $\partial\Omega$ (and g_δ does not). Suppose now that a harmonic function $g_H \in H^1(\Omega)$ is chosen to satisfy

$$g_\delta + g_H = 0 \quad \text{on } \partial\Omega. \tag{5.1.28}$$

Then, since $(\nabla g_H , \nabla v)_\Omega = 0$ for any $v \in H^1_0(\Omega)$, the sum

$$(g_\delta + g_H)$$

satisfies (5.1.3) too and by (5.1.28) is thus identical to the original Green's function g.

It only remains for us to bound $|| \rho^\epsilon \nabla g_H ||_{L_1(\Omega)}$. If the stress-sampling point M_0 (i.e. the singularity of g_δ) is bounded away from $\partial\Omega$ as $h \to 0$ then the boundary values of g_H are bounded, in all norms, independently of h. Therefore since g_H is harmonic it is also bounded in all norms over Ω (by the maximum principle) - independently of h - and by (5.1.25)

$$\begin{aligned} || \rho^\epsilon \nabla g ||_{L_1(\Omega)} &= || \rho^\epsilon \nabla (g_\delta + g_H) ||_{L_1(\Omega)} \\ &\leq || \rho^\epsilon \nabla g_\delta ||_{L_1(\Omega)} \\ &\quad + c \, || \nabla g_H ||_{L_1(\Omega)} \\ &\leq c \, |\log h|^\beta + c \\ &\leq c \, |\log h|^\beta \quad . \end{aligned}$$

Alternatively, suppose that M_0 is not bounded away from $\partial\Omega$ as $h \to 0$ (i.e. $d(M_0 , \partial\Omega) \to 0$) but that M_0 is still bounded away from all of the corners of $\partial\Omega$. Let us now write g_H in the following form:

$$g_H = g^*_\delta + g^*_H \quad . \tag{5.1.29}$$

Here g^*_δ is an image function of the same general form as g_δ (5.1.18); the singularity and direction of differentiation (i.e. the loci $\rho^* = 0$ and $\theta^* = 0$ in Figure 5.1.2(a)) are chosen so that $g_\delta + g^*_\delta$ will vanish on the segment of $\partial\Omega$ which M_0 approaches as h

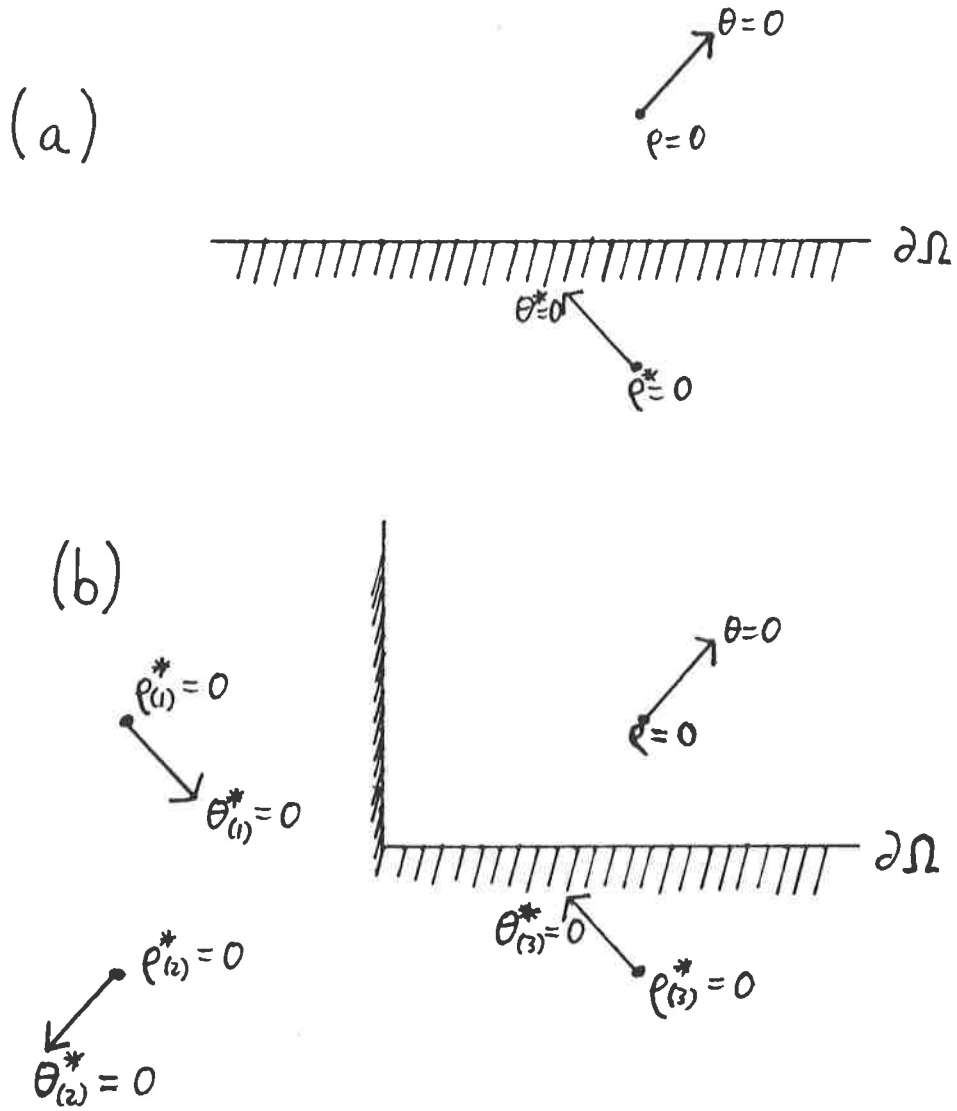

Figure 5.1.2

Image functions for singularities close to ∂Ω

(a) The singularity $\rho = 0$ (i.e. M_0) is close only to one segment of ∂Ω: g^*_δ is the function of the form (5.1.18) with polar coordinates (ρ^*,θ^*) as marked.

(b) The singularity is close to a vertex – i.e. two segments – of ∂Ω. Since Ω is a rectangle, g^*_δ can be given as the sum of three g_δ-type functions $g^*_{\delta(j)}$ $(j = 1,2,3)$.

$\to 0$. Thus g_δ^* satisfies a bound of the form (5.1.25) and furthemore the image point $\rho^* = 0$ is outside Ω, i.e. g_δ^* is harmonic in the interior of Ω.

We see therefore that g_H^* is another harmonic function with values on $\partial\Omega$ such that (5.1.28) still holds. But g_H^* vanishes identically on one segment of $\partial\Omega$ (namely that approached by M_0) and is bounded independently of h, in all norms, on the other segments. (This is because both the limit point of M_0 and its image are bounded away from all these segments.) So, as before,

$$\begin{aligned} & || \rho^{\epsilon} \nabla g ||_{L_1(\Omega)} \\ \leq \quad & || \rho^{\epsilon} \nabla g_\delta ||_{L_1(\Omega)} + || \rho^{\epsilon} \nabla g_\delta^* ||_{L_1(\Omega)} \\ & \qquad + || \rho^{\epsilon} \nabla g_H^* ||_{L_1(\Omega)} \\ \leq \quad & c\, |\log h|^{\beta} + c\, |\log h|^{\beta} + c \\ \leq \quad & c\, |\log h|^{\beta} \quad . \end{aligned}$$

Finally, suppose that the singularity M_0 approaches one of the corners of $\partial\Omega$ as $h \to 0$. Again, we employ the decomposition (5.1.29); this time however g_δ^* is the sum of three image functions (see Figure 5.1.2(b)) such that $g_\delta + g_\delta^*$ vanishes on both the boundary segments neighbouring the vertex V. The weighted norms of g_δ^* and g_H^* are bounded exactly as above and we arrive once again at (5.1.16). ###

5.2 LOGARITHM-FREE ESTIMATES

In this section we will discuss the pointwise bound

$$| (I - R)u |_{1,\infty,\Omega} \leq ch^2 |\log h|^{\beta} ||u||_{3+\epsilon,\infty,\Omega} \quad (5.2.1)$$

where $\epsilon > 0$ and β is as given by (5.1.15) above. (For a parallel discussion of the bound

$$|| Ru - u ||_{L_\infty(\Omega)} \leq ch^2 |\log h|^{\beta} ||u||_{2+\epsilon,\infty,\Omega} \quad ,$$

which has been a subject of widespread speculation for some time, see Levine, 1984. See also Haverkamp, 1984, for an alternative approach to the latter bound.) We have already established (5.2.1) for the case $\epsilon = 0$ but we have not yet shown that the $|\log h|$ factor is necessary. We give here a numerical example of $O(h^2|\log h|)$ convergence; note that (as a particular consequence of the existence of such an example), the bound on $||\nabla g||_{L_1(\Omega)}$ yielded by Lemma 5.1 is sharp. We start however by considering the case $\epsilon > 0$.

Theorem 5.2 Let $u \in W_\infty^{3+\epsilon}(\Omega)$ for some constant $\epsilon > 0$. Then for the model problem discussed in Section 5.1,

$$| (I - R)u |_{1,\infty,\Omega} \leq ch^2 ||u||_{3+\epsilon,\infty,\Omega} . \qquad (5.2.2)$$

Proof As above, it is sufficient to consider just one component of $\nabla(I - R)u$ evaluated at just one stress point $M_0 = (x_0 , y_0)$ in Ω. We arrive again at (5.1.10) and re-examine the x-derivative term

$$\left[\frac{\partial}{\partial x}(Iu - u) , \frac{\partial Rg}{\partial x} \right]_\Omega = \Sigma_k F_{k,Rg}(u) .$$

The result will follow at once if we can bound this sum by

$$ch^2 ||u||_{3+\epsilon,\infty,\Omega} ,$$

for the y-derivative term is treated identically.

We decompose the unknown u thus:

$$u(x,y) = p(x,y) + r(x,y) , \qquad (5.2.3)$$

where p is the cubic defined by

$$D^\alpha p(x_0 , y_0) = D^\alpha u(x_0 , y_0) , \quad |\alpha| \leq 3$$

(α is a multi-index). Now consider an α for which $|\alpha| = 3$. Then by the definitions of r, p and the norm in $W_\infty^{3+\epsilon}(\Omega)$,

$$\begin{aligned} & | D^\alpha r(x , y) | \\ = & | D^\alpha (u(x , y) - p(x , y)) | \\ = & | D^\alpha (u(x , y) - p(x_0 , y_0)) | \end{aligned}$$

$$= \quad | \, D^{\alpha} \, (u(\, x \, , \, y \,) - u(\, x_0 \, , \, y_0 \,)) \, |$$

$$\leq \quad \rho^{\epsilon} \quad ||u||_{3+\epsilon,\infty,\Omega} \qquad (5.2.4)$$

for all $(x,y) \in \Omega$.

Using this decomposition we will show that, because $\epsilon > 0$, all the contributions to logarithmic behaviour either decay radially away from M_0 or cancel transversely. We start by examining $F_{k,Rg}(p)$:

$$F_{k,Rg}(p) \quad = \quad \iint_{A_k} \frac{\partial}{\partial x}(Ip - p) \quad \left[\frac{\partial Rg}{\partial x} \right]_{A_k}$$

$$= \quad F_k(p) \quad \left[\frac{\partial Rg}{\partial x} \right]_{A_k}$$

(say). Now the $F_k(p)$ thus defined depends only on the restriction to A_k of the function p. Also, in the model problem, all element pairs A_k are congruent and aligned in the same direction. So, since p is cubic,

$$[p]_{A_k} \quad = \quad [p]_{A_0} \quad + \quad \textit{quadratic} \quad ,$$

for all k; furthermore all quadratics are in the null-space of F_k (Lemma 2.2). Therefore $F_k(p)$ is independent of k and so (recall $Rg = 0$ on $\partial\Omega$)

$$\Sigma_k \, F_{k,Rg}(p) \quad = \quad F_0(p) \quad \Sigma_k \left[\frac{\partial Rg}{\partial x} \right]_{A_k}$$

$$= \quad F_0(p) \quad ch^{-2} \iint_{\Omega} \frac{\partial Rg}{\partial x}$$

$$= \quad F_0(p) \quad ch^{-2} \oint_{\partial\Omega} Rg \; dy$$

$$= \quad 0 \quad . \qquad (5.2.5)$$

(As an aside, we can easily extend (5.2.5) to the statement

$$(\, \nabla(Ip - p) \, , \, \nabla\phi \,) \quad = \quad 0$$

for all cubic p and all $\phi \in S_0$ whence, by (1.3.2) and (1.3.5) with $\phi = (I - R)p$,

$$| \, (I - R)p \, |_{1,\Omega} \quad = \quad 0 \quad .$$

So on this mesh, the Finite Element approximation Rp is in fact exact at all nodes for all cubic p – compare this with the notes

to (1.4.6) and (1.5.9).)

We consider next the contribution from the remainder term r. This (recall the bounding of the $F_{k,\phi}$ in the last section) is

$$\begin{aligned} & \left| \Sigma_k F_{k,Rg}(r) \right| \\ & \leq ch^2 \Sigma_k |r|_{3,\infty,A_k} \left\| \frac{\partial Rg}{\partial x} \right\|_{L_1(A_k)} . \end{aligned} \tag{5.2.6}$$

Now by (5.2.4) each $|r|_{3,\infty,A_k}$ is bounded by

$$(\rho_k)^{\epsilon} \, \|u\|_{3+\epsilon,\infty,\Omega}$$

where ρ_K is the maximum of the set of distances to points in A_k from M_0. Moreover,

$$\begin{aligned} & (\rho_k)^{\epsilon} \left\| \frac{\partial Rg}{\partial x} \right\|_{L_1(A_k)} \\ & \leq (\rho_k)^{\epsilon} \, \|\nabla Rg\|_{L_1(A_k)} \\ & \leq c \, \|\rho^{\epsilon} \nabla Rg\|_{L_1(A_k)} \\ & \leq c \left[\|\rho^{\epsilon} \nabla g\|_{L_1(A_k)} + \|\rho^{\epsilon} \nabla (Rg - g)\|_{L_1(A_k)} \right] . \end{aligned}$$

So, by (5.2.6), (5.1.5) and Lemma 5.1,

$$\begin{aligned} & \left| \Sigma_k F_{k,Rg}(r) \right| \\ & \leq ch^2 \Sigma_k (\rho_k)^{\epsilon} \|u\|_{3+\epsilon,\infty,\Omega} \left\| \frac{\partial Rg}{\partial x} \right\|_{L_1(A_k)} \\ & \leq ch^2 \|u\|_{3+\epsilon,\infty,\Omega} \Sigma_k (\rho_k)^{\epsilon} \left\| \frac{\partial Rg}{\partial x} \right\|_{L_1(A_k)} \\ & \leq ch^2 \|u\|_{3+\epsilon,\infty,\Omega} \left[\|\rho^{\epsilon} \nabla g\|_{L_1(\Omega)} + \|\nabla (Rg - g)\|_{L_1(\Omega)} \right] \\ & \leq ch^2 \|u\|_{3+\epsilon,\infty,\Omega} . \end{aligned} \tag{5.2.7}$$

The result of the theorem now follows from (5.2.3), (5.2.5) and (5.2.7). ###

We have shown that the $|\log h|$ factor in (5.1.14) is not necessary if the smoothness of u is increased to $W_{\infty}^{3+\epsilon}$ for any $\epsilon > 0$. On the other hand, this factor does remain necessary when $\epsilon = 0$: we demonstrate this by means of a simple example.

Let Ω be the unit square $(-1/2, 1/2)^2$ and let

$$u = x^3 y^2 / (x^2 + y^2) . \tag{5.2.8}$$

(We note that away from the origin u is C^{∞}; overall u is W_{∞}^{3} but not $W_{\infty}^{3+\epsilon}$ for any $\epsilon > 0$.) We partition Ω into squares of side h and thence into triangles with diagonals of slope $+1$; we take $Ru \in S_E$ to be the Finite Element approximation to u via Poisson's equation: Ru solves (1.6.1) with Δu given analytically from (5.2.8).

Since we are concerned with displaying the asymptotic behaviour of the error for a computationally feasible range of h, we examine the point values

$$\left.\begin{array}{lllll} e & = & e(u;h) & = & \left[\frac{\partial}{\partial x}(I - R)u \right]_{M_0} \\ \text{where} \quad M_0 & = & M_0(h) & = & (0 , -h/2) \quad , \end{array}\right\} \quad (5.2.9)$$

rather than the overall supremum of the full gradient. (Note that if we take h^{-1} to be odd then $M_0(h)$ will always be an x-derivative stress point.) In Table 5.2, values of $|e|$, $|e/h^2|$ and $|e/h^2 \log h|$ are presented for $h = 1/3, 1/5, \ldots, 1/15$; in addition we give relative differences between rows in the columns marked Δ. The $|\log h|$ factor is very clear for $h < 1/7$.

We remark that this example was only constructed with some difficulty, by an intuitive matching of the directions of ∇u and ∇g for functions u just in W_{∞}^{3}. Most simple functions in $W_{\infty}^{3} \backslash W_{\infty}^{3+\epsilon}$ do not display this $|\log h|$ behaviour. Further, most W_{∞}^{3} functions are also in $W_{\infty}^{3+\epsilon}$; finally even when the $|\log h|$ term is present it will in general not have a significant effect on the global error for computationally interesting h. For these reasons we conclude this section by repeating our earlier remark that in practical work, the best thing to do with the logarithm is to ignore it.

$\frac{1}{h}$	$\lvert e \rvert$	$\left\lvert \frac{e}{h^2} \right\rvert$	$\left\lvert \frac{e}{h^2 \log h} \right\rvert$	$\left\lvert \Delta\left[\frac{e}{h^2}\right] \right\rvert$	$\left\lvert \Delta\left[\frac{e}{h^2 \log h}\right] \right\rvert$
	$\times 10^3$	$\times 10$	$\times 10$		
3	17.70	1.593	1.450		
				26%	12%
5	8.301	2.076	1.290		
				16%	2.9%
7	4.976	2.438	1.253		
				11%	0.85%
9	3.370	2.730	1.242		
				8.4%	0.32%
11	2.245	2.970	1.238		
				6.6%	0.14%
13	1.877	3.172	1.2367		
				5.4%	0.06%
15	1.488	3.347	1.2359		

Table 5.2

Example of $O(h^2 \log h)$ convergence

u and e are given by (5.2.8) and (5.2.9).

5.3 FURTHER RESULTS

In this final section we take an informal look at two directions in which the model ℓ_∞ result (5.1.14) can be extended: pointwise superconvergence for the generalised problem and "local" superconvergence. We do not go into every detail, partly because this would be unilluminating and partly because crucial theoretical results (properties of the Green's function) are not available to us in sufficient generality.

We consider first – and in brief – a generalisation of pointwise superconvergence to the full problem of Chapter 4 (general self-adjoint, curved mesh, etc.). (Except where noted below, the extended result can be made "logarithm-free" without real difficulty. However the details of this process are especially long and we do not intend to air them here.) As in Chapter 4, we let the superscript * denote the use of numerical quadrature by the centroid rule. Then, in place of (5.1.1),...,(5.1.4) we define the functions δ, g and Rg so that

$$\left[\frac{\partial \phi}{\partial x} \right]_Q = \left[\frac{\partial \phi}{\partial x} , \delta \right]^*_{\Omega_h} \qquad \text{for all } \phi \in S,$$

$$a_{\Omega_h}(g , v) = \left[\frac{\partial v}{\partial x} , \delta \right]_{\Omega_h} \qquad \text{for all } v \in H^1_0$$

and $$a^*_{\Omega_h}(Rg , \phi) = \left[\frac{\partial \phi}{\partial x} , \delta \right]^*_{\Omega_h} \qquad \text{for all } \phi \in S_0.$$

Then (recall Theorem 4.2)

$$\left| \left[\frac{\partial}{\partial x}(I - R)u \right]_Q \right|$$

$$= \left| \left[\frac{\partial}{\partial x}(I - R)u , \delta \right]^*_{\Omega_h} \right|$$

$$= \left| a^*_{\Omega_h}((I - R)u , Rg) \right|$$

$$\leq \quad |a^*_{\Omega_h}(Iu - u , Rg)|$$

$$+ \quad |a^*_{\Omega_h}(u , Rg) - a_{\Omega_h}(u , Rg)|$$

$$+ \quad |(f , Rg)_{\Omega_h} - (f , Rg)^*_{\Omega_h}| \quad .$$

In order to bound these three terms, we must strengthen (4.2.5):

$$\left.\begin{aligned} u \quad &\in \quad H^1_E(\Omega) \cap W^3_\infty(\Omega) \quad , \\ a_{ij} \quad &\in \quad W^2_\infty(\Omega) \quad (i,j = 1,2) \\ \text{and} \qquad f \quad &\in \quad W^2_\infty(\Omega) \quad . \end{aligned}\right\} \quad (5.3.1)$$

Now, as before, we would like to bound these functions in norms defined on Ω_h (which might not be a subset of Ω). We encounter here the difficulty that Calderon's extension theorem does not apply to L_∞ norms. Although the theorem of Stein (1970 - page 181) is applicable, we must accept a restriction: that the domain Ω is convex. (Note also that if we require a logarithm-free estimate then an extra ϵ-tuple order of differentiability must be added to each of the functions in (5.3.1), in the manner of Section 5.2. Unfortunately the result stated by Stein applies only to integer orders of differentiation ; we do not know whether this last restriction - that $\epsilon \geq 1$ - is a necessary one.) Additionally, we replace (4.1.2) by

$$(x,y) \quad \in \quad \left[W^2_\infty(\beta_h) \right]^2$$

on each band.

The next step is similar to Sections 4.3 and 4.4, the difference being that now - as in Section 5.1 - the bounds are in terms of the supremum norms implicit in (5.3.1) and the W^1_1 norm on Rg (as opposed to mean-square norms throughout). We then seek to generalise (5.1.5) and (5.1.7) to the full problem. Rannacher and Scott (1982) state that, in the absence of numerical quadrature, the former bound does indeed carry over to the

generalised problem. There is however a well-posedness condition that the elliptic operator L (4.2.1) is a homeomorphism

$$L: \quad W^1_{p(0)} \cap W^2_p \rightarrow L_p \qquad \text{for all } p \in (\, 1 \,,\, 2+\alpha \,].$$

(Here α can be any fixed, small but positive number; $W^1_{p(0)}$ denotes the $W^1_p(\Omega)$ generalisation of $H^1_0(\Omega)$.) In particular this condition places a restriction on the vertices of Ω: the greatest internal angle must be less than

$$\pi \left[\, 1 - \frac{\alpha}{2+2\alpha} \, \right]$$

(see Grisvard, 1976). Since α is arbitrary, this is satisfied by any convex Ω (a condition already imposed, by Stein's extension theorem).

As far as (5.1.7) is concerned, we recall that Lemma 5.1 depends on explicit knowledge of the form of the free-space Green's function g_δ; (5.1.17) and in particular (5.1.26) apply only to the case of the Laplacian operator $L = -\Delta$. The approach of Krasovskiĭ (1967) may be useful for more general operators; however it is restricted to the generally inapplicable case of regions Ω without vertices. We note here that the image-function treatment of g_H for stess points close to $\partial\Omega$ can be applied (in the standard way) to curved segments of the boundary but not to any vertices which are not right-angled.

We believe that the bound on $|Rg|_{1,1,\Omega}$ for the general problem is fraught with difficulty - from numerical quadrature, the form of L and the shape of Ω. We do not know the extent to which the pointwise superconvergence result is jeopardised. We suspect that situations in which the stress point M_0 is close to a general (convex) vertex of $\partial\Omega$ are those most likely to lead to loss of accuracy. However, we have been completely unable to find any evidence either to confirm or to refute this hypothesis.

We move on now to "local" superconvergence. We assume that the conditions we have placed on the mesh, the unknown u and so on are only satisfied in a subdomain Ω_1 of Ω. In the complement Ω_0 of Ω_1 any or all of these conditions may fail. We claim that superconvergence still takes place at stress points in Ω_1, provided they are not too close to the boundary with Ω_0. For simplicity we present the discussion in terms of the model problem; any possible generalisation of it follows the outline given above.

Let $\{ \Omega_0 , \Omega_1 \}$ partition Ω and let $\Omega_0 \subset \Omega_{00} \subset \Omega$, such that

$$d(\partial\Omega_0 \backslash \partial\Omega , \partial\Omega_{00} \backslash \partial\Omega) > c \quad (>0) .$$

Let Q be any point in $\Omega_1 \backslash \Omega_{00}$ (i.e. bounded away from $\partial\Omega_0$ - see Figure 5.3.1). Let the smoothed x-derivative Green's function (for the Laplacian) associated with Q be g. Since g is harmonic in Ω_0 (the singularity being in $\Omega_1 = \Omega \backslash \Omega_0$), we have

$$\begin{aligned} 0 &= (Iu - u , -\Delta g)_{\Omega_0} \\ &= (\nabla(Iu - u) , \nabla g)_{\Omega_0} \\ &\quad - \langle Iu - u , g_\nu \rangle_{\partial\Omega_0} , \end{aligned}$$

where $\langle \cdot , \cdot \rangle$ and the $\cdot_\nu$ subscript denote a boundary inner-product and the outward normal derivative. So (recall the derivation of (5.1.10))

$$\left.\begin{aligned} &\left[\frac{\partial}{\partial x}(I - R)u \right]_Q \\ &= (\nabla(Iu - u) , \nabla Rg)_{\Omega} \\ &= (\nabla(Iu - u) , \nabla Rg)_{\Omega_1} \\ &\quad + \langle Iu - u , g_\nu \rangle_{\partial\Omega_0} \\ &\quad + (\nabla(Iu - u) , \nabla(Rg - g))_{\Omega_0} \end{aligned}\right\} (5.3.2)$$

We consider these three terms separately. The first is bounded in the usual way (Section 5.1) and, since the conditions of superconvergence are met within Ω_1, presents only one difficulty

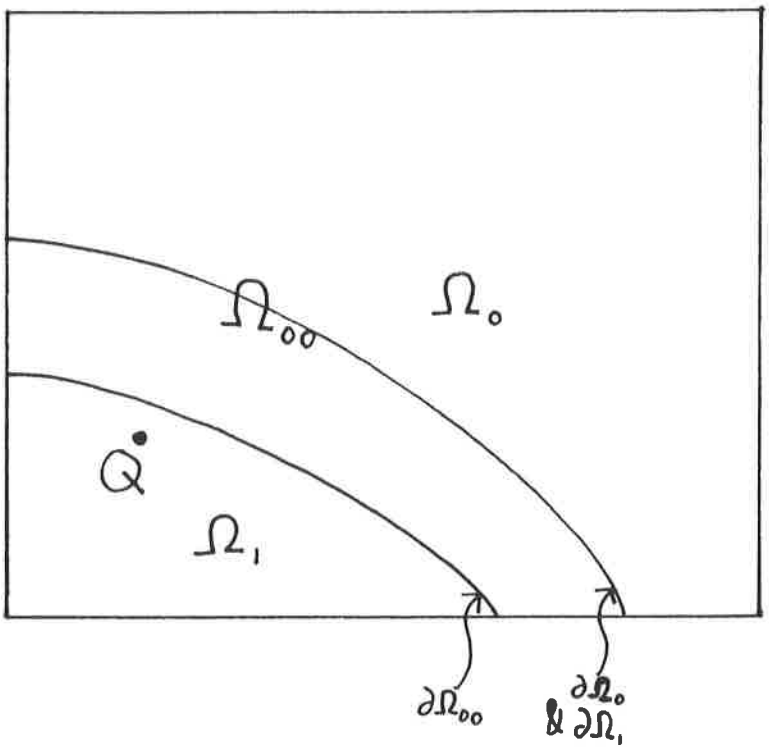

Figure 5.3.1

Partition of Ω for local superconvergence

The sample point Q is excluded from Ω_{oo} and hence bounded away from the subdomain Ω_o of Ω in which the superconvergence requirements break down.

- the bounding of contributions from left-over elements on the internal boundary $\partial\Omega_1 \backslash \partial\Omega$ (on which Rg does not vanish). We pass over this here because it is qualitatively very similar to the bounding of the contribution from Ω_0 (i.e. the remaining terms of (5.3.2)).

The second term is bounded by

$$\begin{aligned} & \|Iu - u\|_{L_\infty(\Omega)} \; |g|_{1,1,\partial\Omega_0} \\ & \leq \; ch^2 \; |u|_{2,\infty,\Omega} \left[\; |g_\delta|_{1,1,\partial\Omega_0} \; + \; |g_H|_{1,1,\partial\Omega_0} \; \right] . \end{aligned}$$

The norm on g_δ is bounded by inspection of (5.1.26); furthermore we recall that all norms on g_H are bounded independently of h. (If Q is close to $\partial\Omega$ then we decompose g_H according to (5.1.29): g_δ^* is bounded as g_δ and g_H^* as g_H above.) Finally the last term in (5.3.2) is bounded thus (under a very mild condition on the smoothness of u in Ω_0):

$$\begin{aligned} & (\nabla(Iu - u) \; , \; \nabla(Rg - g) \;)_{\Omega_0} \\ & \leq \; |Iu - u|_{1,\Omega_0} \; |Rg - g|_{1,\Omega_0} \\ & \leq \; ch \; |u|_{2,\Omega_0} \; |Rg - g|_{1,\Omega_0} \quad . \end{aligned}$$

It remains then to bound $|Rg - g|_{1,\Omega_0}$. Now, according to Nitsche and Schatz (1974),

$$\begin{aligned} & |Rg - g|_{1,\Omega_0} \\ & \leq \; c \left[\; h \; |g|_{2,\Omega_{00}} + \|Rg - g\|_{-s,\Omega_{00}} \; \right] \quad . \qquad (5.3.3) \end{aligned}$$

(Although they restrict this result to regions Ω_{00} which do not meet the main boundary $\partial\Omega$, it is very easily shown that their restriction can be dropped.) Here s is any positive integer; the "negative" (or "dual") Sobolev norm is defined by

$$\|v\|_{-s} \; = \; \sup_{\omega \in H^s \cap H_0^1} \frac{|(v,\omega)|}{\|\omega\|_s} \quad .$$

The first term in (5.3.3) is bounded in exactly the same way

as the W_1^1 norm on g earlier; our problem lies with the local negative norm on the error $Rg - g$. Our most promising approach is to weaken it to a global negative norm (this was suggested by Nitsche and Schatz) and then apply the duality method of Nitsche (1968) (also of Aubin, 1967 and Oganesjan & Ruchovec, 1969).

We set $s=2$ and proceed thus:

$$\begin{aligned} & ||Rg - g||_{-2,\Omega_{00}} \\ \leq\ & ||Rg - g||_{-2,\Omega} \\ =\ & \sup_{\omega \in H^2 \cap H_0^1} \frac{|(\ Rg - g\ ,\ \omega\ )|}{||\omega||_2} \ . \end{aligned}$$

(Here and below, integrals are implicitly over Ω.) Let $\psi = \psi(\omega) \in H_0^1(\Omega)$ satisfy (weakly)

$$-\Delta\psi \ = \ \omega \quad \text{in } \Omega.$$

Then by parts, (1.3.2) and (1.3.5), (5.1.6) and Lemma 5.1,

$$\begin{aligned} & ||Rg - g||_{-2,\Omega_{00}} \\ \leq\ & \sup_\omega \frac{|(\ Rg - g\ ,\ -\Delta\psi\ )|}{||\omega||_2} \\ =\ & \sup_\omega \frac{|(\ \nabla(Rg - g)\ ,\ \nabla\psi\ )|}{||\omega||_2} \\ =\ & \sup_\omega \frac{|(\ \nabla g\ ,\ \nabla(R\psi - \psi)\ )|}{||\omega||_2} \\ \leq\ & \sup_\omega |g|_{1,1,\Omega}\ |R\psi - \psi|_{1,\infty,\Omega}\ ||\omega||_{2,\Omega}^{-1} \\ \leq\ & ch\ |\log h|\ \sup_\omega |\psi|_{2,\infty,\Omega}\ ||\omega||_{2,\Omega}^{-1} \ . \end{aligned}$$

If - hypothetically - all the corners of Ω were strictly acute (!) then by Theorem 5.1 of Grisvard (1976) we would have

$$|\psi|_{2,\infty,\Omega} \ \leq \ c'\ ||\Delta\psi||_{L_\infty(\Omega)} \ .$$

Hence by S.E.

$$|\psi|_{2,\infty,\Omega} \ \leq \ c\ ||\omega||_{2,\Omega} \qquad (5.3.4)$$

and the above supremum would be bounded, whence by (5.3.2)

$$\left|\ \left[\ \frac{\partial}{\partial x}(I - R)u\ \right]_Q\ \right| \ \leq \ c(u)h^2\ |\log h| \ . \qquad (5.3.5)$$

In the (quite reasonable) case that Ω has non-acute (convex)

vertices - and in particular when Ω is the model rectangle - the regularity theorem cannot be applied: (5.3.4) fails and the final supremum may well be unbounded. We do not know how this affects $||Rg - g||_{-2,\Omega}$ - let alone the norm over Ω_{00} or the eventual estimate (5.3.5). We suspect that this result remains valid for all convex Ω, but are again unable to either prove or disprove our claim.

Let us end on a lighter note: a simple numerical example of local superconvergence. Let Ω be the truncated square, as shown and triangulated in Figure 3.1.3. Let u be the quadratic

$$(x - 1)^2 + y^2 .$$

(We choose this function to highlight asymptotic behaviour for computationally reasonable values of h. It has been our experience that when breakdown of superconvergence is due to effects from a subdomain of Ω, in particular the neighbourhood of a line, the error is somewhat smaller than expected and the asymptotic rate may not be obtained for practical values of h.) We take $h = 1/4 , \ldots , 1/12$; as usual we define Ru by (1.6.1).

Now, as predicted in Section 3.1, we obtain

$$E_{rec} \simeq 1.9h^{3/2} .$$

However when we restrict the average to elements in the subdomain

$$\Omega_1 \backslash \Omega_{00} = (0 , 1/2)^2$$

- this is bounded away from the region Ω_0 where the mesh conditions break down - we obtain

$$E_{rec} \simeq 1.9h^2 .$$

CONCLUDING REMARKS

"The stresses are, by the basic assumption, constant within the element. It is usual to assign these to the centroid of the element, and in most of the examples in this chapter this procedure is followed. An alternative consists of obtaining stress values at the nodes by averaging the values in the adjacent elements..." (Zienkiewicz & Cheung, 1967.)

My principal result is that there is nothing at all to be gained by assigning stresses to element centroids. Although the proposal to recover the gradient at a node by taking a six element average (recall Figures 3.3.8 & 3.3.9) is a sound one, the centroids play no part in its justification.

Admittedly the work is not complete: the practical questions of "good" choices for triangulation and recovery algorithms remain open and there are noticeable, if occasionally abstruse, theoretical gaps in the Green's function work of Chapter 5. These cracks, however, are non-structural in nature: I feel that the essential features of superconvergence rest on a solid foundation.

Nick Levine

Yule 1984/5

REFERENCES

DOUGLAS, J., DUPONT, T. & WHEELER, M.F. 1974 "A Galerkin procedure for approximating the flux on the boundary for elliptic and parabolic boundary value problems", R.A.I.R.O. 8 47–59.

DUPONT, T. & SCOTT, R. 1980 "Polynomial approximation of functions in Sobolev spaces", Math. Comp. 34 441–63.

FIX, G.J., GUNZBURGER, M.D. & NICOLAIDES, R.A. 1981 "On mixed finite element methods for first order elliptic systems", Num. Math. 37 29–48.

GRISVARD, P. 1976 "Behaviour of the solutions of an elliptic boundary value problem in a polygonal or polyhedral domain", in "Numerical solution of partial differential equations III" (SYNSPADE 1975), ed. Hubbert, B., 207–74.

HAVERKAMP, R. 1984 "Eine Aussage zur L_∞-Stabilität und zur genauen Konvergenzordnung der H_0^1-Projektionen", Num. Math. 44 393–405.

KRASOVSKIĬ, Ju.P. 1967 "Isolation of singularities of the Green's function", Izv. Akad. Nauk SSSR Ser. Mat. 31, transl. Math. USSR-Izv. 1 935–66.

KŘÍŽEK, M. & NEITTAANMÄKI, P. 1984 "Superconvergence phenomenon in the finite element method arising from averaging gradients", Num. Math. 45 105–16.

LESAINT, P. & ZLÁMAL, M. 1979 "Superconvergence of the gradient of finite element solutions", R.A.I.R.O. 13 139–66.

ADAMS, R.A. 1975 "Sobolev spaces", Academic Press.

AUBIN, J.P. 1967 "Behaviour of the error of the approximate solutions of boundary value problems for linear elliptic operators by Galerkin's and finite difference methods", Ann. Scuola Norm. Sup. Pisa 21 599–637.

BABICH, V.M. 1953 "The problem of the extension of functions", Usp. mat. Nauk. 7 111–3.

BARLOW, J. 1968 "A stiffness matrix for a curved membrane shell", Conf. Recent Advances in Stress Analysis, Roy. Aeron. Soc.

BARLOW, J. 1976 "Optimal stress locations in finite element models", Int. J. Num. Meth. Eng. 10 243–51.

BRAMBLE, J.H. & HILBERT S.R. 1970 "Estimation of linear functions on Sobolev spaces with applications to Fourier transforms and spline interpolation", SIAM J. Numer. Anal. 7 112–24.

BRAMBLE, J.H. & SCHATZ, A.H. 1977 "Higher order local accuracy by averaging in the finite element method", Math. Comp. 31 94–111.

CALDERON, A.P. 1961 "Lebesgue spaces of differentiable functions and distributions", Proc. Symp. Pure Math. IV 33–49.

CIARLET, P.G. 1978 "The finite element method for elliptic problems", North-Holland.

LEVINE, N.D. 1982 "Stress sampling points in the finite element method", Numerical Analysis Report 10/82, University of Reading.

LEVINE, N.D. 1983 "Superconvergent recovery of the gradient from piecewise linear finite element approximations", Numerical Analysis Report 6/83, University of Reading. (To appear in IMAJNA.)

LEVINE, N.D. 1984 "Pointwise logarithm-free estimates for finite elements on linear triangles", Numerical Analysis Report 6/84, University of Reading.

LIN QUN, LU TAO & SHEN SHUMIN 1983 "Asymptotic expansion for finite element approximations", Research Report 11, Institute of Mathematical Sciences, Academia Sinica (Chengdu branch).

MOAN, T. 1974 "Experiences with orthogonal polynomials and best numerical integration formulas on a triangle", Z.A.M.M. 54 501-8.

NITSCHE, J.A. 1968 "Ein Kriterium für die quasi-optimalitat des Ritzchen Verfahrens", Num. Math. 11 346-8.

NITSCHE, J.A. 1978 "L_∞-error analysis for finite elements", in "The mathematics of finite elements and applications, III", ed. Whiteman, J., 174-86.

NITSCHE J.A. & SCHATZ, A.H. 1974 "Interior estimates for Ritz-Galerkin methods", Math. Comp. 28 937-58.

OGANESJAN, L.A. & RUCHOVEC, L.A. 1969 "Investigation of the convergence rate of variational-difference schemes for elliptic second order equations in a two-dimensional domain with a smooth boundary", Z. Vychisl. Mat. i Mat. Fiz. 9, transl. USSR Comp. Math. and Math. Phys. 9 153-83.

RANNACHER, R. & SCOTT, R. 1982 "Some optimal error estimates for piecewise linear finite element approximations", Math. Comp. 38 437-45.

SOBOLEV, S.L. 1950 "Application of functional analysis in mathematical physics", Leningrad, transl. in Math. Monographs 7, American Mathematical Society (1963).

STEIN, E.M. 1970 "Singular integrals and differentiability properties of functions", Princton University Press.

STRANG, G. & FIX G.J. 1973 "An analysis of the finite element method", Prentice-Hall.

THOMÉE, V. 1977 "High order approximations to derivatives in the finite element method", Math. Comp. 31 652-60.

TOO, J.M. 1971 "Two dimensional, plate and finite prism isoparametric elements and their application", PhD Thesis, University of Wales.

VERYARD, D.A. 1971 "Problems associated with the convergence of isoparametric and mixoparametric finite elements", MSc Thesis, University of Wales.

WHEELER, J.A. 1973 "Simulation of heat transfer from a warm pipeline buried in permafrost", presented to the American Institute of Chemical Engineers.

ZIENKIEWICZ, O.C. & CHEUNG, Y.K. 1967 "The finite element method in continuum mechanics", McGraw Hill.

ZLÁMAL, M. 1977 "Some superconvergence results in the finite element method", in "Mathematical aspects of finite element methods", eds. Galligani, I. & Magenes, E., 351–62.

ZLÁMAL, M. 1978 "Superconvergence and reduced integration in the finite element method", Math. Comp. 32 663–85.

WHEELER, J.A. 1973 "Simulation of heat transfer from a warm pipeline buried in permafrost", presented to the American Institute of Chemical Engineers.

ZIENKIEWICZ, O.C. & CHEUNG, Y.K. 1967 "The finite element method in continuum mechanics", McGraw Hill.

ZLÁMAL, M. 1977 "Some superconvergence results in the finite element method", in "Mathematical aspects of finite element methods", eds. Galligani, I. & Magenes, E., 351-62.

ZLÁMAL, M. 1978 "Superconvergence and reduced integration in the finite element method", Math. Comp. 32 663-85.